



The University of
Nottingham

School of Chemistry

Transaminase-Triggered Cascades for the Construction of Complex Alkaloids

Freya Frances Hughes Taday MSci (Hons)

**Thesis Submitted to the University of Nottingham
for the Degree of Doctor of Philosophy**

2021

Contents

Contents	I
Abstract	III
Acknowledgements	VII
Abbreviations.....	VIII
1.0 Introduction.....	1
1.1 Alkaloids.....	1
1.2 Synthesis of Alkaloids	3
1.2.1 Biosynthesis of Alkaloids.....	3
1.2.2 Chemical Synthesis of Alkaloids	7
1.2.3 Biocatalytic Synthesis of Alkaloid Scaffolds.....	16
1.3 Transaminases (TA)	26
1.3.1 Mechanism of ATAs	27
1.3.2 Limitations of ATAs.....	29
1.3.4 Key Synthetic Examples using ATAs	31
1.4 Enzyme Reversibility.....	33
1.5 Shuttle Catalysis.....	37
1.5.1 Shuttle Catalysis as Part of a Larger Cycle	38
1.6 Project Aims.....	42
Part I - Asymmetric Construction of Cyclic β -Enaminones, Employing a Transaminase-Aza-Michael Cascade.....	48
2.1 Introduction.....	49
2.2 Results and Discussion	52
2.2.1 Synthesis of Ketoynones 147 (Scheme 46)	52
2.2.2 Synthesis of β -enaminones using ATA-aza-Michael Cascade	56
2.2.3 Annulation Cascades and Reactions	62
2.3 Summary	68

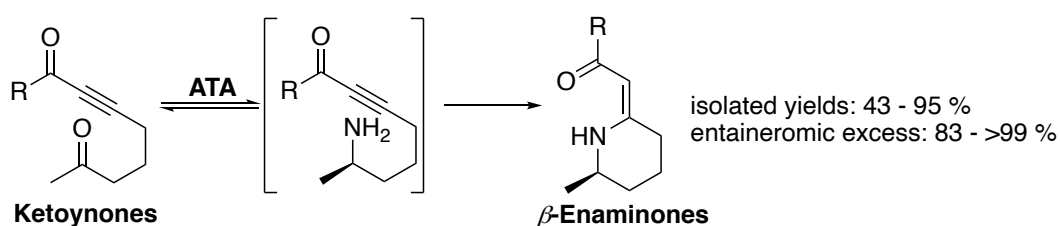
Part II - Development of <i>Amine Borrowing</i> Methodology for the Synthesis of Complex Alkaloids	69
3.0 Investigating the Transaminase-Mannich Cascade	71
3.1 Introduction.....	72
3.2 Results and Discussion	74
3.3 Summary	79
3.4 Future work.....	80
4.0 Exploring the Transaminase-Knorr Pyrrole Synthesis Cascade	82
4.1 Introduction.....	83
4.2 Results and Discussion	86
4.3 Summary	92
4.4 Future Work	93
5.0 Studying the Transaminase-Pictet Spengler Reaction Cascade	94
5.1 Introduction.....	95
5.2 Results and Discussion	97
5.3 Summary	109
5.4 Future Work	110
6.0 Conclusions	112
7.0 Experimental	116
7.1 General Methods	116
7.2 Synthesis of β -Enaminone and corresponding derivatives	117
7.3 Mannich Reaction.....	141
7.4 Pyrrole Synthesis	145
7.5 THIQ Synthesis	153
8.0 References	160

Abstract

The natural defence mechanisms of plants often involve the use of secondary metabolites known as alkaloids. Alkaloids have been shown to act as poisons and herbicides to discourage predators or suppress competition from other plants. This class of metabolite has been found to have biologically useful functions, including acting as antibiotics, anticancer agents and many more. However, synthesis of these molecules often involves the use of harsh, unsustainable methodologies.

During the biosynthesis of alkaloids, there are multiple cascade reactions taking place, for example, in the biosynthesis of pelletierine, where a transaminase (TA)-catalysed reaction proceeds *via* a Mannich reaction. The introduction of biocatalysts into the chemical toolbox means that research can look at ways in which organisms perform a synthesis and mimic this in the laboratory. The overall aim of this project was to use a transaminase reaction to trigger a concurrent cascade and enable access to a range of alkaloid scaffolds, which could then serve as templates for drug-like molecules.

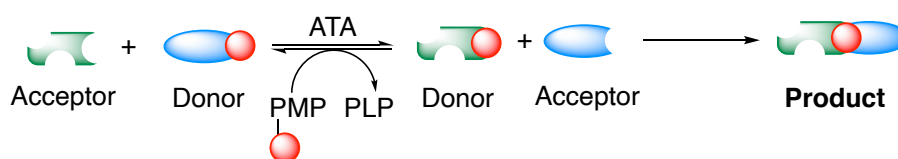
One aspect of this project employed a transaminase-triggered intramolecular aza-Michael reaction for the preparation of cyclic β -enaminones in good yields (43 – 95 %), with excellent enantio and diastereoselectivity, starting from prochiral ketoyones (**Scheme A**). This methodology required only two equivalents of isopropylamine, reflecting the powerful thermodynamic driving force associated with the spontaneous aza-Michael reaction, which displaces the transaminase reaction equilibrium towards product formation.



Scheme A: The retrosynthesis of cyclic β -enaminones from pro-chiral ketoyone scaffolds.

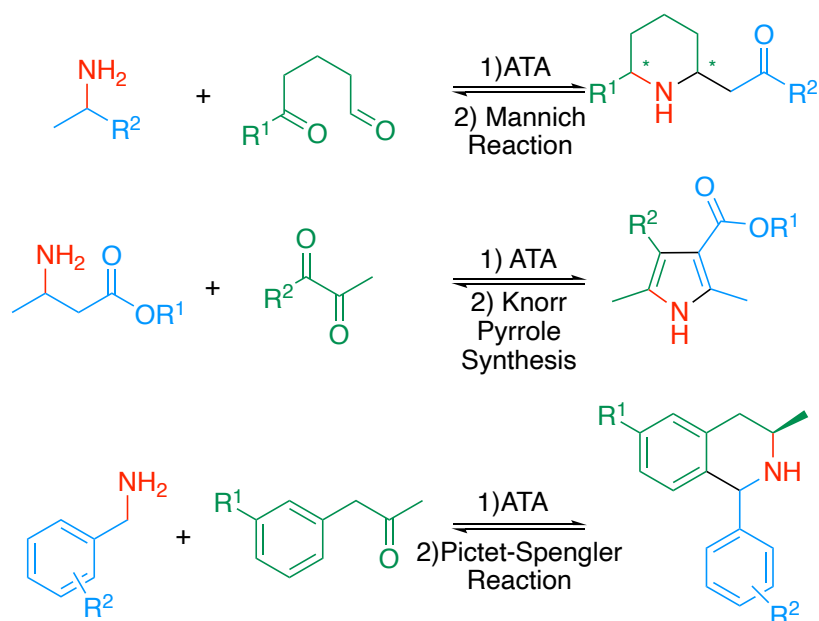
To further demonstrate the potential of this methodology, the original cascade was combined with annulation chemistry, either in a concurrent cascade to provide a range of tetrahydroquinolines (THQ) in a range of yields (10 – 90 %) or in a two-step approach to afford a selection of fused-ring cyclic alkaloids (44 – 92 %).

The second aspect of this work focused on the development of the entirely novel concept of ‘*amine borrowing*’ via shuttle catalysis. Shuttle catalysis is a relatively new methodology and involves *in situ* catalytic shuttling of a functional moiety from one molecule to another. The approach is often employed to avoid the handling of toxic or unstable intermediates. The biocatalytic transaminase reaction lends itself to shuttle catalysis and proved a useful transformation for the development of the concept of *amine borrowing* (**scheme B**).



Scheme B: A depiction of the ability of transaminase to shuttle the amine functionality from the donor molecule (blue) to an acceptor molecule (green) generating two reactive species in situ. These two species react in a concurrent cascade forming the desired product containing the amine functionality.

It was hypothesised that by using a transaminase to shuttle the amine moiety from the donor molecule to the acceptor molecule, two reactive species could be generated *in situ*. These species are then able to undergo an intermolecular reaction, leading to the ‘borrowed’ amine moiety ultimately being incorporated into the target compound and representing the first example of *amine borrowing* (**Scheme B**). Three reactions were chosen to investigate *amine borrowing* including the Mannich, Knorr Pyrrole synthesis and Pictet-Spengler reactions (**Scheme C**).



Scheme C: The proposed synthesis of a range of alkaloid derivatives via different concurrent cascades used to investigate amine borrowing methodology as part of this work.

When delving into the transaminase-Mannich cascade, initial results revealed the Mannich reaction was able to be conducted under biotransformation conditions to afford the natural product pelletierine in a 74 % conversion. However, this observed conversion was not under *amine borrowing* conditions and to date, suitable substrates and conditions have yet to be established for this transaminase triggered Mannich reaction.

Amine borrowing conditions were successfully employed during the synthesis of pyrrole derivatives with good conversions (41 – 99 %) and reasonable yields (32 – 80 %). These conversions result from the pyrrole formation effectively displacing the equilibrium of the transaminase reaction, even in the presence of just one equivalent of available amine donor. The highly reactive intermediate formed *in situ* highlights as to why it is advantageous to use an *amine borrowing* methodology.

To further demonstrate the potential of *amine borrowing*, the conditions were applied to a transaminase-Pictet-Spengler cascade. Multiple screening attempts were conducted to obtain the best conditions for a range of potential amine donors and carbonyls. Despite this, disappointing

conversions (1 – 31 %) were only achieved. However, this project presents important proof-of-concept results for completely novel methodology, which has the potential to impact amine synthesis, in the development of high value chemicals.

Acknowledgements

Firstly, I would like to thank Dr Elaine O'Reilly for providing me with the opportunity to complete my PhD under her guidance and support, without which this would not have been possible. This was alongside Dr Nick Mitchell, who took on the administrative care of another PhD student when Elaine moved back to Ireland.

I would also like to thank Dr James Ryan, for his help in the lab during the early part of my PhD, as well as helpful discussions throughout. Of course, I have to thank the rest of the O'Reilly group both past and present for their camaraderie in the lab, and a special shout out to Dr Chris Peel, who made being in the lab so enjoyable as well as his help bouncing ideas back and forth in the process of writing this thesis.

I'd also like to thank the amazing technical team at the University for keeping the analytical equipment running so well and helping with so many questions, helping to solve several problems that arose during the course of this work, without which analytical chemistry would not be possible. And of course, to Sue, for giving me a space away from the lab when things weren't going to plan, to relax and regroup.

This acknowledgement would not be complete without a huge thank you to Dr Alex Wichlacz, for his unconditional support for the past three and a half years, helping me solve problems in the lab and with my data as well as reading and re-reading this thesis in the course of helping me make it legible. I'd finally like to thank my family for their continued support throughout my studies.

Abbreviations

AcN	Acetonitrile
AcOH	Acetic Acid
ADH	Alcohol Dehydrogenase
Ala	Alanine
AlaDH	Alanine Dehydrogenase
AmDH	Amine Dehydrogenase
ATA	Amine Transaminase
CDI	1,1'-Carbonyldiimidazole
DDQ	2,3-Dichloro-5,6-Dicyanobenzoquinone
<i>d.e.</i>	Diastereomeric Excess
DEAD	Diethyl Azodicarboxylate
DERA	Deoxyribose-5-Phosphate Aldolase
DMSO	Dimethylsulfoxide
DPPA	Diphenylphosphoryl Azide
<i>d.r.</i>	Diastereomeric Ratio
EDG	Electron-Donating Group
<i>e.e.</i>	Enantiomeric Excess
EWG	Electron-Withdrawing Group
FTIR	Fourier Transform Infrared Spectroscopy
GC-FID	Gas Chromatography - Flame Ionising Detection
HHQ	Hexahydroquinolines
HPLC	High Performance Liquid Chromatography
IRED	Imine Reductase
IPA	Isopropylamine
KP_i	Potassium Phosphate Buffer
LDH	Lactate Dehydrogenase
Lys	Lysine
MBA	Methylbenzylamine
MeOH	Methanol
MOA	Monoamine Oxidase
MTase	Methyl Transferase
NAD(H)	Nicotinamide Adenine Dinucleotide

NADP(H)	Nicotinamide Adenine Dinucleotide Phosphate
NCS	Norcochlorine Synthase
NMR	Nuclear Magnetic Resonance
PDB	Protein Data Bank
P_i	Inorganic Phosphate
PLP	Pyridoxal-5'-Phosphate
PNP	Purine Nucleoside Phosphorylase
PMP	Pyridoxamine-5'-Phosphate
PPM	Phosphopentomutase
Red Am	Reductive Amidases
TA	Transaminase
TFA	Trifluoroacetic acid
THF	Tetrahydrofuran
THIQ	Tetrahydroisoquinoline
THQ	Tetrahydroquinolines
TLC	Thin Layer Chromatography
Tyr	Tyrosine

1.0 Introduction

1.1 Alkaloids

The biological effects of alkaloids are well-established and these structures are frequently key components of drugs, medicines, teas, and poisons.¹⁻³ Alkaloids are found as secondary metabolites, mainly in plants,^{4,5} but they have also been found in animals⁶ and microorganisms,⁷ where they are frequently deployed as defensive agents to protect these organisms from predators;^{2,8} they often give plants an undesirable bitter taste, and in the case of caffeine **7** producing plants, the caffeine **7** acts as a herbicide to reduce competition.⁹ The general definition of an alkaloid is a cyclic compound containing nitrogen, either as part of a heterocyclic moiety or as an additional aliphatic or aromatic cyclic moiety, and this amine provides a degree of basicity. The basic property of alkaloids are responsible for their name, which is derived from alkali.¹⁰ The nitrogen in the alkaloid structure stems from amino acids, where the parent amino acid is incorporated into the alkaloid and subsequently decarboxylated.¹¹

The important biological activity observed in alkaloids owes to the structurally intriguing and complex scaffolds, and has led them to be highly investigated natural products and drug leads, despite a large majority of alkaloids being known toxins and poisons.¹² Alkaloids of plant-based origin that have been used clinically include morphine **2** and codeine **1** as analgesics, the gout suppressant colchicine **3**, (+)-tubocurarine **5** and papaverine **4** (muscle relaxants), and also the recreational drug cocaine **6**. In addition, there are many common household names such as caffeine **7**, nicotine **8** and piperine **9**, which can be found in the condiment pepper (**Figure 1**).^{11,13}

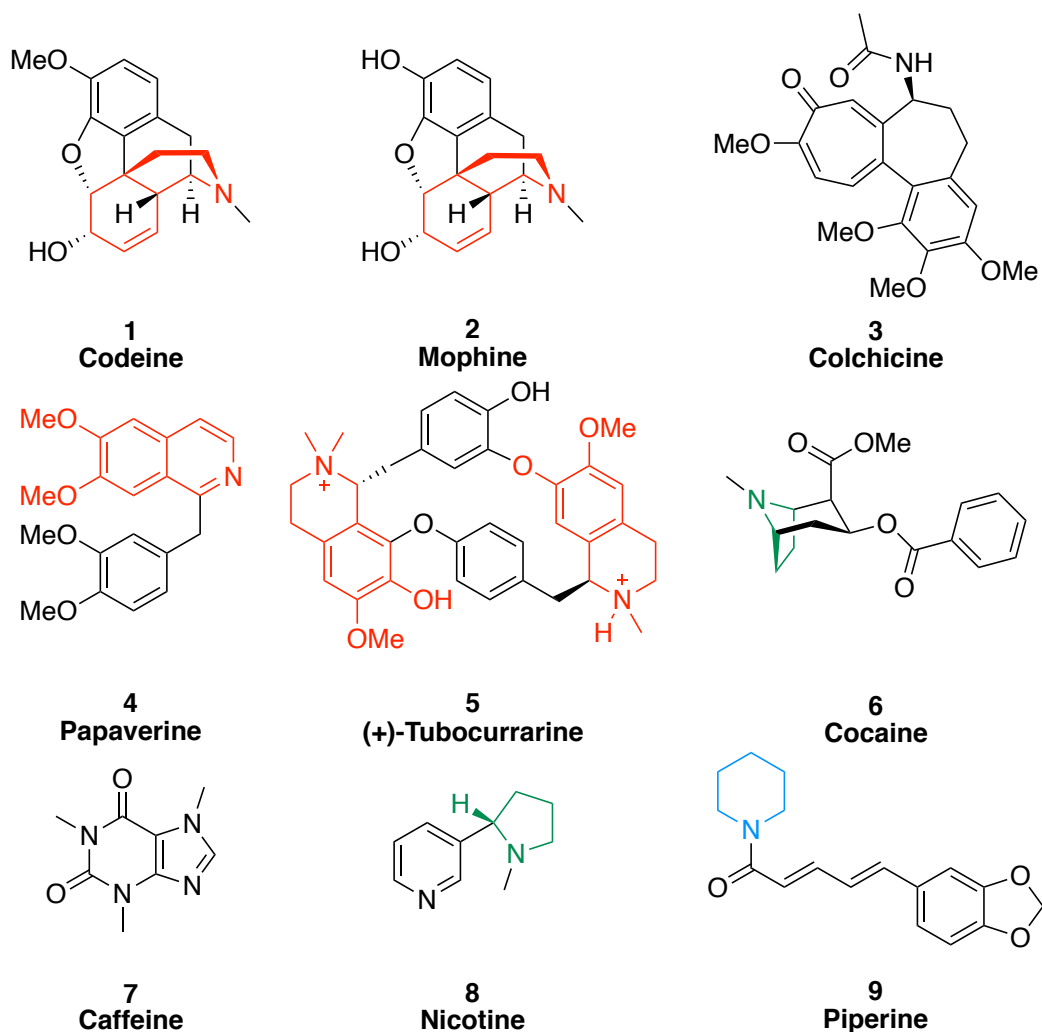


Figure 1: A range of well-known alkaloids that have been used for medicinal purposes as well as common household names, including codeine **1**, morphine **2**, colchicine **3**, papaverine **4**, (+)-tubocurarine **5**, cocaine **6**, caffeine **7**, nicotine **8**, piperine **9**. The sections highlighted denote the nitrogen-containing structure for which alkaloid is classified including, pyrrolidine (green), piperidine (blue), and isoquinoline (red).

Alkaloids are often classified by the nature of the nitrogen-containing structure in the molecule, including pyrrolidine (green), piperidine (blue), quinolone, isoquinolines (red) and more (**Figure 1**).¹³ This classification can then be further divided by the nitrogen-containing precursor that is used during the biosynthesis, principally consisting of ornithine **10**, lysine **13**, tyrosine **11**, tryptophan **14**, histidine, as well as nicotinic acid **12** (vitamin B₃) and anthranilic acid **15** (**Figure 2**).¹³

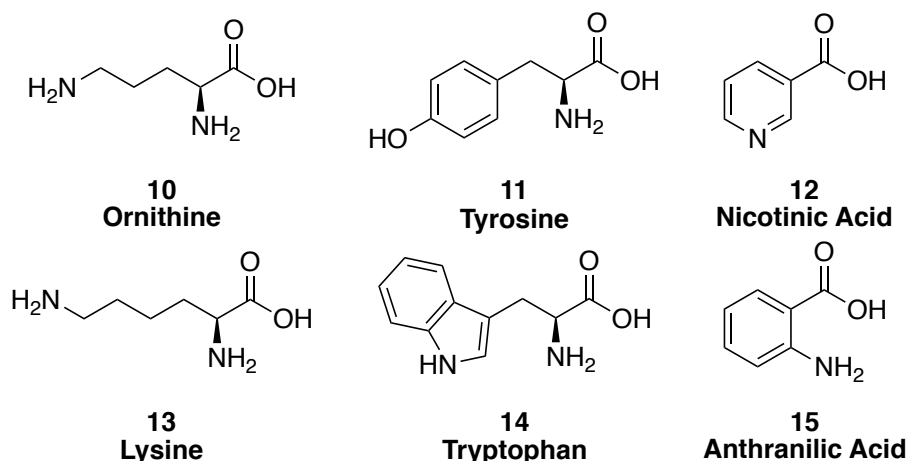


Figure 2: A range of nitrogen-containing precursors including the non-natural amino acid ornithine **10**, as well as the amino acids lysine **13**, tyrosine **11** and tryptophan **14**, as well as nicotinic acid **12** (vitamin B₃) and anthranilic acid **15**.

Furthermore, a separate class of alkaloids have been shown to acquire their nitrogen from a transamination reaction, functionalising either acetate or shikimate scaffolds. These molecules are therefore not derived from amino acids and not true alkaloids, so are known as pseudo-alkaloids. Their biosynthesis is further discussed in **Scheme 3** (page 6).¹³

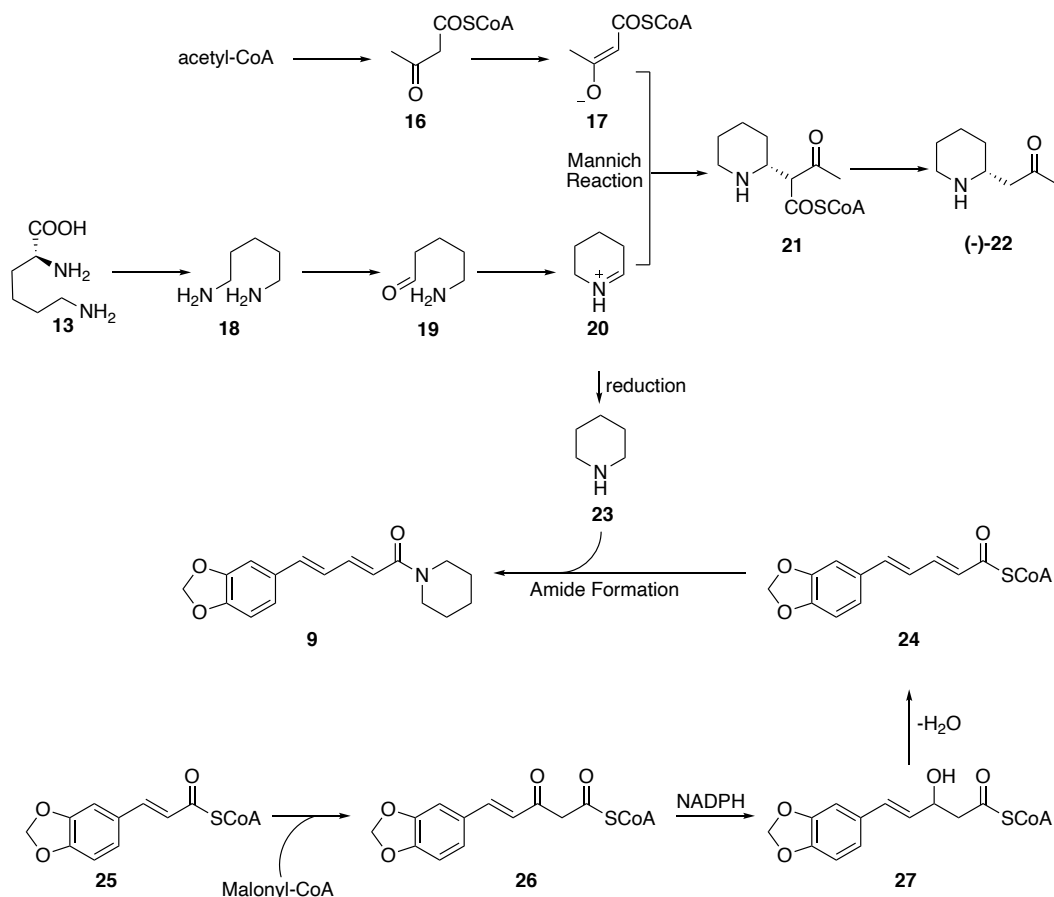
1.2 Synthesis of Alkaloids

1.2.1 Biosynthesis of Alkaloids

As a secondary metabolite, alkaloids are not directly involved in normal growth, development, or reproduction of the organism; however, they play an important defence role. Their production is linked to primary metabolites as they use the same building blocks and biosynthetic enzymes. The class of alkaloid depends upon and is defined by the biosynthetic route utilised.

The proposed biosynthesis of lysine-derived alkaloids such as piperine **9** and pelletierine **22**, involves the decarboxylation of the amino acid to form the diamine, cadaverine **18**,¹⁴ associated with the smell of decomposing flesh. An oxidative deamination *via* a diamine oxidase forms an aldehyde **19**, which spontaneously cyclises to form an imine (piperidinium **20**) (**Scheme 1**). At this point, the biosynthesis can be diversified by varying the

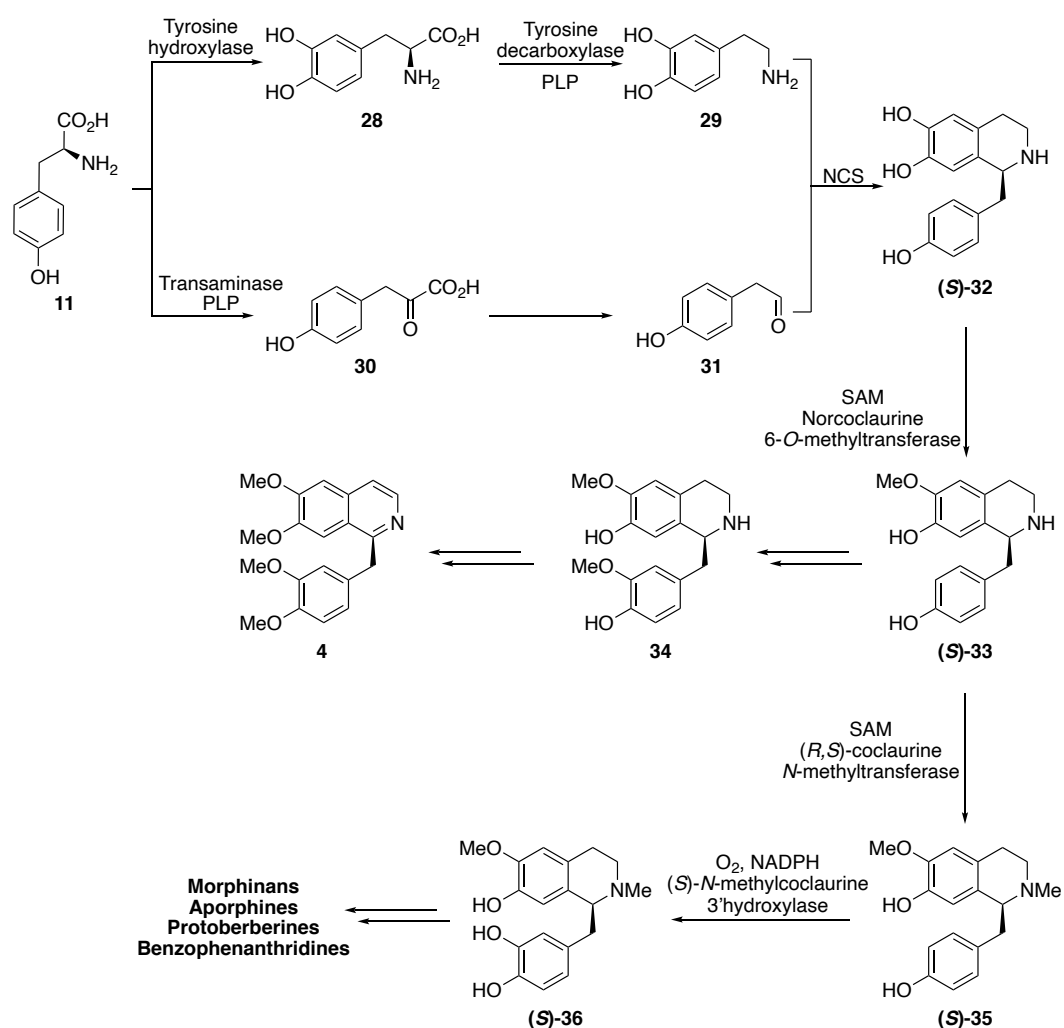
nucleophile that attacks during the Mannich reaction; in the case of **Scheme 1**, acetoacetyl-CoA **16** reacts with the imine **20** before undergoing a decarboxylation to produce (-)-pelletierine **(-)-22**.^{7,13,15}



Scheme 1: The biosynthesis of the lysine-derived alkaloids pelletierine (-)-22 and piperine 9. Both syntheses involve the common intermediate Δ^1 -piperidinium 20, which reacts with a nucleophile or is reduced before reacting further.¹³

The biosynthesis shown in **Scheme 1** can also be further diversified by the reduction of piperidinium **20** to piperidine **23**, which reacts in an amide coupling with piperoyl-CoA **24** forming the alkaloid piperine **9**, which is the compound responsible for the pungency of black pepper.^{13,15}

Another class of these alkaloids are tetrahydroisoquinolines (THIQ), which originate from tyrosine **11** (Tyr), and their biosynthesis is shown below in **Scheme 2**.

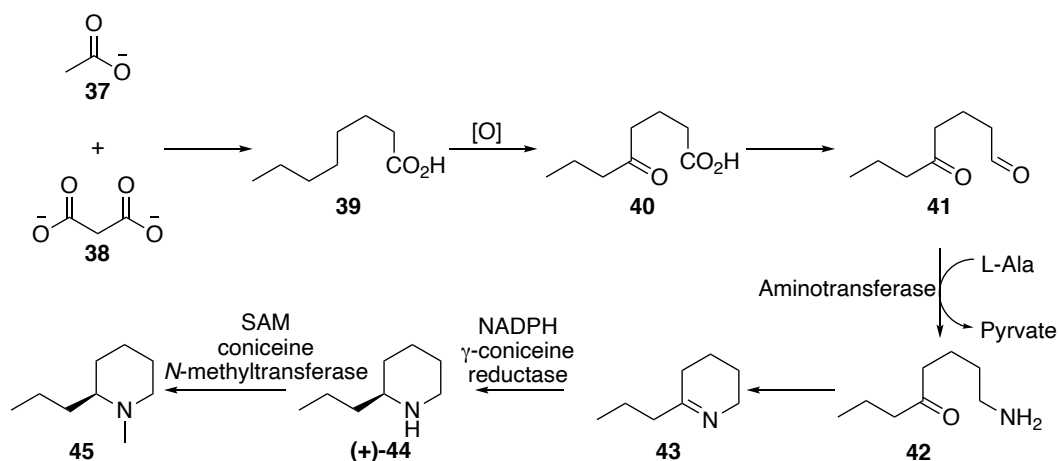


Scheme 2: The biosynthesis of a range of THIQs, including papaverine **4**, norcoclaurine **(S)-32** from two tyrosine **11** precursors, leading to a number of complex biologically active molecules, including a range of fused ring molecules, benzophenanthridines and morphinans.¹³

During the biosynthesis shown above in **Scheme 2**, two tyrosine molecules are used; where one is converted into dopamine **29** via L-DOPA **28**, while the other tyrosine molecule **11** is converted to 4-hydroxyphenylacetaldehyde **31** via reaction with a transaminase (TA) and subsequent decarboxylation. These two products then undergo a Pictet-Spengler type reaction, mediated by the enzyme norcoclaurine synthase (NCS), to provide the THIQ (S)-norcoclaurine **(S)-32**, where a selective methyl transferase methylates the catechol to produce (S)-coclaurine **(S)-33**.¹³ The impressive aspect of this biosynthesis is the ability of different enzymes to modify the THIQ at distinctive positions, allowing access to a wide variety of biologically active

molecules, including morphinans, as well as tetracyclic scaffolds such as aporphine and protoberines.¹³

The term ‘pseudo-alkaloid’ is used to distinguish the alkaloids that are synthesised primarily from non-amino acid precursors, where the nitrogen atom is inserted at a later stage. The nitrogen atom is donated from an amino acid source *via* reaction with an aminotransferase. The structures of ‘pseudo-alkaloids’ are often based on terpenoid and steroidal skeletons, and an example of the biosynthesis of a ‘pseudo-alkaloid’ is shown in **Scheme 3**.¹⁶



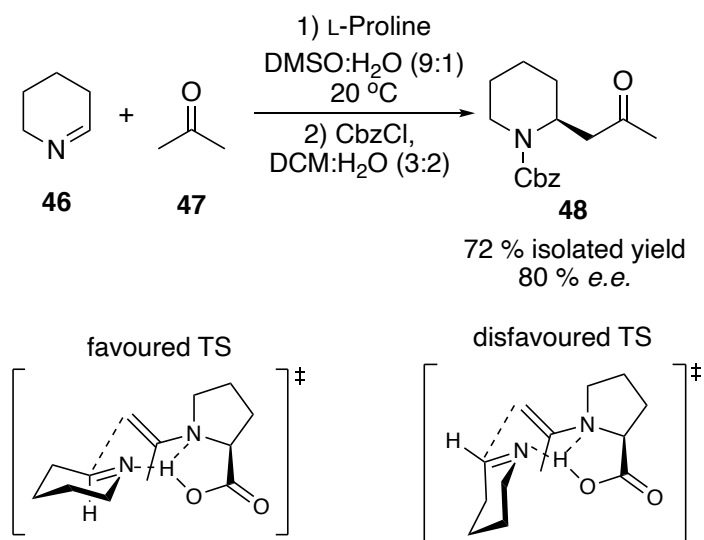
*Scheme 3: The biosynthesis of coniine 44, from the fatty acid precursor octanoic acid 39. The key step utilises an aminotransferase to introduce the amine functionality into the molecule providing the pseudo-alkaloid.*¹⁶

While appearing closely related to lysine-derived compounds such as pelletierine **22**, the hemlock poisons γ -coniceine **43** and coniine **44** have been shown to derive from the fatty acid precursor octanoic acid **39**.¹⁶ Through successive oxidative and reduction steps, the octanoic acid **39** is transformed into 5-oxo-octanal **40**, a substrate for a transamination reaction with the amine group donated from L-alanine, which can then cyclise to form the imine, γ -coniceine **43**. The imine bond of γ -coniceine **43**, is then selectively reduced before being methylated to form *N*-methylconiine **45**.¹⁶

1.2.2 Chemical Synthesis of Alkaloids

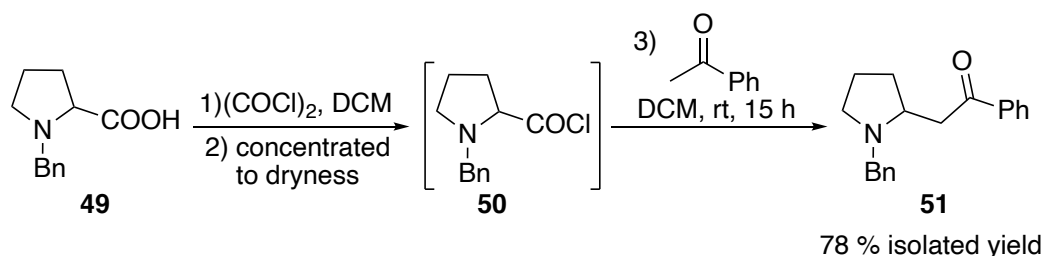
In 2019, 85 % of approved FDA small molecule drugs contained a nitrogen heterocycle, showing the supremacy of these scaffolds when it comes to developing drugs.¹⁷ While the pharmaceutical industry is still using natural products as their inspiration for certain drug molecules, it does entail certain difficulties. Though these products are naturally occurring, extracting them from their natural source is often difficult and expensive, due to their low abundance (between 0.1-2 % dry weight),¹⁰ and therefore the development of sustainable synthetic routes is highly desirable. However the synthetic approach to these alkaloids is often hampered by the limited scope of enantio-controlled reactions.¹⁸

The Mannich reaction proves to be a key step in both the biosynthesis and asymmetric synthesis of alkaloids, but the chemical Mannich reaction often requires a chiral organo- or metal catalyst to be enantioselective.¹⁸ The Mannich reaction has a multitude of applications in organic synthesis, and is particularly of interest due to its utilisation in the development of synthetic amine-containing building blocks and precursors. They have recently been used in the synthesis of protected piperidine type alkaloids **41** (Scheme 4).^{19,20}



Scheme 4: The synthesis of the piperidine type alkaloid, pelletierine via a Mannich reaction. Proline is utilised as an organo-catalyst, showing the potential transition states the reaction can take.¹⁹

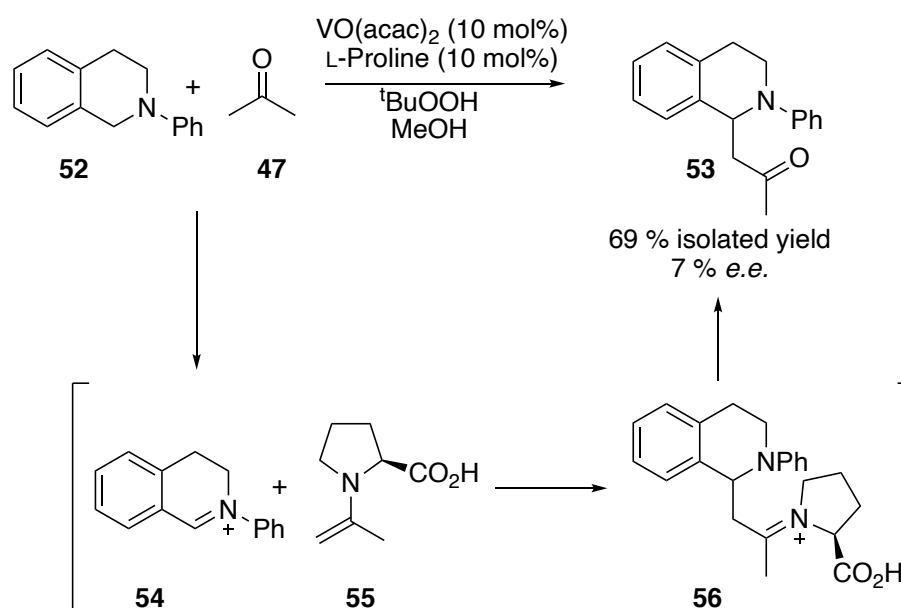
There are multiple examples of proline being used as an organocatalyst in a polar solvent system to ensure the proline remains soluble. Zaidan *et al.* predicted the stereoselectivity of this reaction (**Scheme 4**) would be high due to the use of a chiral organocatalyst, however the reaction *e.e.* was disappointing (80 %). The hypothesis for this lower *e.e.* is that β -keto amines are able to undergo isomerisation *via* a *retro*-Mannich or a *retro*-Michael reaction, before being trapped by Cbz-protection.¹⁹ Protected proline **49** has also been used as a precursor in the synthesis of pyrrolidine scaffolds, found in many natural alkaloids (**Scheme 5**).



Scheme 5: A decarboxylative Mannich reaction via the formation of an acid chloride reported by Shih *et al.*²¹

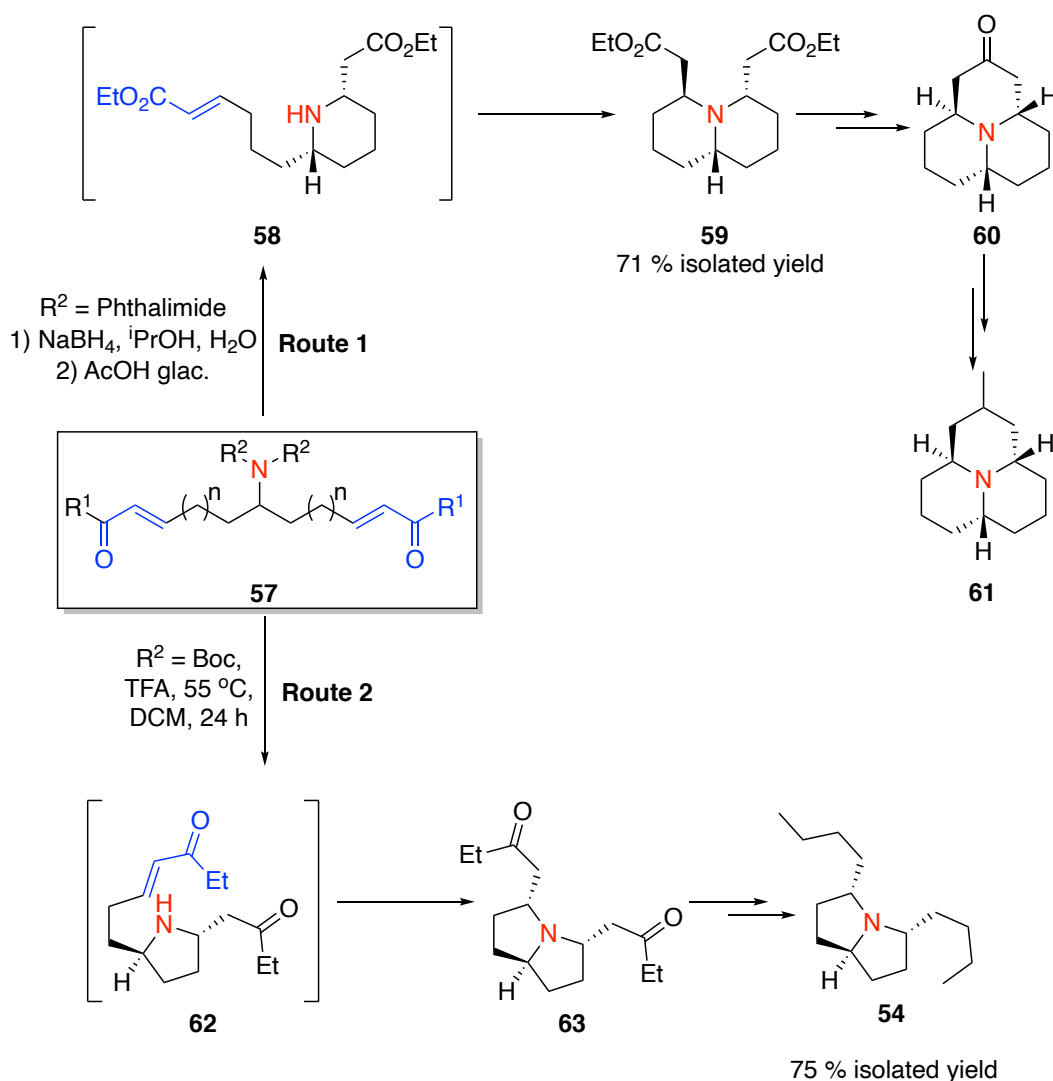
A recent report by Shih *et al.* involved decarboxylative Mannich reactions, during which the protected proline is converted to the corresponding acid chloride **50**. This acid chloride then undergoes C-C bond formation with a methylketone, followed by a spontaneous decarbonylation providing access to protected pyrrolidine alkaloids **51** (**Scheme 5**), however the main drawback for this methodology is the lack of enantioselectivity.²¹

The Mannich reaction requires an electrophilic imine, which is often formed *in situ* by a condensation reaction between the amine and aldehyde in the reaction mixture, before the attack by the activated ketone. Sud *et al.* formed the imine *in situ* from oxidation of a tertiary amine in conjunction with the activation of the organocatalyst by the methyl ketone in the form of a nucleophilic enamine intermediate **54** (**Scheme 6**). Despite the use of L-proline, Sud *et al.* believed that racemisation of **53** under the reaction conditions lead to a poor enantiomeric excess of 7 %.²²



Scheme 6: The production of a THIQ via a Mannich reaction reported by Sud et al.²² A vanadium catalyst oxidises the amine to an imine followed by the attack of a ketone.

There has been extensive research into the utilisation of intramolecular aza-Michael reactions to produce alkaloids starting from a simple scaffold.²³ Key examples of this are the synthesis of natural products hippodiamine^{24,25} **61**, pyrrolizidine *cis*-223B²⁶ **64** (Scheme 7), (±)-perhydrohistrionicotoxin²⁷ and DL-Histrionicotoxin.²⁸



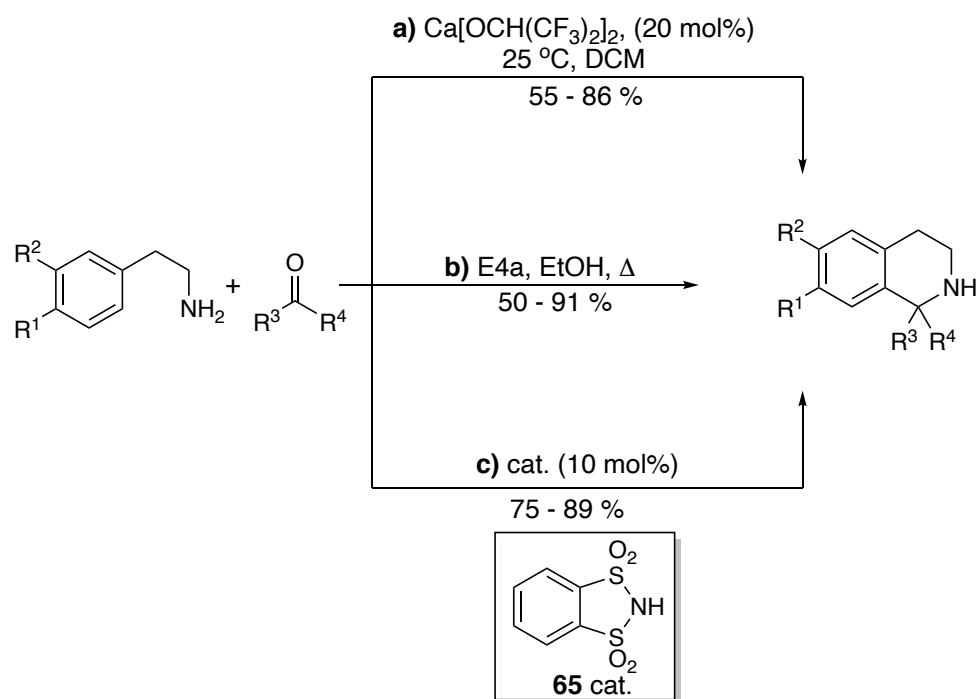
Scheme 7: The synthetic route to natural products *cis*-223B **64** and hippodiamine **61** via intramolecular aza-Michael reactions, demonstrated by Rejzek et al.²⁴ and Legeay et al.²⁶ Both routes entail multiple steps and numerous by-products, reducing the efficiency and sustainability of reactions.

Depending on the nature of the protecting group that is used during the synthesis of the amine, the Boc-protecting group is removed *via* either the acidic, TFA conditions (**Route 2, Scheme 7**) or the phthalimide group is removed by reduction (**Route 1, Scheme 7**). If not already under acidic conditions (**Route 1, Scheme 7**), glacial acetic acid was added to promote the double aza-Michael reaction to lead to the hippodiamine intermediate **59**. While the disubstituted pyrrolizidine (**Route 2, Scheme 7**) is formed in the *cis* conformation **63**, the disubstituted quinolizidines formed selectively in the *trans* conformation **59**, which is believed to be due to the

thermodynamic properties of the products. The larger angle between the side-chains in pyrrolizidine allows for the *cis*-arrangement **63** to be the lowest energy state, whereas the steric properties of the quinolizidine derivative means that the *trans*-arrangement **59** has the lowest energy.^{24–26}

Pictet and Spengler developed their namesake reaction in 1911; by reflux of β -phenylethylamine and formaldehyde dimethylacetal with hydrochloric acid.²⁹ The two compounds undergo a cyclic addition to form the alkaloid compound 1,2,3,4-tetrahydroisoquinoline (THIQ). These privileged scaffolds are key building blocks in many alkaloids and structurally complex synthetic products; several of them having physiological and therapeutic significance.

Extensive research has been performed on the Pictet-Spengler reaction using various catalysts and reaction conditions, dating back to 1911.^{30–33} These reactions often require harsh reaction conditions such as high temperatures under highly acidic catalytic conditions, which are incompatible with many aldehydes and amines causing them to degrade.^{34–36} Vanden Eynden *et al.* found an inorganic catalyst such as calcium hexafluoroisopropoxide was very effective with not only aldehydes, but also inactivated ketones in milder reaction conditions than traditional methods (**Scheme 8a**). The calcium catalyst is able to co-ordinate to the imine nitrogen activating the imine towards nucleophilic attack and hence stabilising the carbocation created forming a covalent nitrogen calcium bond.^{37,38}

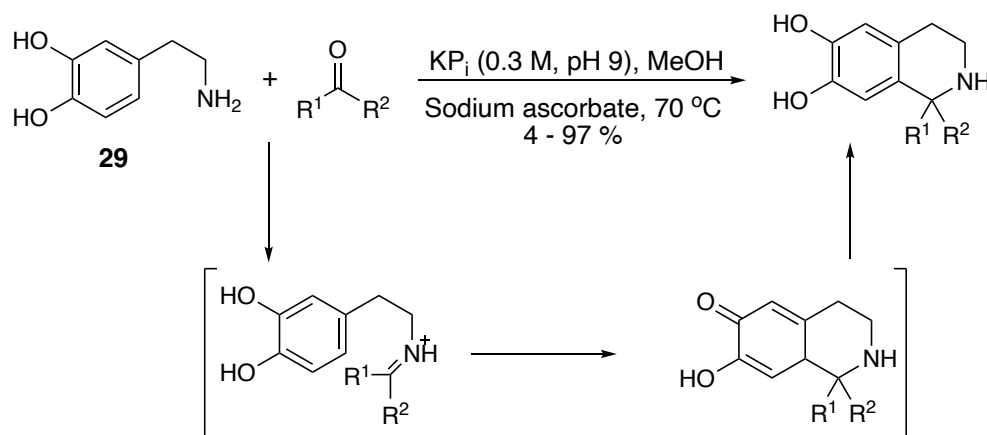


Scheme 8: Catalytic Pictet-Spengler reaction under different conditions: a) calcium complex catalysis via a Lewis acid type mechanism,^{37,38} b) An acidic zeolite-type catalyst allowing adsorption onto the surface,³⁹ c) a reusable Brønsted acid organocatalyst.⁴⁰

Hegedüs *et al.* managed to shorten the reaction time of the traditional conditions by exchanging the catalyst from either trifluoroacetic acid (TFA) or acetic acid (AcOH) to a zeolite catalyst, Ersorb-4, a weakly acidic zeolite-type adsorbent, which has shown good activity in different condensation reactions (**Scheme 8b**).³⁹ A reusable Brønsted acid organocatalyst, *o*-benzenedisulfonimide **65**, combined with mild and green conditions (**Scheme 8c**) was shown to produce THIQ with high yields.⁴⁰ Barbero *et al.* easily isolated the catalyst after the reaction by separation and evaporation of the aqueous layer, and the reused catalyst produced high yield (78 %), whereby the only caveat is that with each cycle the reaction time increased, due to gradual inactivation of the catalyst.⁴⁰

Since the discovery of Pictet-Spenglerases in 1977, there have been multiple groups working with this class of enzyme, as a replacement for the traditional chemical routes. Notably in 2011, Pesnot *et al.*⁴¹ found that when using potassium phosphate buffer (KPi) during the Pictet-Spenglerase reaction there was conversion in the negative control, which did not contain

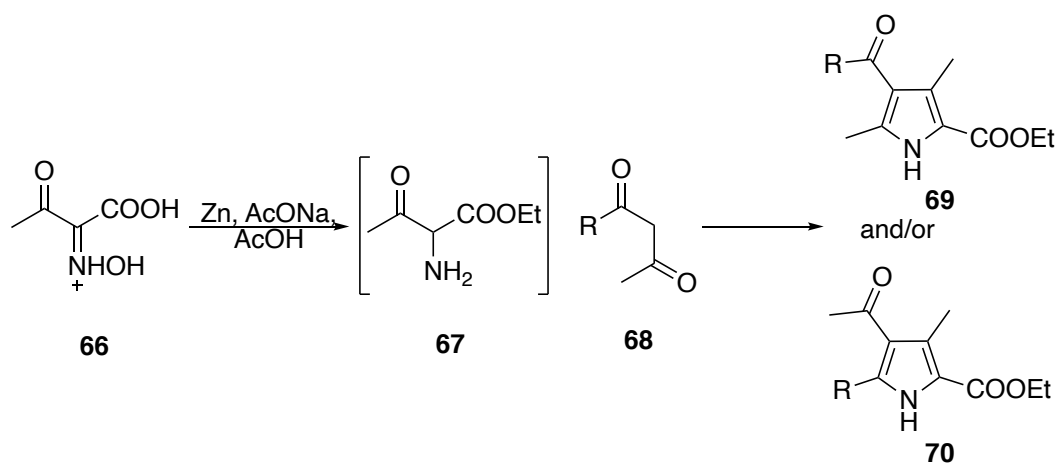
enzyme. It was deduced that the inorganic phosphate ions in the buffer catalysed a background Pictet-Spengler reaction (**Scheme 9**).^{41,42}



Scheme 9: An inorganic phosphate catalysed Pictet-Spengler reaction of dopamine coupling with an aldehyde discovered by Pesnot *et al.*⁴¹ and further expanded by Zhao *et al.*⁴² to include ketones.

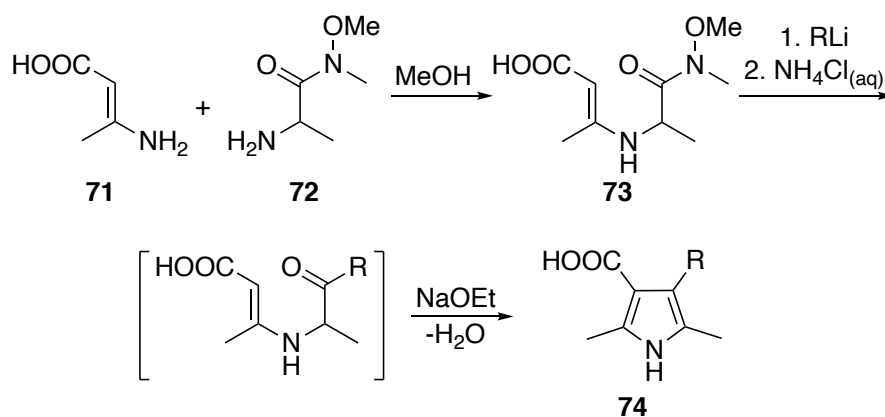
During the optimisation of these reactions, it was found that below pH 4, no product was obtained due to the protonation of the amine group of dopamine **29**, blocking its nucleophilicity. While under alkaline conditions, the dopamine **29** substrate was found to oxidise to a catechol, hence while investigating the Pictet-Spengler reaction at the higher pH 9, an antioxidant (sodium ascorbate) was added.⁴² Investigation into the Pictet-Spengler reaction with aldehydes gave high or moderate yields with a range of aldehydes, however Pesnot *et al.* found that the catalyst only worked when the *meta* position of the β -phenylethylamine was able to be deprotonated, which was aided by the phosphate ions. This therefore limited the substrate scope of this phosphate-catalysed Pictet-Spengler reaction to *meta*-substituted β -phenylethylamines, while proving that this methodology was suitable with a range of aldehydes and ketones.⁴¹

The synthesis of pyrrole derivatives by the condensation of α -amino ketones with a β -keto ester was initially reported by Knorr in 1884.⁴³ Due to α -amino ketones readily self-condensing, they are often generated *in situ*, either from oximes or hydrazones in the presence of zinc dust, NaOAc and AcOH (**Scheme 10**).⁴⁴



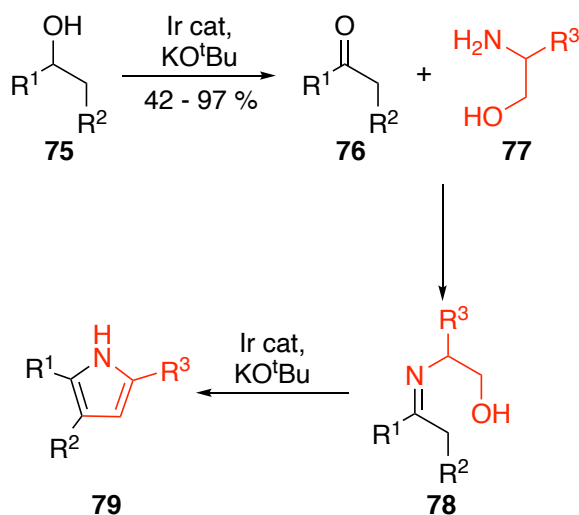
Scheme 10: The synthesis of α -amino ketones in situ from a hydrazine using zinc dust, before the condensation with the β -keto ester in a Knorr pyrrole synthesis, potentially producing two isomers.⁴⁴

However, there is often an issue with regioselectivity, as shown above, where there are two resultant pyrrole compounds formed **69** and **70**. This is often overcome by using more sterically hindered β -ketoesters and α -amino ketones. An alternative method utilises Weinreb α -aminoamides **72** as these have been shown as useful reagents, which have the advantage of not being able to self-condense. The Weinreb α -aminoamide **72** is reacted with the appropriate enaminone **71** and the resultant compound **73** is then reacted with an organometallic compound to produce a carbonyl intermediate, which then undergoes cyclisation to give the pyrrole derivative **74**, shown in **Scheme 11**.^{45,46}



Scheme 11: The reaction between an enaminone and Weinreb amide interaction reacted with the appropriate organolithium compound; during workup, this readily cyclises to form product **74**, as reported by Alberola et al.⁴⁶

Michlik *et al.* took inspiration from the borrowing hydrogen cycle in the synthesis of pyrroles, by using a novel catalyst for the alkylation of amines and novel C-C coupling reactions (**Scheme 12**).⁴⁷



Scheme 12: A borrowing hydrogen inspired iridium catalysed pyrrole synthesis reported by Michlik *et al.*⁴⁷ The first step involves oxidation of the secondary alcohol via liberation of hydrogen followed by an imine formation; step 3 then involves the intramolecular C-C coupling via the loss of hydrogen and water.

In this case, the secondary alcohol **75** is oxidised to give the corresponding ketone **76**, which reacts with the amino alcohol **77** to form an imine **78**. The ring closure can occur *via* an iridium-catalysed amino alcohol dehydrogenation and condensation reaction.⁴⁷ This methodology produced a range of highly substituted pyrroles *via* a series of selective consecutive C-C and C-N bond formations. While this methodology takes inspiration from hydrogen borrowing cycles, it does not come under the classification due to the reaction not recycling the hydrogen originally removed in the initial step.

Synthetic routes for the preparation of these natural products are often long, complex and low yielding, with a lot of wasteful by-products generated, and this reduces the sustainable nature of these reactions. The major challenge in these synthetic approaches is the installation of chiral centres on a large scale, as this often requires an expensive metal catalyst.⁴⁸ These

challenges show that there is a need for the development of new synthetic methodology to access a more diverse set of alkaloids in a cleaner, greener way, which require less synthetic steps with an increased yield and selectivity.

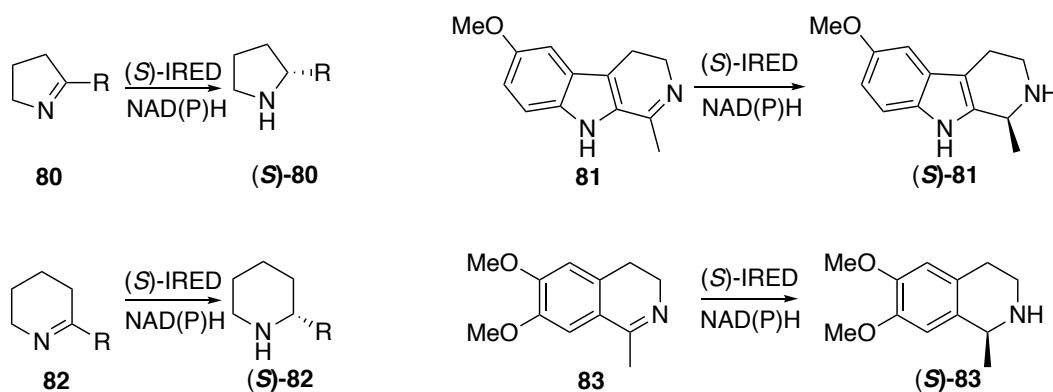
1.2.3 Biocatalytic Synthesis of Alkaloid Scaffolds

Nature is capable of constructing an incredible variety of complex, optically pure natural products containing multiple stereocentres, originating from a very limited set of building blocks. It does so by employing enzymes to build molecular complexity with excellent regio and stereoselectivity. Chemists have long been inspired by nature and have developed synthetic routes and catalysts that attempt to mimic natural biosynthetic pathways.⁴⁹ When undertaking the synthesis of a natural product, organic chemists begin the process by retrosynthesis of the product, using a tool box of known chemical reactions that they have been taught. However, there is now a useful toolbox of biocatalysts available to complement traditional chemical catalysis and these can now be considered alongside other approaches.⁵⁰

There is a growing pressure to follow more sustainable practices, and many industries are now interested in adopting traditional approaches in order to maximise atom economy, reduce the use of solvents and cut out costly purification steps or protecting group manipulations, therefore biocatalysis is becoming increasingly more important.^{51,52} Nature has developed a number of different catalytic methods for the synthesis of chiral amines, including imine reductases (IREDs), monoamine oxidases (MOAs), amine dehydrogenases (AmDH), ammonia lyases, reductive amidases (RedAm) and transaminases (TA). Many of these enzymes have been used in the synthesis of alkaloid scaffolds and drug-based molecules, examples of which will be discussed below.⁵³

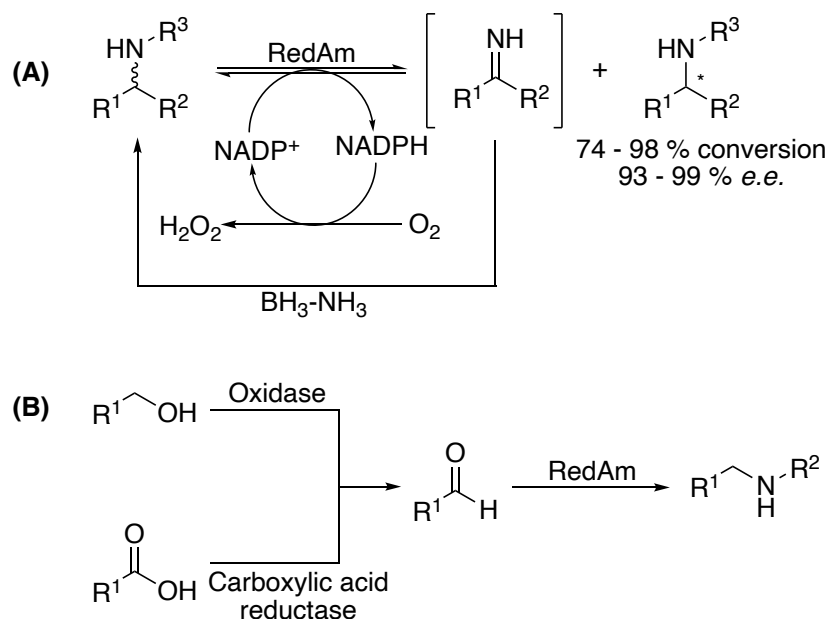
Imine reductases (IREDs) selectively reduce an imine bond using NAD(P)H as the hydride source. Limited attention has been paid to this class of enzymes due to lack of known biocatalysts. IREDs that have been

discovered have low activity and a narrow substrate range, meaning that they are not ideal candidates for chemical synthesis. A number of reports have overcome these issues to produce different classes of alkaloids via a selective reduction of an imine, as shown in **Scheme 13**.^{7,54}



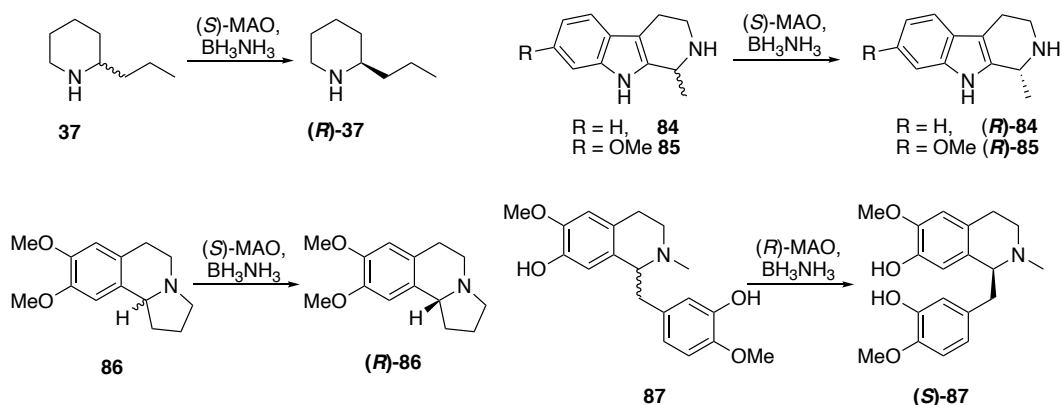
Scheme 13: A range of alkaloid derivatives synthesised via the selective reduction of the precursor imine, using a IRED as the biocatalyst and NAD(P)H as a cofactor.^{7,54}

Aleku *et al.* discovered a subfamily of IREDs that showed remarkable activity towards catalysing reductive amination, hence the name reductive amidase (RedAm).⁵⁵ They went on to report the use of this class of enzyme to deracemise an array of amines with reasonable conversion and high enantioselectivities (**Scheme 14A**).⁵⁶ Ramsdem *et al.* further exploited RedAms in a cascade reaction with an oxidase or a carboxylic acid reductase to produce amines from alcohols or carboxylic acid respectively (**Scheme 14B**).⁵⁷



Scheme 14: A) deracemisation of an array of amines by Aleku *et al.*⁵⁶ (B) The use of a RedAm as part of a cascade reaction with an oxidase or carboxylic acid reductase to produce chiral amines from compounds derived from a suitable renewable feedstock.⁵⁷

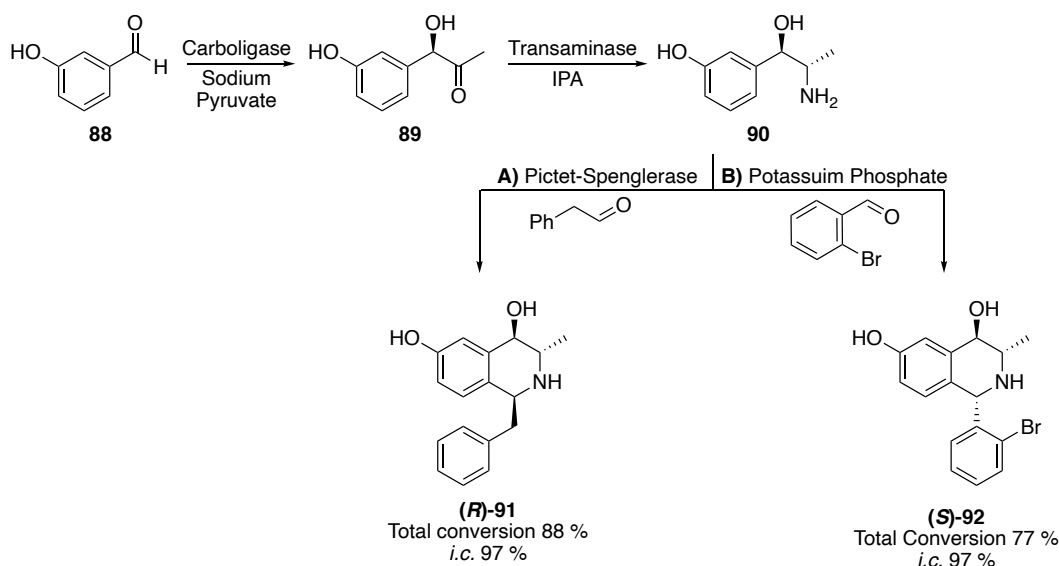
Leipold *et al.* developed the use of a whole-cell biocatalytic system to produce a range of enantiopure piperidine-, pyrrolidine-, THIQ- and indole-based alkaloid scaffolds. The whole-cell system consisted of resting *E. coli* cells with the addition of glucose to enable *in situ* co-factor recycling. This recycling system enables the expensive NADPH to be regenerated during the reaction and thus reducing the need for stoichiometric equivalents.⁵⁴ Similar enantiopure alkaloid scaffolds have been produced *via* deracemisation of the racemic amines using a MAO in conjunction with ammonia borane, as shown in **Scheme 15**.⁵⁸⁻⁶⁰



Scheme 15: Range of enantiopure alkaloids including (*R*)-coniine (**R**-37),⁵⁸ (*R*)-eleagine (**R**-84),⁵⁸ (*R*)-leptaflorin (**R**-85),⁵⁸ (*R*)-crispine A (**R**-86)⁶⁰ and (*S*)-rericuline (**S**-87)⁶⁹ produced via a deracemisation cascade using ammonia borane as the reductant and MAO to catalyse the oxidation.

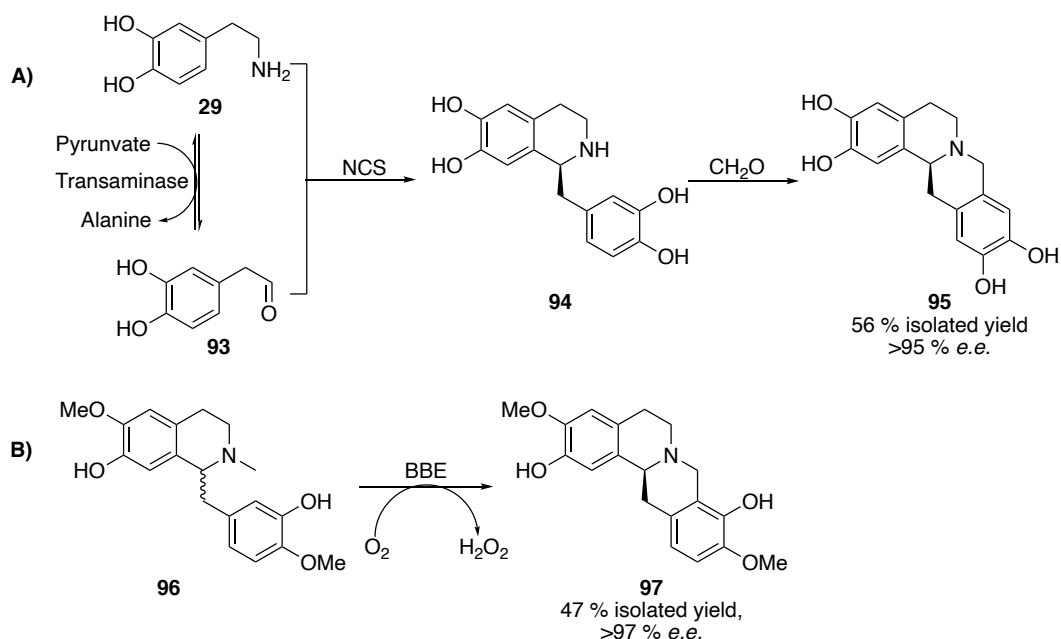
The deracemisation demonstrated in **Scheme 15** proceeded with the selective oxidation of a single enantiomer catalysed by the MAO, which is then followed by the non-selective reduction by ammonia borane. The oxidation-reduction cycle continues leading to the accumulation of one enantiomer, due to the selectivity associated with the selective MAO.^{58–60}

Enzyme mining, along with increased knowledge of biosynthetic pathways has allowed for the discovery of many new classes of enzymes, including Pictet-Spenglerases in 1977. Since then, there have been multiple groups working with this class of enzyme as a replacement for the traditionally harsh chemical routes to THIQ, including approaches employing a Pictet-Spengler reaction as discussed in **1.2.2 Chemical Synthesis of Alkaloids**. Erdman *et al.* reported a three-step (chemo)enzymatic cascade for the stereoselective formation of tri-substituted THIQs as shown in **Scheme 16**.⁶¹



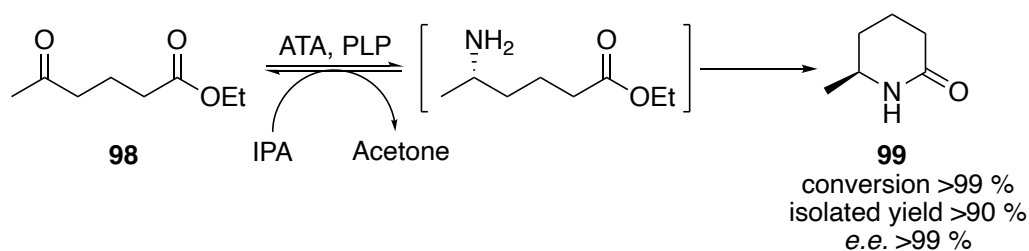
Scheme 16: The three step chemo-enzymatic cascade as reported by Erdman *et al.* to produce the enantiopure trisubstituted THIQs; by employing two different methodologies both enantiomers can be accessed. Route A uses Pictet-Spenglerase to set the stereochemistry, where in route B the Pictet-Spengler reaction is catalysed by inorganic phosphate and the stereochemistry is being set by sterics.⁶¹ $Isomeric\ content = i.c. (\%) = (1/\sum I_i) * 100$

The two diastereomers were accessed *via* a Pictet-Spenglerase or an inorganic phosphate (P_i) catalysed Pictet-Spengler reaction (**Scheme 16**). The Pictet-Spenglerase selectively forms the (*R*)-enantiomer **(R)-91**. However, in the case of the P_i -catalysed reaction, the position of the bromide group on the ring interacts with the hydroxyl group, leading to a steric clash, forcing the formation of exclusively the (*S*)-enantiomer **(S)-92**. Further to this, Lichman *et al.* designed a triangular chemo-enzymatic cascade to synthesise tetrahydroprotoberberine (THPB) alkaloids *via* a THIQ intermediate.⁶² This triangular cascade involves the use of a transaminase, followed by an enzyme catalysed Pictet-Spengler reaction, where formaldehyde was then added which triggered a second Pictet-Spengler Reaction closing the fourth ring in the THPB **95** (**Scheme 17A**). Berberine bridge enzymes (BBE) have also been used in the synthesis of THPBs, including (*S*)-Scoulerine **97**, in a C-C bond formation step (**Scheme 17B**).⁶³



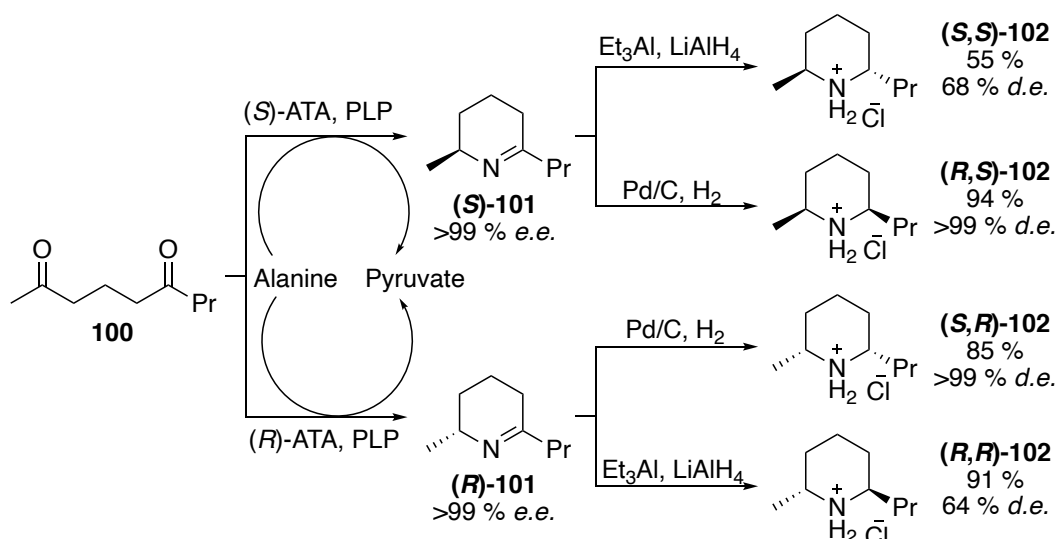
Scheme 17: A) Lichman *et al.* triangular cascade, where dopamine **29** is converted into DOPAL **93** before both are reacted in a Pictet-Spengler reaction catalysed by a NCS. The resulting THIQ **94** reacted further with formaldehyde to form tetrahydroprotoberberine (THPB) **95**.⁶² B) Schrittwieser *et al.* synthesis of THPB **97** via a Berberine bridge enzyme (BBE).⁶³

The key step in the biosynthesis of piperidine and pyrrolidine-based alkaloids is the Schiff base formation of Δ^1 -piperideine **23** and *N*-methylpyrrolinium (**Scheme 1**), which then are able to undergo a Mannich reactions, among other transformations producing a diverse range of alkaloids. Inspired by this methodology, ω -transaminases (ω -TAs) have been used to transform diketones or ketoaldehydes to their corresponding amine before a spontaneous cyclisation takes place in a linear cascade. ω -TAs convert a pro-chiral ketone to a chiral amine using a sacrificial amine donor, a sub-class of these enzymes, amine transaminases (ATA), have been explored by a number of groups due to not requiring a distal carboxyl group. More detail on this class of enzyme is given later in **1.3 Transaminases (TA)**. One of the first examples of this was reported by Truppo *et al.*, where ethyl 4-acetylbutyrate **98** was transaminated and spontaneously cyclised to form a lactam **99**. The reaction was performed on a high substrate concentration (50 g L⁻¹) with excellent conversion and stereocontrol (**Scheme 18**).⁶⁴ This methodology was then applied to the synthesis of a dual orexin receptor antagonist on a kilogram scale.⁶⁵



Scheme 18: The conversion of ethyl 4-acetylbutyrate **98** to the corresponding amine followed by the spontaneous cyclisation to form a lactam **99**.⁶⁵

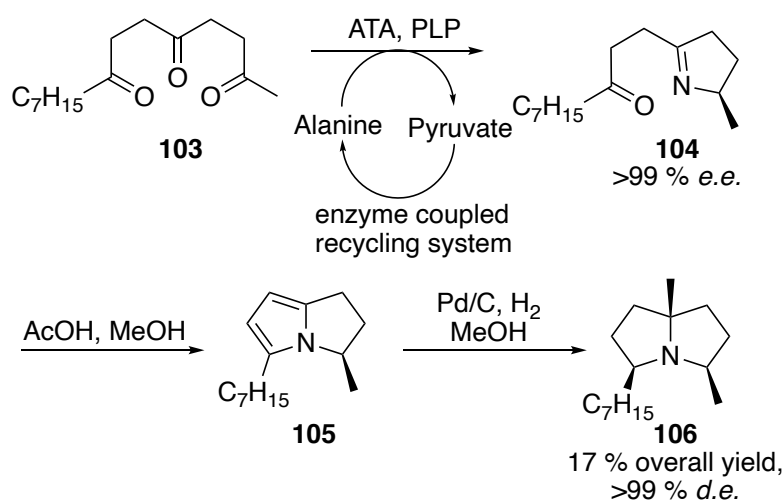
Simon *et al.* completed a further variation of the above methodology to access 2,6-disubstituted piperidines (**Scheme 19**).⁶⁶



Scheme 19: Conversion of a diketone **100** to the corresponding chiral amine, which cyclises to form imine **101**, before selective chemical reduction to produce both the *syn*- and *anti*-diastereomers.⁶⁶

The least sterically hindered ketone was selectively aminated to the corresponding amine, before spontaneous cyclisation to form the chiral imine **101**. The imine formed was selectively reduced forming the *syn*- and *anti*-enantiomers **102**, therefore giving access to all four diastereomers with high diastereomer excess (*d.e.*) and high yields (55 – 94 %).⁶⁷

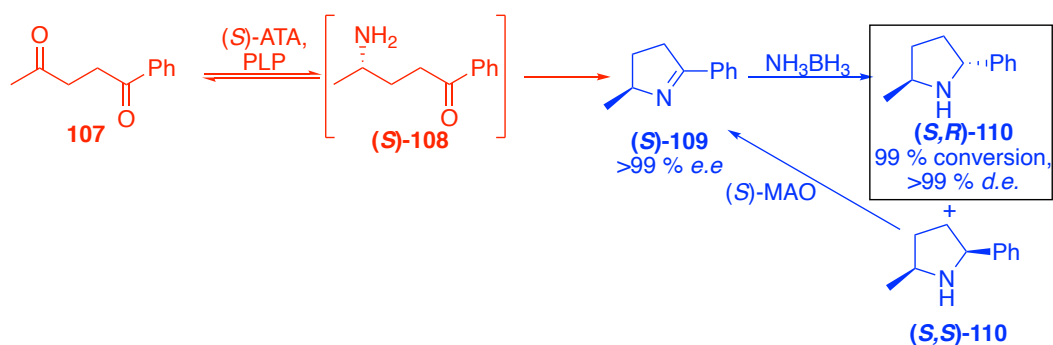
Furthermore, this cascade methodology has been used to synthesise both enantiomers of xenovenine **106** from a triketone **103** in a chemoenzymatic synthesis (**Scheme 20**).⁶⁸



Scheme 20: The chemoenzymatic synthesis of (+)-xenovenine **106** developed by Payer *et al.*,⁶⁸ starting with the selective transamination of triketone **103**, triggering the formation of imine **104**. This then undergoes two chemical steps, including a selective reduction, to form final product (+)-xenovenine **106**.

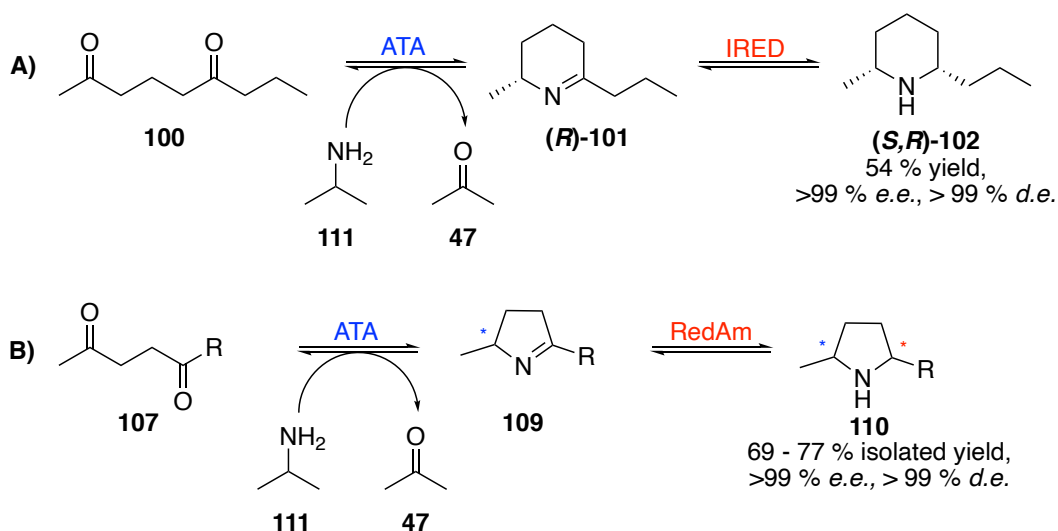
The methyl ketone **103** is selectively aminated by the ATA, to form cyclic imine **104**. Acetic acid then catalyses an aromatisation to form **105** before being selectively reduced to give the desired (5*Z*,8*E*)-diastereomer **106** with high diastereomeric excess (>99 %). The regio and stereoselective amination of the single ketone moiety allowed for a short total synthesis of the bicyclic pyrrolizidine alkaloid xenovernine **106**.⁶⁸

O'Reilly *et al.* used a multienzyme chemoenzymatic cascade to produce highly enantioselective pyrrolidines (**Scheme 21**).⁶⁹



Scheme 21: O'Reilly *et al.*⁶⁹ developed a ATA-MAO chemoenzymatic cascade to produce a range of 2,5-disubstituted pyrrolidines **110**.

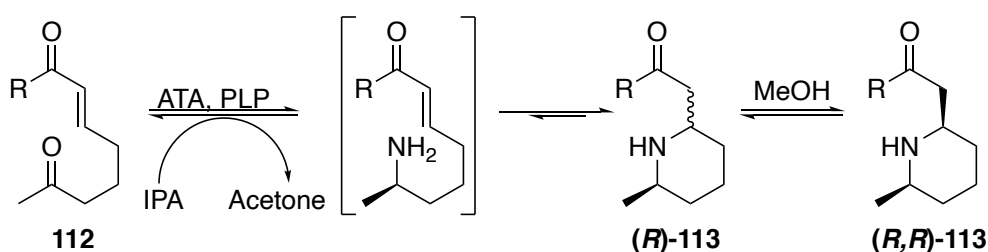
This reaction sequence takes advantage of the regio- and stereoselective nature of the TA to form the corresponding amine **108** from a prochiral diketone **107** in high *e.e.*. The cyclic imine (**S**)-**109** formed is then chemically reduced *in situ* forming both diastereomers **110**. The (*S*)-enantiomer (**S,S**)-**110** is the selectively reduced by the (*S*)-selective-MAO leaving the other diastereomer (**S,R**)-**110** to accumulate over a number of cycles, to provide (**S,R**)-**110**, > 99 % *d.e.* (**Scheme 21**).⁶⁹ The coupling of this linear and cyclic cascade ensures that the stereogenic centre established by the transaminase (TA) is not affected by the monoamine oxidase (MAO), and highlights the potential use of multienzyme cascades for the efficient synthesis of chiral building blocks. To expand on the methodology, France *et al.*⁷⁰ and Alvarenga *et al.*⁷¹ used a concurrent multienzyme cascade coupling the TA reaction with an IRED to reduce the imine biocatalytically (**Scheme 22A**). Furthermore, Costa *et al.* demonstrated the use of RedAm as the reducing catalyst in a one-pot cascade reaction to produce 2,5-disubstituted pyrrolidine scaffolds in reasonable *d.r.* (**Scheme 22B**).⁷²



Scheme 22: A) The concurrent multienzyme cascade reaction as reported by Alvarenga *et al.* for the production of (-)-dihydropinidine (**S,R**)-**102** from diketone **100** using a transaminase and an imine reductase.⁷¹ B) The multienzyme cascade using a transaminase and reductive amidase to produce 2,5-disubstituted pyrrolidine scaffolds **110**.⁷²

To access the key intermediate nonane-2,6-dione **100** (**Scheme 22A**), a pig liver esterase was cyclised by utilisation of a decarboxylation, which together provide a mild alternative to the Krapcho decarboxylation. Intermediate **100** underwent a selective transamination to form imine (**R**)-**101**, which is selectively reduced by IRED leaving the diketone **100** untouched under the reduction conditions. This cascade showcases the ability of enzymes to selectively complete transformations in the presence of other reactive groups without the need for protecting group strategies. In a similar manner, Alvarenga *et al.*⁷¹ used a RedAm to selectively reduce imine **109** without affecting the starting diketone **107**.

More recently, Ryan *et al.* synthesised 2,6-disubstituted piperidine **113** via the coupling of a transamination and an aza-Michael reaction in a cascade (**Scheme 23**).⁷³ This was followed by a key epimerisation step to give the more stable *cis* configuration of the 2,6-disubstituted piperidines **113**. While the previously reported synthetic methods using an amine transaminase (ATA) involve an enzyme cascade to either remove or recycle the co-product or the need for high equivalents of IPA (1.3.2 Limitations of ATAs), Ryan *et al.* reported the use of only 2 equivalents of IPA **111**. This is likely due to the aza-Michael cyclisation displacing the reaction equilibrium towards product formation, allowing high yields and excellence *e.e.* after an epimerisation step, to give the thermodynamically favoured *cis* product.⁷³



*Scheme 23: The synthesis of 2,6-disubstituted piperidines **113** from ketoenones **112**, with a key transaminase-initiated aza-Michael cascade followed by an epimerisation step, using methanol.⁷³*

This investigation exploited the selectivity of ATA, whereby employing a bulky R-group the ketone is selectively aminated over the enone carbonyl group allowing for the aza-Michael reaction to take place, leading to the

generation of two diastereomers. The diastereomers were then able to be epimerised *via* a retro-aza-Michael, aza-Michael reaction in methanol to produce piperidine scaffolds **113** in high *d.e.*.⁷³

1.3 Transaminases (TA)

PLP-dependent enzymes are widespread in cellular signalling and metabolic pathways, and are involved in the synthesis of numerous important biomolecules including amino compounds such as amino acids, and can also be seen in the degradation of amino sugars, polyamines and alkaloids.^{74–76} There are seven major classes of PLP-dependent enzymes, grouped by their fold type. TAs fall into two fold types: I and IV, corresponding to the enantioselectivity of the enzyme.^{77,78}

TAs have been further classified into six subgroups, based on their structural features and sequence similarities.⁷⁹ Furthermore TAs can be classed into either α -TA (subgroup I, II and IV) or ω -TA (subgroup III). α -TAs require the presence of a carboxylic group in the α -position to the carbonyl group undergoing transamination, thus are only capable of forming α -amino acids. ω -TAs are able to aminate carbonyl groups with a distal carboxylic group and have two subgroups, β -TA and amine transaminase (ATA). ATAs are able to convert substrates without a carboxylate group, due to the possibility of these enzymes being able to accept any ketone or aldehyde, with high enantio and regioselectivity. This has meant that they have gained high interest in the pharmaceutical industry.^{80,81}

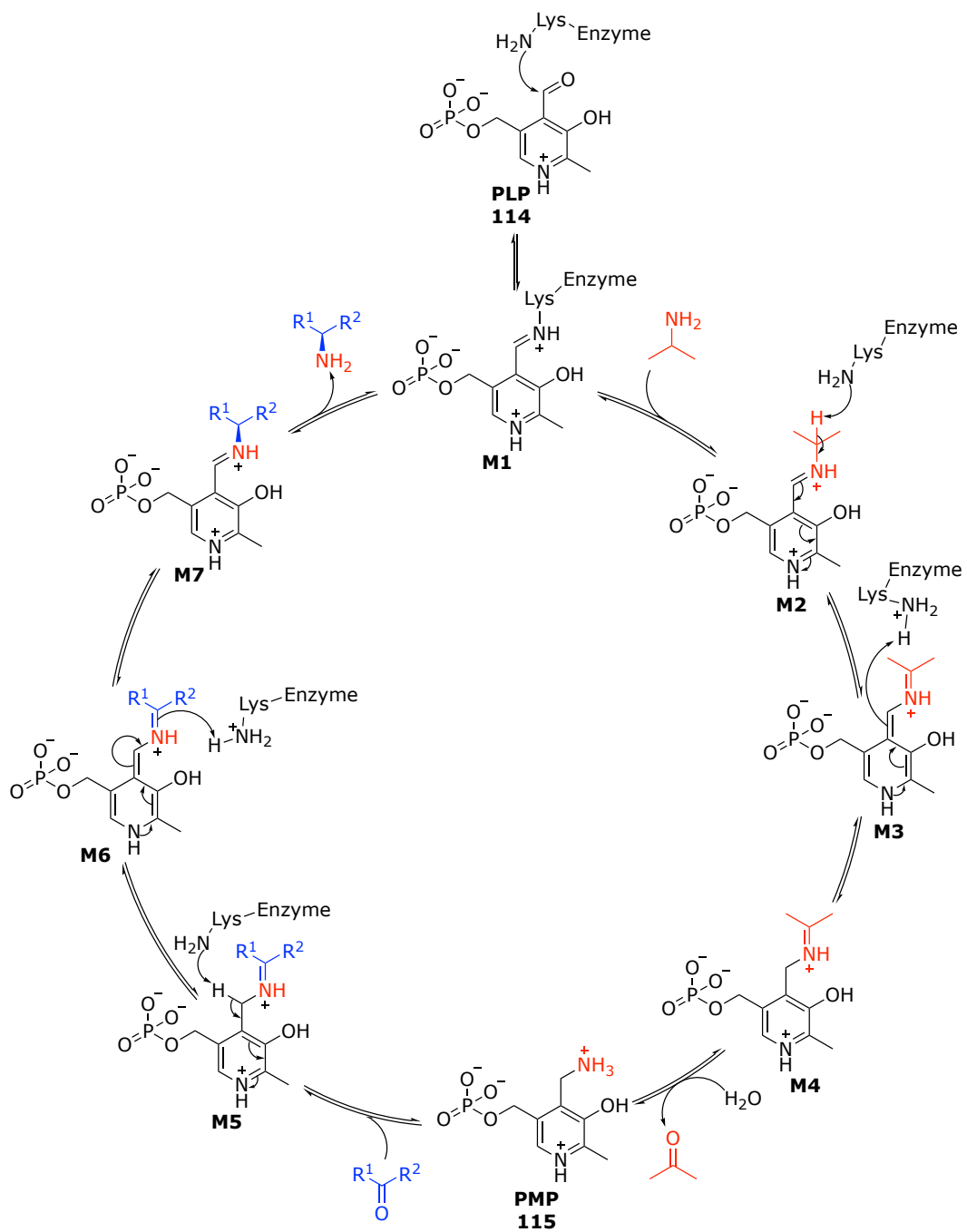
The quaternary protein structure of ATAs consists of a homodimer and the active site is situated on the interface of the monomers, with each unit contributing to the active site.⁸² The active site consists of two binding-pockets: a large pocket, allowing a diverse size distribution of substrates and a small pocket, limited to accepting substrates with a smaller substituent, such as a methyl group. This small binding pocket limits the substrate scope of ATAs, though attributes to the high stereo and regioselectivity of the enzyme.⁸³ For this reason, research has focused upon

engineering the small binding pocket to accept more demanding substrates. An example of this is the work by Pavlidis *et al.* where a successfully engineered (*S*)-selective transaminase from *Ruegeria sp.* TM1040 with four mutations was able to accept bulky ketone substrates. The ability to engineer the small binding pocket of ATAs opens the door to the possibility of using ATA to accept more challenging substrates, increasing the substrate scope for this class of enzymes, leading to a larger range of high value alkaloid products.⁸⁴

1.3.1 Mechanism of ATAs

The transaminase enzymes follow a ping-pong bi-bi mechanism. Where the catalytically active enzyme coordinates PLP **114** *via* hydrogen bonding to the phosphate group, a lysine residue in the active site is covalently bonded to the PLP **114**, forming the internal aldimine **M1**. A Schiff-base formation between the PLP **114** and amine substrate displaces the lysine residue, forming an external aldimine **M2** (**Scheme 24**).^{85,86}

The external aldimine **M2** has a lower energy barrier for the proton abstraction when compared to the free amine substrate, due to the electron sink properties of the PLP **114**. Dunathan's hypothesis means that the proton abstraction occurs in the plane perpendicular to the π -system of the aromatic ring. Water then attacks the ketimine **M4** leading to hydrolysis of the imine bond forming the ketone by-product and pyridoxamine-5'-phosphate (PMP **115**). At this point, the pro-chiral ketone is attacked by the PMP **115** before another planar quinonoid **M6** is formed, which is able to deprotonate the lysine residue in a selective manner. The lysine residue then displaces the imine **M7**, reforming the internal aldimine **M1** and the chiral amine.^{85,86}

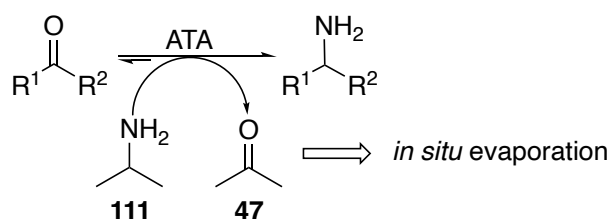


Scheme 24: The catalytic cycle of the transaminase enzyme, using PLP as the co-factor forming an internal aldimine with the lysine residue in the active site.

1.3.2 Limitations of ATAs

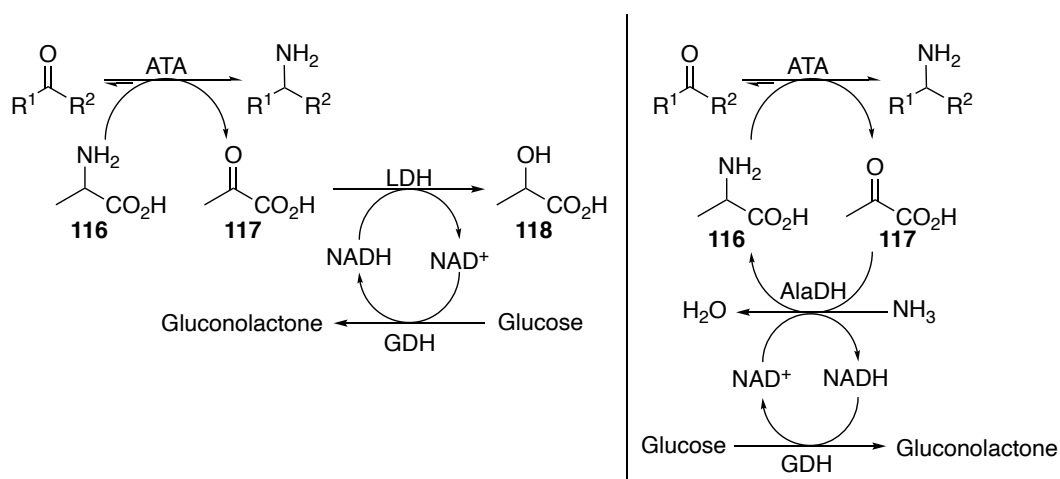
One of the key limitations of ATAs is the steric constraint of the active site with the small binding pocket discussed previously (1.3 Transaminases (TA)). When using ATAs in the asymmetric synthesis of chiral amines, the reaction is often thermodynamically limiting, there are several ways to drive the equilibrium, therefore increasing the conversion of these reactions, detailed below.

The main industrial technique is to use high equivalents of isopropylamine (IPA **111**), which produces acetone **47** as a volatile by-product and is removed *in situ* (**Scheme 25**). While this system uses inexpensive IPA **111** as the amine donor it still requires high equivalents and therefore without protein engineering enzymes will suffer from co-substrate inhibition.⁵³



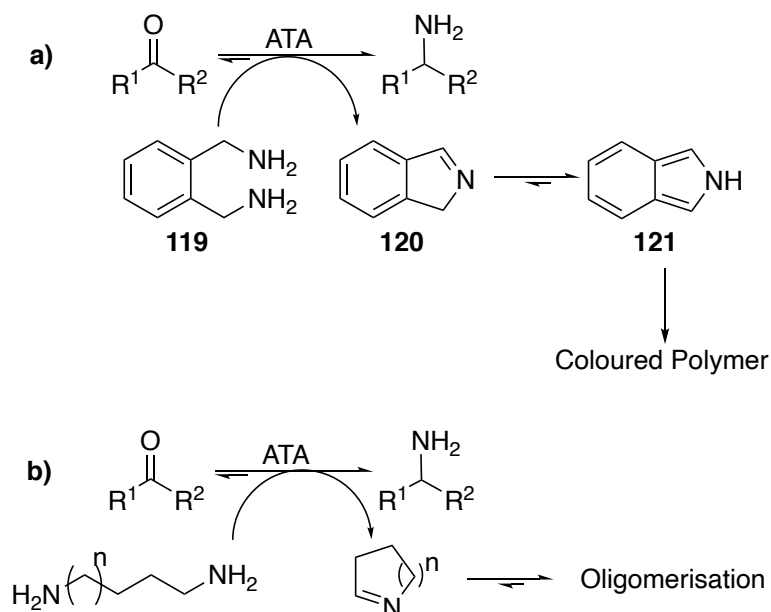
Scheme 25: The transamination reaction, where the equilibrium is directed by the IPA converting to volatile acetone, which can be removed in situ.

Orthogonal enzyme cascades are often used to remove the pyruvate **117** co-product when the amine donor is alanine (Ala) **116** (**Scheme 26**). There are several different classes of enzymes that are able to remove pyruvate **117** from the reaction. The cascade most commonly used is lactate dehydrogenase (LDH), forming lactic acid **118** from pyruvate **117**, however due to the need for an expensive co-factor (NADH), a recycling system of glucose dehydrogenase (GDH) is used (**Scheme 26**) allowing only a small equivalent of NADH to be present in the reaction. Alanine **116** can also be recycled by use of alanine dehydrogenase (AlaDH); in this case pyruvate **117** is reductively aminated at the expense of ammonia and a cheap reducing agent, such as glucose, as part of the recycling system (**Scheme 26**).



Scheme 26: Two different methods of using enzyme cascades in the removal of co-product. A) The removal of pyruvate via an LDH/GDH enzyme cocktail. B) The recycling of alanine from pyruvate using an alanine dehydrogenase (AlaDH) coupled with GDH cofactor recycling system.

More recently the use of ‘smart’ amine donors has been shown to drive the equilibrium towards the desired product. *o*-xylylenediamine **119** is the best-known example of these ‘smart’ amine donors, where following transamination, the aldehyde spontaneously cyclises to form an unstable imine **120**. The imine **120** tautomerises to form **121** and polymerises forming a black precipitate, thus removing the amine donor from the system (**Scheme 27a**).⁸⁷ Due to the expense of *o*-xylylenediamine **119**, this method is not suitable to use on a large scale in industry, where another drawback would be the production of the polymer, which complicates purification. Furthermore, *o*-xylylenediamine **119** is often not accepted by many wild type and (*R*)-selective enzymes.⁸⁷ However, other ‘smart’ amine donors such as terminal diamines **105** such as putrescine, cadaverine **18** and spermidine are also used (**Scheme 27b**). These diamines spontaneously cyclise, and in the case of cadaverine **18**, the cyclised imine trimerises to form isotripiperidene.^{88,89}



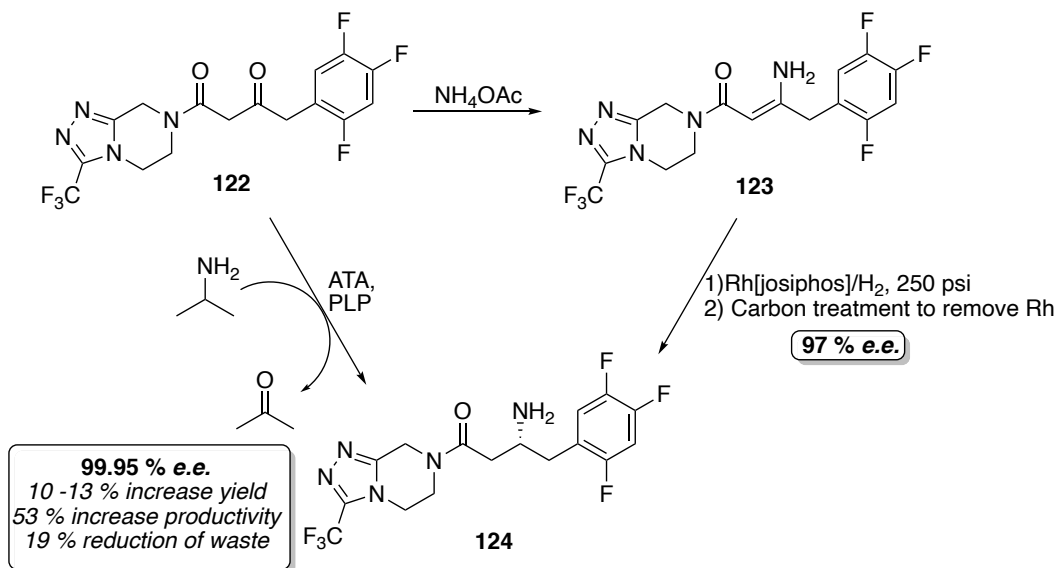
Scheme 27: Example of 'smart' amine donors in ATA reactions: a) *o*-xylylendiamine **119** used as the amine donor spontaneously cyclising after the transamination reaction to form unstable **120**, which tautomerises to **121** before polymerising.⁸⁷ b) The use of terminal diamines as amine donors, forming a cyclised imine after transamination before further reacting to form an oligomer.^{88,89}

Furthermore, ATAs are limited to producing chiral primary amines, while other enzymes such as RedAms can synthesise chiral secondary and tertiary amines with high conversion and selectivity as briefly discussed in **1.2.3 Biocatalytic Synthesis of Alkaloid Scaffolds**. While limiting the product scope available to be produced by ATAs, the nucleophilicity of the primary amines produced opens the door to a number of cascade reactions to take place and be explored, generating useful compounds for further synthesis.

1.3.4 Key Synthetic Examples using ATAs

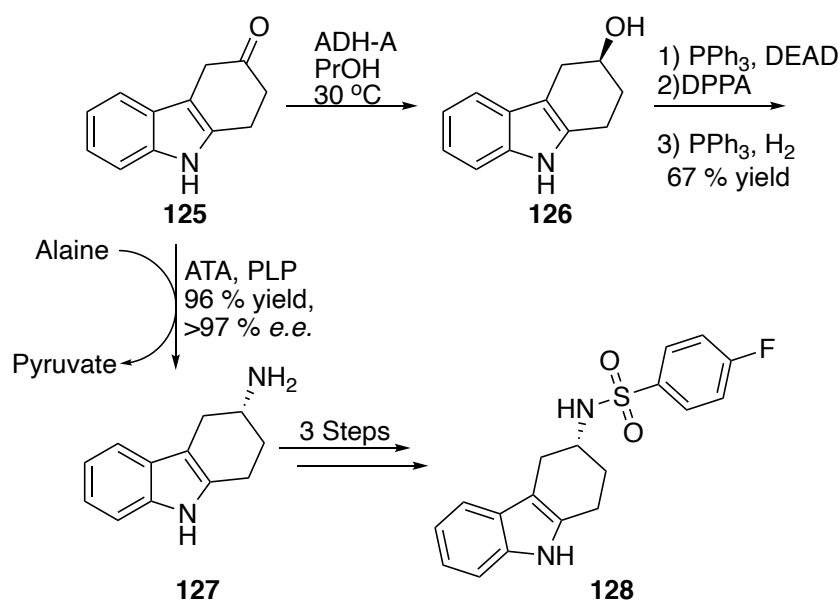
Most notably, a collaboration between Merck and Codexis[®] produced an ATA which was able to accept a Sitagliptin precursor ketone moiety **122** with two bulky constituents (**Scheme 28**). This was a keynote example of the use of transaminase in synthesis, as using this synthetic process not only reduced the number of steps but also, saw a reduction in the amount of waste by 19%. It also avoided using expensive rhodium catalysis and the use of high pressure while also increasing productivity, overall yield and e.e..⁹⁰ This improvement in synthetic method was a real breakthrough on

this methodology, allowing for a cleaner, greener synthesis desired while improving upon the yield and e.e., and improving the energy efficiency and overall safety of the reaction.



Scheme 28: Savile *et al.* uses a highly engineered ATA in the synthesis of Sitagliptin **124**, replacing the two step chemical synthesis from the same common ketone precursor **122**.⁹⁰

Busto *et al.* employed a (*R*)-selective transaminase in the synthesis of Ramatroban **128**, which is used in the treatment of allergic rhinitis and asthma (**Scheme 29**).⁹¹



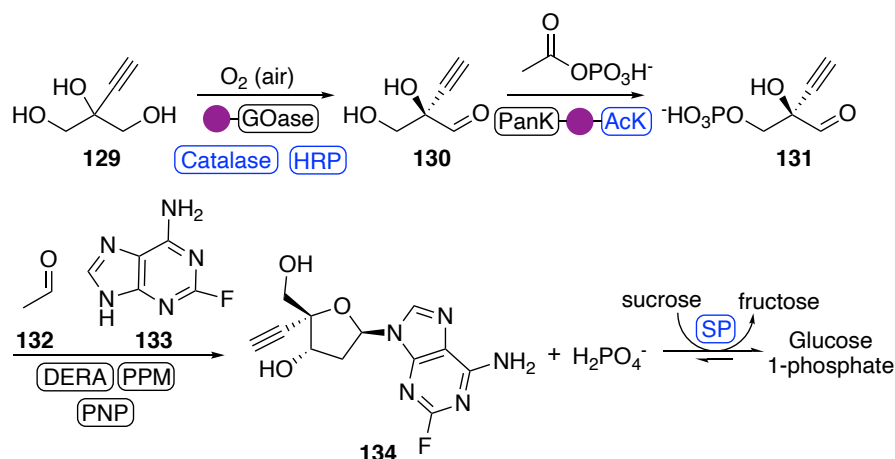
Scheme 29: The chemical and chemo-enzymatic synthesis to the of Ramatroban **128**.⁹¹

During the chemical synthesis of Ramatroban, the chiral alcohol **126** has a tendency to invert its stereochemistry during the Mitsunobu reaction meaning that the final e.e. of the amine **127** suffers. Furthermore, high excess of reagents such as diethyl azodicarboxylate (DEAD) and diphenylphosphoryl azide (DPPA) are required, where due to their toxicity, these need special handling and disposal. By employing the use of an ATA to convert the prochiral ketone **125** to the chiral amine **127**, synthetic routes can be reduced from three steps to one, increasing the productivity and overall yield of the reaction, while removing the need for the use of reagents like DEAD.⁹¹

1.4 Enzyme Reversibility

There are very few truly reversible chemical reactions, which allow for breaking and making of the same bonds. Enzymes have the ability to transform substrates in both directions of a reaction either by addition of functionality or removing the functional group from a molecule. This reversibility is often viewed as a limitation when using enzymes in synthesis, due to the need to drive the reaction equilibrium in one direction (**1.3.2 Limitations of ATAs**). However, when organic chemists perform retrosynthesis on target molecules, they have the ability to use enzymes in both their natural and non-natural directions in many cases, creating more options for disconnections of bonds and increasing the diversity of the subsequent forward synthesis.

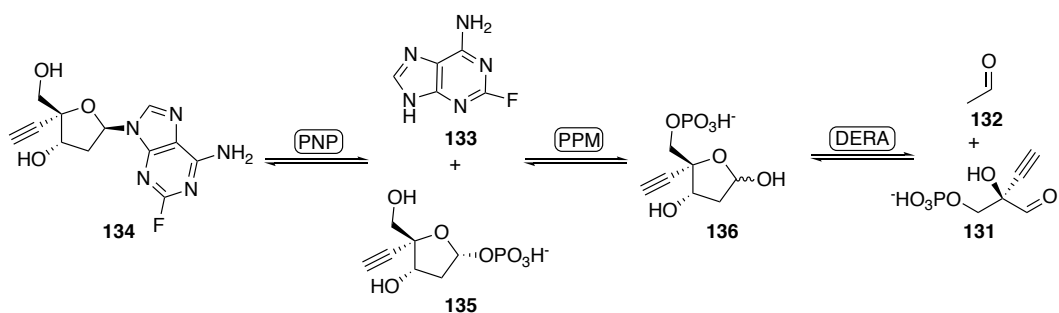
A recent report by Huffman *et al.* showcased the importance of the multi-directionality of enzymes by building the nucleoside type molecule islatravir **134**, in a multi-enzyme cascade in which some were utilised in their non-natural direction (**Scheme 30**). During this cascade, nine enzymes were utilised; five of these biocatalysts are used directly in the synthesis of the islatravir **134**, while the other four used are auxiliary enzymes used to recycle co-factors or to remove by-products of the cascade, thus driving the equilibrium in the desired direction.^{92,93}



Evolved enzymes		Auxiliary enzymes	
(GOase)	Galactose Oxidase from <i>Fusarium graminearum</i>	(Catalase)	Horseradish Peroxidase
(PanK)	Pantothenate Kinase from <i>E. coli</i>	(HRP)	Catalase
(DERA)	Deoxyribose 5-Phosphate Aldolase from <i>Shewanella halifaxensis</i>	(AcK)	Acetate Kinase
(PPM)	Phosphopentomutase from <i>E. coli</i>	(SP)	Sucrose Phosphorylase
(PNP)	Purine Nucleoside Phosphorylase from <i>E. coli</i>	●	Denotes immobilised enzymes

Scheme 30: A fully assembled biocatalytic pathway using five enzymes engineered from the wild type enzymes, and four auxiliary enzymes to regenerate co-factors or remove by-products to drive the equilibrium towards formation of to form the potential HIV drug, islatravir **134**.^{92,93}

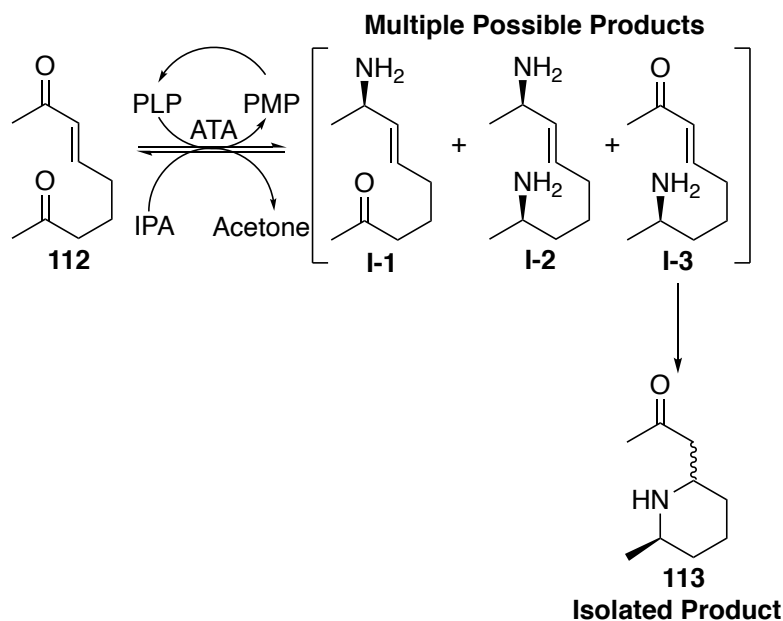
Huffman *et al.* took inspiration from the bacterial nucleoside salvage pathway, which recycles precious nucleosides by breaking them down using a three-enzyme cascade involving purine nucleoside phosphorylase (PNP), phosphopentomutase (PPM) and deoxyribose-5-phosphate aldolase (DERA). While developing this part of the cascade, Huffman *et al.* worked in the natural direction of the enzymes and begun by screening the ability of PNP to cleave islatravir **134** into the nucleobase **133** and the otherwise inaccessible sugar 1-phosphate **135**, which in turn was coupled to screening PPM (**Scheme 31**). This methodology of screening highlights the usefulness of the reversibility of these reactions, as this screen was performed the opposite direction to that of the intended use of the cascade (**Scheme 30**).



Scheme 31: The nucleoside salvage pathway used during the development of the islatravir **134** cascade reported by Huffman *et al.* The first step shows the cleavage of islatravir **134** with PNP to give the nucleoside base **133** and sugar phosphate **135**. This is followed by the transfer of the phosphate group with PPM, and finally the salvage pathway is shown as the retro-aldol reaction completed by DERA.^{92,93}

An extensive screening and engineering effort was made to develop the best enzymes to accept non-natural substrate. While the engineering of enzymes can increase the affinity of certain substrates, the unfavourable equilibrium and by-product inhibition was still a problem. By using an auxiliary enzyme, sucrose phosphorylase, the inorganic phosphate can be removed from the system, thus removing an inhibitor the forward reaction along with providing a driving force towards completion. Using nine enzymes, five involved directly in the construction of islatravir **134** from simple building blocks and four auxiliary enzymes, this route reduces the amount of steps by >50 % when compared to the traditional chemical synthesis of the HIV drug.⁹²

Ryan *et al.* exploited the reversibility of the transaminase by expanding the substrate range, shown in **Scheme 23**, by taking a methyl-methyl keto-enone **112**. The reversible nature of the reaction means that three intermediates were produced by shuttling the amine moiety along the scaffold, where these intermediates are observed to be in equilibrium with one another (**Scheme 32**).⁷³

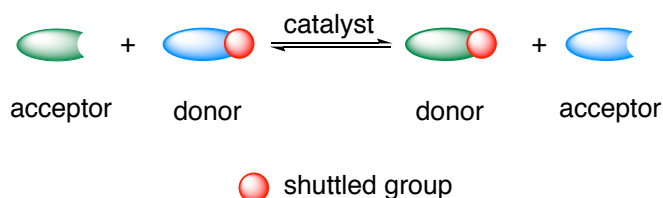


*Scheme 32: Proposed mechanism for the shuttling of the amine moiety from IPA **111** to **112** to provide a range of possible intermediates **I-1,2,3**; the ATA is then able to shuttle the amine to **I-3**, which readily cyclises producing (-)-pinidinone **113**.⁷³*

During the course of this reaction, the enzyme bound PLP is transformed into PMP **115** using IPA **11** as the amine donor, subsequently forming multiple possible intermediates **I-1-3**. The enzyme-bound PMP **115** then shuttles the amine functionality to the more thermodynamically stable ketone **I-3**, restoring the enone conjugation. Intermediate **I-3** then readily undergoes an intramolecular aza-Michael reaction, forming the 2,5-disubstituted piperidine **113**. This reaction proceeded with striking efficiency in 24 h given that there were only two equivalents of amine donor from an internal source, thus showing the ability of a strong thermodynamic driving force. This reaction was only possible due to the reversible nature of the enzyme which allowed the reaction to move between the intermediates.⁷³

1.5 Shuttle Catalysis

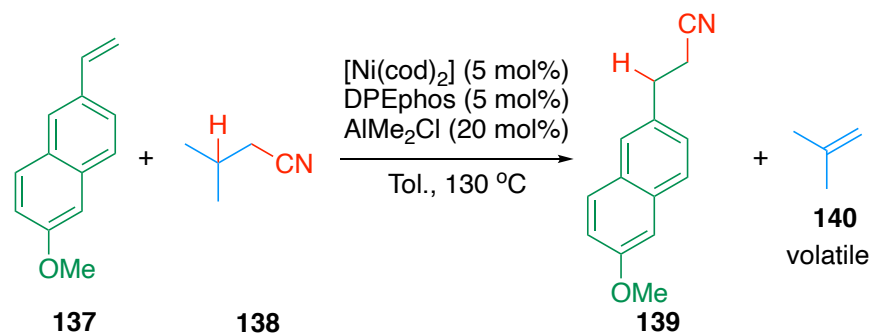
Recently, shuttle catalysis has emerged as a new strategy for the functionalisation and defunctionalisation of organic molecules, by taking advantage of the reversible nature of reactions. The idea of shuttle catalysts is to extend hydrogen transfer to the transfer of functional groups from a donor molecule (blue) to an acceptor molecule (green) (**Scheme 33**), where the sacrificial donor molecule is a simple and inexpensive molecule that can be obtained in bulk to reduce expense and increase atom economy. Shuttle catalysis is particularly appealing when the functional group being transferred is either toxic, a highly reactive compound or avoids an unstable intermediate.^{94–98}



Scheme 33: A depiction of shuttle catalysis, where the red ball is the shuttled group between a donor and an acceptor.^{94–98}

The reversible nature of these shuttle reactions means that they can often suffer from problems with thermodynamics, and therefore need a driving force (e.g. gas release, polymerisation, strain release or chemical trapping). In an ideal scenario, to improve the atom economy of the reaction, the sacrificial donor has a small molecular weight.^{94–98}

An example of this type of catalysis is the hydrocyanation of an alkene with a nickel catalyst, which circumvents the need for toxic and highly dangerous hydrogen cyanide, as observed in traditional synthesis (**Scheme 34**).⁹⁹

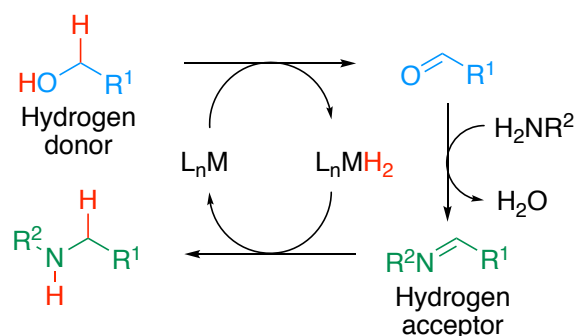


Scheme 34: The transfer of a cyanide group from a sacrificial donor molecule to an acceptor molecule using a nickel catalyst to give a potential drug precursors **139**, as reported by Fang *et al.*⁹⁹

In this case, the sacrificial donor was an inexpensive alkyl cyanide **138** and the acceptors were a range of different alkenes **137**. The forward reaction was driven to completion by the production and removal of volatile isobutene **140**. To show the utility of this reaction, Fang *et al.* prepared potential drug precursor **139**, with high yields and moderate selectivity (**Scheme 34**).⁹⁹

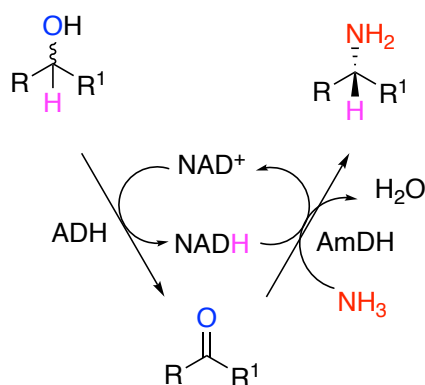
1.5.1 Shuttle Catalysis as Part of a Larger Cycle

Shuttle catalysis can help in the development of novel catalytic reactions in which the transfer event is included in a more complex cycle. A key example of this would be the hydrogen transfer event during the hydrogen borrowing mechanism (**Scheme 35**). There are many different examples of borrowing hydrogen, most of which involve alkane metathesis or amine alkylation that have gained attention due to their high atom economy and their use often negates the need for mutagenic reagents.⁹⁹



Scheme 35: An example of the shuttling of hydrogen can be used as part of a bigger catalytic cycle, borrowing hydrogen.

In the example shown above, the donor is oxidised to an aldehyde, while the hydrogen moieties are transferred on to the metal catalyst. Once the aldehyde is reacted *in situ* with an amine, a Schiff base is formed before being reduced, thus taking the hydrogen atoms back from the metal catalyst and regenerating it. This is a simple example of shuttling the hydrogen moiety from molecule to molecule whilst adding different functionalities across the molecule, ensuring high atom economy and losing water as the only by-product. Hydrogen borrowing has also been used as part of a biocatalytic cycle to produce chiral amines from the corresponding alcohol (**Scheme 36**).^{100–103}

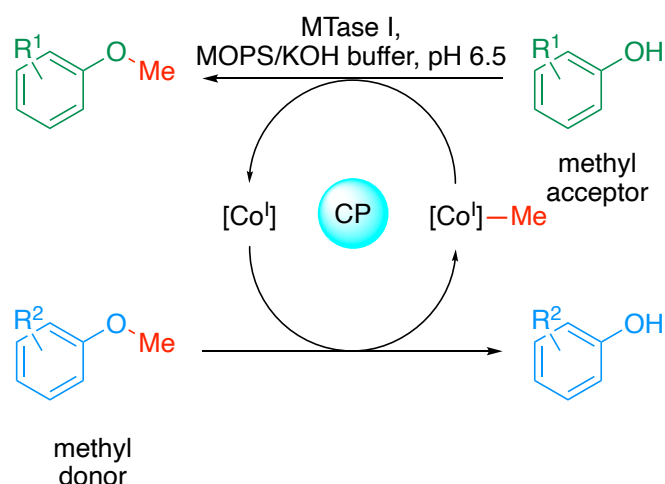


Scheme 36: A biocatalytic hydrogen borrowing cycle, producing a chiral amine from a racemic alcohol, as first reported by Mutti *et al.*¹⁰³

The first biocatalytic hydrogen borrowing cycle was reported by Mutti *et al.*,¹⁰³ which involves the oxidation of an alcohol by an alcohol dehydrogenase (ADH), transferring a hydride onto the co-factor NAD^+ forming NADH (**Scheme 36**). The corresponding ketone is then aminated by an AmDH, and during this part of the cascade, the hydride from NADH is then shuttled back onto the molecule, recycling the NAD^+ . This system allows for only a catalytic amount of the co-factor, as well as utilizing ammonia as the simplest form of nitrogen donor, while the only by-product produced was water. There have since been several further articles published in this area of hydrogen-borrowing.^{100,102,103} Furthermore, Knaus *et al.*¹⁰¹ expanded this methodology to include a more complex redox

cascade to synthesis chiral α -substituted carboxylic acids from the corresponding α,β -unsaturated aldehydes.

There are many examples of biocatalytic hydrogen transfer in a hydrogen borrowing mechanism; the first example of the transfer of a different moiety *via* a biocatalytic method was reported by Farnberger *et al.* using a methyltransferase (MTase I) to shuttle a methyl group (**Scheme 37**).¹⁰⁴



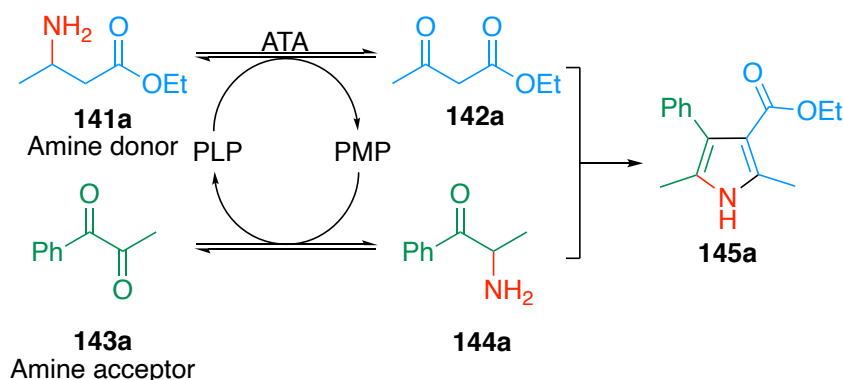
Scheme 37: The MTase I catalysed methyl transfer from a methyl donor molecule to a methyl acceptor molecule via an corrinoid cofactor.¹⁰⁴

MTase I transfers the methyl group to a corrinoid cofactor bound coronoid protein (CP), and a subsequent methylation of the acceptor molecule leads to regeneration of the co-factor. This method avoids the need for generally hazardous reagents (i.e. boron tribromide) and harsh reaction conditions needed to break the C-O-C ether bond. This concept allows for easy deprotection by demethylation, while also allowing for late-stage functionalisation to provide value-added products with mild reaction conditions. However, this is not a true representation of the bio-shuttle catalysis due to the methyl group being transferred onto a different protein than the enzyme.¹⁰⁴

Conceptually, the transaminase mechanism is already an example of a shuttle catalyst, where the amine moiety is transferred from the amine donor, to the pro-chiral ketone or vice versa. ATAs are also capable of

shuttling amine moieties across a molecular framework as shown by Ryan *et al.*⁷³ who reported the synthesis of (-)-pinidinone **113** from ketoenone **112** (**Scheme 32**).

Taking inspiration from both shuttle catalysis and borrowing hydrogen, we propose that ATAs can be used in an *amine borrowing* fashion. The first example of this was demonstrated by Ryan *et al.* (**Scheme 32**).⁷³ Xu *et al.* later demonstrated that combining a transamination reaction with a Knorr pyrrole synthesis was possible (**Scheme 38**) in the preparation of compound **145a**.¹⁰⁵



Scheme 38: The use of a transamination reaction in shuttle catalysis, followed by a Knorr pyrrole synthesis, in a cascade type reaction.¹⁰⁵

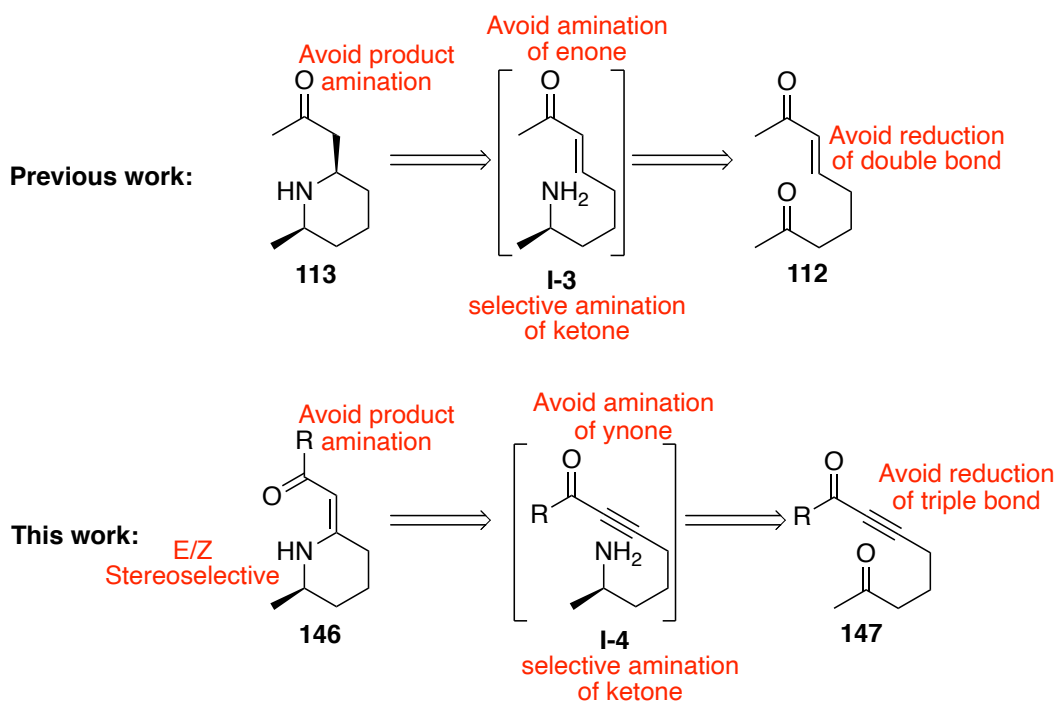
During the course of this reaction, the ATA shuttles the amine from ethyl 3-aminobutanoate **141a** to the diketone acceptor molecule **143a**, before the two products condense in a Knorr pyrrole synthesis (KPS) type reaction. The internal amine transfer exploits the reversible nature of the biocatalytic amination, providing an alternative disconnection for synthesis of the pyrrole. An ATA-Knorr pyrrole synthesis cascade would benefit from 100 % atom economy when completed under stoichiometric amounts. Unfortunately this was not the case during the investigation by Xu *et al.* as they used racemic ethyl 3-aminobutanoate **141a**, requiring ten equivalents.¹⁰⁵ The shuttling of the amine moiety from one starting material to the other *via* a transamination reaction before they are able to condense,

which will provide a driving force for the reaction, would be a great example of *amine borrowing*; although this concept has not yet been reported.

1.6 Project Aims

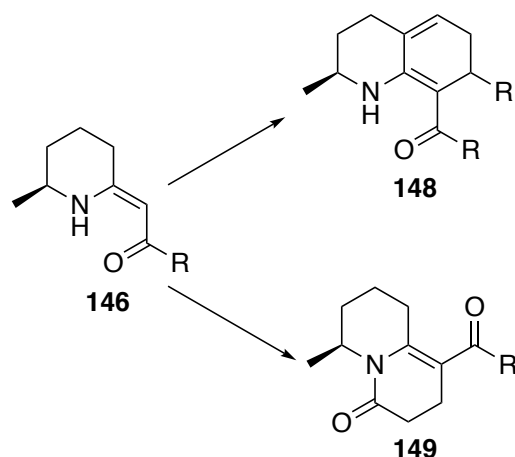
The overall aim of this project is to develop new sustainable methodology for the synthesis of a number of different alkaloid scaffolds. This is to be approached *via* the use of a transaminase cascade, coupling a transaminase reaction with an intra or intermolecular ring closing in a linear cascade.

The first section of this work involves building on the previously reported transaminase-triggered aza-Michael reaction by Ryan *et al.* (**Scheme 39**),⁷³ as stated in **1.2.3 Biocatalytic Synthesis of Alkaloid Scaffolds**, this work showed that when using only two equivalents of amine donor the reaction underwent complete conversion due to the thermodynamically favourable aza-Michael reaction. Ryan *et al.* demonstrated this methodology using a range of ketoenones **112** to produce 2,6-disubstitued piperidine scaffolds **113** with high conversion and high enantioselectivity.⁷³ This work aims to expand the substrate scope of this reaction cascade to include ketoenones **146**, providing an additional functional group handle, with an alkene present in the products.



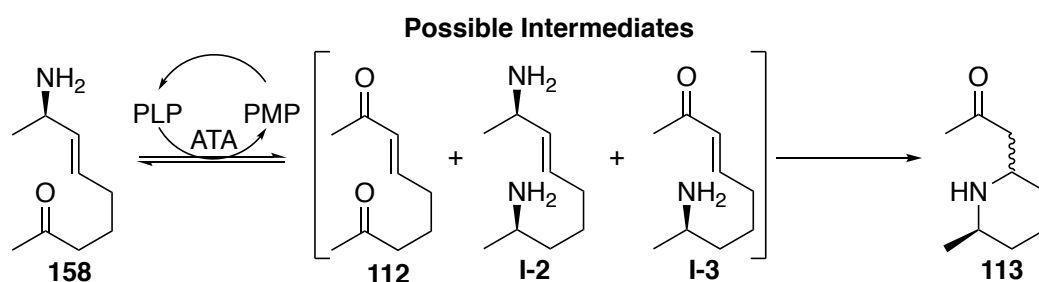
Scheme 39: A) Retrosynthesis used in previous work by Ryan et al.⁷³ during the production of piperidine scaffolds **113** from ketoenones **112**. B) The proposed retrosynthesis used in this work to produce cyclic β -enaminones **146** from ketoynones **147**.

To maximise the number of ketoynones **147** that could be screened, a suitable synthetic route will be devised, as these compounds are not commercially available. Once synthesised, the aim of this project is to screen these compounds to find the best conditions for the biotransformation to obtain the corresponding β -enaminone **146**, before being scaled up for isolation. Furthermore, the transamination of the ketoynones **135** should give highly functional cyclic β -enaminones **146**. To showcase the nucleophilic and electrophilic capabilities of the cyclic β -enaminone products, annulation reactions could be performed to produce further alkaloid scaffolds **148** and **149** (Scheme 40).



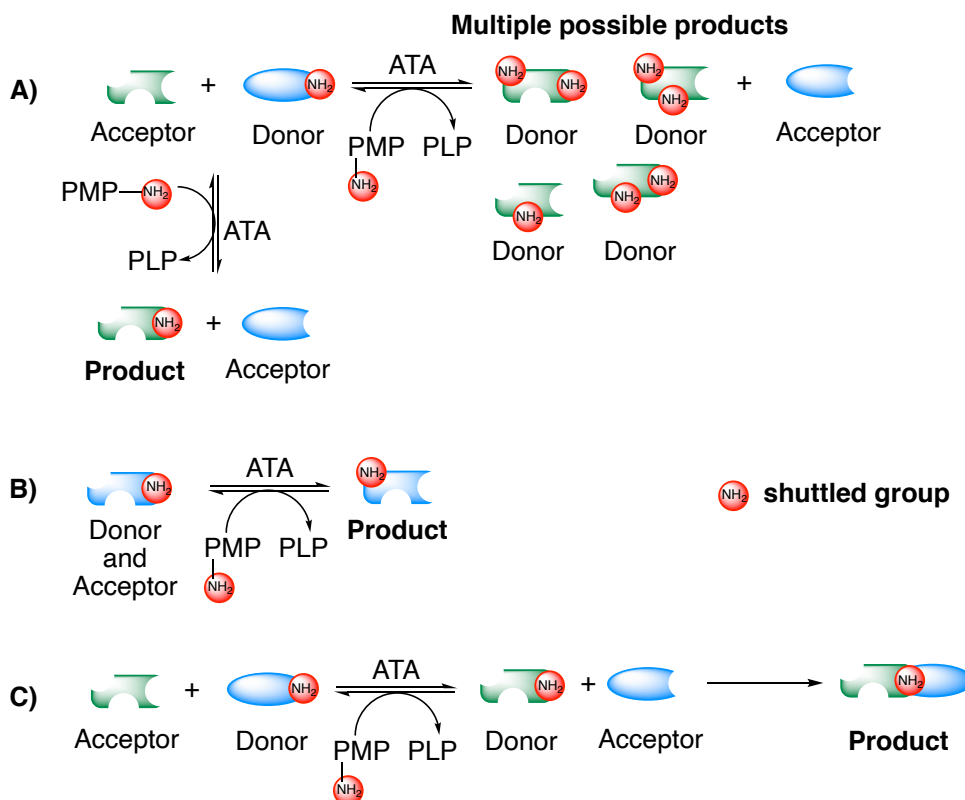
Scheme 40: Proposed annulation chemistry to produce Hexahydroquinolines (HHQ) **148** and lactams **149**.

The second aspect of this project is based upon an idea introduced by Ryan *et al.* where they demonstrated the shuttling of an amine along a molecular framework using an ATA (**Scheme 41**).⁷³



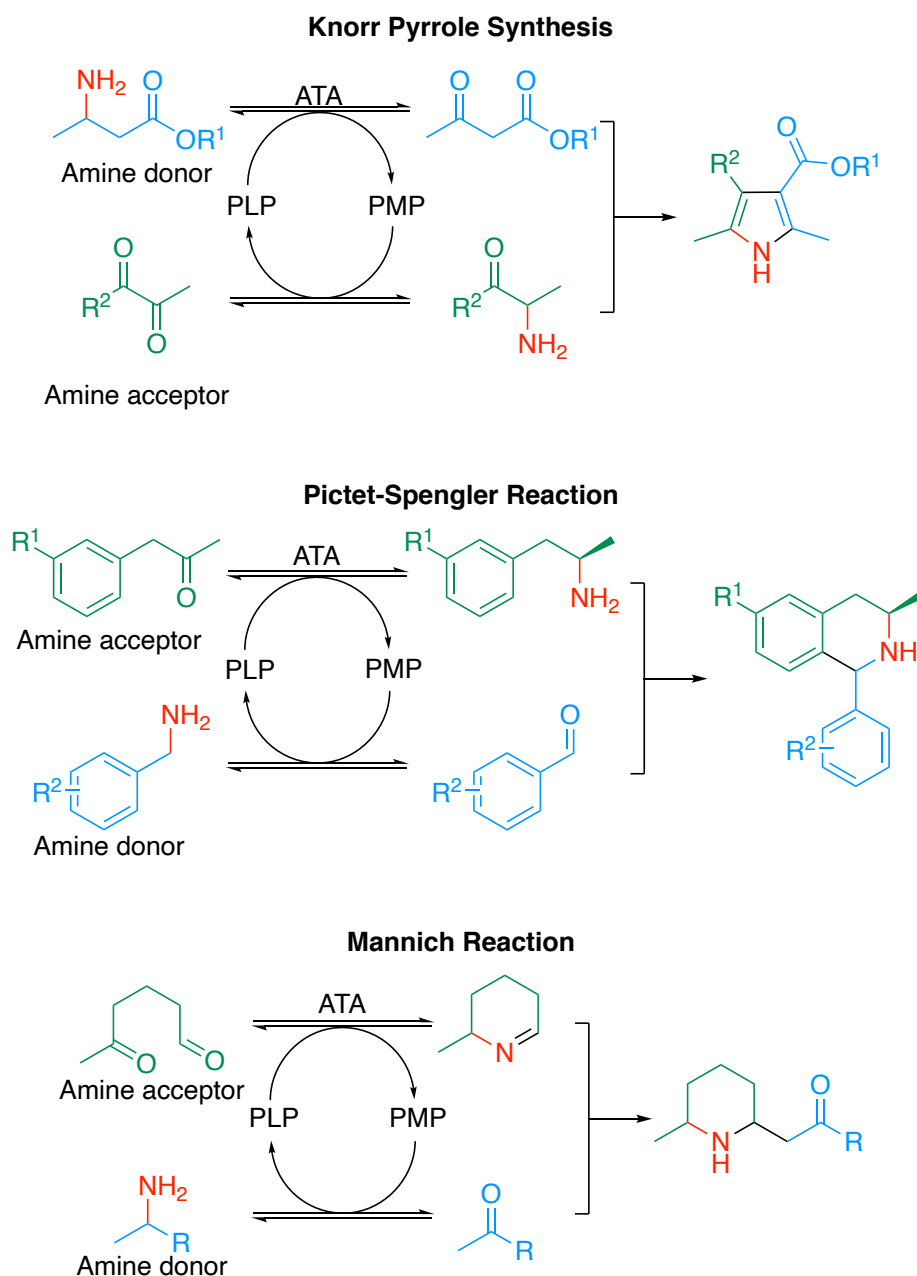
Scheme 41: The shuttling of an amine across a molecule as demonstrated by Ryan *et al.*; this shuttling action provides three potential intermediates, which are all substrates for the ATA. Intermediate **I-3** is able to undergo an aza-Michael reaction to produce the final product **113**.⁷³

The shuttling of the amine moiety across the molecule combines the new methodology of shuttle catalysis with biocatalysis to form a *amine borrowing* cycle by isolating a single product from multiple potential products.^{106,107} This part of the project aims to exploit the natural ability of transaminases to reversibly shuttle an amine moiety from one molecule to another *via* a PLP coenzyme. By taking advantage of the reversible nature of the transaminase reaction there is the possibility that a single product can be isolated from multiple possible products as shown in **Scheme 42A**.



Scheme 42: The overall concept of 'amine borrowing' and shuttle catalysis. **A)** The general concept of shuttle biocatalysis involves the shuttling of a functional group from a donor to an acceptor molecule. The reversible nature of enzymes is exploited to ensure a that single product is isolated from a range of products. **B)** When the donor and acceptor are the same molecule, the amine moiety is 'borrowed' by the PLP and then returned to a different site on the same molecule. **C)** The amine functionality is shuttled to the acceptor molecule and an intermolecular reaction takes place between the two species, meaning that the shuttled group is borrowed and returned to the same molecule.

Furthermore, **Scheme 42B** depicts the shuttling of the amine functionality across the molecule similar to that already demonstrated by the Ryan *et al.* in **Scheme 41**.⁷³ To expand the *amine borrowing* methodology further, it is conceptualised that a linear cascade could be utilised wherein the amine functionality from a donor molecule is shuttled to an acceptor, resulting in the *in situ* formation of two reactive species. During the second step of the cascade, the 'borrowed' amine moiety is reincorporated into the desired target product (**Scheme 42C**).



Scheme 43: The three potential reactions to demonstrate the amine borrowing shuttle reaction. All the examples are initiated by a transamination before undergoing either a Knorr pyrrole synthesis, Pictet-Spengler or Mannich reaction. The acceptor molecules are shown in green and the donor molecules in blue, with the shuttled moiety shown in red.

To demonstrate this action, three named reactions have been identified the Knorr Pyrrole synthesis (KPS), the Pictet-Spengler reaction and the Mannich reaction as shown in **Scheme 43**. The aim of this project is to screen and the optimise conditions for the reactions in **Scheme 43**, before expanding the substrate scope to demonstrate the ability of transaminase as a biocatalyst.

There are multiple possible advantages for the development of this methodology, including the potential for 100 % atom economy, if completed at one equivalent of amine donor. Another potential use is the masking of reactive functionality, such as aldehydes, in whole cell biotransformations, where aldehydes are often unavoidably transformed by endogenous enzymes, when performing whole-cell reactions

**Part I - Asymmetric Construction of Cyclic β -
Enaminones, Employing a Transaminase-Aza-
Michael Cascade**

2.1 Introduction

The work completed in this chapter has been published by Taday *et al.*¹⁰⁸

β -Enaminones contain highly useful functional moieties with both electrophilic and nucleophilic capabilities. This unique reactivity means that β -enaminones are important intermediates in the synthesis of a variety of different *N*-heterocyclic compounds as shown in **Figure 3**.^{109–112}

This report investigates the biocatalytic synthesis of six-membered cyclic β -enaminones, which are proven to be useful building blocks for several biologically active alkaloids including, pinidinone **113**,¹¹³ apomistomycin,¹¹⁴ mesembrenone,¹¹⁵ desoxoprosophylline **156**,¹¹⁶ cassine **155**,¹¹⁷ deoxyfebrifugine **157**,¹¹⁸ sedacryptine **158**,¹¹⁹ selenopsine **154**¹²⁰ and hippodamine **61**¹²¹ (**Figure 3**). β -enaminones are also present in a number of active pharmaceutical ingredients for use as anticonvulsants **150**,^{122–124} anti-inflammatories **151**,¹²⁵ anti-tumour agents **152**¹²⁶ and anti-bacterial agents **153**.¹²⁷

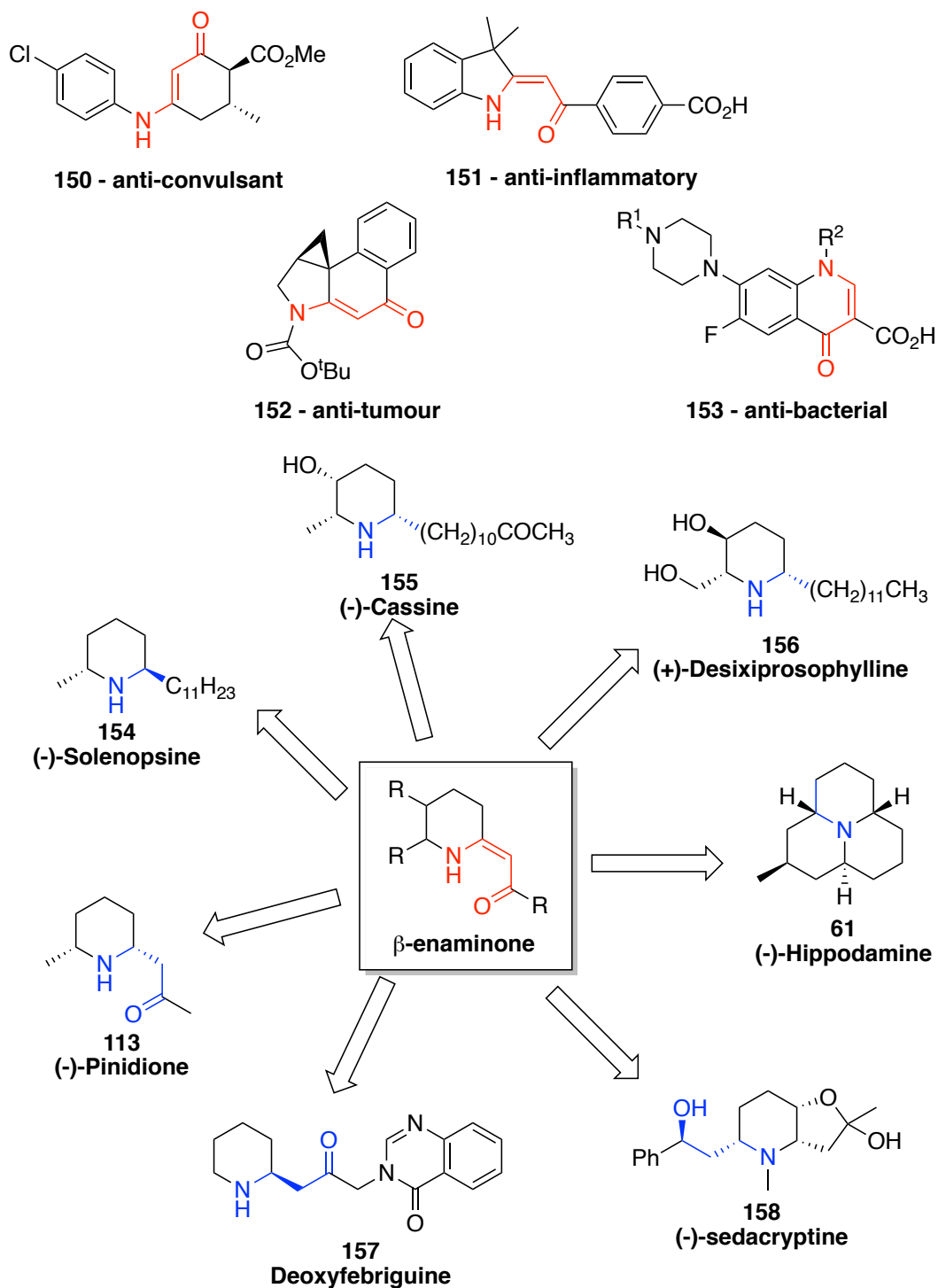
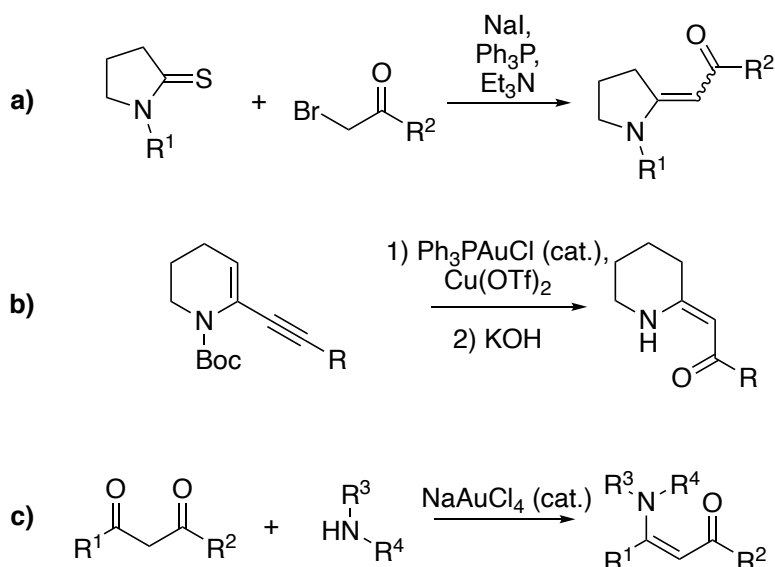


Figure 3: A selection of biologically active compounds containing β -enaminones (red), with examples of natural products that have been synthesised using a key β -enaminone building block including: (-)-solenopsine A **154**, (-)-cassine **155**, (+)-desixiprosophylline **156**, (-)-pinidinone **113**, (-)-hippodamine **61**, deoxyfebriguine **157**, (-)-sedacryptine **158**.

Despite the importance of substituted cyclic β -enaminones as intermediates, there have been few strategies reported for their

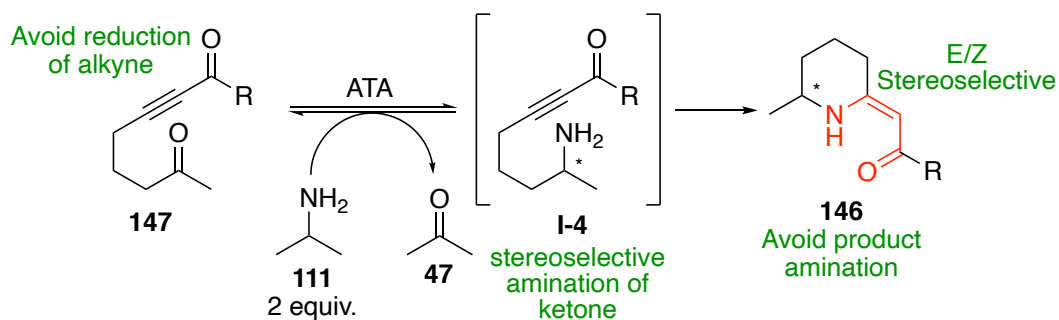
enantioselective synthesis. The simplest current routes to these key synthetic intermediates include the condensation reaction between 1,3-diketones and amines,¹¹⁰ or a sulfide contraction, starting from a thioamide and an α -bromoketone, which was initially reported by Eschenmoser (**Scheme 44a**).¹²⁸



*Scheme 44: Various synthetic routes to β -enaminones. a) Sulfide contraction reported by Eschenmoser.¹²⁸ b) Gold-catalysed reaction of enone in the presence of $\text{Cu}(\text{OTf})_2$ as reported by Scarpi *et al.*¹²⁹ c) Gold-catalysed coupling of diketones and amines forming β -enaminones as completed by Arcadi *et al.*¹³⁰*

More recently, work has been published showing the use of gold (I) as a catalyst for the cyclisation of *N*-Boc-6-alkynyl-3,4-dihydro-2*H*-pyridines to form cyclic β -enaminones (**Scheme 44b**).¹²⁸ Arcadi *et al.* reported the gold (III) catalysed regioselective condensation of diketones and amines in a one-pot procedure (**Scheme 44c**).¹²⁹

By expanding the ω -TA-triggered intermolecular aza-Michael methodology produced by Ryan *et al.*⁷³ by using ketoyrones **147** in place of the original substrates **112**, it was envisaged that a range of cyclic β -enaminones **146** could be prepared with high regio- and stereoselectivity (**Scheme 45**).



Scheme 45: The proposed transamination reaction, using a ketoynone **147** as the starting material.

The products formed have a number of functional handles, including the amine, alkene and carbonyl, meaning further annulation reactions were devised to produce a number of potentially biological active alkaloids containing tetrahydroquinoline (THQ), hexahydroquinoline (HHQ) **148** and quinolizinone moieties, with potentially significant biological activity. The substrates needed for this methodology were not commercially available, so were synthesised. The following section describes the synthesis of these key ketoynone substrates.

2.2 Results and Discussion

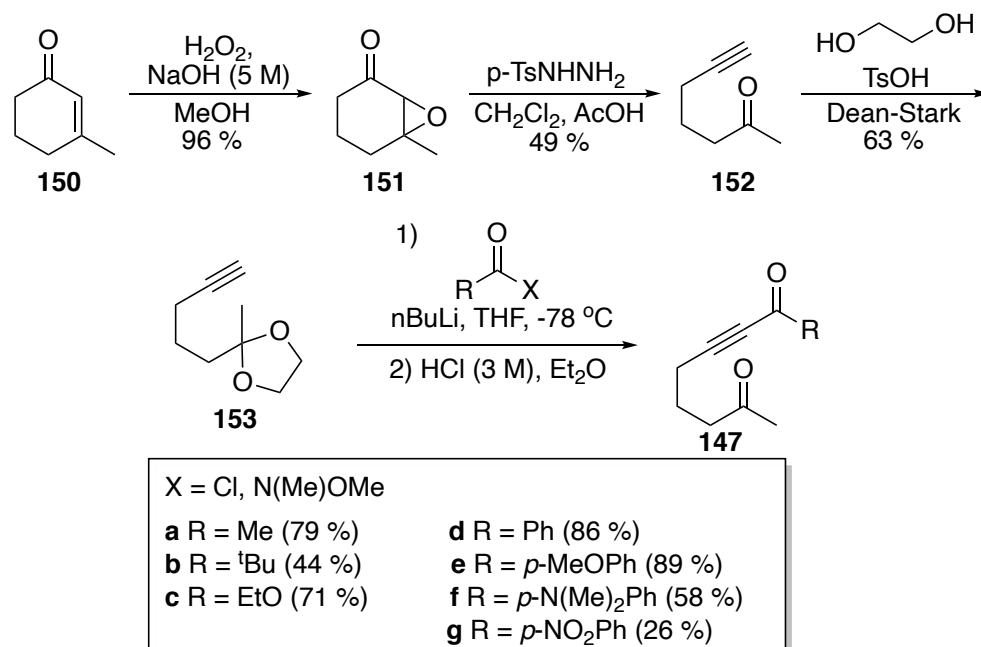
2.2.1 Synthesis of Ketoyrones **147** (Scheme 46)

A number of synthetic routes have previously been reported to obtain a variety of ketoyrones **147**.^{131–133} Ciesielski *et al.* reported a route which does not allow for the late stage functionalisation of the R-groups (**Scheme 46**).¹³¹ The late stage functionalisation is advantageous when building a library of substrates due to the ability to then produce large amounts of the precursor before diversifying the pathway to produce smaller amounts of numerous final products.

The route taken by Chiu *et al.*¹³³ allows for late stage functionalisation of the R-group, with the introduction of the alkyne from the corresponding aldehyde by utilising trimethylsilyldiaomethane with a moderate yield of 54 %. This overall route provided the ketoynone **147** in reasonable yields and includes multiple the oxidative and reductive steps to obtain the aldehyde in

6-steps overall. Prior attempts of this route by previous members of our group did not provide the desired ketoyrones.

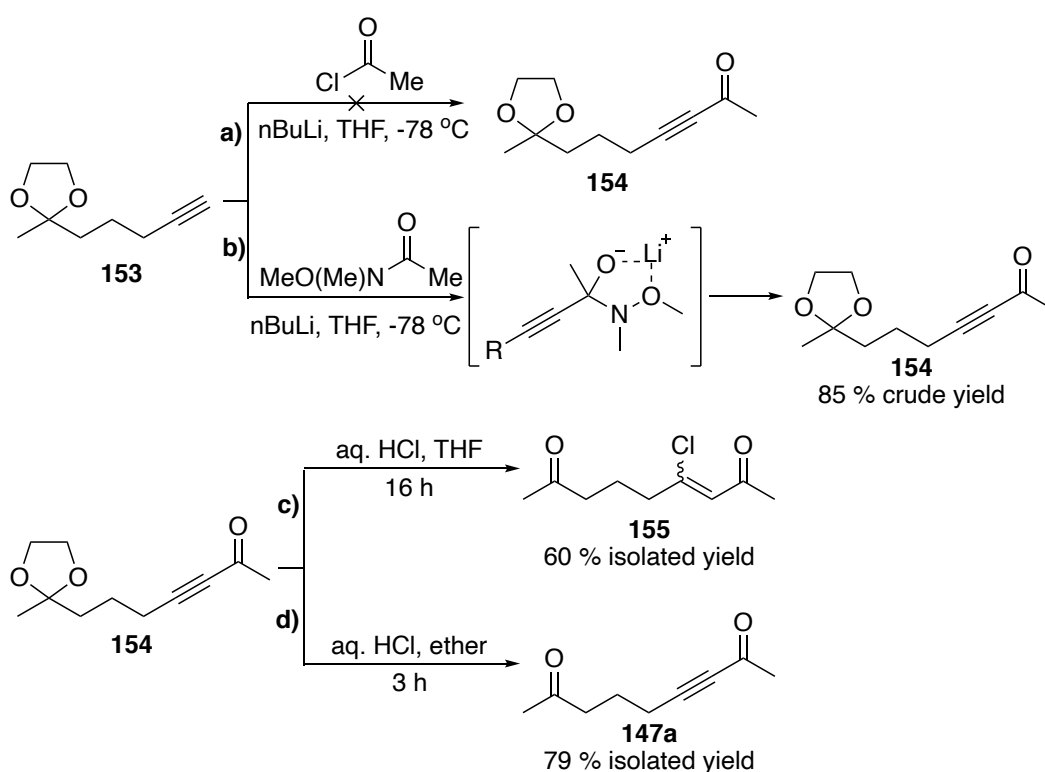
Given the drawbacks associated with some of the established routes, it was postulated that a new route may be preferable (**Scheme 46**), which would involve introducing the alkyne *via* an Eschenmoser fragmentation. Initially, two routes to the ketoyrones **147** were attempted from hept-6-yn-2-one **152**, one being a protection and subsequent acylation and deprotection step, the other utilising a Sonogashira coupling. These routes were attempted in tandem in an attempt to achieve synthesis of the desired compounds.



Scheme 46: Synthesis of the Ketoyrone **147a-g** substrate from 3-methylcyclohexenone **150**.

The ketoyrones **147** were prepared (**Scheme 46**) *via* the epoxidation of commercially available 3-methyl-2-cyclohexenone **150** using hydrogen peroxide, catalysed by sodium hydroxide. While an initial yield of 69 % was achieved, this reaction was further optimised by increasing the time and slowing the addition of the hydrogen peroxide (added dropwise) from 20 min to 40 min. These changes led to the yield increasing to 96 % and removal of the purification step, as it was determined to be sufficiently pure to be

taken forward into the next step. Eschenmoser fragmentation of the epoxide **151** using *p*-toluenesulfonyl hydrazide afforded a poor yield (49%). However, previous reports in the literature also show that this reaction is low-yielding, potentially due to the addition of the hydrazide into the ketone of the product to produce an unwanted by-product.¹³⁴ The acetal protection proceeded with a reasonable yield of 63 % and the subsequent acylation of the alkyne was followed directly with an acidic work-up to deprotect the ketone, which proved to be a more challenging step than expected and required optimisation to achieve the desired results (**Scheme 47**).



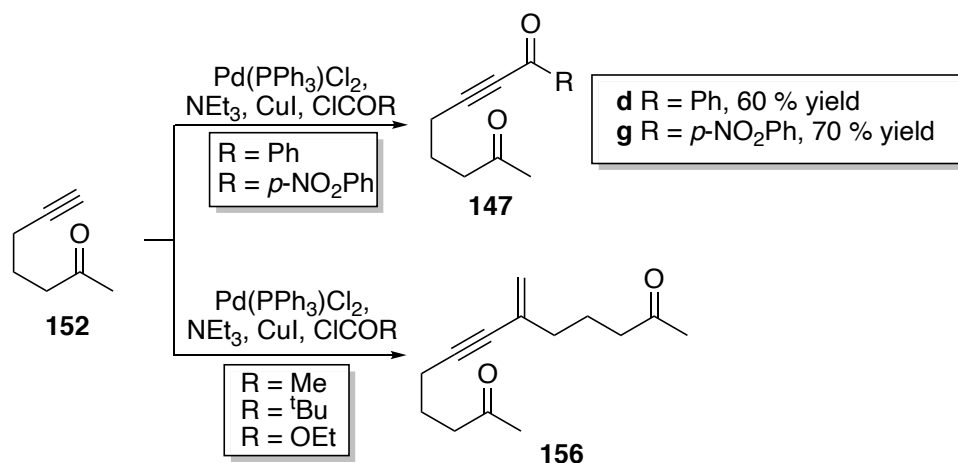
Scheme 47: a) and b) Conditions employed in the acylation of the methyl-methyl derivative **147a**., c) and d) Conditions used in the acetal deprotection to give the desired methyl ketone.

During the acylation to synthesise the methyl-methyl substrate **147a**, it was discovered that reaction of acetyl chloride with the deprotonated alkyne did not afford any of the desired product, and only starting material remained (**Scheme 47a**). Modification of the reaction conditions to substitute the acyl chloride with a Weinreb amide allowed a stabilised tetrahedral intermediate to be formed, which collapses during the work-up to give the desired product

154, which could be detected in the crude ^1H NMR (**Scheme 47b**) (85 % crude yield).

It was then observed that the length of time involved (16 h) in the deprotection step of acetal-protected ketoynone **154** (**Scheme 47c and d**) led to undesired side reactions, due to the chloride ion acting as a nucleophile to complete a 1,4-addition onto the ynone (**Scheme 47c**). Modifications to the procedure using a biphasic reaction mixture were accomplished by switching solvents from THF to ether, designed to slow down the rate of the reaction (**Scheme 47d**). This allowed the chloride ion to remain dissolved in the aqueous layer while the organic methyl ketoynone **147a** was dissolved in the organic diethyl ether layer, reducing the likelihood of reaction between the two. Monitoring the reaction closely by TLC revealed that the deprotection was complete in 3 h, while none of the undesired by-product **155** could be seen *via* TLC.

To remove the need for a protecting group in the synthetic route, an alternative route was attempted utilising a Sonogashira coupling and various acid chlorides (**Scheme 48**). However, it was found that when the reaction was performed with either aliphatic acid chlorides or chloroformates, the homo-coupled product, 8-methylenetridec-6-yne-2,12-dione **156**, was formed in preference to the desired product **147**. This was potentially due to side reactions between the acid chlorides and the triethylamine base leading to formation of the corresponding carbamate,¹³⁵ while the homo-coupled product **156** has been previously reported by Islas *et al.* where the alkyne **152** is coordinated into the Pd catalyst and is likely to undergo a Heck type reaction to form the germinal enyne **156**.¹³⁶ Both of these interactions can be seen in **Scheme 48**, below.



Scheme 48: Sonogashira coupling of hept-6-yn-2-one **152** with acid chlorides to give the desired ketoyones **147** product and the homodimer **156** produced with some acid chlorides.

It was hypothesised that the desired product **147** could be preferentially formed by changing the order in which reagents were added. Unfortunately, this did not have the desired effect and the reactions continued to produce the enyne by-product **156**. Due to the acylation reaction mentioned previously producing the desired products, it was decided to not pursue further optimisation. However, if optimisation of the reaction conditions was pursued further, a selection of sterically hindered bases could be attempted, along with modification of the ligands on the palladium catalyst.

2.2.2 Synthesis of β -enaminones using ATA-aza-Michael Cascade

A range of ketoynone substrates were synthesised to demonstrate the versatility of the methodology, as well as allow for the generation of derivatives with diverse functionality, as shown below in **Figure 4**. The varying R-groups of the substrates were chosen to show a range of different functionalities, varying from a non-bulky methyl substituent to a bulky tert-butyl group, as well as inclusion of aromatic phenyl groups with different electronic groups. Ketoynone **147**, which incorporates an ethyl ester, would also provide an extra functional handle for further derivatisation. It was thought that this class of substrates would be more challenging than the ketoenones used by Ryan *et al.*,⁷³ due to the fixed sterics around the sp^1

centres of the triple bond, meaning there is limited overlap of the π orbitals during the aza-Michael step.

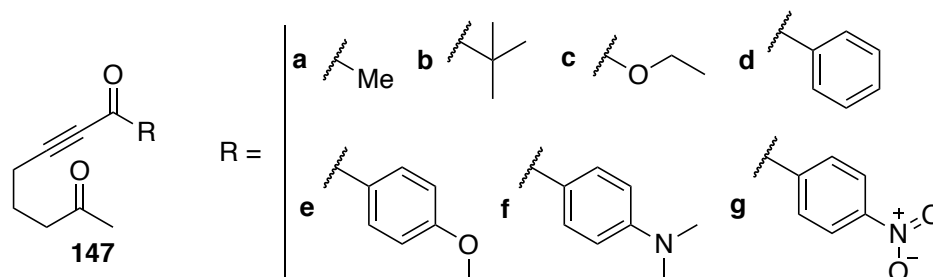
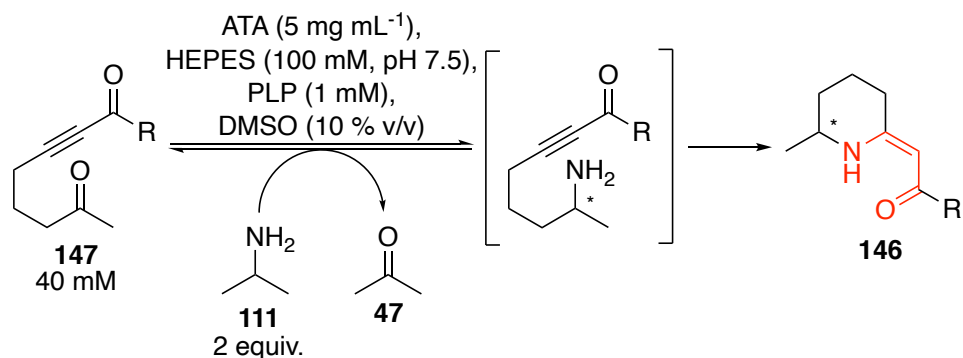


Figure 4: The various ketoyrones synthesised as part of this work, with a range of functional handles for further synthesis.

Following successful synthesis of the ketoyrones, analytical scale biotransformations were conducted with the four compounds **147a-d**, to determine the best conditions for scale-up reactions. The conditions were adapted from the highly optimised reactions in Ryan *et al.*⁷³ Readily available commercial enzymes from Codexis[®] were selected for these transformations to ensure that the methodology was accessible. The four enzymes chosen were **ATA113**, **ATA256** ((*S*)-selective transaminases) and **ATA117**, **ATA025** ((*R*)-selective transaminases). All of these enzymes are highly engineered to increase thermal and solvent stability, enhance activity and reduce substrate inhibition (**1.3.2 Limitations of ATAs**). The initial studies performed involved determining the commercial enzymes which gave the best conversion to the β -enaminone **146** (**Table 1**).



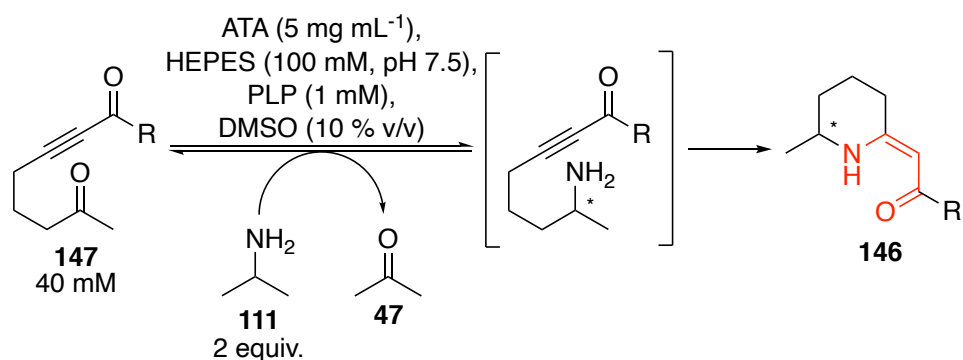
Entry	R	ATA113		ATA256		ATA117		ATA025	
		Conv. (%) ^(a)	e.e. (%) ^(b)						
1	Me	0	-	56	99	71	99	83	99
2	^t Bu	68	95	46	99	28	99	65	94
3	OEt	99	77	91	99	85	64	99	83
4	Ph	72	-	17	-	1	-	100	-

*Table 1: The conversion of the ketonone **147** to the corresponding β -enaminones **146** using different transaminases. Reaction conditions: ATA (5 mg mL⁻¹), **147** (40 mM), isopropylamine **111** (80 mM), DMSO (10%), PLP (1 mM), HEPES buffer (1 mL, 100 mM, pH 7.5), 30 °C, 200 rpm, 24 h. a) conversion determined by GC-FID b) e.e. determined by GC-FID fitted with a chiral column. – denotes no data obtained.*

When choosing the conditions for scaling up the biotransformations, it was necessary to compromise on the conversion to obtain the best enantiomeric excess in the final products. **Table 1** shows that while **ATA113** resulted in higher conversions to the (*S*)-enantiomer of the β -enaminone **147** than **ATA256** with both the tert-butyl **b** (68 % conversion, 95 % e.e. (**Table 1, entry 2**)) and ethoxy **c** (>99 % conversion, 77 % e.e. (**Table 1, entry 3**)) derivatives, the enantiomeric excess was lower than **ATA256**. **ATA256** was therefore selected to produce the (*S*)-enantiomer of the tert-butyl **b** (46 % conversion, >99 % e.e. (**Table 1, entry 2**)) and ethoxy **c** (91 % conversion, >99 % e.e. (**Table 1, entry 3**)) derivatives, due to the increased enantioselectivity. Furthermore, **ATA113** showed no activity towards the methyl substrate **a**, however **ATA256** gave reasonable conversion (56 %) with good enantiomeric excess (99 %) (**Table 1, entry 1**).

ATA113 gave better conversion with the aromatic phenyl substrate **d** (72 % (**Table 1, entry 4**)). Comparing the (*S*)-selective enzymes and substrates shows that **ATA113** seems to accept the larger substrates better, while **ATA256** gave increased *e.e.* for the smaller substrates. This is potentially due to the active site of these enzymes and the large binding pocket in **ATA113** being more receptive towards aromatic substrates. The downside to using these commercial enzymes is that very little information is given about them, so docking in a crystal structure to confirm is not available. The most suitable (*S*)-selective ATA to use in the preparative scale synthesis of **133a**, **b** and **c** was **ATA256**, which can be seen in **Table 2** below. However, for synthesis of the aromatic compounds, **146d-g**, **ATA113** was chosen.

Of the (*R*)-selective enzymes, **ATA025** afforded higher conversion across all of the substrates screened (**Table 1**). **ATA117** gave very low conversion with the bulkier phenyl substituent **d** (1 %) and tert-butyl **b** (23 %) groups, indicating that the 'large' binding pocket of **ATA117** might not have been sufficient to accommodate this class of substrate. The enantiomeric excess of the phenyl derivative **146d** was not measured at this point, as separation of the individual enantiomers by GC or HPLC, fitted with a chiral column, required further optimisation. From these analytical scale reactions, it was thought that the best (*R*)-selective ATA to use in the synthesis of **146a-g** on a preparative scale was **ATA025**; all the above results informed the selection of enzymes for the preparative-scale reactions shown in **Table 2**.



Entry	Subs.	R	ATA	Conv. (%) ^(b)	Yield (%) ^(c)	e.e. (%)
1	a	Me	ATA025	91 ^(a)	78	>99 ^(d) (<i>R</i>)
2	a	Me	ATA256	95 ^(a)	43	>99 ^(d) (<i>S</i>)
3	b	^t Bu	ATA025	99 ^(a)	54	94 ^(d) (<i>R</i>)
4	b	^t Bu	ATA256	97 ^(a)	95	98 ^(d) (<i>S</i>)
5	c	OEt	ATA025	92 ^(a)	73	83 ^(d) (<i>R</i>)
6	c	OEt	ATA256	96 ^(a)	60	>99 ^(d) (<i>S</i>)
7	d	Ph	ATA025	88 ^(a)	72	97 ^(d) (<i>R</i>)
8	d	Ph	ATA113	91 ^(a)	85	>99 ^(d) (<i>S</i>)
9	e	<i>p</i> -MeOPh	ATA025	88 ^(b)	79	94 ^(e) (<i>R</i>)
10	e	<i>p</i> -MeOPh	ATA113	91 ^(b)	85	98 ^(e) (<i>S</i>)
11	f	<i>p</i> -N(Me) ₂ Ph	ATA025	46 ^(b)	43	>99 ^(e) (<i>R</i>)
12	f	<i>p</i> -N(Me) ₂ Ph	ATA113	53 ^(b)	29	98 ^(e) (<i>S</i>)
13	g	<i>p</i> -NO ₂ Ph	ATA025	98 ^(b)	58	>99 ^(e) (<i>R</i>)
14	g	<i>p</i> -NO ₂ Ph	ATA113	94 ^(b)	53	97 ^(e) (<i>S</i>)

Table 2: Reaction conditions: ATA (5 mg mL⁻¹), **147** (40 mM), isopropylamine **111** (80 mM), DMSO (10%), PLP (1 mM), HEPES (5 mL, 100 mM, pH 7.5), 30 °C, 200 rpm, 24-48 h. (a) Conversion determined by GC-FID. (b) Conversion determined by ¹H NMR spectroscopy. (c) Isolated yield after column chromatography. (d) e.e. determined by GC-FID using a chiral column. (e) e.e. determined by HPLC using chiral column.

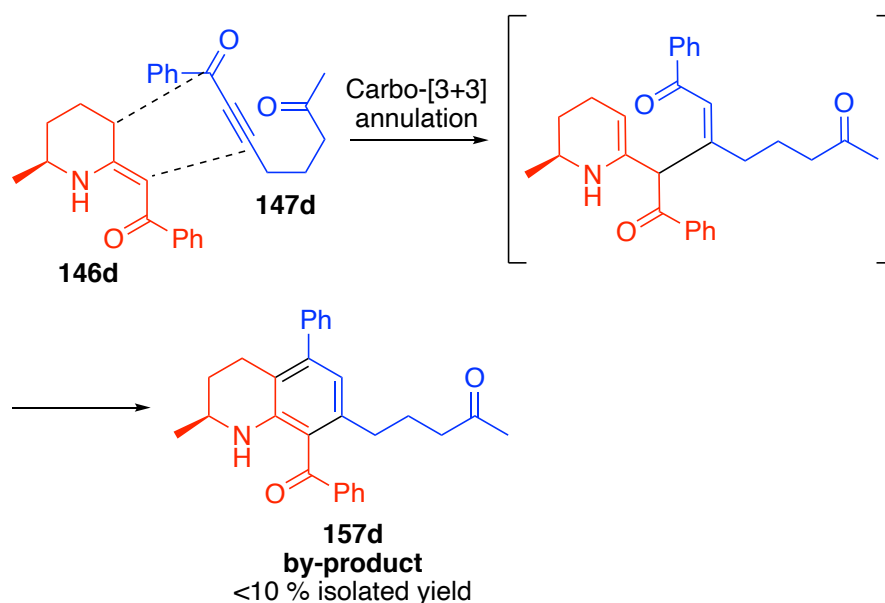
Due to the lack of conversion seen with the (*R*)-selective enzyme **ATA117** with all the ketoyones **147a-g**, **ATA025** was used exclusively for the synthesis of the (*R*)-enantiomers with high conversions achieved (88 - 99 %) (Table 2), with the exception of compound **147g** (46 % conversion (Table 2, entry 11)). This particular substrate proved challenging for both commercial enzymes.

As discussed above, to achieve the best conversion for the (S)-enantiomers, two different ATAs were employed, depending on the substrate being transformed. **ATA256** was found to give better conversions with the non-aromatic ketoynones **135a-c** (95-97 % (**Table 2, entries 1-6**)), while **ATA113** achieved better conversion with the aromatic ketoynones **147d-g** (53-92 % (**Table 2, entries 7-14**)), with **147g** again giving the lowest conversion (53 %, (**Table 2, entry 12**)). Due to issues with extraction during the work up, the isolated yield varied from a low to excellent (29-95 %).

As expected, the enantiomeric excess achieved ranged from good to excellent (83-99 %) in all cases. The β -enaminones **146** were isolated in the Z-configuration, as observed by NOESY NMR spectroscopy. This configuration is likely to be favoured due to the presence of an intramolecular hydrogen bond between the carbonyl and the amine, resulting in a low energy conformation. These results are consistent with previous reports.^{113,117,137}

Notably, the reaction conditions required only two equivalents of amine donor, due to the irreversible cyclisation of the intermediate, which displaces the reaction equilibrium towards product formation. These conditions are in contrast to typical TA biotransformations, which often require extremely high equivalents of amine donor or the removal of co-products *in situ*. (**1.3.2 Limitations of ATAs**). This is a significant improvement to traditional methodology because of the increased sustainability of these reaction conditions.⁵³

The biotransformations of the aromatic compounds proved to be more challenging than those of the aliphatic substrates as seen in **Table 2**, and suspected that this was due to an annulation reaction occurring between the cyclic enaminone product and the starting material, forming a tetrahydroquinolone (THQ) **157d** (**Scheme 49**). By modifying the electronics of the phenyl substrate **147d**, it was thought that the amount of this by-product could be reduced, hence the modifications using substrates **147e-g** were synthesised (**Table 2, entries 9-14**).



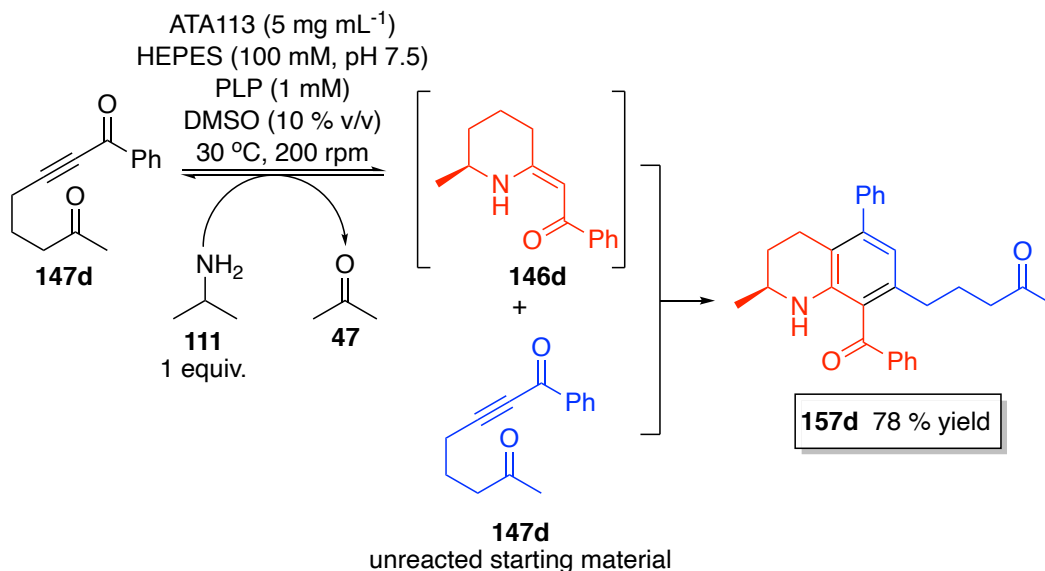
Scheme 49: The carbo-[3+3] annulation between the unreacted ketoynone **147d** and the β -enaminone **146d** produced during the biotransformation to produce THQ **157d** by-product.

In the case of *para*-nitro substrate **147g**, which contained an electron-withdrawing group (EWG), the formation of the by-product appeared to reduce to trace amounts and none could be isolated. Unfortunately, this was not the case with the electron-donating (EDG) substrates **147e** and **147f**, where the conversion to the β -enaminone **146** decreased, and there was a higher proportion of the by-product seen when measuring the conversion, *via* $^1\text{H NMR}$. This by-product was only isolated in sufficient amounts to fully characterise in the case of substrate **147e-f**. The EDG on the aromatic ring would have decreased the electron density around the carbon of atom on the alkyne bond, therefore increasing the amount of by-product produced during the reaction.

2.2.3 Annulation Cascades and Reactions

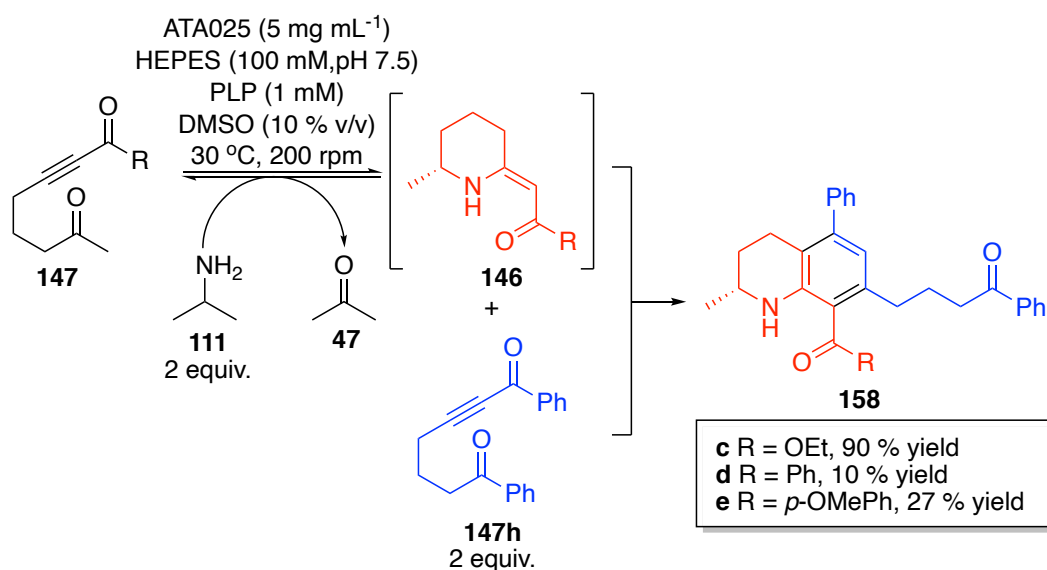
Although the annulation product **157d** was only isolated as the minor component following the above biotransformations (<10 %) (**Scheme 49**), it was thought that by decreasing the equivalents of amine donor the efficiency of the biotransformation would be decreased enough to allow for the annulation reaction to take place. Reducing the equivalents from two to

one appeared to reduce the conversion sufficiently to allow the remaining starting ketoynone **147d** time to undergo a carbo-[3+3] annulation cascade preferentially, affording the desired THQ **157d** in 78 % yield (**Scheme 50**).



*Scheme 50: By reducing the equivalents of amine donor **111** to one, allows for the left-over starting material to react with the β -enaminone **146** in a carbo-[3+3] annulation cascade reaction. Reaction conditions: ATA025 (5 mg mL⁻¹), **147d** (40 mM), isopropylamine **111** (40 mM), DMSO (10%), PLP (1 mM), HEPES (5 mL, 100 mM, pH 7.5), 30 °C, 200 rpm, 24 h.*

To investigate the novel one-pot ATA-annulation cascade further, a coupling partner was chosen that could not readily undergo transamination, due to the ‘bulky’ nature of the substituents (**Scheme 51**). To exploit the nature of the ‘small’ - ‘large’ binding pockets associated with ATAs a ketoynone **147** with phenyl substituents on both carbonyls was chosen **147h** (**1.3 Transaminases (TA)**). The selection of this partner was expected to reduce or eliminate the risk of by-product formation. Since the bulky-ketoynone **147h** was not a substrate for the transaminases, there was no requirement to limit the equivalents of amine donor; hence 2 equivalents were used to effectively displace the equilibrium. The concentration of ketoynone **147c-e** was also reduced to 20 mM, thus ensuring the full conversion to β -enaminone **146c-e**, which can go forward in the annulation reaction.

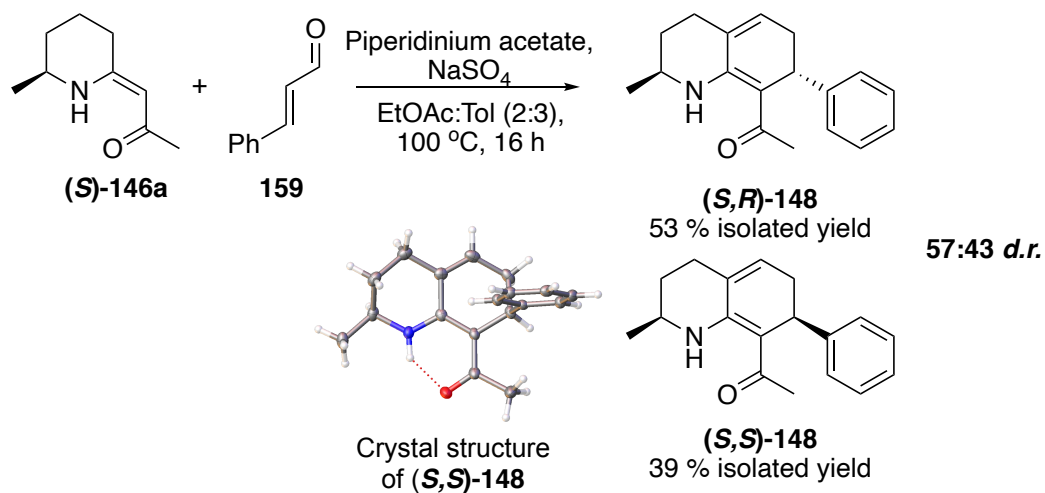


Scheme 51: The one-pot ATA-annulation cascade with a ketonone **147**, which does not readily undergo a transamination reaction. Reaction conditions: ATA (5 mg mL⁻¹), **147** (20 mM), bulky-bulky ketonone **147h** (40 mM), isopropylamine **111** (40 mM), DMSO (10%), PLP (1 mM), HEPES (5 mL, 100 mM, pH 7.5), 30 °C, 200 rpm, 24 h.

The transamination of ethoxy derivative **147c** followed by carbo-[3+3]-annulation with **147h** yields the THQ **158c** target in a 90 % yield when **ATA025** was employed, however when **ATA256** was used, the yield reduced to 39 %. The one-pot cascade proceeded poorly with aromatic substrates **147d** and **147e**, affording isolated yields of 10 % and 27 % respectively. These low yields were most likely due to the poor efficiency of the carbo-[3+3] annulation, as during isolation, the respective β -enaminone **146** intermediate was also present. Furthermore, only a small percentage of the remaining bulky-bulky ketonone **147h** was isolated; it was postulated that this was due to the degradation of the starting material. In light of this, increased equivalents of the ketonone **147h** were used in the annulation reaction; however, this caused issues with solubility in the reaction and thus this did not increase the isolated yield of the THQ product(s) **158** formed.

To show the versatility of cyclic β -enaminones **146** that could be produced, two further annulation reactions were explored using the methyl **146a** and phenyl **146d** β -enaminones. The first of these involved reacting the methyl-

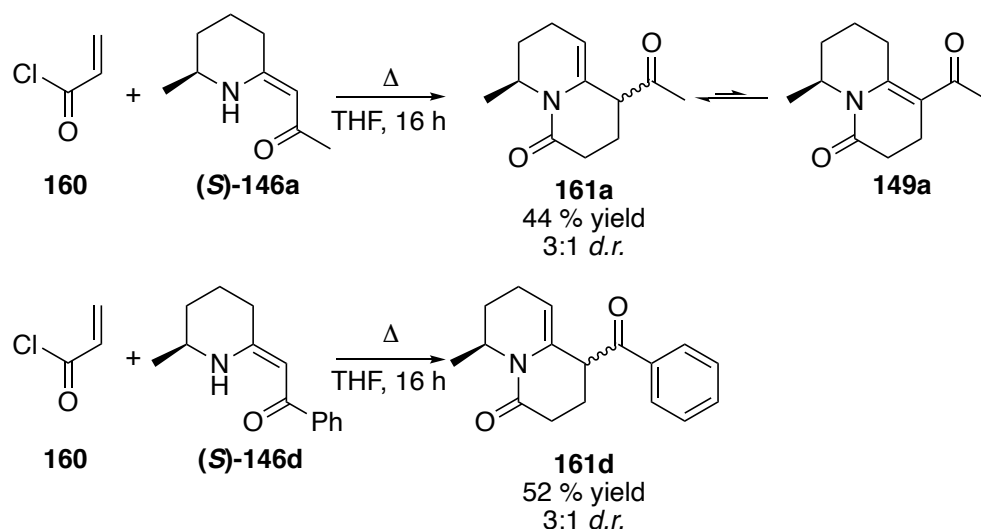
methyl derivative **146a** with cinnamaldehyde **159** in the presence of piperidinium acetate to complete a carbo-[3+3] annulation (**Scheme 52**).



*Scheme 52: The reaction of β -enaminone **(S)-146a** and cinnamaldehyde **159** to form two diastereomers of HHQ **148**, in a carbo-[3+3] annulation. *d.r.* was measured from the crude NMR.*

The carbo-[3+3] annulation provided two separable diastereomers **(S,R)-148** (53 % yield) and **(S,S)-148** (39 % yield). **(S,S)-148** was analysed by X-ray crystallography to determine the relative and absolute configuration of the diastereomers because NoE NMR studies were inconclusive, due to the separation of the chiral centres on the molecule being above the threshold of visualisation (4 Å). While the reaction was high yielding, the diastereomeric ratio (57:43 *d.r.*) produced was poorer than desired, and further efforts were made to epimerise this product, as it was thought that the most stable configuration of the ring system would have the phenyl substituent in the equatorial position. However, attempts to epimerise the products with bases such as potassium carbonate or sodium methoxide resulted in no change to the *d.r.*. It was noted that due to the planar nature of the hexadiene, the effect of axial/equatorial bias would be minimal. To remove the need for epimerisation, Gosh *et al.*¹³⁸ showed that treatment of the HHQ **148** with 2,3-dichloro-5,6-dicyanobenzoquinone (DDQ) would undergo aromatization to form a quinolone, leading to formation of a THQ and removing the second chiral centre.

The second annulation reaction performed took advantage of the nucleophilic amine on the cyclic β -enaminone. An aza-[3+3] annulation was performed by reacting the methyl-methyl derivative **146a** with acryloyl chloride **160** under anhydrous reflux conditions, which provided the lactam **(S)-161a** in a 44 % isolated yield (**Scheme 53**).

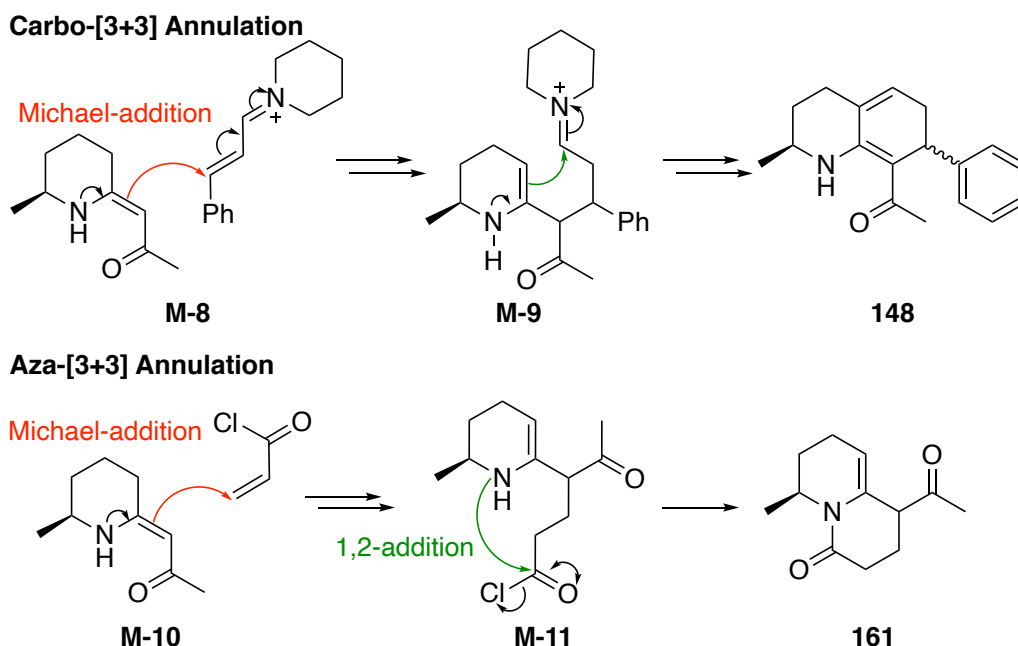


*Scheme 53: Aza-[3+3] annulation between acryloyl chloride and β -enaminone. *d.r.* was measured from crude NMR.*

Although it was assumed the most stable product would be the more conjugated tautomer **149a**, as suggested by previous literature with the 5-membered cyclic β -enaminones,^{139,140} the only product observed was the lactam **161a** with a 3:1 *d.r.*. By substituting the α -methyl **146a** for a bulkier α -phenyl β -enaminone derivative **146d**, it was thought the diastereomeric ratio would be improved due to stereofacial selectivity. In this case, the bulkier constituent gave a better yield (52 %) but showed no improvement of in the diastereomeric ratio (3:1 *d.r.*), suggesting that the substituent on the β -enaminone may have limited effects on the sterics of the ring due to distal proximity.

The different annulation reactions that took place highlight the diversity of the reactivity in the β -enaminones **146**. **Scheme 54** shows the proposed

mechanisms of the two different annulation reactions, taking advantage of the different nucleophilic centres on the β -enaminones **146**.



Scheme 54: The different nucleophilic attacks that take place via conjugate 1,4-addition. The two annulation routes then diversify allowing for two bi-cyclic amine scaffolds to be formed.

In both the carbo-[3+3] and aza-[3+3] annulation reaction it was hypothesised by Gosh *et al.*¹³⁸ that the dominating interaction during the first step would be the strong internal hydrogen bonding. Thus, the initial nucleophilic attack happens at the α -carbon, completing a 1,4-conjugate addition into the corresponding electrophile based on the 'hard-and-soft' concept. At this point, the reaction pathway diversifies depending on the electrophile being used. The iminium ion **M-9** is able to undergo a carbo-[3+3] annulation, to provide the HHQ **148**. In comparison acryloyl chloride derivative **M-11** allows for the nitrogen to attack the carbonyl forming a lactam **161a** in an aza-[3+3] annulation. These two reactions showcase the versatility of β -enaminones **146** reactive sites providing two different bi-cyclic alkaloid scaffolds.

2.3 Summary

Ketoynone substrates **147** were successfully synthesised *via* a four-step synthesis with moderate yields (26 – 89 %). To reduce the number of steps in the synthesis, a Sonogashira coupling was attempted, however, this coupling only worked with the aryl acid chlorides and was not pursued further.

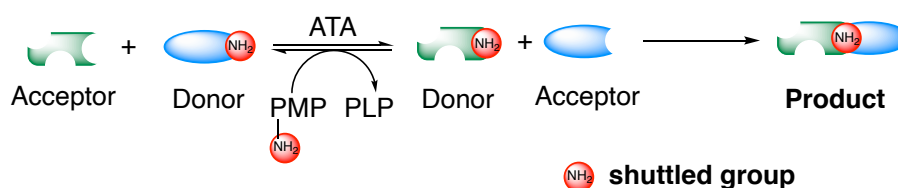
The ketoynone substrates **147** were then used to expand the scope of the ω -TA triggered intramolecular aza-Michael reaction cascade. The stereo and regioselectivity of the transaminase used in the reaction allows for the reaction of the prochiral ketoynone to be converted to β -enaminones **146** in good yields (43 – 95 %) and enantiomeric excess (83 - >99 %).

A novel one-pot tandem ATA-aza-Michael-annulation cascade was developed during these biotransformations, affording the highly functionalised THQ molecules **157** and **158**. This adds a new functional cascade to the toolbox of transamination reactions, which may be used in future synthesis.

To show the versatility of the cyclic β -enaminones and their multiple functional handles, two further annulation reactions were demonstrated, providing HHQ **148** and quinolizinone **161** in good to reasonable yields (92 % and 52 % respectively). Unfortunately, due to the nature of the compounds with no overall driving force for the selectivity, the diastereomeric ratio was low to moderate with the conditions used and further optimisation would be required to achieve a good diastereomeric excess.

**Part II - Development of *Amine Borrowing*
Methodology for the Synthesis of Complex
Alkaloids**

This chapter presents a new concept of *amine borrowing*. The approach involves a linear cascade and relies on the reversible shuttling of amine functionality from a donor molecule to an acceptor, resulting in the *in situ* generation of reactive species (**Scheme 55**). In the next step of the cascade, the ‘borrowed’ amine functionality is subsequently reincorporated into the donor to generate the desired target. While the concept can be extended to encompass a number of cascade sequences (**Scheme 42**), this chapter will focus on a linear cascade, initiated by an ATA (**Scheme 43**). At its best, the methodology allows for high atom economy and near stoichiometric equivalents of donor and acceptor, as well as potentially bypassing the need to handle toxic or highly reactive and unstable reagents. The strategy also enables the generation of complex targets, starting from relatively simple building blocks. Our idea of *amine borrowing* was developed from the catalytic hydrogen borrowing and shuttle catalysis concept, which was previously explained in **1.5 Shuttle Catalysis**.^{106,107}



Scheme 55: Amine functionality is shuttled from a donor to an acceptor molecule, triggering an intermolecular reaction between the species generated in situ, and meaning that the ‘borrowed’ group is reincorporated into the original donor molecule.

It was envisioned that three named reactions would be ideal for examining the scope of this *amine borrowing* methodology (**Scheme 43**). The selected reactions were the Knorr pyrrole synthesis as well as the Pictet-Spengler and Mannich reactions. These three reactions have been previously reported in conjunction with the use of ATAs, although not under the proposed *amine borrowing* conditions.^{88,105,141} This section will briefly introduce the work that has previously been completed using ATAs in a cascade with the above reactions, pointing out the differences, as well as exploring the *amine borrowing* methodology of interest.

3.0 Investigating the Transaminase-Mannich Cascade

3.1 Introduction

As discussed previously in **1.2.1 Biosynthesis of Alkaloids**, the Mannich reaction plays a key role in the biosynthesis of many alkaloids (**Scheme 1**), particularly in the synthesis of pyrrolidine and piperidine type alkaloids, derived from ornithine **10** and lysine **13**. Here, the amino acids undergo a decarboxylation reaction before further transformations to form cyclic imines. Subsequent Mannich-type nucleophilic attack forms a range of 2-substituted pyrroline and piperidine scaffolds that frequently occur in many natural products and active pharmaceutical ingredients (**Figure 5**).^{13,142}

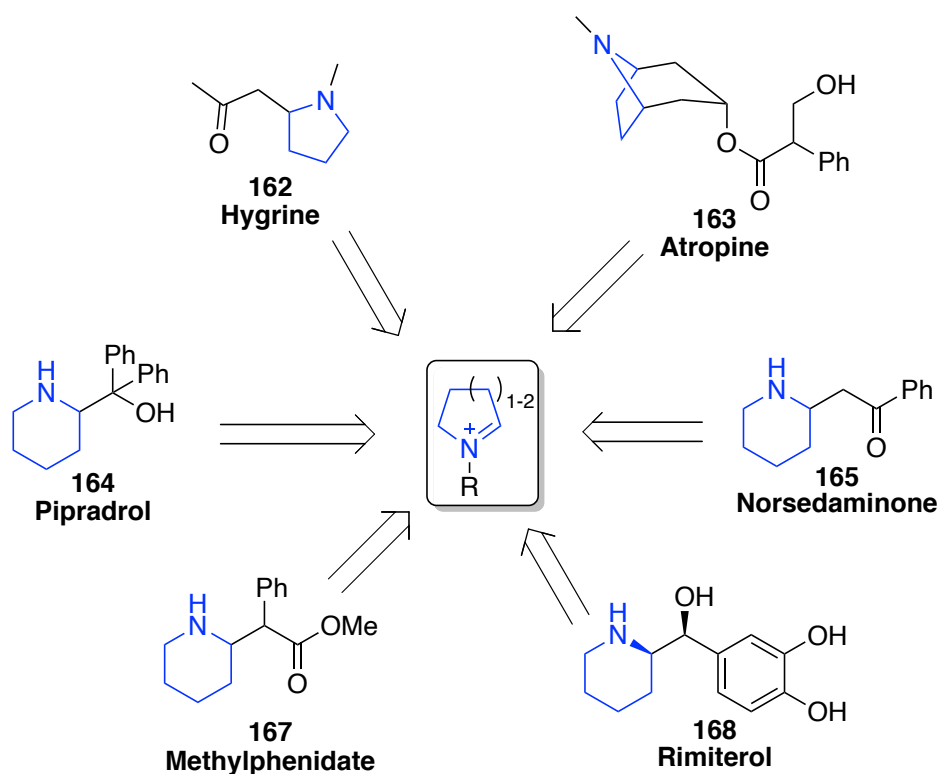
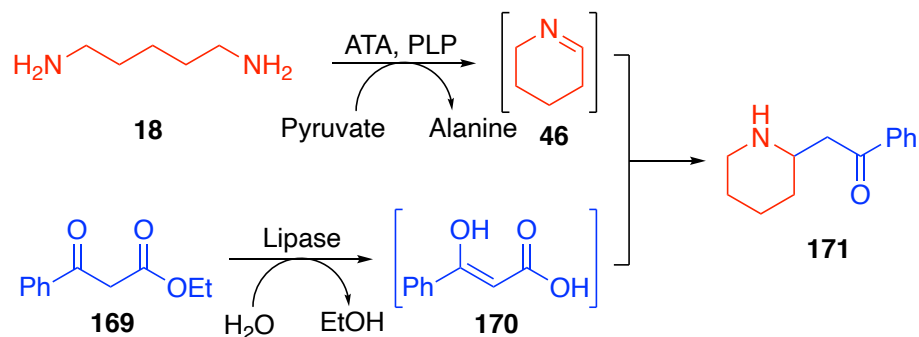


Figure 5: A range of 2-substituted pyrrolidine and piperidine natural products and pharmaceutical active ingredients, which are derived from the amino acids ornithine and lysine in their biosynthesis. These include hygrine **162**, atropine **163**, pipradrol **164**, norsedaminone **165**, methylphenidate **167** and rimiterol **168**.

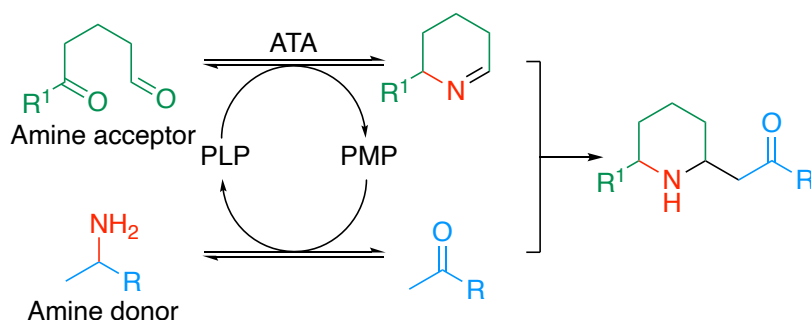
Due to the bioactive nature of the compounds shown in **Figure 5**, the Mannich reaction has been highly investigated, both with and without the presence of an organocatalyst, which is discussed in detail in **1.2.2 Chemical Synthesis of Alkaloids**.

Taking inspiration from the biosynthetic pathway of 2-substituted pyrrolidine and piperidines, Galman *et al.* integrated a transamination reaction with a Mannich reaction cascade (**Scheme 56**).¹⁴³



Scheme 56: The cascade reaction of an ATA-catalysed amination followed by a Mannich type reaction with a dicarbonyl formed by lipase-catalysed hydrolysis of ester **169**.¹⁴³

As in the biosynthesis of piperidine alkaloids, cadaverine **18** undergoes a transamination before cyclisation to form an imine **46**, which is readily attacked by the enolate moiety of 3-hydroxy-3-phenylacrylic acid **170**. Galman *et al.*¹⁴³ used this cascade to produce a range of 2-substituted pyrrolidine and piperidine alkaloid scaffolds in reasonable to high yields (55 – 73 %). It was proposed that by starting with a dialdehyde or keto aldehyde in the place of the cadaverine **18** (**Scheme 57**), this system would be an elegant example of *amine borrowing*.



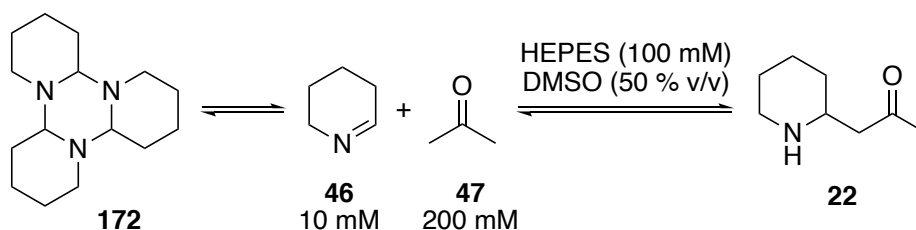
Scheme 57: The proposed scheme for the use of amine borrowing in combination with the Mannich reaction, starting from a dialdehyde/keto aldehyde as both the amine acceptor and external amine donor.

Scheme 57 shows the dicarbonyl undergoing transamination before forming an imine, which then acts as an electrophile for the enolate formed from the amine donor. This methodology differs from the examples demonstrated by Galman *et al.* as the amine donor is incorporated into the final compound.¹⁴³ The scope of the reaction can be increased to develop 2,6-disubstituted piperidine scaffold, accessed *via* incorporating an R¹ group.

3.2 Results and Discussion

3.2.1 Initial Screening of Mannich Reaction Conditions

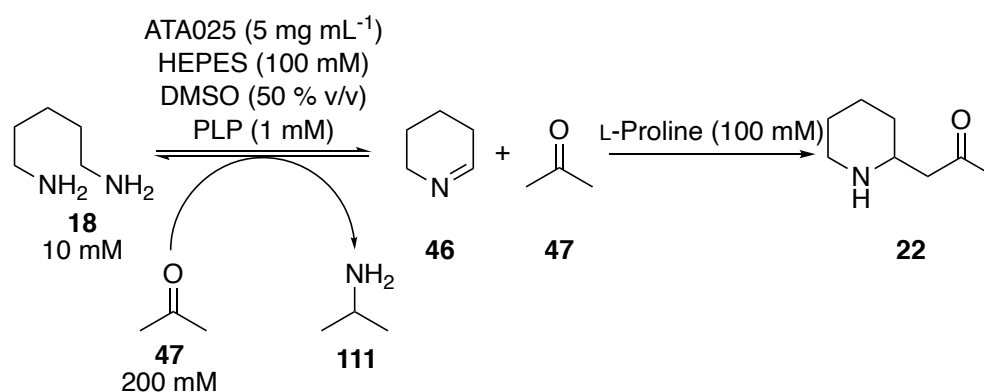
As proof that the Mannich reaction would occur under the conditions needed for the biotransformation to take place, an initial screen was undertaken that involved α -tripiperideine **172** and acetone **47** under these biotransformation conditions, where the results are shown in **Table 3**.



Entry	pH	L-Proline Conc.(mM)	GC Yield (%) 24 h
1	7	0	6
2	8	0	9
3	9	0	9
4	10	0	12
5	7	100	49
6	8	100	>99
7	9	100	99
8	10	100	94

Table 3: The initial screen of α -tripiperideine **172** and acetone **47**. Reaction conditions α -tripiperideine **172** (3.33 mmol), acetone **47** (20 equiv.), L-proline (0 or 10 equiv.), HEPES (100 mM, 1 mL), DMSO (50 % v/v), 30 °C, 200 rpm. Yield was measured by GC-FID. The results in the table are the mean of three replicates.

It is documented within previous work that α -tripiperideine **172** is in equilibrium with piperidine **46** under biotransformation conditions, with higher pHs displacing the equilibrium towards the stabilised trimer **172** formation.^{89,144} To allow for the Mannich reaction to take place with piperidine, this equilibrium needed to be exploited. Basic conditions are often required for the formation of the enolate; this is supported by the results in **Table 3, entries 1-4**, whereas the pH increase the conversion to pelletierine **22** also increases. However, the low conversion observed (12 %) is likely due to the unavailability of piperidine **46** due to the position of the equilibrium. By adding proline to activate the ketone, forming an enamine, the effect of the pH on the progress of the reaction decreases, therefore pH 8 provides the best conversion at >99 % (**Table 3, entry 6**). This screen was then completed with the imine generated *in situ* via a transaminase shown in **Table 4**.



Entry	pH	GC Yield (%)	
		24 h	48 h
1	7	2	6
2	7.5	8	18
3	8	9	19
4	8.5	15	31
5	9	16	38
6	10	29	74

Table 4: The initial test reaction introducing an enzyme into the screened Mannich conditions. Reaction conditions: cadaverine **18** (10 mM), acetone **47** (200 equiv.), L-proline (10 equiv.), ATA025 (5 mg mL⁻¹), HEPES (100 mM, 1 mL), DMSO (50 % v/v), 30 °C, 200 rpm. Yield was measured by GC-FID. The results in the table are the mean of three replicates.

The decrease in conversion to pelletierine **22** at pH 8 from >99 % (**Table 3, entry 6**) to 19 % (**Table 4, entry 3**) conversion, proved that the transaminase reaction is the rate determining step in the cascade and further optimisation of this step is needed. As discussed in Gomm *et al.*, cadaverine **18** gives superior conversions at the higher pHs due to the formation of the trimer **172**.⁸⁹ This correlates with the increase in conversion seen as the pH increases in this experiment and can be seen in **Table 4**, with pH 10 giving the best conversion of 74 % after 48 h. While these reactions show high conversions to the natural product pelletierine **22**, the conditions used are not true *amine borrowing*, due to the amine functionality being shuttled from cadaverine **18** molecule to an external acceptor, acetone **47** forming IPA **111** as a by-product. True *amine borrowing* conditions would involve all components reacting further to be part of the final product, therefore the atom economy of the total reaction is 100 %. As previously discussed, the final aim to implement *amine borrowing* conditions in the ATA-Mannich reaction cascade was to induce a dicarbonyl, as the amine acceptor, which will cyclise forming an imine to react in the Mannich reaction.

3.2.3 Amine Borrowing Screening

An initial screen of the dialdehyde glutaraldehyde **173a** with IPA **111** was conducted, however this showed no conversion to pelletierine **22** with **ATA025**. This reaction was then further investigated with the amine donor *o*-xylylenediamine **119** to explore the ability of glutaraldehyde **173a** as an amine acceptor, as well as a range of different commercial enzymes (**ATA113**, **ATA256**, **ATA025** and **ATA117**), these screens also show no conversion. These results can easily be explained by the common use of glutaraldehyde to cross-link enzymes, meaning that the substrate is not available for the reaction as it has already reacted with the protein.¹⁴⁵

By changing the nature of the dicarbonyl from a dialdehyde to a ketoaldehyde it was thought that the cross-linking effect could be negated,

due to the decrease in reactivity. Therefore, three different dialdehydes and ketoaldehydes (**Figure 6**) were chosen to screen further. These substrates are based off previously reported 'smart' amine donors that have been developed by Gomm *et al.* and Green *et al.*, and these are considered to drive the TA reaction equilibrium towards the desired product by cyclisation and formation of an imine.^{87–89}

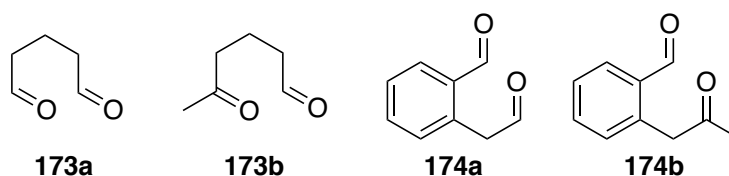
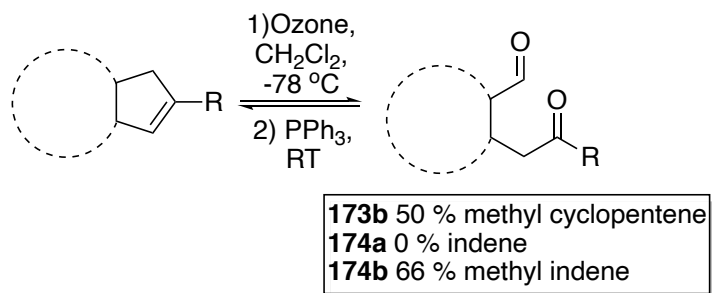


Figure 6: Glutaraldehyde **173a**, and the three potential dicarbonyl substrates for use in the ATA-Mannich reaction cascade.

The new substrates were not commercially available but were easily synthesised in one-step, which involved an ozonolysis reaction from the corresponding cyclic alkene (**Scheme 58**).



Scheme 58: The synthesis of dialdehyde **174a**, and ketoaldehydes **173b** and **174b** via ozonolysis.

The ozonolysis of the methylated alkenes proceeded with reasonable yields to form ketoaldehydes, 5-oxohexanal **173b** (50 %) and 2-(2-oxopropyl)benzaldehyde **174b** (66 %). Further optimisation of this reaction was not undertaken as the yield was viewed to be acceptable. Purification of 2-(2-oxoethyl)benzaldehyde **174a** was difficult due to co-elution of the dialdehyde and triphenylphosphine oxide. To improve the purification in future, the use of dimethyl sulfide could be used as the reaction quench instead of triphenylphosphine.

The initial screen of the substrates was conducted with *o*-xylylenediamine **119**, as there is an indicative colour-change associated with conversion. However, this screen is very sensitive and while a colour change was observed, this did not correspond to detectable activity on GC-FID (**Table 5**).

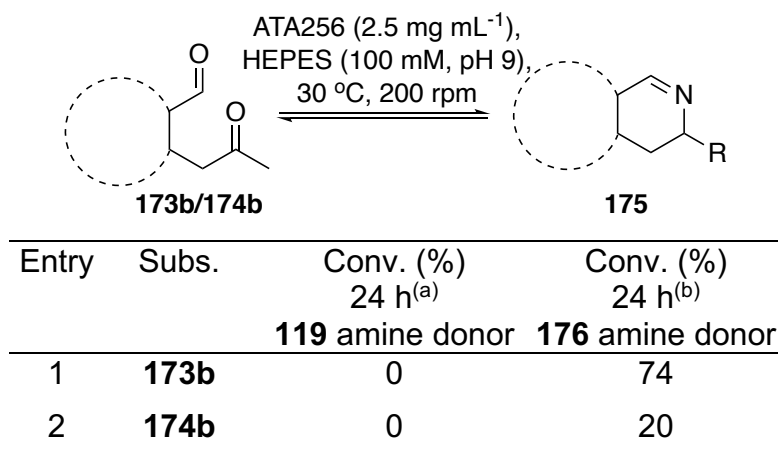
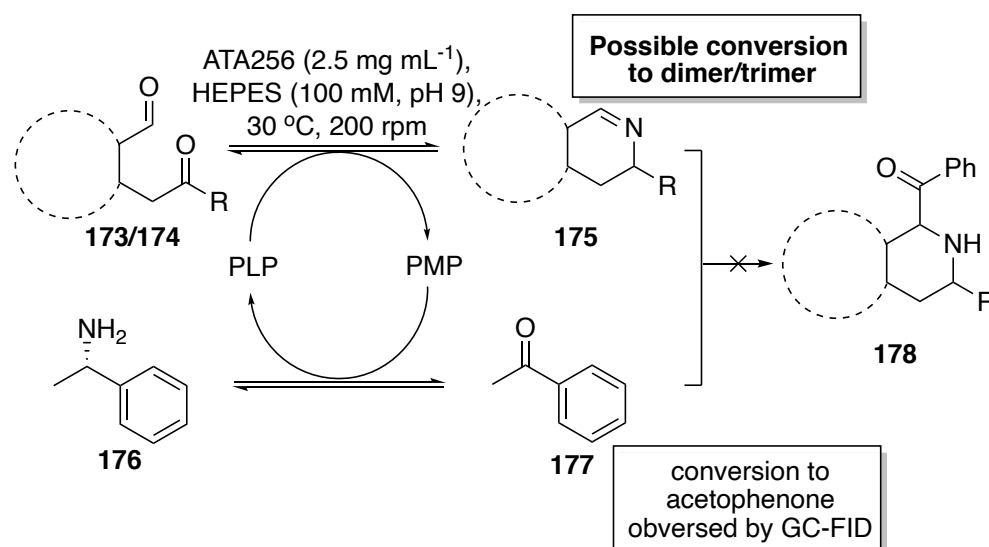


*Table 5: The screen testing the ability of the dicarbonyls to act as amine acceptors. Reaction conditions: dicarbonyl **173/174b** (20 mM), *o*-xylylenediamine **119** or methylbenzylamine **176** (2 equiv.), ATA256 (5 mg mL⁻¹), HEPES (100 mM, pH 8, 1 mL), DMSO (20 % v/v), 30 °C, 200 rpm. Conversion was measured by GC-FID. The results in the table are the mean of three replicates. a) conversion of starting dicarbonyl to cyclic imine. b) conversion of MBA to acetophenone.*

The results from GC-FID analysis often do not provide sufficient information about the progress of a reaction and do not always provide qualitative information. The imine formed in this reaction has the potential to tautomerize and dimerise/trimerise, making GC analysis challenging due to high boiling points. Evidence in support of the formation of alternative products came from performing a reaction with methylbenzylamine (MBA) **167** as the donor (**Table 5**). The GC trace showed the formation of acetophenone **177** but did not show any conversion of the dicarbonyl to the expected Mannich reaction product shown in **Scheme 59**.



Scheme 59: The ATA- Mannich reaction cascade expected to take place with the dicarbonyl as the amine acceptor and MBA **176** as the amine donor.

The lack of conversion to the target product **178** can be explained if the cyclic imine forms a trimer, however with the addition of proline into the reaction mixture there is the potential for the catalytic formation of the final desired compound **178**.

3.3 Summary

This work and previous work by Galman *et al.*¹⁴³ has shown that it is possible to initiate a Mannich reaction with an ATA. The reaction between piperidine **46** and acetone **47** initially took place with disappointing conversion (6 - 12 %) across the range of pH screened. However, when proline was added to the reaction mixture conversion increased to >99 %, the proline acts to activate the ketone, forming an enamine. The other advantage of using proline in the Mannich reaction is the carboxyl group also allows hydrogen bonding between the proline and imine allowing for asymmetric synthesis.^{19,20}

When an ATA is introduced into system to form piperidine **46** *in situ* from cadaverine **18**, the conversion increases as the pH increases, providing a conversion of 74 % to the Mannich product. To introduce *amine borrowing* conditions, glutaraldehyde **173a** was used as the amine acceptor, with the

use of an internal amine donor. However, glutaraldehyde **173a** was found to be a poor acceptor, potentially due to glutaraldehyde **173a** having high reactivity and use as a cross-linker to immobilise enzymes.

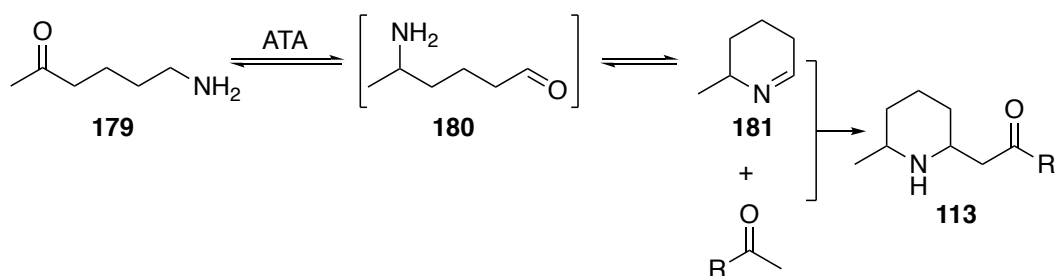
With the poor conversion shown by glutaraldehyde, other dicarbonyls were synthesised *via* an ozonolysis reaction with reasonable yield (50 – 66 %) and investigated to determine whether they were good acceptors. The conversion of MBA **176** to acetophenone **177** with both ketoaldehydes, 5-oxohexanal **173b** and 2-(2-oxopropyl)benzaldehyde **174b** (74 % and 20 % respectively) indicates that these are substrates for the ATA. However, during these reactions none of the expected Mannich product **178** was observed due to the trimerisation of imine **175**. Due to these results showing no conversion to the desired products under *amine borrowing* conditions, further investigation into the reaction conditions is required for the ATA-Mannich cascade to reach its full potential.

3.4 Future work

This study has identified potential dicarbonyl substrates to use in the ATA-Mannich reaction cascade. However, further screening of reaction conditions is required to improve conversion with all of the dicarbonyl substrates. This screening ideally would include a variety of ATAs, both commercial and cultured in house. Transaminases that are known to accept linear diamines would offer a potential solution to this class of acceptor along with many other TAs that might readily accept this class of amine acceptors.

Once an appropriate TA has been found for the dicarbonyl substrates, conditions can be screened to improve the Mannich reaction with a range of substrates. It would also be advantageous to introduce and screen a range of organocatalysts, including proline, allowing for a faster asymmetric reaction to take place.

Furthermore, the ATA- Mannich reaction cascade substrate scope could be increased by using a substrate in which the amine moiety is shuttled across the molecule, without the need for an external amine donor. An example of this type of substrate is 6-aminoheptan-2-one **179** acts the amine donor and acceptor, and the amine moiety is shuttled from the 6-position to the 2-position forming the intermediate **180**, which then readily cyclises forming the imine **181**. This imine **181** is then able to undergo a Mannich reaction with a range of ketones (**Scheme 60**).



*Scheme 60: A potential ATA initiated amine borrowing cascade based on the Mannich reaction of **181** with a range of ketones.*

4.0 Exploring the Transaminase-Knorr Pyrrole Synthesis Cascade

4.1 Introduction

The most prominent biological use of a pyrrole is as a key structural unit of heme- and porphyrinoid-related cofactors, such as heme b, chlorophyll and vitamin B₁₂, with porphobilinogen **184** as a biosynthetic precursor.¹⁴⁶ The pyrrole ring is often found in marine natural products such as marinopyrrole B **185**, which is known to have anti-bacterial properties (**Figure 7**).¹⁴⁷ The biological and pharmacological properties have stimulated the interest in pyrrole scaffolds, where the cholesterol-lowering agent Atorvastatin **182** and cancer treatment Sunitinib **183** are just two examples of the many pyrrole-containing drug molecules.¹⁴⁸

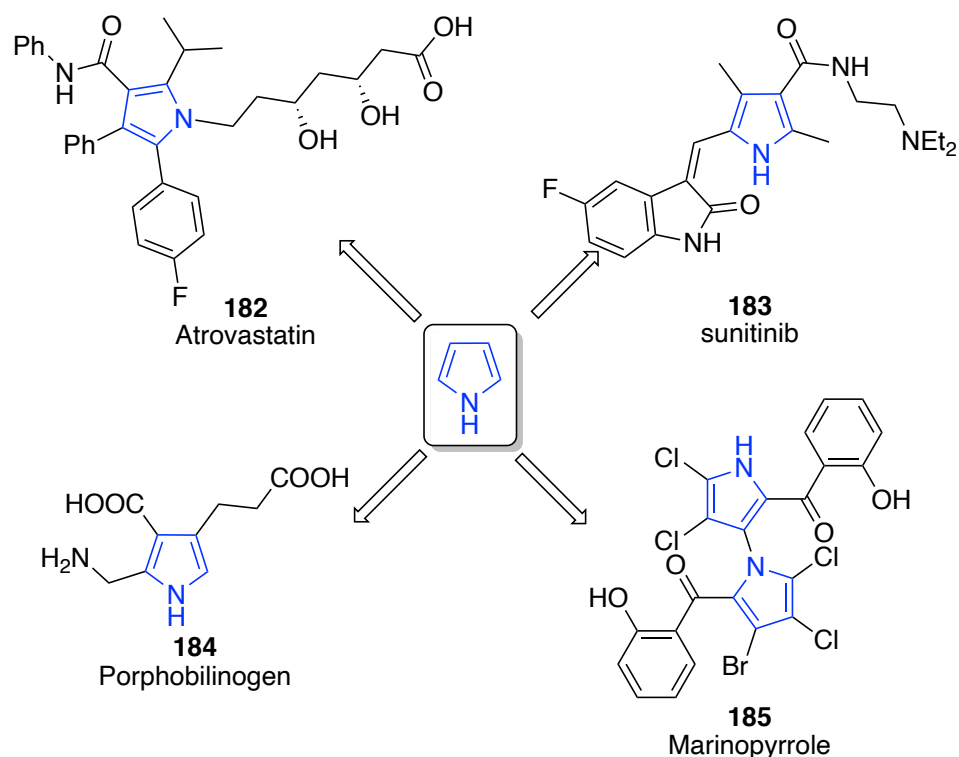
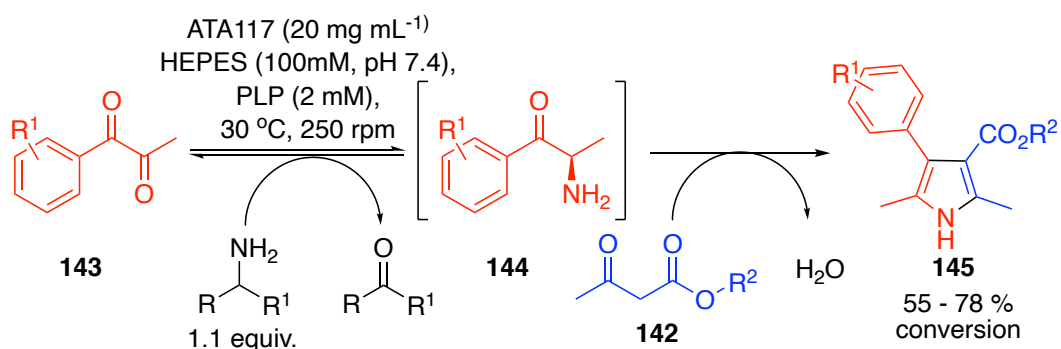


Figure 7: A range of pyrrole containing natural products and pharmaceutical active molecules. These include atorvastatin **182**, sunitinib **183**, porphobilinogen **184**, marinopyrrole B **185**.

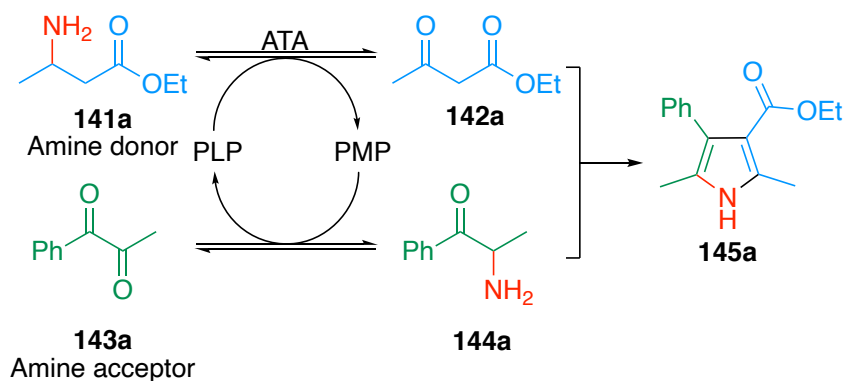
The biological and chemical interest in pyrroles has meant that the synthesis of these scaffolds has been highly investigated. Namely, in 1885 Knorr reported the formation of a highly substituted pyrrole *via* a condensation reaction of an α -aminoketone with a β -dicarbonyl, and this reaction has been investigated more over the years.⁴³ This approach is discussed in more detail in **1.2.2 Chemical Synthesis of Alkaloids**.

Xu *et al.* have recently reported the coupling of an α -diketone **143** with a β -keto ester **142** in an ATA- Knorr Pyrrole Synthesis linear cascade. The α -amino ketone **144** is generated *in situ* via an **ATA117**-catalysed amination of the α -diketone **143** with an external amine donor. **144** is then able to undergo a spontaneous Knorr Pyrrole Synthesis affording pyrrole **145** in reasonable conversion (55 – 78 %) (**Scheme 61**).¹⁰⁵



Scheme 61: A one-pot transamination of an α -diketone **143**, using an external amine donor **144**, followed by spontaneous condensation with β -keto ester **142**, affording pyrrole **145**, reported by Xu *et al.*¹⁰⁵

During the course of the ATA- Knorr Pyrrole Synthesis cascade, there was also the potential for **142** to undergo amination. Xu *et al.* theorised that the unwanted amination of β -keto ester **142** occurs in a reversible manner, and the thermodynamic sink associated with the formation of pyrrole **145** drives the cascade to completion. By replacing the β -keto ester with a β -amino ester, it was anticipated that the reaction could take place without the need for an external amine donor (**Scheme 62**).



Scheme 62: The shuttling of an amine group from a donor molecule to an acceptor molecule with the use of a transaminase, followed by a spontaneous coupling of the products, as demonstrated recently by Xu *et al.*¹⁰⁵

This reaction was previously discussed in **1.5.1 Shuttle Catalysis as Part of a Larger Cycle** as an introduction to *amine borrowing*. While Xu *et al.* showed the first example of this type of shuttle catalysis, the high enzyme loading, high amine donor equivalents and low substrate concentrations used meant that the conditions are not optimal.¹⁰⁵ It was proposed that a stoichiometric ratio of reagents would provide a reaction with high atom economy, with water remaining as the only by-product, therefore opening the door to a greener, more sustainable synthetic route to pyrrole scaffolds. The reaction cascade shown in **Scheme 62** shows compound **144a** being formed *in situ*, as it readily self-condenses under traditional Knorr pyrrole synthesis conditions. Following its generation *in situ*, compound **144a** can undergo reaction with ester **142a** to form the desired product **145a**.

4.2 Results and Discussion

4.2.1 Optimisation of ATA- Knorr Pyrrole Synthesis Cascade

Initial screening concentrated on the same substrates reported by Xu *et al.*¹⁰⁵ and shown in **Scheme 38**. The reported conditions were sub-optimal as a result of high enzyme-loading (20 mg mL⁻¹), 10 equivalents of amine donor and low substrate concentration (5 mM). Enzymes are viewed as a more cost-effective and sustainable alternative to expensive metal catalysts, and they do not typically require high loading. For example, between 1 - 10 mg mL⁻¹ of lyophilised cell free extract is typically sufficient for most biotransformations with substrate loading of 10 – 100 mg mL⁻¹.^{69,87,149,150} Therefore it was believed that the enzyme loading could be decreased from that initially reported by Xu *et al.*¹⁰⁵

The first step in the optimisation process was to determine the necessary enzyme loading, as shown in **Table 6, entries 1-5**. This was followed by a pH screen (**Table 6, entries 6-10**) and concentration screen (**Table 6, entries 11-20**).

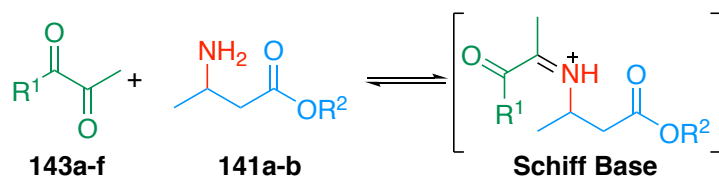
The reported conversion of 58 % by Xu *et al.*¹⁰⁵ was improved to 73 % under conditions with the reported enzyme loading, but lower equivalents of racemic amine donor (2 equiv.) (**Table 6, entry 1**). This means that only one equivalent of the amine (the (*R*)-enantiomer) is actually available to the (*R*)-selective **ATA117**. As expected, when the enzyme loading was decreased, the conversion also decreased. A compromise was needed between the enzyme loading and conversion; therefore, we proposed that by using 5 mg mL⁻¹, which gave a conversion of 48 % (**Table 6, entry 3**), the potential to further optimise would allow an increase in the conversion.

Further screening of suitable pHs with 5 mg mL⁻¹ (**Table 6, entries 6-10**) increased the conversion from 55 % (**Table 6, entry 8**) after 48 h to 75 % (**Table 6, entry 10**) after 72 h; indicating that the ATA- Knorr Pyrrole Synthesis perform better at higher pHs This is potentially due to the transamination reaction preferring the more alkali conditions by ensuring the amine is unprotonated and hence, is increasing its availability as a nucleophile.

The final stage of the screening process involved altering the concentration of diketone **130a** (**Table 6, entries 11-20**). Increasing the concentration of diketone to 10 mM increased the conversion to pyrrole product **145a** from 75 % to 93 %. This positive correlation trend continues until 40 mM (97 %, **Table 6, entry 14**) and is most likely due to an increased rate in the Knorr pyrrole synthesis reaction with the increase in concentration. As the concentration increases further between 50 – 100 mM (**Table 6, entries 15-20**), the conversion to the final pyrrole product **145a** decreases. This is likely due to enzyme inhibition at higher concentrations. At higher concentration (50 - 100 mM), the HPLC trace indicated an additional peak, suggesting that there was degradation in the reaction mixture or further side reactions were occurring. For these reasons, optimal concentration was determined to be 40 mM (**Table 6, entry 14**).

In these reaction conditions there is the possibility of the two starting materials reactivity, forming a Schiff base as shown in **Scheme 63**. This

Schiff base does not react further to form a by-product as there is no nucleophilic characteristic due to its highly conjugated nature. Water can then act as a nucleophile and hydrolyse the Schiff base, pushing the equilibrium into the backwards directing towards into the starting material, providing an equilibrium in the reaction so the ATA- Knorr Pyrrole Synthesis cascade can take place.



Scheme 63: The reaction between diketone **143a-f** and β -amino ester **141a-b** to form a Schiff base in equilibrium.

This initial screen established that the best conditions for the ATA- Knorr Pyrrole Synthesis cascade were 5 mg mL⁻¹, 40 mM diketone substrate at pH 9 and therefore these conditions were used to screen a range of diketone substrates as discussed below.

4.2.2 Preparative Scale of ATA- Knorr Pyrrole Synthesis Cascade

Using the optimised conditions discussed above, the reaction was scaled-up with a number of substrates, as shown in **Table 7**.

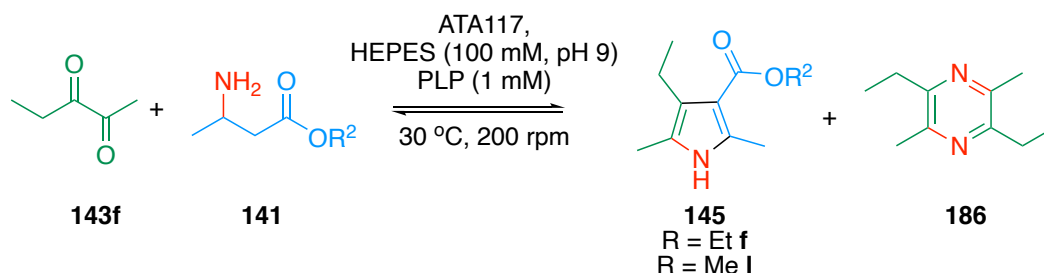
Reaction scheme: Diketone **143a-f** (R¹-substituted) + β-amino ester **141a-b** (OR²-substituted) → Pyrrole **145a-l** (R¹ and OR² substituents).

Entry	Product	R ¹	R ²	β-amino ester Equiv.	Conv. (%) 72 h ^(a)	Yield (%) ^(b)
1	a	Ph	Et	2 ^(e)	90	52
2	b	<i>p</i> -CF ₃ Ph	Et	2 ^(e)	99	64
3	c	(<i>m</i> -Cl) ₂ Ph	Et	2 ^(e)	78	46
4	d	<i>p</i> -NO ₂ Ph	Et	2 ^(e)	41	25
5	e	<i>p</i> -NH ₂ Ph	Et	2 ^(e)	83	54 ^(c)
6	f	Et	Et	2 ^(e)	34	28
7	g	Ph	Me ^(d)	1 ^(d)	87	55
8	h	<i>p</i> -CF ₃ Ph	Me ^(d)	1 ^(d)	44	15
9	i	(<i>m</i> -Cl) ₂ Ph	Me ^(d)	1 ^(d)	95	80
10	j	<i>p</i> -NO ₂ Ph	Me ^(d)	1 ^(d)	44	32
11	k	<i>p</i> -NH ₂ Ph	Me ^(d)	1 ^(d)	76	55 ^(c)
12	l	Et	Me ^(d)	1 ^(d)	25	19

*Table 7: Preparative scale reactions with a range of diketone substrates. Reaction conditions, diketone **143a-f** (40 mM), ethyl 3-aminobutanoate **141a** (80 mM (racemic)), HEPES (100 mM, pH 9, 10 mL), **ATA117** (5 mg ml⁻¹), DMSO (10 % v/v), 30 °C, 200 rpm. (a) Conversion was measured on the HPLC, (b) isolated yield after column chromatography, (c) isolated yield after prep HPLC, (d) concentration of enantiopure methyl (R)-3-aminobutanoate (**R**)-**141b** reduced to 40 mM. (e) racemic ethyl 3-aminobutanoate **141a**, only 1 equiv. available to the enzyme.*

The diketone substrates **143a-f** were chosen to show a range of electronic variations on the aromatic ring from weakly (**143b**) to strongly (**143d**) electron withdrawing groups and an electron donating group **143e**, along with an aliphatic diketone **143f**. This range of electronics on R¹ was designed to investigate the efficiency and diversity of the Knorr pyrrole synthesis.

ATA117 showed good conversion across the aromatic substrate range to the corresponding pyrrole products **145a-e** (41 - 90 %) (**Table 7, entries 1-5**). There seemed to be no correlation between conversion and the electronic substituent effects on the ring, indicating that the electronics on the ring do not have an effect in the Knorr pyrrole synthesis. Furthermore, the poor conversion of the alkyl diketone **143f** with both amine donors (34 % (**Table 7, entry 6**), 25 % (**Table 7, entry 12**)) was expected due to the reported production of the pyrazine homodimer product **186** (**Scheme 64**). However, this potential side product was never isolated. It has been previously reported that the production of pyrazine **186** decreases at lower pHs,¹⁰⁵ however previous screening (**Table 6**) shows higher conversion to the pyrrole **145f** as the pH increases, and this is most likely due to the increased efficiency of the transaminase reaction. As a result, the formation of pyrazine **186** side product has been deemed to be unavoidable.



*Scheme 64: The potential products from the transamination reaction of diketone **143f**, including the coupling of the two products to give pyrrole **145f,l**, and the homocoupling of the amine produced to give pyrazine **186**.*

Having achieved good conversion with racemic ethyl 3-aminobutanoate **141a**, using racemic amine meant that only one equivalent of donor was available to the enzyme. To investigate the substrate scope further, one equivalent of enantiopure methyl (*R*)-3-aminobutanoate (*R*)-**141b** was introduced into the reaction (**Table 7, entries 7-12**). In most cases the conversion was slightly reduced across the range of substrates tested, with the exception of (*m*-Cl)₂Ph substrate where the conversion increased from 78 % to 95 % (**Table 7 entries 3 and 9**). The reduced conversion is

potentially due to the enzyme accepting both enantiomers of the racemic amine donor **141a**, thus driving up the number of equivalents in the reaction.

4.3 Summary

A range of pyrrole derivatives **145a-I** were successfully synthesised *via* an ATA-Knorr pyrrole synthesis cascade, with the aryl substrates showing good to excellent conversion (41 - 99%). Notably, these conversions were achieved with only one equivalent of amine donor available to the enzyme, due to it being used in its racemic form. Unfortunately, when an aliphatic R-group was used, the conversion dropped significantly to 25 % or 34 % depending on the amine donor used, which was thought to be due to a side reaction that was occurring. These results improved upon previously reported results by Xu *et al.*¹⁰⁵ and reduced the enzyme loading, increased the substrate range and increased the overall conversion of the substrates.

The potential side reaction that can be seen to occur (**Scheme 64**) highlights the reasons that the production of reactive amino ketones *in situ* is advantageous to the Knorr pyrrole synthesis. It is well documented that during the Knorr pyrrole synthesis, the α -amino ketone **144f** readily condenses, forming pyrazine **186**.¹⁵¹ This example is the perfect justification for the development of shuttle biocatalysis methodology, and more specifically, *amine borrowing* methodology. However, perhaps a less elegant aspect of this approach is the loss of the ATA-installed chiral centre during the condensation reaction. It can therefore be proposed that this *amine borrowing* shuttle methodology is better suited to the synthesis of more complex chiral products, and this will be the subject of the next section (**5.0 Studying the Transaminase-Pictet Spengler**).

These results show the ability of ATAs to shuttle amine functionality across molecular frameworks as part of an *amine borrowing* cycle, forming a thermodynamic sink to drive the reaction to completion. The enzyme-triggered Knorr pyrrole reactions presented here represent a rare example of the use of stoichiometric equivalents of an amine donor to achieve near quantitative conversions of products and beautifully demonstrates the

power of developing biocatalytic reactions coupled to thermodynamically favourable spontaneous cyclisation reactions as an alternative to more traditional methods.

4.4 Future Work

During this work, the effect of altering the R¹-substituent was investigated with a range of aromatic rings **143a-e** incorporating differing electronic properties. Additionally, a single aliphatic derivative **143f** was studied. Screening the conditions used for the successful ethyl derivative **143f** would potentially increase the low conversions obtained (25 and 34 %) during this investigation, balancing the production of pyrrole **145** and pyrazine **186**. Once these conditions are optimised further, screening other aliphatic groups at the R¹ position could increase the substrate scope, and diversify the pool of products that can be generated by this optimised methodology.

Exploration of the ATA- Knorr Pyrrole Synthesis cascade could also be expanded by altering the R²-substituent to an alternative ester or an amide and a range of electron withdrawing groups could also be explored. Increasing the substrate scope by substituting at this position also offers the possibility of adding extra functional handles to the pyrrole, which can be used in further synthetic manipulations in the generation of higher value chemicals.

5.0 Studying the Transaminase-Pictet Spengler Reaction Cascade

5.1 Introduction

A portion of the work completed in this chapter was carried out in collaboration Dr James Ryan.

Tetrahydroisoquinolines (THIQ) are privileged scaffolds and core motifs in many alkaloids and structurally complex synthetic products. Several THIQs have physiological and therapeutic significance, and many are registered drugs, including solifenacin **187** (bladder control), emetine **188** (anti-protozoal) and norcoclaurine **32**, which is used as an intermediate in the total synthesis of morphine **2**¹⁵² (**Figure 8**). THIQ-containing molecules have also been applied as ligands in asymmetric catalysis.^{153–156}

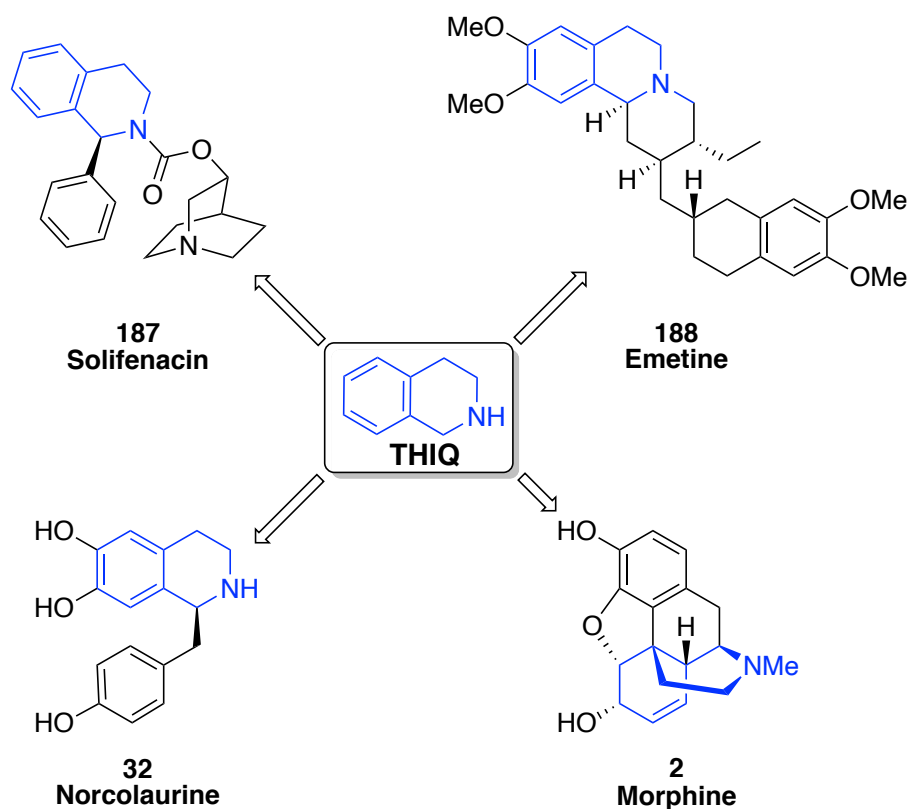
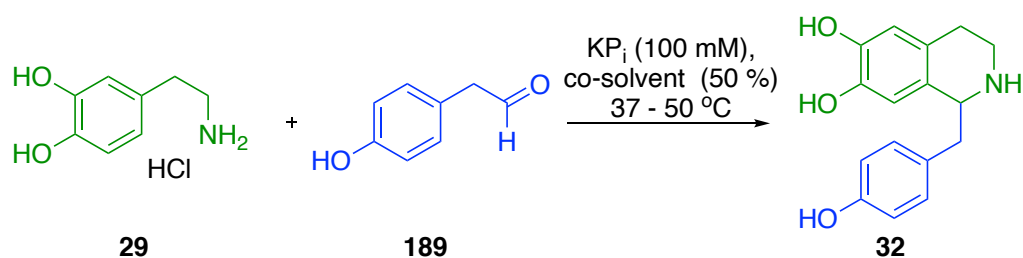


Figure 8: Pharmaceutically relevant molecules Solifenacin **187**, and emetine **188** containing a THIQ moiety highlighted in blue, along with the key intermediate Norcoclaurine **32**, used in the synthesis of morphine **2**.

While working with norcoclaurine synthases (NCSs), Pesnot *et al.* discovered that the background chemical reaction observed was due to the

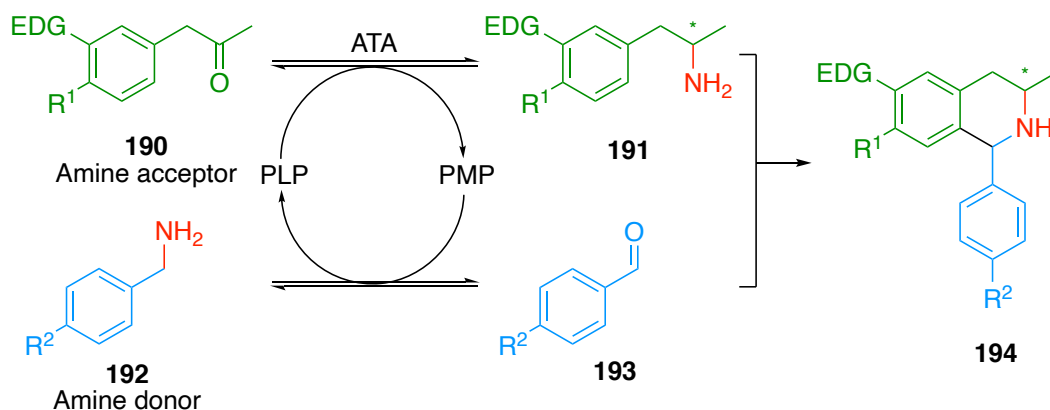
KP_i catalysing the Pictet-Spengler reaction (**Scheme 65**), as discussed previously in **1.2.2 Chemical Synthesis of Alkaloids**.^{38,39}



Scheme 65: The KP_i-catalysed background reaction that takes place during the NCS biotransformation, as discovered by Pesnot *et al.*⁴¹

Once the catalytic capability of the KP_i buffer was established, Pesnot *et al.* further explored this with a range of aldehydes, achieving reasonable to good conversions (41 – 88 %).⁴¹ More recently Zhao *et al.* reported the use of KP_i to catalyse a Pictet-Spengler reaction between dopamine and a range of more challenging ketones. While some ketones gave excellent conversions (95 %), there were a few cases where significantly lower conversion (11 %) was achieved.⁴²

We envisaged optimising the ATA- Pictet-Spengler reaction cascade under *amine borrowing* conditions (**1.5.1 Shuttle Catalysis as Part of a Larger Cycle**) (**Scheme 66**).



Scheme 66: General reaction scheme for proposed amine borrowing ATA-Pictet-Spengler cascade reaction.

KP_i-catalysed Pictet-Spengler reactions offer an ideal opportunity to showcase the *amine borrowing* methodology. Unlike the previous examples of the ATA- Knorr Pyrrole Synthesis cascade, where the chiral centre installed by the ATA is lost, the Pictet-Spengler reaction example uses a pro-chiral ketone **190** and leads to the installation of a chiral centre. This reaction generates the reactive intermediates, which undergo a Pictet-Spengler reaction and form a chiral THIQ **194**.

5.2 Results and Discussion

5.2.1 Chemical Synthesis of Substrates **190**

Previous studies have shown phenylethylamines with an electron-donating group (EDG) in the *meta* position play a key role in the reaction mechanism (**Scheme 9**), as they possess increased electron density at the point of ring closure, which facilitates the nucleophilic attack of the imine.^{36,41} Therefore, the substrates used in the studies conducted here were limited to those bearing an electron-donating group (EDG) in the *meta* position on the ring (**Figure 9**). It was envisaged that a range of different EDGs could be tested and a potential pattern may be established. Given that ATAs convert pro-chiral ketones to chiral amines, typically with high enantiomeric excess,⁵³ the focus was placed on developing the methodology using ketones **190**, rather than aldehydes **195**.

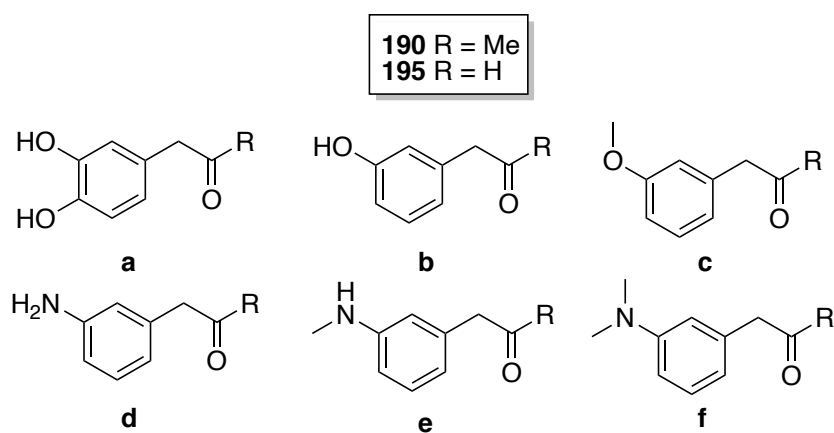
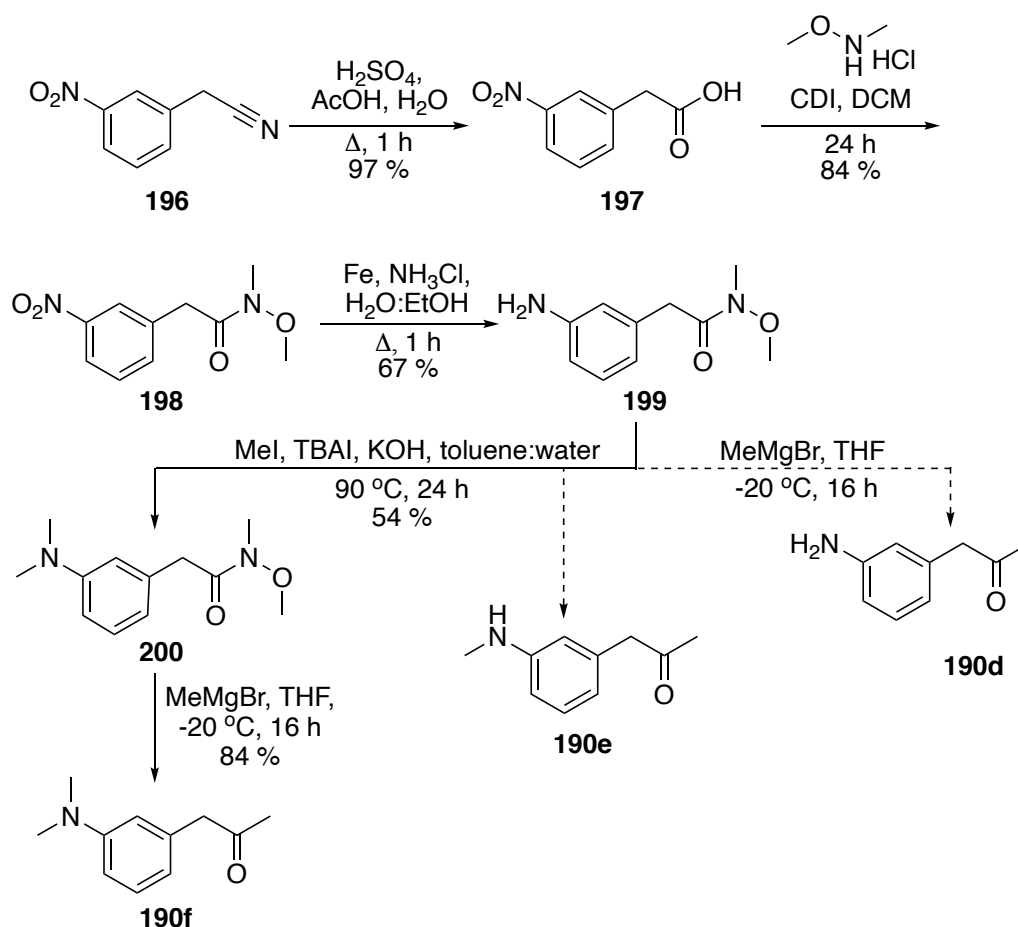


Figure 9: Selected ketone substrates used to explore the ATA-Pictet-Spengler cascade.

Only a handful of the proposed substrates were commercially available, and the others were readily synthesised (**Scheme 67** and **Table 8**). The nitrogen-substituted derivatives were the more challenging substrates to synthesise, having previously been prepared by a palladium-coupled reaction using Zheda-Phos or an indole-based ligand.^{159,160} These ligands are not commercially available and their preparation requires several synthetic steps and so an alternative synthesis was devised (**Scheme 67**).



*Scheme 67: The synthetic pathway starting from the commercially available 2-(3-nitrophenyl)acetonitrile **196**, forming the Weinreb amide **198**, before the nitro group is fully reduced and the pathway diverged to give three separate potential substrates **190d-f**.*

The hydrolysis of 2-(3-nitrophenyl)acetonitrile **196** proceeded in high yield (97 %), and the product was carried forward without the need for purification. Formation of Weinreb amide **198** was achieved using the peptide coupling agent 1,1'-carbonyldiimidazole (CDI) in good yield (84 %). Reduction of the nitro group was carried out using iron, and at this point the

synthetic route be could diversified to form either the dimethylated amine **190f** or the aniline derivative **190d**. Methylation of the aniline using methyl iodide gave moderate yield due to over methylation of the amine to give *N,N,N*-trimethyl-3-(2-oxopropyl)benzenaminium as the prevalent by-product, however this by-product was not isolated during purification, merely seen by analytical methods. The addition of the Grignard reagent methylmagnesium bromide into the Weinreb amide proceeded in good yield (84 %) to afford **190f**, whereas addition of methyl magnesium bromide into the aniline Weinreb amide derivative **190d** did not produce the desired product, but instead appeared to result in polymerisation, which was observed *via* NMR spectroscopy. It was decided that the dimethyl derivative **190f** would be taken forward while the synthesis of the aniline was optimised.

The hydroxy-substituted derivative **190b** was previously synthesised from 1-(3-methoxyphenyl)propan-2-one **190c** by demethylation using BBr₃, however when this methodology was used, no product was observed under several different reaction conditions shown in the **Table 8** below.



Entry	Reagent	Equiv.	Temp / °C	Conv. ^(a) / %	Isolated yield ^(b) / %
1	BBr ₃	2.5	-78 ^(c)	0	-
2	BBr ₃	2	-78 ^(c)	0	-
3	BBr ₃	1.5	-78 ^(c)	0	-
4	HBr	8	120	-	59

*Table 8: The reaction conditions used in the demethylation of m-methoxyphenylacetone **190c** to form m-hydroxyphenylacetone **190b**. (a) Conversion measured in the crude NMR spectra. (b) Isolated yield after column chromatography. (c) After 1 h the reaction was warmed to room temperature for 2 h.*

During the reaction with boron tribromide, degradation of the reagents was observed, therefore it was hypothesised that reducing the number of

equivalents boron tribromide (**Table 8, entries 1-3**) would decrease any chance of side reaction, which was leading to degradation. However, this proved unsuccessful. Further research into the reaction provided an alternative route. Changing the source of the nucleophilic bromide to hydrobromic acid led to complete demethylation and afforded a 59 % isolated yield (**Table 8, entry 4**). Optimisation of the reaction conditions above were run in tandem with the screening efforts described below.

5.2.2 Screening the Pictet-Spengler Reaction

The hypothesis was that the Pictet-Spengler reaction would be the driving force for the dynamic equilibrium associated with the transamination reaction. This should mean that almost stoichiometric equivalents of amine donor should still allow good conversions to the THIQ. The conditions for the Pictet-Spengler reaction were first optimised (**Figure 10**). The substrate chosen for the initial screening process was the dimethylaniline derivative **190f**, which was thought to be the most challenging substrate, due to the proposed mechanism by Pesnot *et al.*⁴¹ where the *meta* position of the phenylacetone derivative **190** is deprotonated by the P_i. The initial conditions for these reactions were based on the highly optimised reaction conditions reported by Pesnot *et al.* for dopamine.⁴¹ However, in these experiments, the co-solvent was changed from acetonitrile to DMSO as the commercial ATA enzymes are known to be stable in DMSO. The first condition screened was pH (**Figure 10A**), followed by a co-solvent screen (**Figure 10B**) and finally, a co-solvent percentage screen (**Figure 10C**).

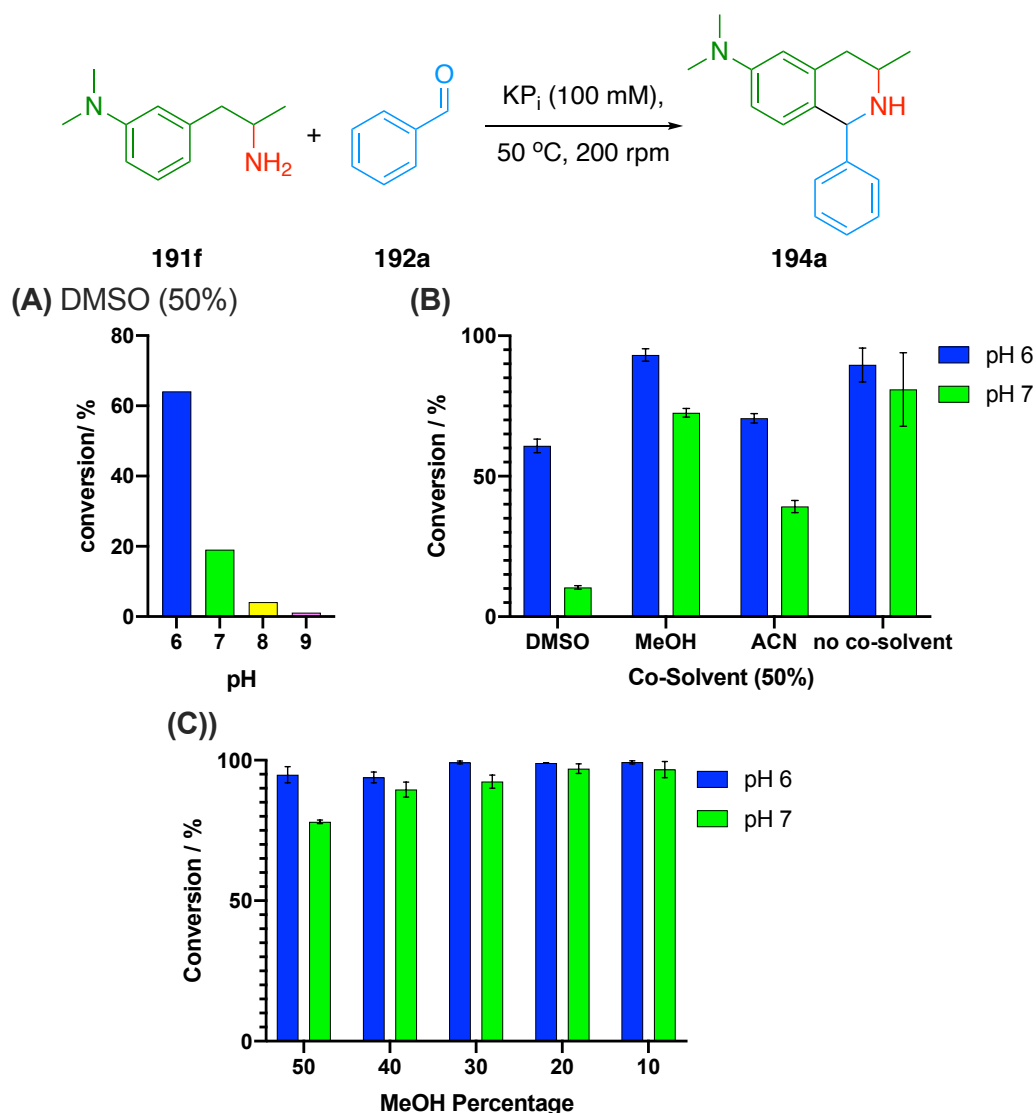


Figure 10: A) pH screen of the Pictet-Spengler reaction. Reaction conditions, substrate **191f** (20 mM), benzylamine **192a** (22 mM), potassium phosphate buffer (100 mM, 1 mL), DMSO (50 % v/v), 50 °C, 200 rpm, 24 h. B) Graph showing the conversion from **191f** to THIQ **194a** with different co-solvents. Reaction conditions: substrate **191f** (20 mM), benzylamine **192a** (22 mM), potassium phosphate buffer (100 mM, 1 mL), co-solvent (50 % v/v), 50 °C, 200 rpm, 24 h. C) Graph showing the conversion from **191f** to THIQ **194a** with different co-solvents. Reaction conditions: substrate **191f** (20 mM), benzylamine **192a** (22 mM), potassium phosphate buffer (100 mM, 1 mL), MeOH (percentage v/v), 50 °C, 200 rpm, 24 h. Conversion measured via GC-FID

As expected, **Figure 10A** shows that the conversion of 3-(2-aminopropyl)-N,N-dimethylaniline **191f** to THIQ **194a** decreased from 64 % at pH 6 to 1 % at pH 9, due to the reaction being acid-catalysed.^{30–33} While the conversion to the THIQ **194a** was reasonably low, there was increased conversion to Schiff base as the pH increased, observed by GC-MS. The

Schiff base is an intermediate in the reaction mechanism of the Pictet-Spengler reaction (**Scheme 9**), and by visualising this on the GC trace, it indicates that the ring closure was not occurring. While pH 6 showed the best conversion to the THIQ **194a**, there was a potential compatibility issue when it came to using the ATA and Pictet-Spengler reaction in a tandem cascade as ATAs commonly provide better conversions at higher pHs.¹⁴⁹ Due to this potential compatibility issue, the subsequent two screens (**Figure 10B/C**) were completed at pH 6 and pH 7, and the results compared to explore the best compromise conditions.

Commercial ATAs are known to be stable in DMSO but are also active in alternative co-solvents, which may affect the conversion of the Pictet-Spengler reaction, shown in **Figure 10B**. Adjusting the co-solvent from DMSO to methanol or acetonitrile increased the conversion to THIQ at both pH values. Notably the largest increase in conversion proved to be from the DMSO at pH 7 (10 %) to methanol (73 %), which proves to be promising for future reactions with the ATAs. As with the pH screen, when lower conversions to the THIQ were observed, an increase in the Schiff base formation was seen, again observed by GC-MS.

While the commercial ATAs stability towards DMSO have been well documented by Codexis[®],¹⁴⁹ this greater stability does not necessary transfer across to other co-solvents such as methanol (MeOH) and acetonitrile (AcN). For this reason, it was decided to complete a screen to explore the viability of the Pictet-Spengler reaction at lower percentages of co-solvent (**Figure 10C**). Interestingly, when decreasing the amount of methanol as a co-solvent, the conversion did not significantly change at pH 6. The conversion increased slightly at pH 7 as the amount of co-solvent decreased. These results are promising when thinking about combining the ATA reaction with Pictet-Spengler reaction as they indicate that the Pictet-Spengler reaction is able to take place under more ATA-friendly conditions.

5.2.3 Screening ATA- Pictet-Spengler Reaction Cascade Reaction

Having established that the Pictet-Spengler reaction could proceed with excellent conversion to the THIQ under the optimised conditions discussed above (**5.2.2 Screening the Pictet-Spengler Reaction**), it was anticipated that the thermodynamically favourable condensation would help to displace the ATA reaction. Two of the commercially available ATAs were selected for screening using the conditions optimised above; **ATA025** as the (*R*)-selective and **ATA256** as the (*S*)-selective enzyme. The results of this screen are shown in **Figure 11** below.

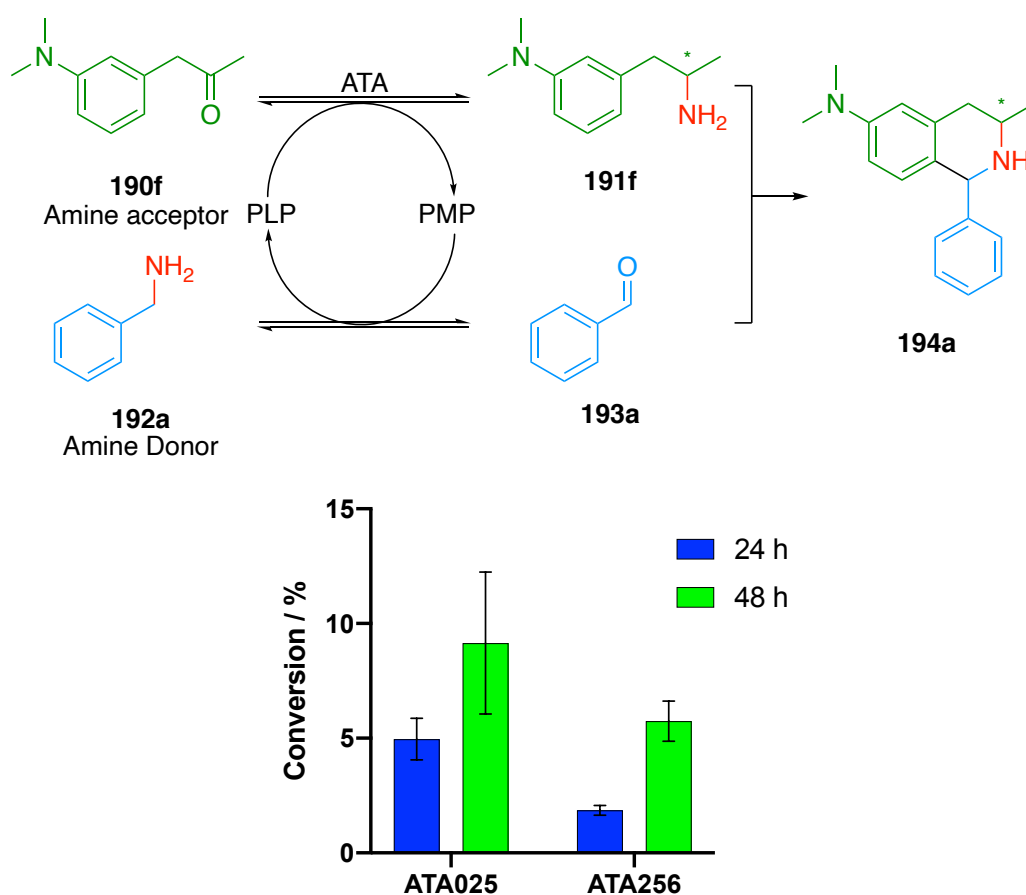


Figure 11: Graph showing the conversion from **190f** to THIQ **194a** with different co-solvents. Reaction conditions: substrate **190f** (20 mM), benzylamine **192a** (22 mM), ATA (5 mg mL⁻¹), potassium phosphate buffer (100 mM, pH 7, 1 mL), MeOH (10 % v/v), 50 °C, 200 rpm. Conversion measured via GC-FID.

ATA025 and **ATA256** enzymes have both been shown by Codexis® to be stable and active at a maximum temperature of 50 °C, however, both

enzymes provided low conversion (< 10 %). There are two possibilities for the poor conversion to the THIQ **194a** - the enzyme failing to convert the ketone to the corresponding amine or the Pictet-Spengler reaction coupling not taking place. To ascertain which section of the cascade was causing the problem with the poor conversion, NMR analysis of the reaction was employed. NMR analysis suggested that the enzyme was failing to convert the ketone **190f** to its corresponding amine **191f**, which meant that it was then unavailable to undergo the Pictet-Spengler reaction, meaning that further optimisation of the enzyme reaction was required. For this reason, further exploration into the other available amine donors (**Figure 12**) was completed by James Ryan. It was theorised that by changing the electronics of the amine donor, the efficiency of the Pictet-Spengler reaction would increase, thus driving the reaction equilibrium in the desired direction towards completion.

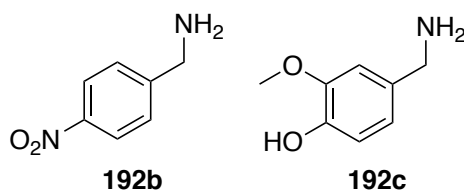
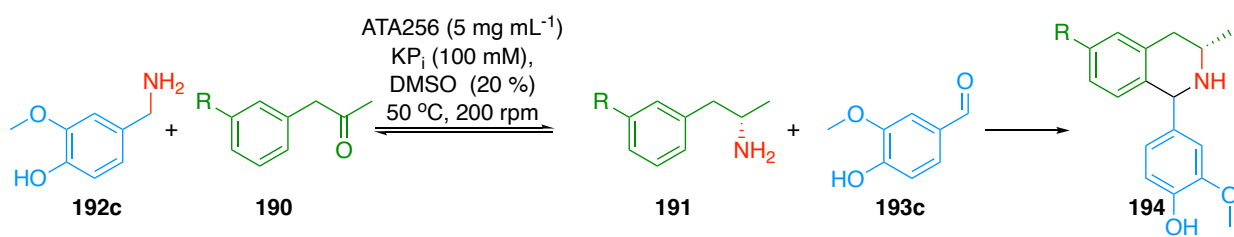


Figure 12: The two potential amine donors used as part of the ATA- Pictet-Spengler reaction cascade.

When using amine donor **192b** in biotransformation conditions, James Ryan found that the corresponding aldehyde preferentially condensed together, thus adding a competing reaction into ATA- Pictet-Spengler reaction cascade, which was highly undesirable. However, vanillamine **192c** offered a viable alternative for the synthesis of THIQ **194**. **Table 9** shows the screening process with a range of ketones **190** utilising vanillamine **192c** as the amine donor, in an attempt to achieve optimum reaction conditions. This screen was initially conducted with methanol as the co-solvent however this yielded low conversions, initially thought to be due to the stability of enzyme in methanol, so the screen was carried out using DMSO as the co-solvent.



Entry	R	Conc. of ketone 190 / mM	Equiv. amine 192c	pH	% DMSO (v/v)	Conv. to amine 191 (%) 48 h	Conv. to THIQ 194 (%) 48 h
1	NMe ₂ f	40	1.1	7	20	3	2
2	NMe ₂ f	40	1.1	7.5	20	3	1
3	NMe ₂ f	40	1.1	8	20	2	1
4	NMe ₂ f	40	2	7.5	20	4	2
5	NMe ₂ f	10	1.1	7.5	20	5	4
6	NMe ₂ f	50	1.1	7.5	20	3	2
7	NMe ₂ f	100	1.1	7.5	20	3	3
8	OMe c	50	1.1	7.5	20	32	0
9	OH b	40	1.1	6	20	17	7
10	OH b	40	1.1	7	20	15	15
11	OH b	40	1.1	7.5	20	14	17
12	OH b	40	1.1	8	20	13	13
13	OH b	40	1.1	9	20	13	8
14	OH b	40	2	7.5	20	21	27
15	OH b	40	5	7.5	20	27	31
16	OH b	10	1.1	7.5	20	13	4
17	OH b	25	1.1	7.5	20	14	12
18	OH b	50	1.1	7.5	20	14	17
19	OH b	75	1.1	7.5	20	15	20
20	OH b	100	1.1	7.5	20	14	22
21	OH b	100	1.1	7.5	15	11	26
22	OH b	100	1.1	7.5	10	11	28
23	OH b	100	1.1	7.5	5	10	22

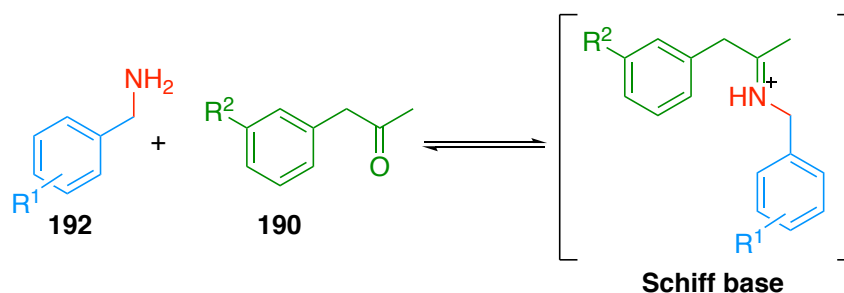
Table 9: pH and concentration of substrate screen, with samples taken at 48 h. Reaction conditions, phenylacetone derivate **190**, vanillamine **192c**, HEPES (100 mM, 0.5 mL), DMSO (v/v), 50 °C, 200 rpm. Conversion was measured by NMR against a standard. The results in the table are the mean of three replicates.

The conversion of ketone **190f** to amine **191f** proved to be a major challenge in this cascade, with the conversion ranging from 2 - 5 % (**Table 9, entries 1-7**). This poor conversion was not improved by an increase of amine donor **192c** equivalents (**Table 9, entry 4**), change in pH or in concentration of the reactants in solvent. When looking more closely at the reaction, it was suggested that changing the ketone substrate might provide better conversions, and with this in mind, synthesis with 1-(3-(methoxy)phenyl)propan-2-one **190c** was attempted (**Table 9, entry 8**), which gave reasonable conversion to the corresponding amine **191c**, 32 %, however, no THIQ **194** product was observed. Presot *et al.* also reported no conversion with the methoxy-compound during their investigation into the KP_i -catalysed Pictet-Spengler reaction. They hypothesised that the mechanism for this reaction required a *meta*-substituent that was not only electron donating but was capable of deprotonation. Therefore, a 1-(3-(hydroxy)phenyl)propan-2-one ketone **190b** was also investigated (**Table 9, entries 9-23**).

More success was afforded during the screening of the *meta*-hydroxy ketone **190b** than previous substrates. During the pH screen of this compound, it was observed that the conversion to the THIQ **194** increased as the pH increased 6 to 7.5 (**Table 9, entries 9-11**) as the transaminase reaction proceeded more efficiently. As the pH is increased from 8 to 9 (**Table 9, entries 12-13**), the conversion to the THIQ **194** drops to 13 % and 8 % respectively, which is likely caused by the decrease of acid catalysed Pictet-Spengler reaction. When the amine donor was increased to 2 and 5 equivalents (**Table 9, entries 14-15**) the conversion to the amine **191b** increased (21 and 27 % respectively) as did the conversion to the THIQ **194** (27 and 31 % respectively). But this conversion was still rather disappointing due to the vast increase to the number of equivalents of amine donor, it was thought that reaction equilibrium would be driven further towards the THIQ product **194**. This indicates that while both amine donor **192c** and ketone **190b** are substrates for ATA, there is potential for screening of different ATA that these compounds may be better substrates for. While increasing the number equivalents of amine donor improved the conversion to the THIQ

product **194**, these are not the ideal *amine borrowing* conditions, as they do not maintain stoichiometric equivalents of amine donor **192c**. Therefore, more work was required to find the best conditions of this cascade under *amine borrowing* conditions.

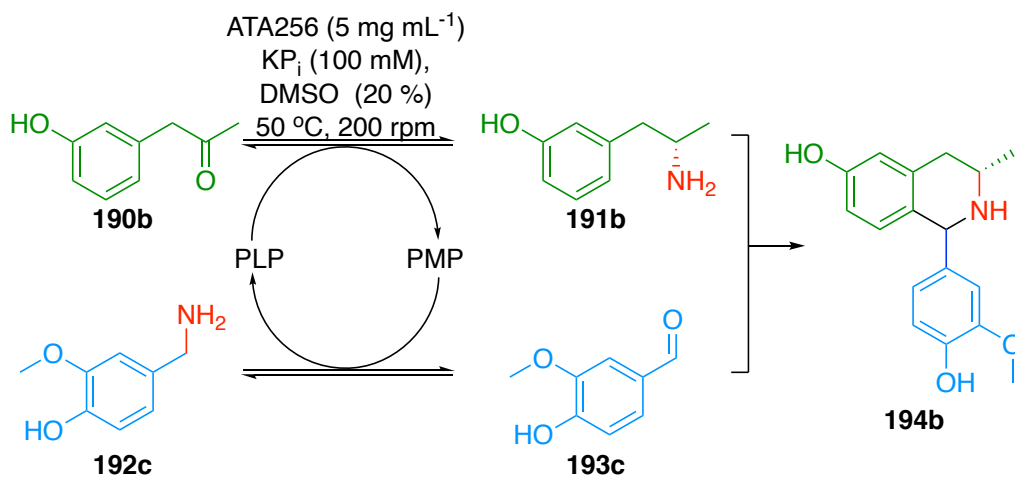
As in the ATA- Knorr Pyrrole Synthesis cascade the two starting materials have the ability to react and form a Schiff base (**Scheme 68**). In theory this Schiff base can undergo a ring closure reaction, however this reaction is would be unfavourable due to the formation of a highly strained four membered ring. Therefore, the Schiff base is hydrolysed back into the starting amine **192** and ketone **190**, forming an equilibrium favouring the starting materials, these are then able to undergo the ATA- Pictet-Spengler reaction cascade to form the corresponding THIQ.



Scheme 68: The reversible formation of Schiff base between the starting amine **192** and the ketone **190**.

The concentration screen (**Table 9, entries 15-19**) showed that as the concentration of the substrate increased, so too did the conversion to THIQ **149**. This trend is understandable due to bimolecular nature of the reaction, though it is surprising that the transamination reaction was not the bottleneck of the reaction as the concentration increases due to the seemingly low affinity for the substrate that the enzyme has. However, during the concentration screen for this substrate, it was discovered that there was a discrepancy between the conversion to amine **191b** and the conversion to vanillin **193c** as shown in **Table 10**. It is also worth noting that the lower concentration screens turned dark brown in colour, potentially indicating degradation of a compound in the reaction mixture after 24 h ,

whereas this colour change was not observed at higher concentrations. It was concluded that at the lower concentration, amine **191b** was degrading faster than the Pictet-Spengler reaction could occur.



Entry	Conc. of ketone 190b /mM	Conv. to amine 191b (%) 48 h	Conv. to Vanillin 193c (%) 48 h
1	10	13	42
2	25	14	35
3	50	14	24
4	75	15	19
5	100	14	15

Table 10: Concentration of substrate screen, with samples taken at 48 h. Reaction conditions, *m*-1-(3-(hydroxyphenyl)propan-2-one **190b**, vanillamine **192c**, HEPES (100 mM, 0.5 mL), DMSO (20 % *v/v*), 50 °C, 200 rpm. Conversion was measured by NMR against a standard. The results in the table are the mean of three replicates.

During the investigation of how the co-solvent affects the Pictet-Spengler reaction in the absence of enzyme, as seen in **Figure 10B**, it was demonstrated that the Pictet-Spengler reaction afforded 81 % conversion to the THIQ without the need of co-solvent. Therefore, it was envisaged that decreasing the amount of co-solvent in the enzyme screen, may increase conversion to THIQ **194** (**Table 9, entries 21-23**). However, some co-solvent was necessary to dissolve the ketone substrate and therefore 5 % DMSO was selected. Decreasing the percentage from 20 % to 15 and 10 % increased the conversion to THIQ **194** from 22 % to 26 % and 28 %

respectively. When this was decreased further to 5 % DMSO, the same conversion of 22 % was observed, suggesting that conversion is relatively unaffected by the decrease concentration in co-solvent.

5.3 Summary

Two transaminase substrates x and y were synthesised in reasonable yields. **Compound 109f** had a five-step synthetic route to obtain the final dimethyl amine (24 % over 5 steps), where the most challenging step was the alkylation of aniline **199**, due to over-methylation leading to the production of the trimethylated product. 1-(3-(hydroxy)phenyl)prop-2-one **190b** was produced in a reasonable yield of 59 % *via* demethylation of 1-(3-(methoxy)phenyl)propan-2-one **190c**.

The easily accessed amine derivate **191f** was coupled with benzaldehyde **193a** to investigate the Pictet-Spengler reaction without the prerequisite enzyme reaction. These results showed that the Pictet-Spengler aspect of this reaction occurred with reasonable conversion in a number of conditions and limiting the amount of co-solvent afforded the THIQ **194a** in high conversion.

However, attempts to generate the PS reactants *in situ* using an ATA resulted in a decreased conversion to THIQ **194a** 10 %. This indicated that a compromise between conditions suitable for the transaminase reaction and Pictet-Spengler reaction needed to be made. Along with further NMR investigation into the reaction, it was discovered that benzylamine **192a** was a poor amine donor, as no conversion to the corresponding benzaldehyde **193a** was observed. This poor conversion indicated that a more suitable amine donor should be found. James Ryan undertook some preliminary work that indicated that vanillamine **192c** could potentially offer a viable alternative.

The screen of a range of phenylacetone derivatives **190** with vanillamine **192c** was conducted with varying reaction success. 1-(3-

(dimethylamino)phenyl)propan-2-one **190f** produced disappointing conversions of 2 - 4 %; with further screening and optimisation of concentration, pH and co-solvents, these conversions can potentially be increased. In the case of 1-(3-(methoxy)phenyl)propan-2-one **190c**, conversion to the corresponding amine **191c** was achieved (32 %), however the nature of this substrate meant that the THIQ **194** was not formed. The most successful of the substrates screen during this project was 1-(3-(hydroxy)phenyl)propan-2-one **190b**, giving the best conversion of 31 % to THIQ **194b**. However, this reaction did not proceed under true *amine borrowing* conditions and therefore further investigation into the conditions needed for this reaction to be completed with higher conversion is required.

5.4 Future Work

The full potential of the ATA- Pictet-Spengler reaction cascade has yet to be realised and additional synthesis and screening of ketones **190a-f** and aldehydes **195a-f** (**Figure 13**), would increase the substrate scope of this chemo-enzymatic cascade.

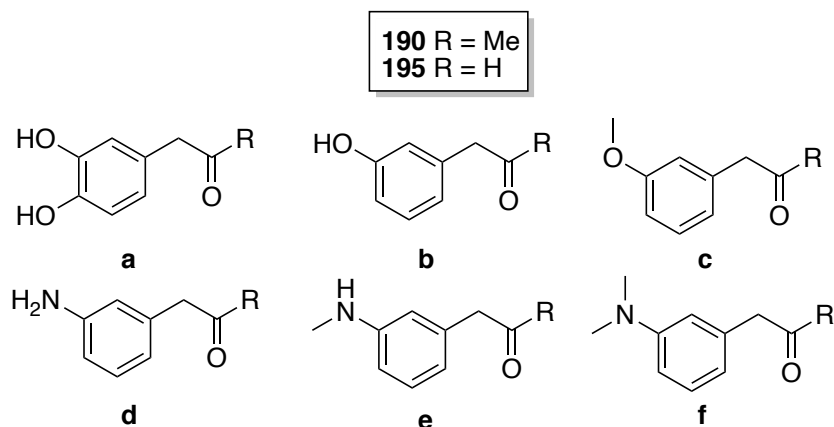


Figure 13: Selected examples of the ketone substrates that will be used in future studies in the ATA- Pictet-Spengler cascade.

Once optimum ATA- Pictet-Spengler reaction conditions for the carbonyls **190a-f** and **195a-f** have been established, they can then be used for the scale-up and subsequent isolation of the resulting THIQs, ensuring this methodology is easily translated to preparative-scale synthesis. To further increase the substrate scope of the ATA- Pictet-Spengler reaction cascade,

a range of amine donors could be screened, enabling access to a selection of highly functionalised THIQ molecules.

During the course of the phosphate-catalysed Pictet-Spengler reaction no control of stereochemistry was observed, resulting in the production of two diastereomers being produced. By introducing a Pictet-Spenglerase into the cascade to act as the catalyst, the Pictet-Spengler reaction would proceed with control of the stereochemistry and allowing the synthesis of molecules with the desired stereocentres. Therefore, in the case of the ketone **190a-f** substrates, THIQ would only give one diastereomer and aldehydes **195a-f** would produce one enantiomer, therefore enhancing the ability of this chemo-enzymatic cascade.

6.0 Conclusions

The initial aim of this work was to use a transaminase-triggered aza-Michael reaction in the synthesis of cyclic β -enaminones **146**, which are key building blocks in the synthesis of alkaloid scaffolds. In order to achieve this objective, a range of ketoynone substrates **147** were synthesised in moderate yields (26 – 89 %).

The ketoynones **147a-g** were then incorporated as substrates in a transaminase-triggered aza-Michael reaction cascade to give cyclic β -enaminones **146a-g** in moderate to high conversions (46 – 99 %), and these β -enaminones **146a-g** were then purified by column chromatography providing reasonable to high yields (29 – 95 %) in high enantiomeric excess (83 - >99 %).¹⁰⁸

During the course of the biotransformations, it was noticed that a side reaction was also occurring. This side reaction was caused by unreacted ketoynone **147d** undergoing a carbo-[3+3] annulation with the β -enaminones **146d** producing THQ **157d** in <10 % yield. This side reaction was then exploited by decreasing amine donor equivalents, which led to the annulation reaction becoming the main reaction to form THQ **157d** in a 78 % yield. The selectivity of the transaminase was then explored as part of an ATA-aza-Michael-annulation cascade, by using bulky-bulky ketoynone **147h**. The unoptimised cascade produced a range of THQs **158c-e** with varying success (10 – 90 % yield).

To further demonstrate the ability of the cyclic β -enaminones **146** as key building blocks in the synthesis of alkaloid scaffolds, two further annulation reactions were undertaken to show the multiple functional handles present in β -enaminones **146**. A carbo-[3+3] annulation produced HHQ **148** in reasonable 92 % yield, however with no apparent stereoselective control (57:43 *d.r.*). The aza-[3+3] annulation reaction produced quinolizones **161a** and **161d** in reasonable yields (44 and 52 %), however, this reaction also had poor stereoselective control (3:1 *d.r.*). Further optimisation of these

reaction has the potential to give higher diastereomeric excess, meaning they are a useful downstream reaction for cyclic β -enaminones.

The second aim of this project was to develop the novel concept of *amine borrowing*. This approach involves a linear cascade where the ATA shuttles the amine moiety from the donor molecule to an acceptor molecule generating two reactive species. These two species react in the next step of the cascade, subsequently the 'borrowed' amine moiety becomes part of the final product. It was envisaged that three named reactions: Mannich, Pictet-Spengler and Knorr Pyrrole synthesis, could be used to examine the scope of the *amine borrowing* methodology.

While investigating if *amine borrowing* could be used in an ATA-Mannich cascade, it was shown that a Mannich reaction could be undertaken between piperidine **46** and acetone **47** to produce pelletierine **22** with disappointing conversion (6 - 12 %). However, when proline was added to the reaction mixture the conversion increased to >99 %. The transamination of cadaverine **18**, allowed for the generation of piperidine **46** *in situ*, this was then able to react with excess acetone **47** in the reaction mixture forming pelletierine **22** in a conversion of 74 %. This provides evidence that the Mannich reaction proceeds under biotransformation conditions.

However, when introducing *amine borrowing* conditions by using glutaraldehyde **173a** as the amine acceptor, it was found that this is a poor amine acceptor, potentially due to the ability of glutaraldehyde **173a** to cross-link enzymes. With this in mind, other dicarbonyls were synthesised *via* ozonolysis in reasonable yields (50 - 66 %). Further screening of these molecules with a range of ATAs, as well as optimisation of the reaction conditions is needed to develop optimum conditions for the ATA-Mannich cascade to occur.

Amine borrowing conditions were successfully used in the synthesis of a range of pyrrole derivatives **145a-l** with good to excellent conversions (41 – 99 %) for the aryl substrates **143a-e** and disappointing conversion with the

aliphatic derivative **145f** and **145I** (25 or 34 %). This poor conversion was determined to be due to the self-condensation reaction between the α -amino keto **144f** forming pyrazine **161**. This reaction is a perfect justification for developing the *amine borrowing* methodology, as generating the reactive α -amino keto **144** limits ability of this compound to self-condense. With further optimisation of the conditions with aliphatic compound **143f**, the production of pyrazine **161** could be reduced. The loss of the ATA-installed chiral centre during the Knorr pyrrole synthesis is the biggest downfall of this methodology. The ATA-triggered Knorr pyrrole reactions presented in this work are a rare example of the successful use stoichiometric equivalents of amine donor being able to be employed.

The final example of an ATA-triggered cascade explored in this project was an ATA - Pictet-Spengler reaction cascade. As part of this reaction cascade, two ketones **190b** and **190f** were synthesised. Conditions for the P_i -catalysed Pictet-Spengler reaction were initially screened, which indicated that the Pictet-Spengler reaction could be performed under biotransformation conditions.

When ATA was introduced into the cascade, the conversion to THIQ **194** dropped to >10 %. Further investigation into this poor conversion proved that there was a lack of conversion in the ATA reaction to form the corresponding amine **191f** and benzaldehyde **193a**. Further screening of a range of potential amine donors **192b-c** was undertaken, and the most promising was taken forward and screened against a number of ketones **190b-c** and **f**. However, the best conversion of 32 % was obtained with the reaction of 1-(3-hydroxyphenyl)propan-2-one **190b** to THIQ **194b**. A greater screening effort is needed to decide whether these results can be improved, with the aim of scale up of these reactions.

The second part of this project has provided a proof of concept toward the development of shuttle biocatalysis, and more specifically, *amine borrowing*. Further work and screening are needed to obtain optimum conditions for the ATA-MR and ATA- Pictet-Spengler reaction cascades.

Amine borrowing conditions were successfully implemented into the synthesis of a range of pyrrole derivatives **145a-l** in and ATA- Knorr Pyrrole Synthesis cascade to give reasonable conversions, notably with only one equivalent of amine donor.

7.0 Experimental

7.1 General Methods

General: NMR spectra were recorded on a Bruker DPX 400 or Bruker AV(III)500 spectrometer (400 MHz for ^1H and 100 MHz for ^{13}C). The chemical shift values (δ) are reported in ppm with the residual solvent referenced to CDCl_3 : δ 7.26 for ^1H -NMR, δ 77.0 for ^{13}C NMR or MeOD δ 3.31 for ^1H -NMR, δ 49.0 for ^{13}C NMR. Coupling constants (J) are reported in Hz and refer to the observed peak multiplicities, where needed, 2D NMR was performed to assign specific carbon atoms and stereochemistry of compounds. GC-FID analysis was performed on a Bruker Trace 1310 series GC equipped with an autosampler and a Chirasil Dex CB (25 m x 0.25 mm x 0.25 mm) column, the oven was held at 40 °C for 2 min, before the temperature was increased to 150 °C at a rate of 20 °C min $^{-1}$ and held for 5 min, the temperature was then increased to 200 °C at a rate of 30 °C min $^{-1}$ and held for 18 min. Analytical HPLC was performed on a Thermo Ultimate 3000 uHPLC system equipped with PDA e λ detector (λ = 210 – 400 nm). The mobile phase composed of 0.1% trifluoroacetic acid in H_2O (Solvent A) and 0.1% trifluoroacetic acid in acetonitrile (Solvent B). The analysis of the chromatograms was conducted using Chromeleon 7 software. Mass spectra were recorded on a Bruker MicroTOF II spectrometer using Electron Spray Ionisation (ESI). IR spectra were recorded on a Bruker ATR or solution cell. Single crystal X-ray diffraction data were collected by Dr Stephen Argent, on an Oxford Diffraction GV1000 (AtlasS2 CCD area detector, mirror-monochromated Cu-K α radiation source; λ = 1.54184 Å, ω scans).

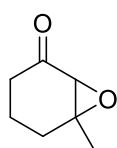
Preparative reverse-phase HPLC was performed using a Waters 1525 binary pump HPLC equipped with a dual wavelength UV detector set to 210 nm and 280 nm. Preparative HPLC was performed on a Waters Sunfire 5 μm (C-18) preparative column with 5- μm particle size, 19 x 150 mm, operating at a flow rate of 6 mL min $^{-1}$ using a mobile phase of 0.1% trifluoroacetic acid in water (Solvent A) and 0.1% trifluoroacetic acid in

acetonitrile (Solvent B) using the gradient specified in the experimental section.

Materials: Commercially available reagents and solvents were purchased from Acros Chemicals, Fluorochem, Sigma Aldrich and Thermo Fisher Scientific. Commercially available transaminases ATA113, ATA256, ATA025 and ATA117 were purchased from Codexis® in the form of lyophilised cell extract.

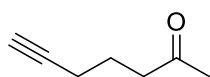
7.2 Synthesis of β -Enaminone and corresponding derivatives

Chemical synthesis of 2-methyl-2-(pent-4-yn-1-yl)-1,3-dioxolane (150) 6-Methyl-7-oxobicyclo[4.1.0]heptan-2-one (151)^{108,161,162}



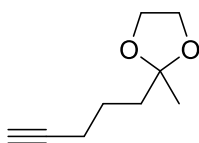
To a solution of 3-methylcyclohex-2-en-1-one **150** (13.6 mL, 119 mmol) in MeOH (120 mL) at 0 °C was added 30% solution of hydrogen peroxide (36.6 mL, 323 mmol) dropwise over 40 min. Sodium hydroxide solution (5 M, 2.00 mL) was then added dropwise, and the mixture stirred at ~10 °C for 3 h and a further 16 h at room temperature. The reaction was diluted with brine (150 mL) and extracted with CH₂Cl₂ (3 x 250 mL) and the combined organic layers were dried over anhydrous magnesium sulfate and concentrated *in vacuo*. The crude product was purified by vacuum distillation (bp 110 °C at 45 mbar) to yield a colourless oil (14.37 g, 96 %). ¹H NMR (400 MHz, CDCl₃) δ_{H} 3.06 (1H, s, CH), 2.53-2.43 (1H, m, CH₂), 2.16-1.80 (4H, m, CH₂), 1.67-1.58 (1H, m, CH₂), 1.44 (3H, s, CH₃); ¹³C NMR (100 MHz, CDCl₃) δ_{C} 206.8 (C=O), 62.1 (CH), 35.8 (CH₂), 28.5 (CH₂), 22.3 (CH₃), 17.3 (CH₂); FTIR (solution) ν_{max} : 3019, 1705, 1327, 1287, 960 cm⁻¹; HRMS-ESI (m/z): C₇H₁₁O₂⁺ [M+H]⁺ theoretical 127.0754, found 127.0753. Data in accordance with literature data.^{161,162}

Hept-6-yn-2-one (**152**)^{108,161,162}



To a solution of 6-methyl-7-oxabicyclo[4.1.0]heptan-2-one (**151**, 12.2 g, 97.1 mmol) in CH₂Cl₂/AcOH (2:1 mixture, 150 mL) at -20 °C, was added a solution of (*p*-tolylsulfonyl)hydrazine (19.9 g, 106 mmol) in CH₂Cl₂/AcOH (2:1 mixture, 150 mL) and the mixture was stirred for 7 h and warmed to room temperature over 16 h. The mixture was concentrated *in vacuo* to remove the CH₂Cl₂, dissolved in Et₂O (100 mL) and filtered. Water (100 mL) was added to the filtrate and the mixture was separated. The aqueous phase was extracted with Et₂O (2 x 200 mL) and the combined organic layers were dried over anhydrous magnesium sulfate and concentrated *in vacuo*. The crude product was purified by vacuum distillation (bp 120 °C, 40 mbar) to yield a colourless oil (5.2 g, 49 %). ¹H NMR (400 MHz, CDCl₃) δ_H 2.59 (2H, t, *J* = 7.2 Hz, CH₂), 2.23 (2H, td, *J* = 6.9, 2.6 Hz, CH₂), 2.16 (3H, s, CH₃), 1.96 (1H, t, *J* = 2.6 Hz, CH), 1.79 (2H, *pseudo p*, CH₂); ¹³C NMR (100 MHz, CDCl₃) δ_C 208.3 (CO), 83.6 (CCH), 69.2 (CH), 42.1 (CH₂), 30.2 (CH₃), 22.3 (CH₂), 17.8 (CH₂); FTIR (solution) ν_{max}: 3308, 3014, 2945, 2117, 1714 cm⁻¹; HRMS-ESI (*m/z*): C₇H₁₁O⁺ [M+H]⁺ theoretical 111.0804, found 111.0811. Data in accordance with literature data.^{161,162}

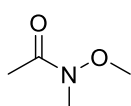
2-Methyl-2-(pent-4-yn-1-yl)-1,3-dioxolane (**153**)^{108,163}



Ethylene glycol (4.04 mL, 72 mmol) and *p*-toluenesulfonic acid (691 mg, 3.60 mmol) were dissolved in anhydrous toluene (30 mL) and heated under reflux under Dean-Stark conditions for 1 h, before heptan-6-yn-2-one (**152**, 2.00 g, 18.0 mmol) was added. The reaction mixture was heated under reflux for 2 h, before being cooled and diluted in Et₂O (30 mL). The organic layer was washed with saturated sodium hydrogen carbonate solution (2 x 50 mL), brine (2 x 50 mL) and dried over anhydrous sodium sulfate and the solvent removed *in vacuo*. The crude product was purified by flash column chromatography (Et₂O:pentane, 1:19) to produce a colourless oil (1.75 g, 63 %). ¹H NMR (400 MHz, CDCl₃) δ_H 3.98-3.90 (4H, m, OCH₂), 2.22 (2H, td, *J* = 7.0, 2.6 Hz, CH₂), 1.94 (1H, t, *J* = 2.6 Hz, CH), 1.79-1.73 (2H, m, CH₂), 1.68-1.59 (2H,

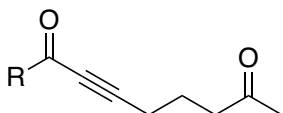
m, CH₂), 1.32 (3H, s, CH₃); ¹³C NMR (100 MHz, CDCl₃) δ_C 109.6 (CO₂), 84.4 (C≡CH), 68.6 (C≡CH), 64.8 (OCH₂), 38.2 (CH₂), 24.0 (CH₂), 23.2 (CH₃), 18.7 (CH₂); FTIR (solution) ν_{max}: 3308, 3039, 2117, 1221, 1063 cm⁻¹; HRMS-ESI (m/z): C₉H₁₅O₂ [M+H]⁺ theoretical 155.1067, found 155.1050. ¹H NMR in accordance with literature data.¹⁶³

Preparation of N-methoxy-N-methylacetamide (201)^{108,164}



To *N,O*-dimethylhydroxyamine hydrochloride (9.75 g, 100 mmol) and triethylamine (29.8 mL, 200 mmol) in CH₂Cl₂ (150 mL) at 0 °C, was added dropwise acetyl chloride (7.1 mL, 100 mmol). The reaction mixture was stirred at room temperature for 17 h and then quenched with saturated sodium hydrogen carbonate (50 mL). The layers were separated, and the aqueous layer was extracted with CH₂Cl₂ (2 x 50 mL). The combined organic layers were washed with hydrochloric acid (1 M, 100 mL), brine (100 mL), dried over anhydrous sodium sulfate and concentrated *in vacuo*. The crude product was purified by distillation to give a colourless oil (5.73 g, 56 %). ¹H NMR (400 MHz, CDCl₃) δ_H 3.68 (3H, s, CH₃), 3.17 (3H, s, CH₃), 2.12 (3H, s, CH₃); ¹³C NMR (100 MHz, CDCl₃) δ_C 172.0 (C=O), 61.1 (NCH₃), 32.0 (OCH₃), 19.8 (H₃C-CO). FTIR (ATR) ν_{max}: 2940, 2823, 1723, 1559, 1180, 1027 cm⁻¹; HRMS-ESI (m/z): C₄H₉NO₂Na⁺ [M+Na]⁺ theoretical 126.0525, found 126.0530. Data in accordance with literature data.¹⁶⁴

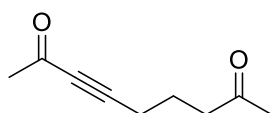
General procedure for the synthesis of methylketoynonones (147)¹⁰⁸



To a solution of 2-methyl-2-(pent-4-yn-1-yl)-1,3-dioxolane (**153**, 500 mg, 3.24 mmol, 1 equiv.) in anhydrous THF (30 mL) at -78 °C, was added *n*-butyllithium (2.43 mL, 3.89 mmol, 1.6 M solution in hexane, 1.2 equiv.) dropwise and the reaction mixture stirred for 10 min. The reaction was warmed to 0 °C and stirred for a further 10 min and then cooled to -78 °C before the corresponding acid chloride or Weinreb amide (1.2 equiv) was added. After 30 min, the reaction was warmed to room temperature and monitored by TLC. The reaction mixture was quenched with water (30 mL)

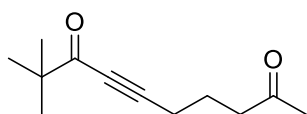
and the aqueous layer extracted with Et₂O (3 x 60 mL). The combined organic layers were dried over anhydrous magnesium sulfate and concentrated *in vacuo*. The crude residue was dissolved in Et₂O (5 mL) and aq. HCl (3 M, 2 mL) and stirred for 3 h. The reaction was separated between Et₂O (25 mL) and water (20 mL) and the aqueous layer was the extracted with Et₂O (2 x 20 mL). The combined organic layers were washed with saturated sodium hydrogen carbonate solution (40 mL), dried over anhydrous magnesium sulfate and the solvent removed *in vacuo*. The crude product was purified by flash column chromatography.

Non-3-yne-2,8-dione (**147a**)^{108,133}



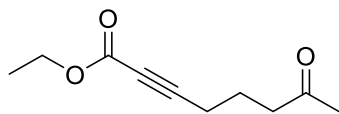
The reaction of **153** with *N*-methoxy-*N*-methylacetamide **201** (816 mg, 7.91 mmol) provided **147a** as a colourless oil (783 mg, 79 %) after column chromatography (Et₂O:pentane 1:4). ¹H NMR (400 MHz, CDCl₃) δ_H 2.57 (2H, t, *J* = 7.1 Hz, CH₂), 2.41 (2H, t, *J* = 7.0 Hz, CH₂), 2.31 (3H, s, CH₃), 2.16 (3H, s, CH₃), 1.83 (2H, *pseudo p*, CH₂); ¹³C NMR (100 MHz, CDCl₃) δ_C 207.8 (CO), 184.9 (CO), 92.8 (C_q), 82.0 (C_q), 41.9 (CH₂), 32.9 (CH₃), 30.2 (CH₂), 21.6 (CH₂), 18.3 (CH₃); FTIR (ATR) ν_{max}: 2943, 2207, 1717, 1690, 1358, 1227 cm⁻¹; HRMS-ESI (*m/z*): C₉H₁₂O₂Na⁺ [M+Na]⁺ theoretical 175.0730, found 175.0741. Data in accordance with literature data.¹³³

9,9-Dimethyldec-6-yne-2,8-dione (**147b**)¹⁰⁸



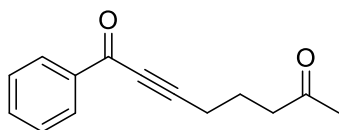
The reaction of **153** with pivaloyl chloride (467 mg, 3.87 mmol) provided **147b** as a colourless oil (276 mg, 44 %) after column chromatography (Et₂O:pentane 1:2). ¹H NMR (400 MHz, CDCl₃) δ_H 2.58 (2H, t, *J* = 7.1 Hz, CH₂), 2.44 (2H, t, *J* = 6.9 Hz, CH₂), 2.16 (3H, s, CH₃), 1.83 (2H, *pseudo p*, CH₂), 1.18 (9H, s, CH₃); ¹³C NMR (100 MHz, CDCl₃) δ_C 207.8 (CO), 194.5 (CO), 94.4 (C_q), 79.5 (C_q), 44.8 (C_q), 42.0 (CH₂), 30.2 (CH₃), 26.2 (CH₃), 21.8 (CH₂), 18.4 (CH₃); FTIR (ATR) ν_{max}: 2967, 2933, 2300, 1714, 1709, 1364, 1150, 941 cm⁻¹; HRMS-ESI (*m/z*): C₁₂H₁₈O₂Na⁺ [M+Na]⁺ theoretical 217.1199, found 217.1207.

Ethyl 7-oxooct-2-ynoate (**147c**)¹⁰⁸



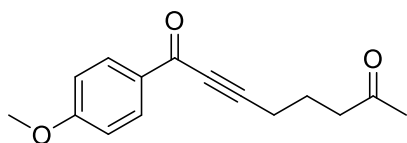
The reaction of **153** with ethyl chloroformate (131 mg, 1.00 mmol) provided **147c** as a colourless oil (130 mg, 71 %) after column chromatography (Et₂O:pentane 1:4). ¹H NMR (400 MHz, CDCl₃) δ_H 4.20 (2H, q, *J* = 7.2 Hz, OCH₂CH₃), 2.58 (2H, t, *J* = 7.1 Hz, CH₂), 2.38 (2H, t, *J* = 6.9 Hz, CH₂), 2.15 (3H, s, CH₃), 1.83 (2H, *pseudo p*, CH₂), 1.30 (3H, t, *J* = 7.2 Hz, OCH₂CH₃); ¹³C NMR (100 MHz, CDCl₃) δ_C 207.7 (CO), 153.8 (COO), 88.3 (C_q), 74.0 (C_q), 62.0 (OCH₂CH₃), 41.9 (CH₂), 30.2 (CH₃), 21.4 (CH₂), 18.0 (CH₂), 14.6 (OCH₂CH₃); FTIR (ATR) ν_{max}: 3032, 3018, 2964, 2236, 1711, 1368, 1260, 1079 cm⁻¹; HRMS-ESI (*m/z*): C₁₀H₁₅O₃⁺ [M+H]⁺ theoretical 183.1016, found 183.1011.

1-Phenyl oct-2-yne-1,7-dione (**147d**)¹⁰⁸



The reaction of **153** with benzoyl chloride (136 mg, 0.97 mmol) provided **147d** as a yellow oil (149 mg, 86 %) after column chromatography (EtOAc:hexanes 1:4). ¹H NMR (400 MHz, CDCl₃) δ_H 8.14-8.11 (2H, m, ArCH), 7.63-7.58 (1H, m, ArCH), 7.51-7.45 (2H, m, ArCH), 2.65 (2H, t, *J* = 7.1 Hz, CH₂), 2.56 (2H, t, *J* = 7.0 Hz, CH₂), 2.18 (3H, s, CH₃), 1.94 (2H, *pseudo p*, CH₂); ¹³C NMR (100 MHz, CDCl₃) δ_C 207.8 (CO), 178.2 (CO), 136.9 (ArC_q), 134.2 (ArCH), 129.7 (ArCH), 128.7 (ArCH), 95.5 (C_q), 80.3 (C_q), 42.0 (CH₂), 29.8 (CH₂), 21.8 (CH₃), 18.6 (CH₂); FTIR (ATR) ν_{max}: 3033, 2928, 2855, 2237, 2204, 1715, 1642, 1450, 1267 cm⁻¹; HRMS-ESI (*m/z*): C₁₄H₁₈NO₂⁺ [M+NH₄]⁺ theoretical 232.1332, found 232.1339.

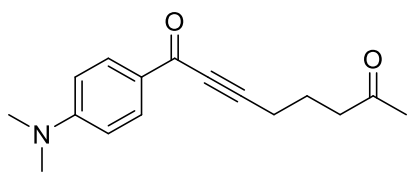
1-(4-Methoxyphenyl) oct-2-yne-1,7-dione (**147e**)¹⁰⁸



The reaction of **153** with 4-methoxybenzoyl chloride (1.294 g, 7.59 mmol) provided **147e** as a yellow oil (1.375 g, 89 %) after column chromatography (EtOAc:hexanes 1:4). ¹H NMR (400 MHz, CDCl₃) δ_H 8.11-8.07 (2H, m, ArCH), 6.97-6.92 (2H, m,

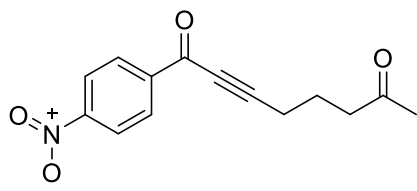
ArCH), 3.88 (3H, s, OCH₃), 2.65 (2H, t, *J* = 7.1 Hz, CH₂), 2.54 (2H, t, *J* = 7.0 Hz, CH₂), 2.17 (3H, s, CH₃), 1.93 (2H, *pseudo p*, CH₂); ¹³C NMR (100 MHz, CDCl₃) δ_C 207.9 (CO), 176.9 (CO), 164.5 (ArC_q), 132.1 (ArCH), 130.4 (ArC_q), 113.9 (ArCH), 94.6 (C_q), 80.3 (C_q), 55.7 (CH₂), 42.1 (CH₂), 30.2 (CH₃), 21.8 (CH₂), 18.6 (CH₃); FTIR (ATR) ν_{max}: 2937, 2842, 2236, 2130, 1712, 1633, 1593, 1251, 1164 cm⁻¹; HRMS-ESI (m/z): C₁₅H₁₆O₃Na⁺ [M+Na]⁺ theoretical 267.0992, found 267.1005.

1-(4-(Dimethylamino)phenyl)oct-2-yne-1,7-dione (147f)¹⁰⁸



The reaction of **153** with 4-(dimethylamino)benzoyl chloride (1.389g, 7.57 mmol) provided **147f** as a yellow solid (941 mg, 58 %) after column chromatography (EtOAc:hexanes 1:4). m.p. 43-45 °C; ¹H NMR (400 MHz, CDCl₃) δ_H 8.04-7.98 (2H, m, ArCH), 6.68-6.62 (2H, m, ArCH), 3.08 (6H, s, CH₃), 2.65 (2H, t, *J* = 7.1 Hz, CH₂), 2.52 (2H, t, *J* = 6.9 Hz, CH₂), 2.17 (3H, s, CH₃), 1.92 (2H, *pseudo p*, CH₂); ¹³C NMR (100 MHz, CDCl₃) δ_C 207.9 (CO), 176.2 (CO), 154.1 (ArC_q), 135.0 (ArCH), 125.5 (ArC_q), 110.6 (ArCH), 93.0 (C_q), 80.5 (C_q), 42.1 (CH₂), 40.1 (CH₂), 30.1 (CH₃), 21.8 (CH), 18.5 (CH₂); FTIR (ATR) ν_{max}: 2906, 2296, 2234, 1711, 1616, 1588 cm⁻¹; HRMS-ESI (m/z): C₁₆H₁₉NO₂Na⁺ [M+Na]⁺ theoretical 280.1308, found 280.1309.

1-(4-Nitrophenyl)oct-2-yne-1,7-dione (147g)¹⁰⁸

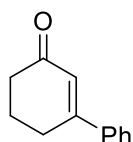


The reaction of **153** with 4-nitrobenzoyl chloride (1.285 g, 6.93 mmol) provided **147g** as a yellow solid (389 mg, 26 %) after column chromatography (EtOAc:hexanes 1:4), m.p. 30-31 °C; ¹H NMR (400 MHz, CDCl₃) δ_H 8.36-8.24 (4H, m, ArCH), 2.65 (2H, t, *J* = 7.0 Hz, CH₂), 2.60 (2H, t, *J* = 7.0 Hz, CH₂), 2.19 (3H, s, CH₃), 1.97 (2H, *pseudo p*, CH₂); ¹³C NMR (100 MHz, CDCl₃) δ_C 207.5 (CO), 176.1 (CO), 151.0 (ArC_q), 141.0 (ArC_q), 130.6 (ArCH), 123.9 (ArCH), 98.1 (C_q), 79.9 (C_q), 42.0 (CH₂), 30.3 (CH₂), 21.7 (CH₃), 18.7 (CH₂); FTIR (ATR) ν_{max}:

3106, 2948, 2856, 2232, 2199, 1711, 1644, 1522, 1342, 1257 cm^{-1} ; HRMS-ESI (m/z): $\text{C}_{14}\text{H}_{13}\text{NO}_4\text{Na}^+$ $[\text{M}+\text{Na}]^+$ theoretical 282.0737, found 282.0748.

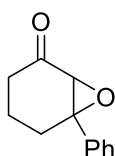
Procedure for the synthesis of 1,7-Diphenylhept-2-yne-1,7-dione (147h)

5,6-Dihydro-[1,1'-biphenyl]-3(4H)-one (202)¹⁰⁸



To a solution of 3-ethoxy-2-cyclohexenone (6 mL, 41.2 mmol) in Et_2O (30 mL) at $-20\text{ }^\circ\text{C}$ was added phenylmagnesium bromide solution in Et_2O (3 M, 16.5 mL, 49.5 mmol), the reaction mixture was then warmed to room temperature and stirred for 16 h. The reaction was diluted with aqueous HCl solution (1 M, 50 mL) and stirred for 0.5 h before extracted with Et_2O (2 x 50 mL). The combined organic layers were washed with brine (50 mL), dried over anhydrous magnesium sulfate and concentrated *in vacuo*. The crude product was purified by flash column chromatography ($\text{EtOAc}:\text{Hexanes}$ (1:19)) to yield a white solid (7.0 g, 98 %), m.p. $50\text{-}52\text{ }^\circ\text{C}$; ^1H NMR (400 MHz, CDCl_3) δ_{H} 7.58-7.49 (2H, m, ArCH), 7.48-7.35 (3H, m, ArCH), 6.42 (1H, t, $J = 1.5\text{ Hz}$, CH), 2.78 (2H, td, $J = 6.0, 1.5\text{ Hz}$, CH_2), 2.49 (2H, m, CH_2), 2.21-2.10 (2H, m, CH_2); ^{13}C NMR (100 MHz, CDCl_3) δ_{C} 199.9 (C=O), 159.7 (ArC_q), 138.8 (C_q=CH), 129.9 (ArC), 128.7 (ArC), 126.0 (ArC), 125.4 (C=CH), 37.2 (CH_2), 28.1 (CH_2), 22.8 (CH_2); FTIR (solution) ν_{max} : 3057, 2937, 2894, 1651, 1602, 1453, 1134 cm^{-1} ; HRMS-ESI (m/z): $\text{C}_{12}\text{H}_{12}\text{ONa}^+$ $[\text{M}+\text{Na}]^+$ theoretical 195.0780, found 195.0786.

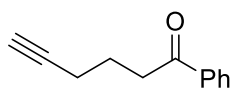
6-Phenyl-7-oxabicyclo[4.1.0]heptan-2-one (203)¹⁰⁸



To a solution of 5,6-dihydro-[1,1'-biphenyl]-3(4H)-one (**202**, 7.0 g, 40.6 mmol) in MeOH (120 mL) at $0\text{ }^\circ\text{C}$ was added 30% solution of hydrogen peroxide (10 mL, 109 mmol) dropwise over 40 min. Sodium hydroxide solution (5 M, 1 mL) was then added dropwise, and the mixture stirred at $\sim 10\text{ }^\circ\text{C}$ for 3 h and a further 16 h at room temperature. The reaction was diluted with brine (50 mL) and extracted with CH_2Cl_2 (3 x 250 mL), the combined organic layers were dried over anhydrous magnesium

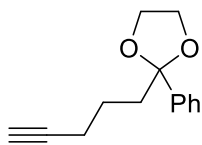
sulfate and concentrated *in vacuo*. The crude product was purified by flash column chromatography (EtOAc:Hexanes (1:4)) to yield a white solid (7.4 g, 97 %), m.p. 34-36 °C; ¹H NMR (400 MHz, CDCl₃) δ_H 7.39-7.31 (5H, m, ArCH), 3.26 (1H, s, CH), 2.67-2.55 (1H, m, CH₂), 2.51-2.39 (2H, m, CH₂), 2.24-2.07 (2H, s, CH₃), 1.87-1.77 (1H, m, CH₂); ¹³C NMR (100 MHz, CDCl₃) δ_C 205.3 (C=O), 138.7 (ArC_q), 128.6 (ArCH), 128.3 (ArCH), 125.2 (ArCH), 64.3 (CH), 64.3 (C_q), 35.8 (CH₂), 27.1 (CH₂), 16.79 (CH₂); FTIR (ATR) ν_{max}: 3061, 2952, 2926, 1709, 1390, 1261, 923 cm⁻¹; HRMS-ESI (m/z): C₁₂H₁₃O₂⁺ [M+H]⁺ theoretical 189.0910, found 189.0901.

1-Phenylhex-5-yn-1-one (**204**)¹⁰⁸



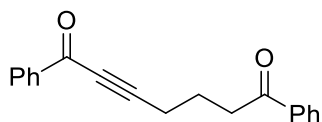
To a solution of 6-phenyl-7-oxabicyclo[4.1.0]heptan-2-one (**203**, 8.5 g, 45.2 mmol) in CH₂Cl₂/AcOH (2:1 mixture, 66 mL) at -20 °C, was added a solution of (*p*-tolylsulfonyl)hydrazine (8.4 g, 45.2 mmol) in CH₂Cl₂/AcOH (2:1 mixture, 66 mL) and the mixture was stirred for 7 h and warmed to room temperature over 16 h. The mixture was concentrated *in vacuo* to remove the CH₂Cl₂, dissolved in Et₂O (50 mL) and filtered. Water (50 mL) was added to the filtrate and the mixture was separated. The aqueous phase was extracted with Et₂O (2 x 100 mL), the combined organic layers were dried over anhydrous magnesium sulfate and concentrated *in vacuo*. The crude product was purified by flash column chromatography (EtOAc:Hexanes (1:19)) to yield a brown oil (1.1 g, 14 %). ¹H NMR (400 MHz, CDCl₃) δ_H 8.01-7.95 (2H, m, ArCH), 7.60-7.53 (1H, m, ArCH), 7.50-7.43 (2H, m, ArCH), 3.14 (2H, t, *J* = 7.2 Hz, CH), 2.34 (2H, td, *J* = 6.8, 2.6 Hz, CH₂), 2.05-1.93 (3H, m, CH₂ and ≡CH); ¹³C NMR (100 MHz, CDCl₃) δ_C 199.6 (CO), 136.9 (ArC_q), 133.1 (ArCH), 128.6 (ArCH), 128.0 (ArCH), 83.7 (C≡CH), 69.1 (C≡CH), 37.0 (CH₂), 22.7 (CH₂), 17.9 (CH₂); FTIR (ATR) ν_{max}: 3295, 3061, 2938, 1682, 1448, 1230, 979 cm⁻¹; HRMS-ESI (m/z): C₁₂H₁₂ONa⁺ [M+Na]⁺ theoretical 195.0780, found 195.0782.

2-(pent-4-yn-1-yl)-2-phenyl-1,3-dioxolane (**205**)¹⁰⁸



Ethylene glycol (1.3 mL, 23.2 mmol) and *p*-toluenesulfonic acid (221 mg, 1.16 mmol) were dissolved in anhydrous toluene (30 mL) and heated under reflux in Dean-Stark conditions for 1 h, before 1-phenylhex-5-yn-1-one (**204**, 1.0 g, 5.81 mmol) was added. The reaction mixture was heated to reflux for a further 16 h, before being cooled down and diluted in Et₂O (30 mL). The organic layer was washed with saturated sodium hydrogen carbonate solution (2 x 50 mL) and brine (2 x 50 mL), dried over anhydrous sodium sulfate and the solvent removed *in vacuo*. The crude product was a yellow oil (1.14 g, 99 %) and carried forward without purification. ¹H NMR (400 MHz, CDCl₃) δ_H 7.49-7.41 (2H, m, ArCH), 7.38-7.26 (3H, m, ArCH), 4.06-3.96 (2H, m, OCH₂), 3.82-3.72 (2H, m, OCH₂), 2.18 (2H, td, *J* = 7.2, 2.6 Hz, CH₂), 2.05-1.96 (2H, m, CH₂), 1.91 (1H, t, *J* = 2.6 Hz, CH), 1.66-1.54 (2H, m, CH₂); ¹³C NMR (100 MHz, CDCl₃) δ_C 142.4 (ArC_q), 128.1 (ArCH), 127.8 (ArCH), 125.7 (ArCH), 110.2 (CO₂), 84.3 (C≡CH), 68.4 (C≡CH), 64.5 (OCH₂), 39.5 (CH₂), 22.7 (CH₂), 18.4 (CH₂).

1,7-Diphenylhept-2-yne-1,7-dione (**147h**)¹⁰⁸



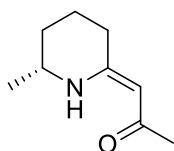
To a solution of 2-(pent-4-yn-1-yl)-1,3-dioxolane (**205**, 1.14 g, 5.27 mmol) in anhydrous THF (20 mL) at -78 °C, was added *n*-butyllithium (1.6 M solution in hexane, 4.9 mL, 6.33 mmol) dropwise, and the reaction mixture stirred for 10 min, before being warmed to 0 °C and stirred for a further 10 min. The reaction mixture was then cooled to -78 °C and benzoyl chloride (734 μL, 6.33 mmol) was added dropwise. After 30 min the reaction was warmed to room temperature and monitored by TLC. The reaction was quenched with water (30 mL), the aqueous layer was extracted with Et₂O (3 x 50 mL), and the combined organic layers were dried over anhydrous magnesium sulfate and concentrated *in vacuo*. The crude residue was dissolved in Et₂O (5 mL) and aq. HCl (3 M, 2 mL) and stirred for 3 h. The reaction was separated between Et₂O (25 mL) and water (20 mL) and the aqueous layer was the extracted with Et₂O (2 x 20 mL). The combined

organic layers were washed with saturated sodium hydrogen carbonate solution and dried over anhydrous magnesium sulfate and the solvent removed *in vacuo*. The crude product was purified by flash column chromatography (EtO₂:pentane 1:4) to yield **147h** as a cream coloured solid (795 mg, 50 %), m.p. 33-35 °C; ¹H NMR (400 MHz, CDCl₃) δ_H 8.15-8.08 (2H, m, ArCH), 8.01-7.95 (2H, m, ArCH), 7.63-7.53 (2H, m, ArCH), 7.51-7.41 (4H, m, ArCH), 3.20 (2H, t, *J* = 7.0 Hz, CH₂), 2.67 (2H, t, *J* = 6.9 Hz, CH₂), 2.14 (2H, *pseudo p*, CH₂); ¹³C NMR (100 MHz, CDCl₃) δ_C 199.0 (CO), 178.1 (CO), 136.8 (ArC_q), 136.7 (ArC_q), 133.7 (ArCH), 133.2 (ArCH), 129.5 (ArCH), 128.7 (ArCH), 128.5 (ArCH), 128.0 (ArCH), 95.53 (C≡C), 80.2 (C≡C), 36.9 (CH₂), 22.1 (CH₂), 16.7 (CH₂); FTIR (ATR) ν_{max}: 3063, 2960, 2236, 2201, 1683, 1635, 1593, 1265, 1200 cm⁻¹; HRMS-ESI (*m/z*): C₁₉H₁₇O₂⁺ [M+H]⁺ theoretical 277.1223, found 277.1221.

General procedure for biotransformations for the preparation of β-enaminones

Commercially available ATA (5 mg/mL) was rehydrated in HEPES buffer (4.5 mL, 100 mM, pH 7.5) containing PLP (1.1 mM) and isopropylamine (89 mM). To this, was added the corresponding ketoynone **2** (0.5 mL, 400 mM stock in DMSO) and the mixture was incubated at 30 °C for 24-48 h in a shaking incubator (200 rpm). The reaction mixture was extracted with Et₂O (3 x 20 mL) and the combined organic layers were washed with water (20 mL), dried over anhydrous sodium sulfate and the solvent removed *in vacuo*. The corresponding β-enaminones **1** were purified by flash column chromatography.

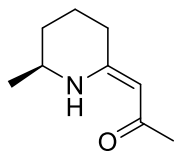
(*R,Z*)-1-(6-Methylpiperidin-2-ylidene)propan-2-one [(*R*)-146a]¹⁰⁸



The reaction of **147a** with ATA025 proceeded in 91 % conversion after 24 h. (*R*)-**146a** was obtained as a colourless oil (24 mg, 78 %, 99 % e.e.) after flash chromatography (EtOAc:hexanes 1:4). ¹H NMR (400 MHz, CDCl₃) δ_H 11.03 (1H, s, NH), 4.85 (1H, s, C=CH), 3.51-3.39 (1H, m, CH), 2.35-2.27 (2H, m, CH₂), 1.98 (3H, s, CH₃), 1.96-1.86 (1H, m, CH₂), 1.85-

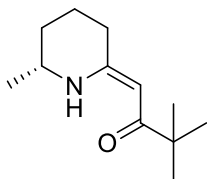
1.74 (1H, m, CH₂), 1.68-1.53 (1H, m, CH₂), 1.41-1.30 (1H, m, CH₂), 1.24 (3H, d, *J* = 6.5 Hz, CH₃); ¹³C NMR (100 MHz, CDCl₃) δ_C 194.3 (CO), 163.8 (C=CH), 93.2 (C=CH), 47.5 (CH₂), 30.7 (CH₂), 28.8 (CH₂), 28.3 (CH₃), 22.9 (CH₃), 19.0 (CH₂); FTIR (ATR) ν_{max}: 3004, 2961, 2927, 2869, 1670, 1670, 1453, 1347 cm⁻¹; HRMS-ESI (m/z): C₉H₁₆NO⁺ [M+H]⁺ theoretical 154.1226, found 154.1232. *e.e.* determination by analysis on a chiral GC column, CP-Chirasil-DEX CB column, retention times: t_r(*R*) = 11.6 min (99.5 %), t_r(*S*) = 12.0 (0.5 %).

(*S,Z*)-1-(6-Methylpiperidin-2-ylidene)propan-2-one [(*S*)-146a]¹⁰⁸



The reaction of **147a** with ATA256 proceeded in 95 % conversion after 24 h. (***S***)-**146a** was obtained as a colourless oil (13 mg, 43 %, 99 % *e.e.*) after flash chromatography (EtOAc:hexanes 1:4). ¹H NMR (400 MHz, CDCl₃) δ_H 11.04 (1H, s, NH), 4.85 (1H, s, C=CH), 3.51-3.40 (1H, m, CH), 2.35-2.28 (2H, m, CH₂), 1.98 (3H, s, CH₃), 1.96-1.87 (1H, m, CH₂), 1.84-1.75 (1H, m, CH₂), 1.66-1.57 (1H, m, CH₂), 1.41-1.30 (1H, m, CH₂), 1.24 (3H, d, *J* = 6.5 Hz, CH₃); ¹³C NMR (100 MHz, CDCl₃) δ_C 194.2 (CO), 163.7 (C=CH), 93.0 (C=CH), 47.3 (CH₂), 30.6 (CH₂), 28.7 (CH₂), 28.2 (CH₃), 22.8 (CH₃), 18.9 (CH₂); FTIR (ATR) ν_{max}: 2944, 2870, 1701, 1663, 1602, 1567, 1292 cm⁻¹; HRMS-ESI (m/z): C₉H₁₆NO⁺ [M+H]⁺ theoretical 154.1226, found 154.1232. *e.e.* determination by analysis on a chiral GC column, CP-Chirasil-DEX CB column, retention times: t_r(*R*) = 11.6 min (not observed), t_r(*S*) = 12.0 (only enantiomer).

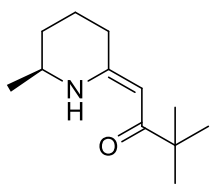
(*R,Z*)-3,3-Dimethyl-1-(6-methylpiperidin-2-ylidene)butan-2-one [(*R*)-146b]¹⁰⁸



The reaction of **147b** with ATA025 proceeded in 99 % conversion after 24 h. (***R***)-**146b** was obtained as a colourless oil (21 mg, 54 %, 94 % *e.e.*) after flash chromatography (EtOAc:hexanes 1:4). ¹H NMR (400 MHz, CDCl₃) δ_H 11.22 (1H, s, NH), 5.02 (1H, s, C=CH), 3.49-3.39 (1H, m, CH), 2.39-2.33 (2H, m, CH₂), 1.95-1.85 (1H, m, CH₂), 1.84-1.75 (1H, m, CH₂),

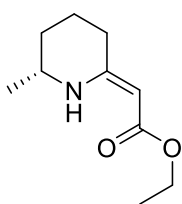
1.65-1.58 (1H, m, CH₂), 1.39-1.32 (1H, m, CH₂), 1.24 (3H, d, *J* = 6.5 Hz, CH₃), 1.13 (9H, s, CH₃); ¹³C NMR (100 MHz, CDCl₃) δ_C 203.4 (CO), 164.6 (C=CH), 88.4 (C=CH), 47.6 (CH₂), 41.2 (C_q), 30.9 (CH₂), 28.8 (CH₂), 28.2 (CH₃), 22.9 (CH₃), 19.3 (CH₂); FTIR (ATR) ν_{max}: 2957, 2864, 1600, 1558, 1291, 1176 cm⁻¹; HRMS-ESI (*m/z*): C₁₂H₂₂NO⁺ [M+H]⁺ theoretical 196.1696, found 196.1700. *e.e.* determination by analysis on a chiral GC column, CP-Chirasil-DEX CB column, retention times: *t_r*(*R*) = 13.7 min (97 %), *t_r*(*S*) = 13.9 (3%).

(*S,Z*)-3,3-Dimethyl-1-(6-methylpiperidin-2-ylidene)butan-2-one [(*S*)-**146b**]¹⁰⁸



The reaction of **147b** with ATA256 proceeded in 97 % conversion after 24 h. (*S*)-**146b** was obtained as a colourless oil (37 mg, 95 %, 98 % *e.e.*) after flash chromatography (EtOAc:hexanes 1:4). ¹H NMR (400 MHz, CDCl₃) δ_H 11.21 (1H, s, NH), 5.02 (1H, s, C=CH), 3.50-3.37 (1H, m, CH), 2.40-2.31 (2H, m, CH₂), 1.95-1.86 (1H, m, CH₂), 1.84-1.75 (1H, m, CH₂), 1.66-1.56 (1H, m, CH₂), 1.41-1.29 (1H, m, CH₂), 1.23 (3H, d, *J* = 6.5 Hz, CH₃), 1.12 (9H, s, CH₃); ¹³C NMR (100 MHz, CDCl₃) δ_C 203.4 (CO), 163.6 (C=CH), 88.4 (C=CH), 47.6 (CH₂), 41.2 (C_q), 30.9 (CH₂), 28.8 (CH₂), 28.2 (CH₃), 22.8 (CH₃), 19.3(CH₂); FTIR (ATR) ν_{max}: 2954, 2868, 1600, 1555, 1293, 1176 cm⁻¹; HRMS-ESI (*m/z*): C₁₂H₂₂NO⁺ [M+H]⁺ theoretical 196.1696, found 196.1703. *e.e.* determination by analysis on a chiral GC column, CP-Chirasil-DEX CB column, retention times: *t_r*(*R*) = 13.7 min (not observed), *t_r*(*S*) = 13.9 (only enantiomer).

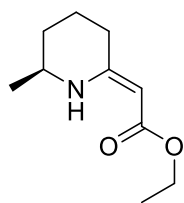
Ethyl (*R,Z*)-2-(6-methylpiperidin-2-ylidene)acetate [(*R*)-**146c**]^{108,165}



The reaction of **147c** with ATA025 proceeded in 92 % conversion after 24 h. (*R*)-**146c** was obtained as a colourless oil (26 mg, 73 %, 83 % *e.e.*) after flash chromatography (EtOAc:hexanes 1:4). ¹H NMR (400 MHz, CDCl₃) δ_H 8.65 (1H, s, NH), 4.34 (1H, s, C=CH), 4.07 (2H, q, *J* = 7.1 Hz, OCH₂CH₃), 3.44-

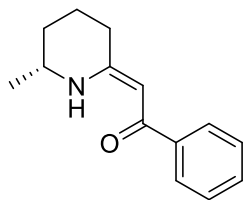
3.33 (1H, m, CH), 2.35-2.27 (2H, m, CH₂), 1.93-1.84 (1H, m, CH₂), 1.82-1.72 (1H, m, CH₂), 1.65-1.52 (1H, m, CH₂), 1.39-1.28 (1H, m, CH₂), 1.24 (3H, t, *J* = 7.1 Hz, OCH₂CH₃), 1.21 (3H, d, *J* = 6.4 Hz, CH₃); ¹³C NMR (100 MHz, CDCl₃) δ_C 170.8 (CO), 162.8 (C=CH), 80.1 (C=CH), 58.3 (OCH₂CH₃), 47.7 (CH₂), 31.3 (CH₂), 29.1 (CH₂), 23.1 (CH₃), 19.7 (CH₂), 14.8 (OCH₂CH₃); FTIR (ATR) ν_{max}: 3271, 2940, 2868, 1645, 1598, 1231, 1146, 1058 cm⁻¹; HRMS-ESI (m/z): C₁₀H₁₇NO₂Na⁺ [M+Na]⁺ theoretical 206.1151, found 206.1152. Data in accordance with literature data.¹⁶⁵ e.e. determination by analysis on a chiral GC column, CP-Chirasil-DEX CB column, retention times: t_r(*R*) = 10.7 min (91.5 %), t_r(*S*) = 10.8 (8.5 %).

Ethyl (S,Z)-2-(6-methylpiperidin-2-ylidene)acetate [(S)-146c]^{108,165}



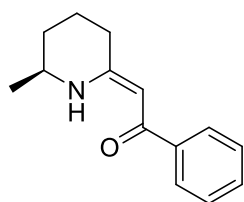
The reaction of **147c** with ATA256 proceeded in 96 % conversion after 24 h. (**S**)-**146c** was obtained as a colourless oil (21 mg, 60 %, 99 % e.e.) after flash chromatography (EtOAc:hexanes 1:4). ¹H NMR (400 MHz, CDCl₃) δ_H 8.66 (1H, s, NH), 4.35 (1H, s, C=CH), 4.08 (2H, q, *J* = 7.1 Hz, OCH₂CH₃), 3.44-3.34 (1H, m, CH), 2.34-2.28 (2H, m, CH₂), 1.92-1.84 (1H, m, CH₂), 1.82-1.73 (1H, m, CH₂), 1.64-1.53 (1H, m, CH₂), 1.39-1.27 (1H, m, CH₂), 1.24 (3H, t, *J* = 7.1 Hz, OCH₂CH₃), 1.21 (3H, d, *J* = 6.4 Hz, CH₃); ¹³C NMR (100 MHz, CDCl₃) δ_C 170.8 (CO), 162.8 (C=CH), 80.1 (C=CH), 58.3 (OCH₂CH₃), 47.7 (CH₂), 31.3 (CH₂), 29.1 (CH₂), 23.1 (CH₃), 19.8 (CH₂), 14.9 (OCH₂CH₃); FTIR (ATR) ν_{max}: 3270, 2940, 2869, 1644, 1597, 1232, 1147, 1058 cm⁻¹; HRMS-ESI (m/z): C₁₀H₁₈NO₂⁺ [M+H]⁺ theoretical 184.1332, found 184.1341. Data in accordance with literature data.¹⁶⁵ e.e. determination by analysis on a chiral GC column, CP-Chirasil-DEX CB column, retention times: t_r(*R*) = 10.7 min (not observed), t_r(*S*) = 10.8 (only enantiomer).

(R,Z)-2-(6-Methylpiperidin-2-ylidene)-1-phenylethan-1-one **[(R)-146d]**¹⁰⁸



The reaction of **147d** with ATA025 proceeded in 88 % conversion after 48 h. **(R)-146d** was obtained as a yellow oil (31 mg, 72 %, 97 % e.e.) after flash chromatography (EtOAc:hexanes 1:9). ¹H NMR (400 MHz, CDCl₃) δ_H 11.66 (1H, s, NH), 7.88-7.81 (2H, m, ArCH), 7.43-7.34 (3H, m, ArCH), 5.56 (1H, s, C=CH), 3.61-3.50 (1H, m, CH), 2.52-2.45 (2H, m, CH₂), 2.02-1.92 (1H, m, CH₂), 1.91-1.82 (1H, m, CH₂), 1.75-1.62 (1H, m, CH₂), 1.48-1.37 (1H, m, CH₂), 1.31 (3H, d, J = 6.5 Hz, CH₃); ¹³C NMR (100 MHz, CDCl₃) δ_C 187.2 (CO), 165.6 (C=CH), 140.8 (ArC_q), 130.3 (ArCH), 128.2 (ArCH), 126.9 (ArCH), 90.1 (C=CH), 47.7 (CH), 30.6 (CH₂), 28.9 (CH₂), 22.9 (CH₃), 19.1 (CH₂); FTIR (ATR) ν_{max}: 3057, 2941, 2867, 1579, 1540, 1285 cm⁻¹; HRMS-ESI (m/z): C₁₄H₁₈NO⁺ [M+H]⁺ theoretical 216.1383, found 216.1383. e.e. determination by analysis on a chiral GC column, CP-Chirasil-DEX CB column, retention times: t_r(R) = 22.1 min (98.5 %), t_r(S) = 22.3 (1.5 %).

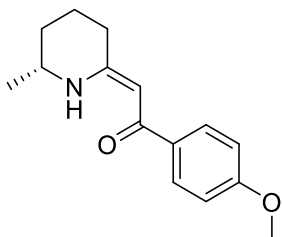
(S,Z)-2-(6-Methylpiperidin-2-ylidene)-1-phenylethan-1-one **[(S)-146d]**¹⁰⁸



The reaction of **147d** with ATA113 proceeded in 91 % conversion after 48 h. **(S)-146d** was obtained as a yellow oil (37 mg, 85 %, 99 % e.e.) after flash chromatography (EtOAc:hexanes 1:9). ¹H NMR (400 MHz, CDCl₃) δ_H 11.66 (1H, s, NH), 7.87-7.81 (2H, m, ArCH), 7.41-7.35 (3H, m, ArCH), 5.56 (1H, s, C=CH), 3.63-3.50 (1H, m, CH), 2.52-2.44 (2H, m, CH₂), 2.04-1.93 (1H, m, CH₂), 1.93-1.82 (1H, m, CH₂), 1.77-1.62 (1H, m, CH₂), 1.49-1.37 (1H, m, CH₂), 1.32 (3H, d, J = 6.5 Hz, CH₃); ¹³C NMR (100 MHz, CDCl₃) δ_C 187.1 (CO), 165.5 (C=CH), 140.6 (ArC_q), 130.2 (ArCH), 128.1 (ArCH), 126.8 (ArCH), 90.0 (C=CH), 47.6 (CH), 30.6 (CH₂), 28.7 (CH₂), 22.7 (CH₃), 18.9 (CH₂); FTIR (ATR) ν_{max}: 3057, 2924, 2853, 1580, 1542, 1287 cm⁻¹; HRMS-ESI (m/z): C₁₄H₁₈NO⁺ [M+H]⁺ theoretical 216.1383, found 216.1389. e.e. determination by analysis on a chiral GC column, CP-Chirasil-DEX CB

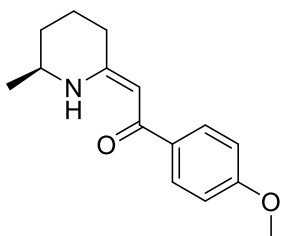
column, retention times: $t_r(R)$ = 22.1 min (not observed), $t_r(S)$ = 22.3 (only enantiomer).

(*R,Z*)-1-(4-Methoxyphenyl)-2-(6-methylpiperidin-2-ylidene)ethan-1-one
[(*R*)-146e]¹⁰⁸



The reaction of **147e** with ATA025 proceeded in 88 % conversion after 48 h. (***R***)-**146e** was obtained as a yellow solid (31 mg, 79 %, 94 % e.e.) after flash chromatography (EtOAc:hexanes 1:9). m.p. 49-54 °C; ¹H NMR (400 MHz, CDCl₃) δ_H 11.55 (1H, s, NH), 7.86-7.80 (2H, m, ArCH), 6.92-6.86 (2H, m, ArCH), 5.52 (1H, s, C=CH), 3.84 (3H, s, CH₃) 3.59-3.48 (1H, m, CH), 2.50-2.44 (2H, m, CH₂), 2.01-1.92 (1H, m, CH₂), 1.90-1.80 (1H, m, CH₂), 1.73-1.63 (1H, m, CH₂), 1.44-1.38 (1H, m, CH₂), 1.30 (3H, d, J = 6.5 Hz, CH₃); ¹³C NMR (100 MHz, CDCl₃) δ_C 186.4 (CO), 164.9 (C=CH), 161.4 (ArC_q), 133.3 (ArC_q), 128.5 (ArCH), 113.3 (ArCH), 89.4 (C=CH), 55.3 (CH), 47.5 (CH₃), 30.6 (CH₂), 28.8 (CH₂), 22.8 (CH₃), 19.0 (CH₂); FTIR (ATR) ν_{max} : 2925, 2854, 1581, 1537, 1251, 1155 cm⁻¹; HRMS-ESI (m/z): C₁₅H₂₀NO₂⁺ [M+H]⁺ theoretical 246.1489, found 246.1501. e.e. determination by analysis on a chiral HPLC column, lux cellulose-2 column, flow 1 mL min⁻¹, water/ACN 4:9, retention times: $t_r(R)$ = 5.6 min (97 %), $t_r(S)$ = 4.0 (3 %).

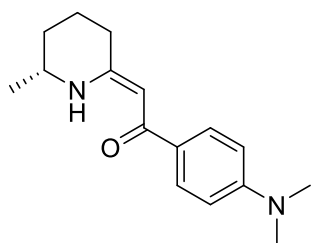
(*S,Z*)-1-(4-Methoxyphenyl)-2-(6-methylpiperidin-2-ylidene)ethan-1-one
[(*S*)-146e]¹⁰⁸



The reaction of **147e** with ATA113 proceeded in 92 % conversion after 48 h. (***S***)-**146e** was obtained as a yellow solid (23 mg, 52 %, 98 % e.e.) after flash chromatography (EtOAc:hexanes 1:9). m.p. 50-53 °C ; ¹H NMR (400 MHz, CDCl₃) δ_H 11.55 (1H, s, NH), 7.86-7.9 (2H, m, ArCH), 6.91-6.85 (2H, m, ArCH), 5.52 (1H, s, C=CH), 3.83 (3H, s, CH₃) 3.58-3.49 (1H, m, CH), 2.50-2.42 (2H, m, CH₂), 2.01-1.92 (1H, m, CH₂), 1.90-1.79 (1H, m, CH₂), 1.74-1.61 (1H, m, CH₂), 1.44-1.38 (1H, m, CH₂), 1.30 (3H, d, J = 6.5 Hz, CH₃); ¹³C NMR (100 MHz, CDCl₃) δ_C 187.5

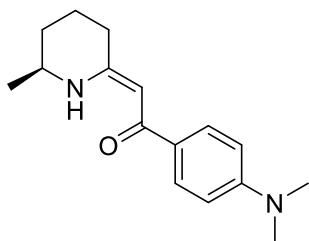
(CO), 165.1 (C=CH), 161.5 (ArC_q), 133.4 (ArC_q), 128.7 (ArCH), 113.4 (ArCH), 89.5 (C=CH), 55.4 (CH), 47.7 (CH₃), 30.8 (CH₂), 28.9 (CH₂), 22.9 (CH₃), 19.2(CH₂); FTIR (ATR) ν_{\max} : 2926, 2853, 1579, 1537, 1247, 1154 cm⁻¹; HRMS-ESI (m/z): C₁₅H₂₀NO₂⁺ [M+H]⁺ theoretical 246.1489, found 246.1500. e.e. determination by analysis on a chiral HPLC column, lux cellulose-2 column, flow 1 mL min⁻¹, water/ACN 4:9, retention times: t_r(R) = 5.6 min (99 %), t_r(S) = 4.0 (1 %).

(R,Z)-1-(4-(Dimethylamino)phenyl)-2-(6-methylpiperidin-2-ylidene)ethan-1-one [(R)-146f]¹⁰⁸



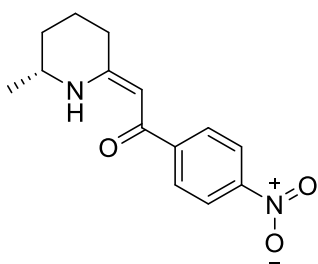
The reaction of **147f** with ATA025 proceeded in 46 % conversion after 48 h. **(R)-146f** was obtained as a yellow solid (20 mg, 43 %, 99 % e.e.) after flash chromatography (EtOAc:hexanes 1:9). m.p. 126-129 °C; ¹H NMR (400 MHz, CDCl₃) δ_{H} 11.45 (1H, s, NH), 7.83-7.77 (2H, m, ArCH), 6.70-6.64 (2H, m, ArCH), 5.53 (1H, s, C=CH), 3.57-3.47 (1H, m, CH), 3.01 (6H, s, CH₃), 2.49-2.43 (2H, m, CH₂), 1.99-1.90 (1H, m, CH₂), 1.89-1.80 (1H, m, CH₂), 1.71-1.63 (1H, m, CH₂), 1.43-1.37 (1H, m, CH₂), 1.29 (3H, d, *J* = 6.4 Hz, CH₃); ¹³C NMR (100 MHz, CDCl₃) δ_{C} 187.0 (CO), 164.1 (C=CH), 152.0 (ArC_q), 128.5 (ArCH), 128.4 (ArC_q), 111.2 (ArCH), 89.2 (C=CH), 47.6 (CH), 40.3 (CH₃), 30.9 (CH₂), 29.0 (CH₂), 23.0 (CH₃), 19.4 (CH₂); FTIR (ATR) ν_{\max} : 2923, 2852, 1582, 1505, 1283, 1169 cm⁻¹; HRMS-ESI (m/z): C₁₆H₂₃N₂O⁺ [M+H]⁺ theoretical 259.1805, found 259.1814. e.e. determination by analysis on a chiral HPLC column, lux cellulose-2 column, flow 1 mL min⁻¹, water/ACN 4:9, retention times: t_r(R) = 7.0 min (99.5 %), t_r(S) = 4.3 (0.5 %).

(S,Z)-1-(4-(Dimethylamino)phenyl)-2-(6-methylpiperidin-2-ylidene)ethan-1-one [(S)-146f]¹⁰⁸



The reaction of **147f** with ATA113 proceeded in 53 % conversion after 48 h. **(S)-146f** was obtained as a yellow solid (12 mg, 29 %, 98 % e.e.) after flash chromatography (EtOAc:hexanes 1:9). m.p. 127-129 °C; ¹H NMR (400 MHz, CDCl₃) δ_H 11.47 (1H, s, NH), 7.86-7.79 (2H, m, ArCH), 6.86-6.79 (2H, m, ArCH), 5.55 (1H, s, C=CH), 3.59-3.49 (1H, m, CH), 3.03 (6H, s, CH₃), 2.51-2.45 (2H, m, CH₂), 2.01-1.92 (1H, m, CH₂), 1.90-1.81 (1H, m, CH₂), 1.73-1.65 (1H, m, CH₂), 1.45-1.38 (1H, m, CH₂), 1.31 (3H, d, *J* = 6.5 Hz, CH₃); ¹³C NMR (100 MHz, CDCl₃) δ_C 187.0 (CO), 164.1 (C=CH), 152.0 (ArC_q), 128.5 (ArCH), 128.4 (ArC_q), 111.2 (ArCH), 89.2 (C=CH), 47.6 (CH), 40.3 (CH₃), 30.9 (CH₂), 29.0 (CH₂), 23.0 (CH₃), 19.4 (CH₂); FTIR (ATR) ν_{max}: 2924, 2855, 1585, 1506, 1285, 1174 cm⁻¹; HRMS-ESI (*m/z*): C₁₆H₂₃N₂O⁺ [M+H]⁺ theoretical 259.1805, found 259.1819. e.e. determination by analysis on a chiral HPLC column, lux cellulose-2 column, flow 1 mL min⁻¹, water/ACN 4:9, retention times: *t*_r(*R*) = 7.0 min (99 %), *t*_r(*S*) = 4.3 (1 %).

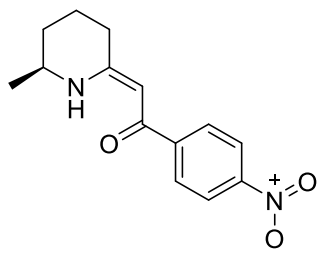
(R,Z)-2-(6-Methylpiperidin-2-ylidene)-1-(4-nitrophenyl)ethan-1-one [(R)-146g]¹⁰⁸



The reaction of **147g** with ATA025 proceeded in 98 % conversion after 48 h. **(R)-146g** was obtained as a yellow solid (30 mg, 58 %, 99 % e.e.) after flash chromatography (EtOAc:hexanes 1:9). m.p. 141-143 °C; ¹H NMR (400 MHz, CDCl₃) δ_H 11.84 (1H, s, NH), 8.26-8.20 (2H, m, ArCH), 8.00-7.93 (2H, m, ArCH), 5.56 (1H, s, C=CH), 3.65-3.55 (1H, m, CH), 2.56-2.47 (2H, m, CH₂), 2.07-1.96 (1H, m, CH₂), 1.95-1.85 (1H, m, CH₂), 1.78-1.66 (1H, m, CH₂), 1.52-1.40 (1H, m, CH₂), 1.34 (3H, d, *J* = 6.5 Hz, CH₃); ¹³C NMR (100 MHz, CDCl₃) δ_C 183.9 (CO), 167.1 (C=CH), 148.8 (ArC_q), 146.5 (ArC_q), 127.8 (ArCH), 123.6 (ArCH), 90.8 (C=CH), 48.0 (CH), 30.4 (CH₂), 28.9 (CH₂), 22.9 (CH₃), 18.8 (CH₂); FTIR (ATR) ν_{max}: 3065, 2919, 2851, 1583, 1543, 1337,

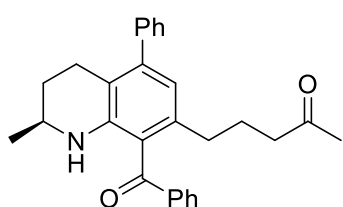
1260 cm^{-1} ; HRMS-ESI (m/z): $\text{C}_{14}\text{H}_{17}\text{N}_2\text{O}_3^+$ $[\text{M}+\text{H}]^+$ theoretical 261.1234, found 261.1244. e.e. determination by analysis on a chiral HPLC column, lux cellulose-2 column, flow 1 mL min^{-1} , water/ACN 4:9, retention times: $t_r(\text{R}) = 11.1 \text{ min}$ (99.5 %), $t_r(\text{S}) = 9.6$ (0.5 %).

(S,Z)-2-(6-Methylpiperidin-2-ylidene)-1-(4-nitrophenyl)ethan-1-one
[(S)-146g]¹⁰⁸



The reaction of **147g** with ATA113 proceeded in 94 % conversion after 48 h. **(S)-146g** was obtained as a yellow solid (28 mg, 53 %, 97 % e.e.) after flash chromatography (EtOAc:hexanes 1:9). m.p. 142-145 $^{\circ}\text{C}$; $^1\text{H NMR}$ (400 MHz, CDCl_3) δ_{H} 11.83 (1H, s, NH), 8.24-8.18 (2H, m, ArCH), 7.99-7.92 (2H, m, ArCH), 5.54 (1H, s, C=CH), 3.64-3.53 (1H, m, CH), 2.54-2.47 (2H, m, CH_2), 2.05-1.95 (1H, m, CH_2), 1.93-1.84 (1H, m, CH_2), 1.77-1.64 (1H, m, CH_2), 1.49-1.39 (1H, m, CH_2), 1.33 (3H, d, $J = 6.5 \text{ Hz}$, CH_3); $^{13}\text{C NMR}$ (100 MHz, CDCl_3) δ_{C} 183.3 (CO), 167.1 (C=CH), 148.8 (ArC_q), 146.4 (ArC_q), 127.7 (ArCH), 123.5 (ArCH), 90.7 (C=CH), 48.0 (CH), 30.4 (CH_2), 28.8 (CH_2), 22.7 (CH_3), 18.7 (CH_2); FTIR (ATR) ν_{max} : 3078, 2925, 2852, 1585, 1546, 1338, 1270 cm^{-1} ; HRMS-ESI (m/z): $\text{C}_{14}\text{H}_{17}\text{N}_2\text{O}_3^+$ $[\text{M}+\text{H}]^+$ theoretical 261.1234, found 261.1238. e.e. determination by analysis on a chiral HPLC column, lux cellulose-2 column, flow 1 mL min^{-1} , water/ACN 4:9, retention times: $t_r(\text{R}) = 11.1 \text{ min}$ (98.5 %), $t_r(\text{S}) = 9.6$ (1.5 %).

By-product (S)-5-(8-benzoyl-2-methyl-5-phenyl-1,2,3,4-tetrahydroquinolin-7-yl)pentan-2-one (157d)¹⁰⁸



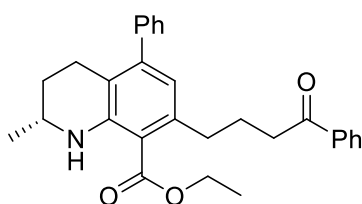
Yellow oil after flash chromatography (EtOAc:hexanes 1:9). $^1\text{H NMR}$ (400 MHz, CDCl_3) δ_{H} 7.90-7.86 (2H, m, ArCH), 7.62-7.56 (1H, m, ArCH), 7.50-7.32 (7H, m, ArCH), 6.44 (1H, s, ArCH), 4.41 (1H, s, NH), 3.41-3.31 (1H, m, CH), 2.75-2.55 (2H, m, CH_2), 2.32-2.17 (4H, m, CH_2), 2.01 (3H, s, CH_3), 1.86-1.77 (1H, m, CH_2), 1.70 (2H, m, CH_2), 1.46-1.34 (1H, m, CH_2), 1.07 (3H, d, $J = 6.3 \text{ Hz}$, CH_3); $^{13}\text{C NMR}$

(100 MHz, CDCl₃) δ_c 208.7, 200.7, 143.6, 143.0, 141.7, 138.6, 137.5, 133.9, 129.6, 129.0, 128.8, 128.0, 127.0, 122.0, 119.0, 117.2, 47.0, 43.0, 33.0, 29.7, 29.5, 25.5, 25.1, 22.4; FTIR (ATR) ν_{\max} : 3057, 2941, 2867, 1579, 1541, 1285, 1175 cm⁻¹; HRMS-ESI (m/z): C₂₈H₃₀NO₂⁺ [M+H]⁺ theoretical 412.2271, found 412.2281.

General procedure for ATA-Carbo-[3+3] annulation cascade¹⁰⁸

Commercially available ATA025 (5 mg/mL) was rehydrated in HEPES buffer (9 mL, 100 mM, pH 7.5) containing PLP (1.1 mM) and isopropylamine (44 mM). To this, was added the selected ketoynone **2** (0.5 mL, 400 mM stock in DMSO), and 1,7-Diphenylhept-2-yne-1,7-dione **2h** (0.5 mL, 400 mM stock in DMSO). The mixture was incubated at 30 °C for 24-72 h in a shaking incubator (200 rpm). The reaction mixture was extracted with EtOAc (3 x 40 mL) and the combined organic layers were washed with water (40 mL), dried over anhydrous sodium sulfate and the solvent removed *in vacuo*. The corresponding products were purified by flash column chromatography.

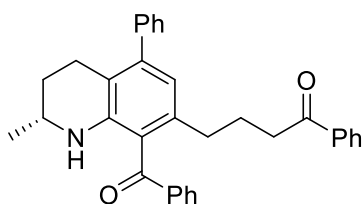
Ethyl (R)-2-methyl-7-(4-oxo-4-phenylbutyl)-5-phenyl-1,2,3,4-tetrahydroquinoline-8-carboxylate (**158c**)¹⁰⁸



The reaction of **147c** with ATA025 and **147h** (0.2 mmol in 500 μ L DMSO) after 48 h gave **158c** as a yellow oil (40 mg, 90 %) after flash column chromatography (EtOAc:hexanes (1:19)). ¹H NMR (400 MHz, CDCl₃) δ_H 7.95 – 7.90 (2H, m, ArCH), 7.56 – 7.51 (1H, m, ArCH), 7.48 – 7.29 (6H, m, ArCH), 7.25 – 7.23 (1H, m, ArCH), 6.38 (1H, s, ArCH), 4.37 (2H, q, *J* = 7.2 Hz, OCH₂CH₃), 3.53 – 3.44 (1H, m, CH), 2.98 (2H, t, *J* = 7.3 Hz, CH₃), 2.92 – 2.81 (2H, m, CH₂), 2.69 – 2.52 (2H, m, CH₂), 2.05 (2H, m, CH₂), 1.87 – 1.79 (1H, m, CH₂), 1.46 - 1.37 (4H, m, CH₂ and CH₃), 1.24 (3H, d, *J* = 6.4 Hz, CH₃).; ¹³C NMR (100 MHz, CDCl₃) δ_c 200.2 (CO), 169.8 (CO), 146.4 (ArC_q), 144.6 (ArC_q), 141.5 (ArC_q), 140.4 (ArC_q), 137.1 (ArC_q), 132.9 (ArCH), 128.8 (ArCH), 128.6 (ArCH), 128.1 (ArCH), 128.0 (ArCH), 127.0 (ArCH), 119.7 (ArCH), 117.3 (ArC_q), 111.4

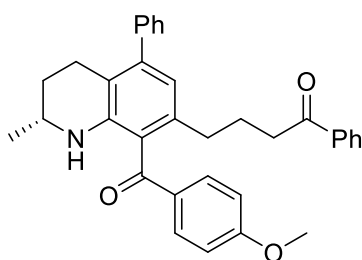
(ArC_q), 60.7 (OCH₂CH₃), 46.8 (CH), 38.2 (CH₂), 35.0 (CH₂), 29.1 (CH₂), 26.1 (CH₂), 25.6 (CH₂), 22.7 (CH₃), 14.3 (OCH₂CH₃); FTIR (ATR) ν_{max} : 3386, 2958, 2926, 1725, 1671, 1253, 1223, 1171 cm⁻¹; HRMS-ESI (m/z): C₂₉H₃₂NO₃⁺ [M+H]⁺ theoretical 442.2377, found 442.2376.

(R)-4-(8-benzoyl-2-methyl-5-phenyl-1,2,3,4-tetrahydroquinolin-7-yl)-1-phenylbutan-1-one (158d)¹⁰⁸



The reaction of **147d** with ATA025 and **147h** (0.2 mmol in 500 μ L DMSO) after 48 h gave **158d** as a yellow oil (9 mg, 10 %) after flash column chromatography (EtO₂:petane (1:4)). ¹H NMR (400 MHz, CDCl₃) δ_{H} 7.90 – 7.87 (2H, m, ArCH), 7.85 – 7.81 (2H, m, ArCH), 7.60 – 7.55 (1H, m, ArCH), 7.48 – 7.43 (3H, m, ArCH), 7.42 – 7.37 (4H, m, ArCH), 7.35 – 7.30 (3H, m, ArCH), 6.49 (1H, s, ArCH), 3.41 – 3.32 (1H, m, CH), 2.76 (2H, t, *J* = 7.4 Hz, CH₂), 2.70 – 2.57 (2H, m, CH₂), 2.37 (2H, t, *J* = 6.7 Hz, CH₂), 1.91 – 1.84 (2H, m, CH₂), 1.84 – 1.78 (1H, m, CH₂), 1.47 – 1.37 (1H, m, CH₂), 1.09 (3H, d, *J* = 6.3 Hz, CH₃); ¹³C NMR (100 MHz, CDCl₃) δ_{C} 200.7 (CO), 199.9 (CO), 143.60 (ArC_q), 142.77 (ArC_q), 141.59 (ArC_q), 138.61 (ArC_q), 137.55 (ArC_q), 136.87 (ArC_q), 133.45 (ArCH), 132.80 (ArCH), 129.54 (ArCH), 128.96 (ArCH), 128.72 (ArCH), 128.44 (ArCH), 128.00 (ArCH), 127.98 (ArCH), 126.91 (ArCH), 122.16 (ArC_q), 119.27 (ArCH), 117.37 (ArC_q), 47.00 (CH), 37.82 (CH₂), 33.11 (CH₂), 29.39 (CH₂), 25.51 (CH₂), 25.45 (CH₂), 22.34 (CH₃); FTIR (ATR) ν_{max} : 3058, 3027, 2927, 1681, 1592, 1448, 1262, 908 cm⁻¹; HRMS-ESI (m/z): C₃₃H₃₂NO₂ [M+H]⁺ theoretical 474.2428, found 474.2438.

(R)-4-(8-(4-methoxybenzoyl)-2-methyl-5-phenyl-1,2,3,4-tetrahydroquinolin-7-yl)-1-phenylbutan-1-one (158e)¹⁰⁸



The reaction of **147e** with ATA025 and **147h** (0.25 mmol, in 500 μ L DMSO) after 72 h gave **158e** as a yellow oil (27 mg, 27 %) after flash column chromatography (EtOAc:hexanes (1:99)). ¹H NMR (400 MHz, CDCl₃) δ_{H} 7.93 –

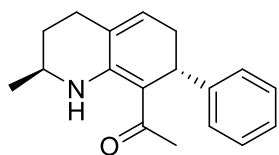
7.79 (4H, m, ArCH), 7.61 – 7.44 (2H, m, ArCH), 7.44 – 7.36 (4H, m, ArCH), 7.36 – 7.28 (2H, m, ArCH), 6.96 – 6.90 (2H, m, ArCH), 6.50 (1H, s, ArCH), 3.87 (3H, s, OCH₃), 3.41 – 3.29 (1H, m, CH), 2.80 (2H, t, *J* = 7.4 Hz, CH₂), 2.74 – 2.54 (2H, m, CH₂), 2.41 (2H, t, *J* = 6.7 Hz, CH₂), 1.96 – 1.75 (3H, m, CH₂), 1.49 – 1.36 (1 H, m, CH₂), 1.08 (3H, d, *J* = 6.3 Hz, CH₃); ¹³C NMR (100 MHz, CDCl₃) δ_C 200.1 (CO), 199.1 (CO), 164.0 (ArC_q), 143.2 (ArC_q), 142.4 (ArC_q), 141.8 (ArC_q), 137.0 (ArC_q), 132.8 (ArCH), 132.1 (ArCH), 131.2 (ArC_q), 129.0 (ArCH), 128.7 (ArC_q), 128.5 (ArCH), 128.0 (ArCH), 128.0 (ArCH), 126.9 (ArCH), 122.9 (ArC_q), 122.0, 119.1 (ArCH), 117.2 (ArC_q), 114.0 (ArCH), 55.5 (OCH₃), 47.0 (CH), 37.9 (CH₂), 32.9 (CH₂), 29.6 (CH₂), 25.5 (CH₂), 25.5 (CH₂), 22.4 (CH₃); FTIR (ATR) ν_{max}: 3058, 2931, 2854, 1682, 1596, 1448, 1256, 1162 cm⁻¹; HRMS-ESI (*m/z*): C₃₄H₃₄NO₃Na [M+Na]⁺ theoretical 526.2353, found 526.2358.

Annulation reactions of chiral enamines

1-((2*S*)-2-Methyl-7-phenyl-1,2,3,4,6,7-hexahydroquinolin-8-yl)ethan-1-one (**148**)^{108,138}

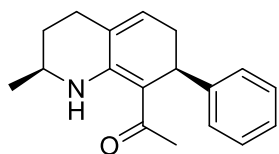
Anhydrous sodium sulfate (222 mg, 1.57 mmol), pyridinium acetate (106 mg, 0.73 mmol) and *trans*-cinnamaldehyde (91 μL, 0.73 mmol) were dissolved in ethyl acetate:toluene (2:3, 1 mL) and the mixture heated at 100 °C for 0.5 h. (*S,Z*)-1-(6-Methylpiperidin-2-ylidene)propan-2-one (**S**)-**146a** (80 mg, 0.52 mmol) was added and the reaction mixture was heated at 100 °C for 16 h. The solid formed was removed by filtration and was washed with ethyl acetate. The organic solution was concentrated *in vacuo* and the crude mixture was purified by flash column chromatography to produce a mixture of diastereoisomers as a yellow oil (132 mg, 95 %, 57:43 *d.r.*). Further column chromatography (CH₂Cl₂) allowed the separation of diastereoisomers (**S,R**)-**148** and (**S,S**)-**148**.

1-((2*S*,7*R*)-2-Methyl-7-phenyl-1,2,3,4,6,7-hexahydroquinolin-8-yl)ethan-1-one ((*S*,*R*)-148)¹⁰⁸



Yellow oil (73 mg, 53 %). ¹H NMR (400 MHz, CDCl₃) δ_H 11.94 (1H, s, NH), 7.25-7.22 (2H, m, ArCH), 7.20-7.14 (3H, m, ArCH), 5.77-5.72 (1H, m, C=CH), 3.96-3.91 (1H, m, CH), 3.70-3.60 (1H, m, CH), 2.89-2.78 (1H, m, CH₂), 2.50-2.73 (3H, m, CH₂), 2.02-1.94 (1H, m, CH₂), 1.93 (3H, s, CH₃), 1.52-1.39 (1H, m, CH₂), 1.30 (3H, d, *J* = 6.4 Hz, CH₃); ¹³C NMR (100 MHz, CDCl₃) δ_C 194.8 (CO), 154.6 (C=CH), 145.5 (ArC_q), 131.1 (ArCH), 128.7 (ArCH), 128.1 (ArCH), 127.5, 126.0, 98.4 (C=CH), 46.9 (CH), 38.3 (CH₂), 33.1 (CH₂), 29.5 (CH₃), 27.0 (CH₂), 25.6, 22.4; FTIR (ATR) ν_{max}: 3365, 2923, 2851, 1641, 1565, 1449, 1374 cm⁻¹; HRMS-ESI (*m/z*): C₁₈H₂₂NO⁺ [M+H]⁺ theoretical 268.1696, found 268.1712.

1-((2*S*,7*S*)-2-Methyl-7-phenyl-1,2,3,4,6,7-hexahydroquinolin-8-yl)ethan-1-one ((*S*,*S*)-148)¹⁰⁸



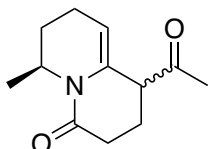
Yellow solid (54 mg, 39 %), m.p. 45-49 °C; ¹H NMR (400 MHz, CDCl₃) δ_H 12.07 (1H, s, NH), 7.25-7.21 (2H, m, ArCH), 7.20-7.13 (3H, m, ArCH), 5.81-5.76 (1H, m, C=CH), 3.62-3.52 (1H, m, CH), 2.87-2.77 (1H, m, CH), 2.59-2.32 (3H, m, CH₂), 1.95-1.86 (4H, m, CH₃, CH₂), 1.57-1.48 (1H, m, CH₂), 1.35 (3H, d, *J* = 6.5 Hz, CH₃); ¹³C NMR (100 MHz, CDCl₃) δ_C 194.8 (CO), 154.6 (C=CH), 145.5 (ArC_q), 131.1 (ArCH), 128.7 (ArCH), 128.1 (ArCH), 127.5, 126.0, 98.4 (C=CH), 46.9 (CH), 38.3 (CH₂), 33.1 (CH₂), 29.5 (CH₃), 27.0 (CH₂), 25.6, 22.4; FTIR (ATR) ν_{max}: 3360, 2960, 2925, 1658, 1562, 1449, 1374 cm⁻¹; HRMS-ESI (*m/z*): C₁₈H₂₂NO⁺ [M+H]⁺ theoretical 268.1696, found 268.1712.

Crystal Data for (*S,S*)-148 C₁₈H₂₁NO (*M* = 267.36 g/mol): orthorhombic, space group P2₁2₁2₁ (no. 19), *a* = 7.13890(10) Å, *b* = 11.77050(10) Å, *c* = 17.23630(10) Å, *V* = 1448.34(3) Å³, *Z* = 4, *T* = 120(2) K, μ(CuKα) = 0.582 mm⁻¹, *D*_{calc} = 1.226 g/cm³, 21960 reflections measured (9.098° ≤ 2θ ≤ 145.85°), 2866 unique (*R*_{int} = 0.0210, *R*_{sigma} = 0.0102) which were used in

all calculations. The final R_1 was 0.0259 ($I > 2\sigma(I)$) and wR_2 was 0.0661 (all data). CCDC 1945711.

(6S)-1-acetyl-6-methyl-1,2,3,6,7,8-hexahydro-4H-quinolizin-4-one

(161a)



(S,Z)-1-(6-Methylpiperidin-2-ylidene)propan-2-one **(S)-**

146a (10 mg, 0.07 mmol) was dissolved in THF (1 mL)

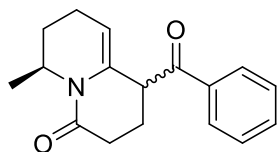
before acryloyl chloride (7 μ L, 0.08 mmol) was added and

the reaction mixture was heated to reflux for 16 h. The reaction was quenched with saturated sodium hydrogen carbonate solution (2 mL) and the aqueous layer was extracted into CH_2Cl_2 (2 x 4 mL). The combined organic layers were dried over anhydrous magnesium sulfate and concentrated *in vacuo*. The crude product was purified by flash column chromatography (CH_2Cl_2) to give a yellow oil (6 mg, 44 %, 3:1 *d.r.*). ^1H NMR (400 MHz, CDCl_3) δ_{H}

4.97 (1H, m, CH_3CH), 4.93 – 4.87 (1H, m, $\text{C}=\text{CH}$ (major)), 4.73 – 4.69 (1H, m, $\text{C}=\text{CH}$ (major)), 3.35 – 3.31 (1H, t, $J = 4.9$ Hz, CH (minor)), 3.25 (1H, t, $J = 4.3$ Hz, CH (major)), 2.61 – 2.39 (2H, m, CH_2), 2.24 – 2.21 (1H, m, CH_2), 2.25 (3H, s, CH_3 (minor)), 2.20 (3H, s, CH_3 (major)), 2.13 – 2.03 (1H, m, CH_2), 1.95 – 1.85 (1H, m, CH_2), 1.79 – 1.70 (2H, m, CH_2), 1.13 (3H, d, $J = 6.7$ Hz, CH_3 (major)), 1.11 (3H, d, $J = 6.5$, CH_3); ^{13}C NMR (101 MHz, CDCl_3) δ_{C} 208.2 (CO (minor)), 207.5 (CO (major)), 167.3 (CO (minor)), 167.0 (CO (major)), 132.7 ($\text{C}=\text{CH}$ (minor)), 132.5 ($\text{C}=\text{CH}$ (major)), 107.6 ($\text{C}=\text{CH}$ (major)), 106.2 ($\text{C}=\text{CH}$ (minor)), 52.6 (CH (major)), 52.4 (CH (minor)), 44.8 (CH (major)), 43.4 (CH (minor)), 30.6 (CH_2 (major)), 29.7 (CH_3 (minor)), 28.8 (CH_2 (minor)), 28.0 (CH_3 (minor)), 26.3 (CH_2 (minor)), 26.2 (CH_2 (major)), 21.6 (CH_2 (minor)), 21.4 (CH_2 (major)), 18.6 (CH_2 (minor)), 18.5 (CH_2 (major)), 16.8 (CH_3 (minor)), 16.1 (CH_3 (major)); HRMS-ESI (m/z): $\text{C}_{12}\text{H}_{17}\text{NO}_2\text{Na}^+$ $[\text{M}+\text{Na}]^+$ theoretical 230.1151, found 230.1149.

(6S)-1-Benzoyl-6-methyl-1,2,3,6,7,8-hexahydro-4H-quinolizin-4-one

(161d)^{108,139}



(*S,Z*)-2-(6-Methylpiperidin-2-ylidene)-1-phenylethan-1-one (**S**)-**146d** (10 mg, 0.07 mmol) was dissolved in THF (1 mL) before acryloyl chloride (7 μ L, 0.08 mmol)

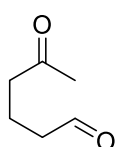
was added and the reaction mixture was heated under reflux for 16 h. The reaction was quenched with saturated sodium hydrogen carbonate solution (2 mL) and the aqueous layer was extracted into CH_2Cl_2 (2 x 4 mL). The combined organic layers were dried over anhydrous magnesium sulfate and concentrated *in vacuo*. The crude product was purified by flash column chromatography (CH_2Cl_2) to give a yellow oil (23 mg, 52 %, 3:1 *d.r.*). ^1H NMR (400 MHz, CDCl_3) δ_{H} 8.01-7.96 (2H, m, ArCH (minor)), 7.96-7.91 (2H, m, ArCH (major)), 7.64-7.55 (1H, m, ArCH), 7.54-7.45 (2H, m, ArCH), 5.02-4.92 (1H, m, CH_3CH), 4.80-4.75 (1H, m, $\text{C}=\text{CH}$ (major)), 4.56-4.51 (1H, m, $\text{C}=\text{CH}$ (minor)), 4.35-4.27 (1H, m, CHCO), 2.51-2.44 (2H, m, CH_2), 2.25-2.08 (3H, m, CH_2), 2.08-1.95 (1H, m, CH_2), 1.85-1.65 (2H, m, CH_2), 1.17 (3H, d, J = 6.6 Hz, CH_3); ^{13}C NMR (100 MHz, CDCl_3) δ_{C} 199.4 (CO (minor)), 199.2 (CO (major)), 167.0 (CO (minor)), 166.8 (CO (major)), 136.2 (Ar C_q (minor)), 135.5 (Ar C_q (major)), 133.7 (ArCH (minor)), 133.4 (ArCH (major)), 133.4 ($\text{C}=\text{CH}$ (minor)), 132.5 ($\text{C}=\text{CH}$ (major)), 128.9 (ArCH (minor)), 128.8 (ArCH (major)), 128.6 (ArCH (minor)), 128.5 (ArCH (major)), 106.5 ($\text{C}=\text{CH}$ (major)), 106.0 ($\text{C}=\text{CH}$ (minor)), 46.4 (CH (major)), 46.3 (CH (minor)), 44.1 (CH_2 (minor)), 43.7 (CH (major)), 30.8 (CH_2 (minor)), 29.4 (CH_2 (major)), 26.2 (CH_2 (major)), 26.0 (CH_2 (minor)), 22.9 (CH_2 (major)), 22.8 (CH_2 (minor)), 18.5 (CH_2 (major)), 18.4 (CH_2 (minor)), 16.4 (CH_3 (minor)), 15.8 (CH_3 (major)). FTIR (ATR) ν_{max} : 2959, 2922, 2849, 1713, 1672, 1399 cm^{-1} ; HRMS-ESI (m/z): $\text{C}_{17}\text{H}_{19}\text{NO}_2\text{Na}^+$ [$\text{M}+\text{Na}$] $^+$ theoretical 292.1308, found 292.1308.

7.3 Mannich Reaction

General Procedure for the synthesis of keto aldehydes

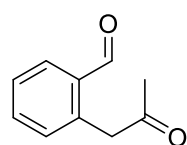
Ozone was bubbled through a solution of the corresponding alkene (8.6 mmol) in dichloromethane (50 mL) at -78 °C until a light blue colour was observed. Triphenyl phosphine (11.2 mmol) was added to the solution and the reaction mixture was allowed warm to room temperature overnight. The mixture was then concentrated *in vacuo* and redissolved in diethyl ether (20 mL) and the white solid was removed *via* filtration. The filtrate was concentrated *in vacuo* and the crude product was purified by column chromatography (Et₂O:pentane (1:9)) to provide the title compound.

5-Oxohexanal (173b)¹⁶⁶



The reaction of methyl cyclopentane (3.00 g, 36.5 mmol) with ozone to produce 5-oxohexanal as a colourless oil (2.08 g, 50 %). ¹H NMR (400 MHz, CDCl₃) δ_H 9.75 (1H, t, *J* = 1.4 Hz, HC=O), 2.53 – 2.45 (4H, q, *J* = 7.1, CH₂), 2.13 (3H, s, CH₃), 1.88 (2H, p, *J* = 7.1 Hz, CH₂); ¹³C NMR (100 MHz, CDCl₃) δ_C 208.1 (C=O), 202.0 (C=O), 43.0 (CH₂), 42.4 (CH₂), 30.1 (CH₂), 16.1 (CH₃); FTIR (ATR) ν_{max}: 2949, 1703, 1409, 1359, 1154, 1068 cm⁻¹; HRMS-ESI (*m/z*): C₆H₁₀O₂Na⁺ [M+Na]⁺ theoretical 137.0573, found 137.0570. Data in accordance with literature data.^{73,166}

2-(2-oxopropyl)benzaldehyde (174b)

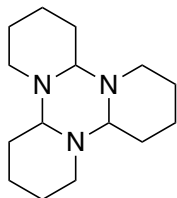


The reaction of methyl indene (1.00 g, 7.68 mmol) with ozone to produce 2-(2-oxopropyl)benzaldehyde as a colourless oil (817 mg, 66 %). ¹H NMR (400 MHz, CDCl₃) δ_H 10.00 (1H, s, HC=O), 7.81 (1H, dd, *J* = 7.4, 1.6 Hz, ArCH), 7.55 (1H, td, *J* = 7.5, 1.7 Hz, ArCH), 7.49 (1H, td, *J* = 7.5, 1.4 Hz, ArCH), 7.21 (1H, dd, *J* = 7.3, 1.3 Hz, ArCH), 4.13 (2H, s, CH₂), 2.31 (3H, s, CH₃); ¹³C NMR (101 MHz, CDCl₃) δ_C 205.4 (C=O), 193.6 (HC=O), 136.0 (ArC_q), 135.5 (ArCH), 134.2 (ArC_q), 133.9 (ArCH), 132.8 (ArCH), 127.9 (ArCH), 48.5 (CH₂), 30.2 (CH₃); FTIR (ATR) ν_{max}: 3004, 2745, 1716, 1691 cm⁻¹; HRMS-ESI (*m/z*): C₁₀H₁₁O₂⁺ [M+H]⁺

theoretical 163.0754, found 163.0755. Data in accordance with literature data.¹⁶⁷

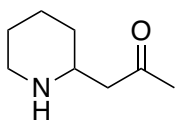
Chemical Synthesis of Pelletierine (22)

α -Tripiperideine (172)⁸⁹



N-Chlorosuccinimide (1.70 g, 52.4 mmol) was dissolved in Et₂O (50 mL) and cooled in an ice bath, piperidine (4.90 mL, 49.6 mmol) was added dropwise before the reaction mixture was left to stir for 2 h. The resulting mixture was washed with water (50 mL) and dried with anhydrous magnesium sulfate and concentrated *in vacuo* (without heating) to give crude 1-chloropiperidine as a yellow oil. The crude 1-chloropiperidine was dissolved in ethanol (50 mL) and potassium hydroxide (5.00 g, 89.1 mmol) was added, the resulting mixture was heated under reflux for 2 h, before being filtered and the solvent removed *in vacuo* to give α -tripiperideine as yellow oil (2.349 g, 57 %). ¹H NMR (400 MHz, CDCl₃) δ_{H} 3.11 (3H, dt, *J* = 10.4, 4.9 Hz), 2.85 – 2.73 (3H, m), 2.08 – 1.93 (3H, m), 1.78 – 1.60 (9H, m), 1.60 – 1.47 (6H, m), 1.35 – 1.23 (3H, m); ¹³C NMR (101 MHz, CDCl₃) δ_{C} 82.0 (CH), 46.5 (CH₂), 29.2 (CH₂), 25.9 (CH₂), 22.4 (CH₂); HRMS-ESI (*m/z*): C₁₅H₂₈N₃⁺ [M+H]⁺ theoretical 250.2278, found 250.2286. In accordance with literature data.⁸⁹

Pelletierine (22)¹⁶⁸



α -tripiperideine (1.00 g, 4.01 mmol), L-Proline (276 mg, 2.41 mmol) and acetone (6.37 mL, 72.17 mmol) were dissolved in acetonitrile (56 mL) before being stirred at room temperature for 16 h. The reaction mixture was diluted in dichloromethane (70 mL) and wash with brine (40 mL x3), the organic layer was dried with anhydrous sodium sulfate and concentrated *in vacuo*. The crude product was purified *via* column chromatography (MeOH:CH₂Cl₂ (3:25)) to give pelletierine as a colourless oil (527 mg, 93 %). ¹H NMR (400 MHz, CDCl₃) δ_{H} 3.04 – 2.98 (1H, m, CH₂), 2.94 (1H, dtd, *J* = 11.0, 6.3, 2.6 Hz, CH), 2.66 (1H, td, *J* = 11.8, 2.8 Hz, CH₂), 2.51 (2H, d, *J* = 6.3 Hz, CH₂), 2.32 (1H, s, broad, NH), 2.13 (3H, s, CH₃), 1.79 – 1.70 (1H, m, CH₂), 1.63 – 1.51 (2H, m, CH₂), 1.47

– 1.30 (2H, m, CH₂), 1.22 – 1.10 (1H, m, CH₂); ¹³C NMR (100 MHz, CDCl₃) δ_C 208.6 (C=O), 52.5 (CH), 50.7 (CH₂), 46.9 (CH₂), 32.5 (CH₂), 30.8 (CH₃), 26.1 (CH₂), 24.7 (CH₂); FTIR (ATR) ν_{max}: 2929, 2854, 1709, 1565, 1165 cm⁻¹; HRMS-ESI (m/z): C₈H₁₆NO⁺ [M+H]⁺ theoretical 142.1226, found 142.1231. In accordance with literature data.¹⁶⁸

General Procedure for Analytical Scale Mannich Reaction with α -Tripiperideine 172 and Acetone 47

Stock solution of α -tripiperideine (33 mM, 5 mL) in HEPES buffer (100 mM) was pH adjusted before 150 μ L being aliquoted into separate microcentrifuge tubes, to this 400 μ L of pH adjusted L-proline stock (350 mM in HEPES buffer (100 mM) and 750 μ L of acetone stock (400 mM in DMSO) were added. The total volume was then made up to 1500 μ L with HEPES buffer (100 mM) and incubated (200 rpm, 37 °C) for 24 h. To a 500 μ L sample conc. sodium hydroxide (100 μ L) and ethyl acetate (750 μ L) was added, the resulting suspension was centrifuged (13000 rpm, 5 min) and the dried organic layer was analysed on the GC-FID.

General Procedure for Analytical Scale Mannich Reaction Biotransformation

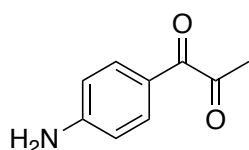
Cadaverine hydrochloride was dissolved HEPES buffer (100 mM) containing PLP (1 mM) the resulting stock (100 mM) was pH adjusted before 100 μ L was aliquoted into separate microcentrifuge tubes, to this 100 μ L of pH adjusted L-proline stock (1 M in HEPES buffer (100 mM) containing PLP (1 mM)) and 500 μ L of acetone stock (400 mM in DMSO) were added. The total volume was then made up to 1000 μ L with enzyme stock solution commercially available ATA025, HEPES buffer (100 mM) conation PLP (1mM)) and incubated (200 rpm, 37 °C) for 24 h. To a 500 μ L sample conc. sodium hydroxide (100 μ L) and ethyl acetate (750 μ L) was added, the resulting suspension was centrifuged (13000 rpm, 5 min) and the dried organic layer was analysed on the GC-FID.

General Procedure for Analytical Scale Amine Acceptor Screen

The corresponding amine donor hydrochloride was dissolved in HEPES buffer (100 mM) containing PLP (1 mM) the resulting stock (100 mM) was pH adjusted before 100 μ L was aliquoted into separate microcentrifuge tubes, to this 200 μ L of dicarbonyl stock solution (100 mM in DMSO) was added. The total volume was then made up to 1000 μ L with enzyme stock solution commercially available ATA256, HEPES buffer (100 mM) containing PLP (1 mM) and incubated (200 rpm, 37 °C) for 24 h. To a 500 μ L sample conc. sodium hydroxide (100 μ L) and ethyl acetate (750 μ L) was added, the resulting suspension was centrifuged (13000 rpm, 5 min) and the dried organic layer was analysed on the GC-FID.

7.4 Pyrrole Synthesis

1-(4-Aminophenyl)propane-1,2-dione (**143e**)



To a solution of 1-(4-nitrophenyl)propane-1,2-dione **143d** (1.976 g, 10.23 mmol) in H₂O:EtOH (34 mL(8:5)) was added iron powder (1.713 g, 30.96 mmol), and ammonium chloride (2.736 g, 51.15 mmol). The reaction mixture was heated under reflux for 1 h. Once the reaction was completed celite was added to from a slurry and the mixture was filtered through a pad of celite and washed with dichloromethane (40 mL). The aqueous layer was separated and washed with dichloromethane (40 mL x2), the combined organic layers were washed with brine (50 mL) and dried with anhydrous magnesium sulfate, filtered and concentrated *in vacuo*. The crude product was purified by column chromatography (Et₂O) to give the title compound as a brown oil (872 mg, 52 %). ¹H NMR (400 MHz, CDCl₃) δ_H 7.85 (2H, d, *J* = 8.7 Hz, ArCH), 6.65 (2H, d, *J* = 8.7 Hz, ArCH), 4.32 (2H, s, NH₂), 2.51 – 2.43 (3H, m, CH₃); ¹³C NMR (100 MHz, CDCl₃) δ_C 202.1 (C=O), 189.9 (C=O), 152.7 (ArC_q), 133.2 (ArCH), 121.9 (ArC_q), 114.1 (ArCH), 26.8 (CH₃); FTIR (ATR) ν_{max}: 3467, 3363, 3233, 1703, 1578, 1320, 1151 cm⁻¹; HRMS-ESI (*m/z*): C₉H₁₀NO₂⁺ [M+H]⁺ theoretical 164.0706, found 164.0704.

General Procedure for Analytical Scale Biotransformations for the Preparation of Pyrroles (**145a**)

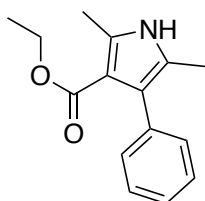
The corresponding amount of β-amino-ester **141a** was dissolved in a HEPES buffer (100 mM) containing PLP (1 mM) the resulting stock was then pH adjusted before 250 μL was aliquoted into separate microcentrifuge tubes. To this 1-phenylpropane-1,2-dione **143a** stock (in DMSO) was added, after which 200 μL of enzyme stock solution (commercially available ATA117 rehydrated in HEPES buffer containing PLP (1 mM)), to give a total volume 500 μL. The resulting mixture was incubated at 30 °C for 72 h in a shaking incubator (200 rpm). 100 μL samples were taken at 24 h intervals, the samples where diluted to a total volume of 500 μL and analysed *via*

reverse phase HPLC using a Waters Sunfire 5 μm , 2.1 x 150 mm column (C-18) at a flow rate of 0.6 mL min^{-1} with a 40 to 100 % gradient.

General Procedure for Biotransformations for the Preparation of Pyrroles (145)

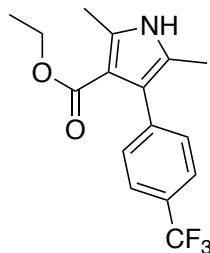
Commercially available ATA117 (5 mg/mL) was rehydrated in HEPES buffer (9.5 mL, 100 mM, pH 9) containing PLP (1 mM) and corresponding β -amino-ester **141** (84 mM or 42 mM). To this, was added the corresponding diketone **143** (1 mL, 400 mM stock in DMSO) and the mixture was incubated at 30 °C for 72 h in a shaking incubator (200 rpm). The reaction mixture was acidified using aq. HCl (4 M, 1 mL) and extracted with EtOAc (3 x 20 mL) and the combined organic layers were washed with water (20 mL), dried over anhydrous sodium sulfate and the solvent removed *in vacuo*. The corresponding pyrrole **145** were purified by flash column chromatography.

Ethyl 2,5-dimethyl-4-phenyl-1H-pyrrole-3- carboxylate (145a)



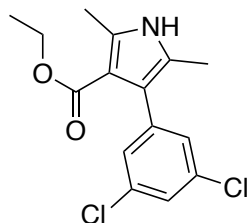
The reaction of 1-phenylpropane-1,2-dione **143a** and ethyl 3-aminobutanoate **141a** (80 mM) with ATA117 proceeded in 90 % conversion after 72 h. **145a** was obtained as a white solid (51 mg, 52 %) after flash chromatography (CH_2Cl_2). m.p. 105-107 °C; ^1H NMR (500 MHz, MeOD) δ_{H} 7.32 – 7.24 (2H, m, ArCH), 7.22 – 7.14 (3H, m, ArCH), 4.00 (2H, q, $J = 7.1$ Hz, OCH_2CH_3), 2.45 (3H, s, CH_3), 2.05 (3H, s, CH_3), 1.04 (3H, t, $J = 7.1$ Hz, OCH_2CH_3); ^{13}C NMR (126 MHz, MeOD) δ_{C} 168.1 (C=O), 138.3 (ArC_q), 135.8 (ArC_q), 131.6 (ArC_q), 128.2 (ArC_q), 126.6 (ArC_q), 124.9 (ArC_q), 123.5 (ArC_q), 110.6 (ArC_q), 60.0 (OCH_2CH_3), 14.4 (CH_3), 13.5 (CH_3), 11.0 (OCH_2CH_3); FTIR (ATR) ν_{max} : 3262, 2982, 2906, 1655, 1382, 1290, 1082, 751, 698 cm^{-1} ; HRMS-ESI (m/z): $\text{C}_{15}\text{H}_{18}\text{O}_2^+$ [M+H]⁺ theoretical 244.1332, found 244.1244. In accordance to literature data.¹⁰⁵

Ethyl 2,5-dimethyl-4-(4-(trifluoromethyl)phenyl)-1H-pyrrole-3-carboxylate (145b)



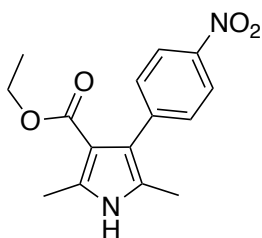
The reaction of 1-(4-(trifluoromethyl)phenyl)propane-1,2-dione **143b** and ethyl 3-aminobutanoate **141a** (80 mM) with ATA117 proceeded in 99 % conversion after 72 h. **145b** was obtained as a pale yellow solid (80 mg, 64 %) after flash chromatography (CH₂Cl₂). m.p. 88-90 °C; ¹H NMR (500 MHz, MeOD) δ_H 7.54 – 7.40 (4H, m, ArCH), 4.01 (2H, q, *J* = 7.1 Hz, OCH₂CH₃), 2.47 (3H, s, CH₃), 2.07 (3H, s, CH₃), 1.02 (3H, t, *J* = 7.1 Hz, OCH₂CH₃); ¹³C NMR (126 MHz, MeOD) δ_C 167.7 (C=O), 139.4 (ArC_q), 136.5 (ArC_q), 135.2 (ArCH), 129.0 (ArCH), 128.3 (ArC_q), 125.6 (ArC_q), 123.3 (ArC_q), 121.9 (ArC_q), 110.5 (ArC_q), 60.1 (OCH₂CH₃), 14.3 (CH₃), 13.4 (CH₃), 10.9 (OCH₂CH₃); FTIR (ATR) ν_{max}: 3317, 2949, 2865, 1673, 1445, 1327, 1013 cm⁻¹; HRMS-ESI (*m/z*): C₁₆H₁₇F₃NO₂⁺ [M+H]⁺ theoretical 312.1206, found 312.1212. In accordance to literature data.¹⁰⁵

Ethyl 4-(3,5-dichlorophenyl)-2,5-dimethyl-1H-pyrrole-3-carboxylate (145c)



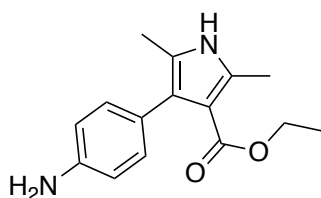
The reaction of 1-(3,5-dichlorophenyl)propane-1,2-dione **143c** and ethyl 3-aminobutanoate **141a** (80 mM) with ATA117 proceeded in 78 % conversion after 72 h. **145c** was obtained as a pale yellow solid (58 mg, 46 %) after flash chromatography (CH₂Cl₂). m.p. 103-105 °C; ¹H NMR (500 MHz, MeOD) δ_H 7.29 (1 H, t, *J* = 1.9 Hz, ArCH), 7.15 (2H, d, *J* = 2.0 Hz, ArCH), 4.07 (2H, q, *J* = 7.1 Hz, OCH₂CH₃), 2.47 (3H, s, CH₃), 2.10 (3H, s, CH₃), 1.12 (3H, t, *J* = 7.1 Hz, OCH₂CH₃); ¹³C NMR (126 MHz, MeOD) δ_C 167.5 (C=O), 141.8 (ArC_q), 134.7 (ArC_q), 130.2 (ArCH), 126.3 (ArCH), 125.2 (ArC_q), 120.7 (ArC_q), 110.4 (ArC_q), 60.2 (OCH₂CH₃), 14.4 (CH₃), 13.4 (CH₃), 10.9 (OCH₂CH₃); FTIR (ATR) ν_{max}: 3294, 3075, 2981, 2938, 1662, 1587, 1557, 1419, 1096, 1016, 799 cm⁻¹; HRMS-ESI (*m/z*): C₁₅H₁₆Cl₂NO₂⁺ [M+H]⁺ theoretical 312.0553, found 312.0547. In accordance to literature data.¹⁰⁵

Ethyl 2,5-dimethyl-4-(4-nitrophenyl)-1H-pyrrole-3-carboxylate (**145d**)



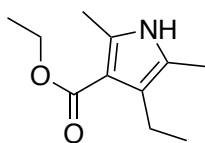
The reaction of 1-(4-nitrophenyl)propane-1,2-dione **143d** and ethyl 3-aminobutanoate **141a** (80 mM) with ATA117 proceeded in 41 % conversion after 72 h. **145d** was obtained as a pale yellow solid (29 mg, 25 %) after flash chromatography (CH₂Cl₂). m.p. 123-125 °C; ¹H NMR (500 MHz, MeOD) δ_H 8.20 – 8.15 (2H, m, ArCH), 7.44 – 7.39 (2H, m, ArCH), 4.06 (2H, q, *J* = 7.1 Hz, OCH₂CH₃), 2.46 (3H, s, CH₃), 2.11 (3H, s, CH₃), 1.10 (3H, t, *J* = 7.1 Hz, OCH₂CH₃); ¹³C NMR (126 MHz, MeOD) δ_C 166.1 (C=O), 145.8 (ArC_q), 144.4 (ArC_q), 135.4 (ArC_q), 131.0 (ArCH), 124.9 (ArCH), 122.0 (ArCH), 120.1 (ArC_q), 109.1 (ArC_q), 58.9 (OCH₂CH₃), 13.1 (CH₃), 12.0 (CH₃), 9.7 (OCH₂CH₃); FTIR (ATR) ν_{max}: 3306, 2980, 2923, 1773, 1668, 1593, 1511, 1341, 1089 cm⁻¹; HRMS-ESI (m/z): C₁₅H₁₇N₂O₄⁺ [M+H]⁺ theoretical 298.1183, found 298.1193.

Ethyl 2,5-dimethyl-4-(4-aminophenyl)-1H-pyrrole-3-carboxylate (**145e**)



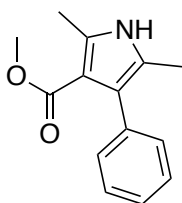
The reaction of 1-(4-amino)propane-1,2-dione **143e** and ethyl 3-aminobutanoate **141a** (80 mM, 3 mL) with ATA117 proceeded in 83 % conversion after 72 h. The acidified reaction mixture was centrifuged (10 min, 4000 rpm) before being directly injected onto the preparative HPLC (20 to 80 % gradient), **145e** was obtained as a pale yellow solid (17 mg, 54 %). m.p. degrades at 147 °C; ¹H NMR (400 MHz, MeOD) δ_H 7.37 – 7.28 (4H, m, ArCH), 4.04 (2H, q, *J* = 7.1 Hz, OCH₂CH₃), 2.46 (3H, s, CH₃), 2.06 (3H, s, CH₃), 1.10 (3H, t, *J* = 7.1 Hz, OCH₂CH₃); ¹³C NMR (101 MHz, MeOD) δ_C 167.8 (C=O), 139.1 (ArC_q), 136.3 (ArC_q), 133.2 (ArCH), 130.1 (ArC_q), 125.5 (ArC_q), 122.6 (ArCH), 121.9 (ArC_q), 110.5 (ArC_q), 60.1 (OCH₂CH₃), 14.5 (OCH₂CH₃), 13.5 (CH₃), 10.9 (CH₃); FTIR (ATR) ν_{max}: 2981, 2922, 1646, 1172, 1135 cm⁻¹; HRMS-ESI (m/z): C₁₄H₁₇N₂O₂⁺ [M+H]⁺ theoretical 259.1441, found 259.1454.

Ethyl 4-ethyl-2,5-dimethyl-1*H*-pyrrole-3- carboxylate (**145f**)



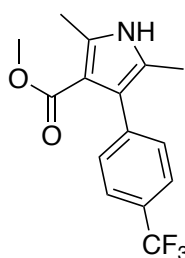
The reaction of pentane-1,2-dione **143f** and ethyl 3-aminobutanoate **141a** (80 mM) with ATA117 proceeded in 34 % conversion after 72 h. **145f** was obtained as a white solid (21 mg, 28 %) after flash chromatography (CH₂Cl₂). m.p. 94-96 °C; ¹H NMR (500 MHz, MeOD) δ_H 4.20 (2H, q, *J* = 7.1 Hz, OCH₂CH₃), 2.59 (2H, q, *J* = 7.4 Hz, CH₂CH₃), 2.38 (3H, s, CH₃), 2.07 (3H, s, CH₃), 1.33 (3H, t, *J* = 7.1 Hz, OCH₂CH₃), 1.04 (3H, t, *J* = 7.4 Hz, CH₂CH₃); ¹³C NMR (126 MHz, MeOD) δ_C 168.5 (C=O), 135.5 (ArC_q), 123.5 (ArC_q), 123.0 (ArC_q), 109.9 (ArC_q), 60.0 (OCH₂CH₃), 19.4 (CH₂CH₃), 16.5 (CH₃), 14.8 (OCH₂CH₃), 13.8 (CH₃), 10.1 (CH₂CH₃); FTIR (ATR) ν_{max}: 3270, 2924, 2422, 1649, 1243, 1148, 1100 cm⁻¹; HRMS-ESI (*m/z*): C₁₁H₁₈NO₂⁺ [M+H]⁺ theoretical 196.1332, found 196.1328.

Methyl 2,5-dimethyl-4-phenyl-1*H*-pyrrole-3- carboxylate (**145g**)



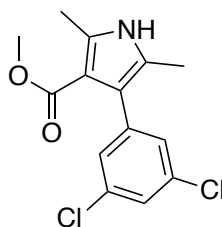
The reaction of 1-phenylpropane-1,2-dione **143a** and ethyl 3-aminobutanoate (**R**)-**141b** (40 mM) with ATA117 proceeded in 87 % conversion after 72 h. **145g** was obtained as a white solid (50 mg, 55 %) after flash chromatography (CH₂Cl₂). m.p. 135-138 °C; ¹H NMR (500 MHz, MeOD) δ_H 7.31 – 7.24 (2H, m, ArCH), 7.21 – 7.13 (3H, m, ArCH), 3.55 (3H, s, OCH₃), 2.45 (3H, s, CH₃), 2.05 (3H, s, CH₃); ¹³C NMR (126 MHz, MeOD) δ_C 168.53 (C=O), 135.8 (ArC_q), 131.5 (ArC_q), 130.0 (ArCH), 128.3 (ArCH), 126.6 (ArCH), 125.1 (ArC_q), 123.5 (ArC_q), 110.4 (ArC_q), 50.6 (OCH₃), 13.5 (CH₃), 11.0 (CH₃); FTIR (ATR) ν_{max}: 3281, 2951, 2500, 1660, 1446, 1403, 1163, 1080 cm⁻¹; HRMS-ESI (*m/z*): C₁₄H₁₆NO₂⁺ [M+H]⁺ theoretical 230.1176, found 230.1182. In accordance to literature data.¹⁰⁵

Methyl 2,5-dimethyl-4-(4-(trifluoromethyl)phenyl)-1H-pyrrole-3-carboxylate (145h)



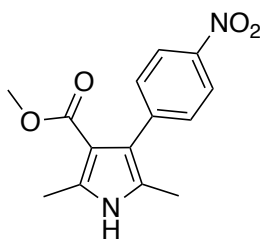
The reaction of 1-(4-(trifluoromethyl)phenyl)propane-1,2-dione **143b** and methyl 3-aminobutanoate (**R**)-**141b** (40 mM) with ATA117 proceeded in 44 % conversion after 72 h. **145h** was obtained as a pale yellow solid (18 mg, 15 %) after flash chromatography (CH₂Cl₂). m.p. 109-113 °C; ¹H NMR (500 MHz, CDCl₃) δ_H 7.53 – 7.48 (2H, m, ArCH), 7.46 – 7.41 (2H, m, ArCH), 3.60 (3H, s, OCH₃), 2.53 (3H, s, CH₃), 2.13 (3H, s, CH₃); ¹³C NMR (126 MHz, CDCl₃) δ_C 166.0 (C=O), 137.0 (ArC_q), 134.7 (ArCH), 133.8 (ArC_q), 127.9 (ArCH), 127.3 (ArC_q), 124.1 (ArC_q), 122.8 (ArC_q), 121.3 (ArC_q), 110.4 (ArC_q), 50.5 (OCH₃), 13.9 (CH₃), 11.4 (CH₃); FTIR (ATR) ν_{max}: 3317, 2949, 455, 1672, 1327, 1113, 1069 cm⁻¹; HRMS-ESI (m/z): C₁₅H₁₅F₃NO₂⁺ [M+H]⁺ theoretical 298.1049, found 298.1048.

Methyl 4-(3,5-dichlorophenyl)-2,5-dimethyl-1H-pyrrole-3-carboxylate (145i)



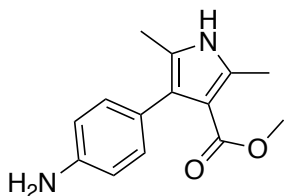
The reaction of 1-(3,5-dichlorophenyl)propane-1,2-dione **143c** and methyl 3-aminobutanoate (**R**)-**141b** (40 mM) with ATA117 proceeded in 95 % conversion after 72 h. **145i** was obtained as a pale yellow solid (93 mg, 80 %) after flash chromatography (CH₂Cl₂). m.p. 103-105 °C; ¹H NMR (500 MHz, MeOD) δ_H 7.27 (1H, t, J = 2.0 Hz, ArCH), 7.12 (2H, d, J = 1.9 Hz, ArCH), 3.61 (3H, s, OCH₃), 2.44 (3H, s, CH₃), 2.08 (3H, s, CH₃); ¹³C NMR (126 MHz, CDCl₃) δ_C 166.0 (C=O), 137.0 (ArC_q), 134.7 (ArC_q), 133.8 (ArC_q), 127.9 (ArCH), 127.3 (ArCH), 124.1 (ArC_q), 121.3 (ArC_q), 110.4 (ArC_q), 50.5 (OCH₃), 13.9 (CH₃), 11.4 (CH₃); FTIR (ATR) ν_{max}: 3320, 2945, 2450, 1674, 1415, 1170, 1094 cm⁻¹; HRMS-ESI (m/z): C₁₄H₁₄Cl₂NO₂⁺ [M+H]⁺ theoretical 298.0396, found 298.0388.

Methyl 2,5-dimethyl-4-(4-nitrophenyl)-1H-pyrrole-3-carboxylate (**145j**)



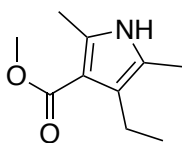
The reaction of 1-(4-nitrophenyl)propane-1,2-dione **145d** and methyl 3-aminobutanoate (**R**)-**141b** (40 mM) with ATA117 proceeded in 44 % conversion after 72 h. **145j** was obtained as a pale yellow solid (35 mg, 32 %) after flash chromatography (CH₂Cl₂). m.p. 145-149 °C; ¹H NMR (500 MHz, MeOD) δ_H 8.19 – 8.15 (2H, m, ArCH), 7.43 – 7.38 (2H, m, ArCH), 3.59 (3H, s, OCH₃), 2.46 (3H, s, CH₃), 2.11 (3H, s, CH₃); ¹³C NMR (126 MHz, MeOD) δ_C 167.9 (C=O), 147.1 (ArC_q), 145.6 (ArC_q), 136.9 (ArC_q), 132.2 (ArCH), 126.4 (ArC_q), 123.5 (ArCH), 121.5 (ArC_q), 110.3 (ArC_q), 50.8 (OCH₃), 13.5 (CH₃), 11.1 (CH₃); FTIR (ATR) ν_{max}: 3314, 2948, 2447, 1667, 1593, 1328, 1077 cm⁻¹; HRMS-ESI (m/z): C₁₄H₁₅N₂O₄⁺ [M+H]⁺ theoretical 275.1026, found 275.1032.

Methyl 2,5-dimethyl-4-(4-aminophenyl)-1H-pyrrole-3-carboxylate (**145k**)



The reaction of 1-(4-amino)propane-1,2-dione **143e** and methyl 3-aminobutanoate (**R**)-**141b** (40 mM, 3 mL) with ATA117 proceeded in 76 % conversion after 72 h. The acidified reaction mixture was centrifuged (10 min, 4000 rpm) before being directly injected onto the preparative HPLC (20 to 80 % gradient), **145k** was obtained as a pale yellow solid (16 mg, 55 %). m.p. degrade at 150 °C; ¹H NMR (400 MHz, MeOD) δ_H 7.36 – 7.28 (4H, m, ArCH), 3.58 (3H, s, OCH₃), 2.45 (3H, s, CH₃), 2.06 (3H, s, CH₃); ¹³C NMR (126 MHz, MeOD) δ_C 168.1 (C=O), 139.1 (ArC_q), 136.3 (ArC_q), 133.1 (ArCH), 129.9 (ArC_q), 125.6 (ArC_q), 122.7 (ArCH), 121.9 (ArC_q), 110.2 (ArC_q), 50.7 (OCH₃), 13.6 (CH₃), 10.9 (CH₃); FTIR (ATR) ν_{max}: 2966, 2922, 1638, 1453, 1407, 1129 cm⁻¹; HRMS-ESI (m/z): C₁₄H₁₇N₂O₂⁺ [M+H]⁺ theoretical 245.1285, found 245.1289.

Methyl 4-ethyl-2,5-dimethyl-1*H*-pyrrole-3- carboxylate (**145I**)

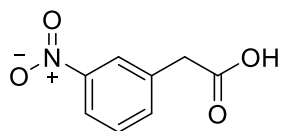


The reaction of pentane-1,2-dione **143f** and methyl 3-aminobutanoate (**R**)-**141b** (40 mM) with ATA117 proceeded in 25 % conversion after 72 h. **145I** was obtained as a white solid (14 mg, 19 %) after flash chromatography (CH₂Cl₂). m.p. 129-132 °C; ¹H NMR (500 MHz, MeOD) δ_H 3.74 (3H, s, OCH₃), 2.58 (2H, q, *J* = 7.4 Hz, CH₂CH₃), 2.37 (3H, s, CH₃), 2.07 (3H, s, CH₃), 1.03 (3H, t, *J* = 7.4 Hz, 3 CH₂CH₃); ¹³C NMR (126 MHz, MeOD) δ_C 168.9 (C=O), 135.5 (ArC_q), 123.6 (ArC_q), 123.0 (ArC_q), 109.7 (ArC_q), 50.6 (OCH₃), 19.4 (CH₂CH₃), 16.4 (CH₃), 13.8 (CH₃), 10.1 (CH₂CH₃); FTIR (ATR) ν_{max}: 3294, 2954, 2865, 2447, 1660, 1410, 1283, 1093 cm⁻¹; HRMS-ESI (*m/z*): C₁₀H₁₆NO₂⁺ [M+H]⁺ theoretical 182.1176, found 182.1173.

7.5 THIQ Synthesis

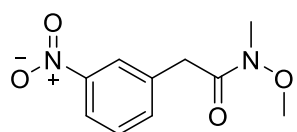
Synthesis of Ketones for ATA- Pictet-Spengler reaction Cascade

2-(3-nitrophenyl)acetic acid (**197**)



To a solution of concentrated sulfuric acid (8 mL), glacial acetic acid (8 mL), in water (8 mL) was added 2-(3-nitrophenyl)acetonitrile **196** (5 g, 30.8 mmol) the reaction mixture was heated under reflux for 1 h. The reaction mixture was cooled and diluted with water (20 mL) washed with EtOAc (30 mL x3). The combined organic layers were washed with water (40 mL x3), brine (40 mL), dried with anhydrous magnesium sulfate and filtered. The resultant residue was concentrated *in vacuo* to give the title compound as a white solid with no further purification (5.393 g, 29.7 mmol, 97 %). m.p 102-105 °C; ¹H NMR (400 MHz, CDCl₃) δ_H 8.20-8.14 (2H, m, ArH), 7.65-7.61 (1H, m, ArH), 7.57-7.50 (1H, m, ArH), 3.79 (2H, s, CH₂); ¹³C NMR (100 MHz, CDCl₃) δ_C 176.2 (C=O), 148.5 (ArC_q), 135.8 (ArCH), 135.1 (ArC_q), 129.7 (ArCH), 124.7 (ArCH), 122.7 (ArCH), 40.4 (CH₂); FTIR (ATR) ν_{max}: 3068, 2927, 1703, 1523, 1347, 713 cm⁻¹; HRMS-ESI (m/z): C₇H₈NO₄⁺ [M+H]⁺ theoretical 182.0448, found 182.0450. In accordance to literature data.¹⁶⁹

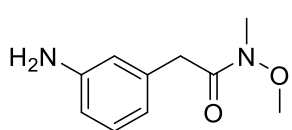
N-methoxy-N-methyl-2-(3-nitrophenyl)acetamide (**198**)



2-(3-nitrophenyl)acetic acid **197** (5.390 g, 29.7 mmol) and 1,1'-carbonyldiimidazole (4.825 g, 29.8 mmol) were dissolved in dichloromethane (100 mL) and mixed for 1 h before N,O-dimethylhydroxylamine (3.61 g, 59.5 mmol) was added. The reaction mixture was stirred for 24 h. Once the reaction was completed it was diluted in water (50 mL), the organic layer was separated, and the aqueous layer was washed with dichloromethane (50 mL x2). The combined organic layers were dried with anhydrous magnesium sulfate, filtered and concentrated *in vacuo* to give N-methoxy-N-methyl-2-(3-nitrophenyl)acetamide as a white solid (5.638 g, 24.7 mmol, 84 %) without further purification. m.p 90-92 °C; ¹H NMR (400 MHz, CDCl₃)

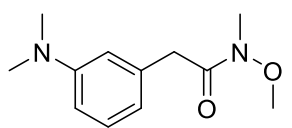
δ_{H} 8.17 – 8.09 (2H, m, ArCH), 7.67 – 7.61 (1H, m, ArCH), 7.49 (1H, t, $J = 7.9$ Hz, ArCH), 3.88 (2H, s, CH₂), 3.71 (3H, s, OCH₃), 3.21 (3H, s, CH₃); ¹³C NMR (100 MHz, CDCl₃) δ_{C} 171.1 (C=O), 148.4 (ArC_q), 136.9 (ArC_q), 136.0 (ArCH), 129.4 (ArCH), 124.7 (ArCH), 122.2 (ArCH), 61.6 (OCH₃), 38.7 (CH₂), 32.4 (CH₃); FTIR (ATR) ν_{max} : 3038, 2920, 1654, 1518, 1342 cm⁻¹; HRMS-ESI (m/z): C₁₀H₁₃N₂O₄⁺ [M+H]⁺ theoretical 225.0870, found 225.0873.

2-(3-aminophenyl)-N-methoxy-N-methylacetamide (199)



To a solution of *N*-methoxy-*N*-methyl-2-(3-nitrophenyl)acetamide **198** (5.60 g, 24.9 mmol) in H₂O:EtOH (39 mL(8:5)) was added iron powder (4.18 g, 74.9 mmol), and ammonium chloride (6.670 g, 124 mmol). The reaction mixture was heated under reflux for 1 h. Once the reaction was completed celite was added to form a slurry and the mixture was filtered through a pad of celite and washed with dichloromethane (40 mL). The aqueous layer was separated and washed with dichloromethane (40 mL x2), the combined organic layers were washed with brine (40 mL) and dried with anhydrous magnesium sulfate, filtered and concentrated *in vacuo*. The crude product was purified by column chromatography (Et₂O) to give the title compound as a brown oil (3.242, 16.7 mmol, 67 %). ¹H NMR (400 MHz, CDCl₃) δ_{H} 7.10 (1H, t, $J = 8.0$ Hz, ArCH), 6.71 (2H, m, ArCH), 6.68 – 6.55 (1H, m, ArCH), 3.68 (3H, s, CH₂), 3.60 (3H, s, OCH₃), 3.19 (3H, s, CH₃); ¹³C NMR (100 MHz, CDCl₃) δ_{C} 172.3 (C=O), 136.2 (ArC_q), 129.6 (ArC_q), 120.4 (ArCH), 116.5 (ArCH), 114.3 (ArCH), 61.5 (OCH₃), 39.5 (CH₂), 32.4 (CH₃); FTIR (ATR) ν_{max} : 3437, 3351, 2936, 1646, 1602, 1406, 994 cm⁻¹; HRMS-ESI (m/z): C₁₀H₁₅N₂O₂⁺ [M+H]⁺ theoretical 195.1128, found 195.1127. In accordance to literature data.¹⁷⁰

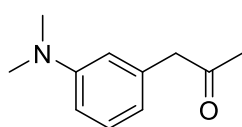
2-(3-(dimethylamino)phenyl)-N-methoxy-N-methylacetamide (200)



To 2-(3-aminophenyl)-*N*-methoxy-*N*-methylacetamide **199** (3.200 g, 16.4 mmol), tetrabutylammonium iodide (426 mg, 1.15 mmol) and potassium hydroxide (2.300 g, 41.2 mmol) dissolved in toluene:water (24

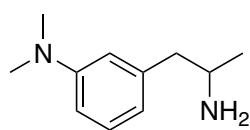
mL (7:1)), iodomethane (2.56 mL, 41.2 mmol) was added dropwise. The reaction mixture was heated at 90 °C for 24 h. The reaction was diluted in water (10 mL) and extracted into ethyl acetate (30 mL x3), the combined organic layers were dried with anhydrous magnesium sulfate, filtered and concentrated *in vacuo*. The crude residue was purified by column chromatography (EtO₂) to yield 2-(3-(dimethylamino)phenyl)-N-methoxy-N-methylacetamide (1.966 g, 8.84 mmol, 54 %). ¹H NMR (400 MHz, CDCl₃) δ_H 7.18 (1H, t, *J* = 7.9 Hz, ArCH), 6.67 (3H, m, ArCH), 3.73 (3H, s, CH₂), 3.60 (3H, s, OCH₃), 3.19 (3H, s, CH₃), 2.95 (6H, s, CH₃); ¹³C NMR (100 MHz, CDCl₃) δ_C 172.9 (C=O), 150.9 (ArCH), 135.8 (ArC_q), 129.2 (ArCH), 117.7 (ArC_q), 113.6 (ArCH), 111.3 (ArCH), 61.4 (OCH₃), 40.7 (CH₃), 40.0 (CH₂), 32.4 (CH₃); FTIR (ATR) ν_{max}: 3436, 3351, 2936, 1636, 1602, 1461, 1382, 1096 cm⁻¹; HRMS-ESI (m/z): C₁₂H₁₉N₂O₂⁺ [M+H]⁺ theoretical 223.1441, found 223.1464.

1-(3-(dimethylamino)phenyl)propan-2-one (190f)



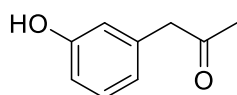
To a solution of 2-(3-(dimethylamino)phenyl)-N-methoxy-N-methylacetamide **200** (1.900 g, 8.5 mmol), in dry THF (20 mL) at -20 °C was added methyl magnesium bromide (4.3 mL, 3 M solution in CH₂Cl₂, 12.8 mmol) dropwise and the reaction mixture was warmed to room temperature and was stirred for 16 h. Water (10 mL) was added to the reaction and the mixture was basified and extracted into with dichloromethane (20 mL x3). The combined organic layers were dried with anhydrous magnesium sulfate, filtered and concentrated *in vacuo* to give 1-(3-(dimethylamino)phenyl)propan-2-one (1.27 g, 7.17 mmol, 84 %) with no further purification. ¹H NMR (500 MHz, CDCl₃) δ_H 7.20 (1H, t, *J* = 7.8 Hz, ArCH), 6.67 – 6.63 (1H, m, ArCH), 6.59 – 6.53 (2H, m, ArCH), 3.63 (2H, s, CH₂), 2.94 (6H, s, CH₃), 2.14 (3H, s, CH₃); ¹³C NMR (126 MHz, CDCl₃) δ_C 207.2 (C=O), 151.1 (ArC_q), 135.3 (ArC_q), 129.6 (ArCH), 117.7 (ArC_q), 113.4 (ArCH), 111.4 (ArC_q), 51.9 (CH₃), 40.7 (CH₃), 29.2 (CH₂); FTIR (ATR) ν_{max}: 2920, 2803, 1706, 1600, 1497, 1352 cm⁻¹; HRMS-ESI (m/z): C₁₁H₁₆NO⁺ [M+H]⁺ theoretical 178.1226, found 178.1230. In accordance to literature data.¹⁵⁹

3-(2-aminopropyl)-*N,N*-dimethylaniline (191f)



1-(3-(Dimethylamino)phenyl)propan-2-one **190f** (200 mg, 1.23 mmol), sodium cyanoborohydride (71 mg, 1.23 mmol) and ammonium acetate (870 mg, 11.28 mmol) were dissolved in methanol (10 mL), the reaction mixture was stirred overnight. The reaction was diluted with water (10 mL) and the methanol removed *in vacuo* before being basified to pH 9 with sodium hydroxide (5M), the aqueous layer was washed with ethyl acetate (20 mL, x3). The combined organic layers were dried with anhydrous magnesium sulfate, filtered and concentrated *in vacuo*. The crude product was purified by column chromatography (CH₂Cl₂:MeOH (95:5)) to give title compound as a brown oil (70 mg, 39 %). ¹H NMR (400 MHz, CDCl₃) δ_H 7.17 (1H, t, *J* = 8.0 Hz, ArCH), 6.63 – 6.59 (1H, m, ArCH), 6.58 – 6.54 (2H, m, ArCH), 3.27 – 3.19 (1H, m, CH), 2.94 (6H, s, CH₃), 2.75 – 2.68 (1H, m, CH₂), 2.58 – 2.51 (1H, m, CH₂), 1.17 (3H, d, *J* = 6.4 Hz, CH₃); ¹³C NMR (101 MHz, CDCl₃) δ_C 150.9 (ArC_q), 140.2 (ArC_q), 129.3 (ArCH), 117.7 (ArCH), 113.7 (ArCH), 110.8 (ArCH), 48.8 (CH), 46.6 (CH₂), 40.8 (CH₃), 23.0 (CH₃); FTIR (ATR) ν_{max}: 3349, 2957, 2802, 1601, 1497, 1348, 1060 cm⁻¹; HRMS-ESI (*m/z*): C₁₁H₁₉N₂⁺ [M+H]⁺ theoretical 179.1543, found 179.1556.

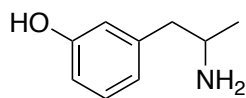
1-(3-Hydroxyphenyl)propan-2-one (190b)



A solution of hydrogen bromide (9 mL, 48 % solution in water) and 1-(3-methoxyphenyl)propan-2-one **190c** (500 mg, 3.04 mmol) was heated at 120 °C for 2 h. Once cooled the reaction was diluted with water (10 mL) and neutralised with sat. sodium hydrogen carbonate solution before being extracted into dichloromethane (20 mL X3), the combined organic extracts were dried over anhydrous magnesium sulfate, filtered and concentrated *in vacuo* (water bath at room temperature). The crude product was then purified by column chromatography (Et₂O:pentane (3:7)) to yield the product as a yellow oil (267 mg, 1.78 mmol, 59%). ¹H NMR (400 MHz, CDCl₃) δ_H 7.20 (1H, t, *J* = 7.8 Hz, ArCH), 6.79 – 6.73 (2H, m, ArCH), 6.70-6.67 (1H, m, ArCH), 3.65 (2H, s, CH₂), 2.16 (3H, s, CH₃); ¹³C NMR (101 MHz, CDCl₃) δ_C 207.3 (C=O), 156.2 (ArC_q), 135.8 (ArC_q), 130.2 (ArCH), 121.9 (ArCH), 116.4 (ArCH),

114.4 (ArCH), 51.0 (CH₂), 29.4 (CH₃); FTIR (ATR) ν_{\max} : 3335, 2962, 1696, 1587, 1356, 1156 cm⁻¹; HRMS-ESI (m/z): C₉H₁₀NaO₂⁺ [M+Na]⁺ theoretical 173.0753, found 173.0783.

3-(2-Aminopropyl)phenol (191b)



1-(3-(hydroxyphenyl)propan-2-one **190b** (100 mg, 0.66 mmol), sodium cyanoborohydride (46 mg, 0.80 mmol) and ammonium acetate (1.00 g, 13.2 mmol) were dissolved in methanol (10 mL), the reaction mixture was stirred overnight. The reaction was diluted with water (10 mL) and the methanol removed *in vacuo* before being basified to pH 9 with sodium hydroxide (5M), the aqueous layer was washed with ethyl acetate (20 mL, x3). The combined organic layers were dried with anhydrous magnesium sulfate, filtered and concentrated *in vacuo*. The crude product was purified by column chromatography (EtOAc:MeOH (NH₃ 7 N) (95:5)) to give title compound as a white solid (30 mg, 30 %). ¹H NMR (400 MHz, MeOD) δ_{H} 7.09 (1H, t, *J* = 8.0 Hz, ArCH), 6.67 – 6.60 (3H, m, ArCH), 3.09 (1H, dt, *J* = 7.5, 6.2 Hz, CH), 2.62 – 2.49 (2H, m, CH₂), 1.08 (3H, d, *J* = 6.4 Hz, CH₃); ¹³C NMR (101 MHz, MeOD) δ_{C} 158.8 (ArC_q), 142.0 (ArC_q), 130.3 (ArCH), 121.3 (ArCH), 117.1 (ArCH), 114.4 (ArCH), 49.5 (CH), 46.5 (CH₂), 22.4 (CH₃); FTIR (ATR) ν_{\max} : 3342, 3289, 2961, 2854, 1592, 1454, 1259 cm⁻¹; HRMS-ESI (m/z): C₉H₁₄NO⁺ [M+H]⁺ theoretical 152.1070, found 152.1075.

Analytical Scale Synthesis of THIQ (194) via Biotransformations

The corresponding amount of amine was dissolved in a KP_i buffer (100 mM) containing PLP (1 mM) the resulting stock was then pH adjusted before 250 μ L was aliquoted into separate microcentrifuge tubes. To this ketone **190** stock (in DMSO) was added, after which 200 μ L of enzyme stock solution (commercially available ATA rehydrated in HEPES buffer containing PLP (1 mM)), to give a total volume 1000 μ L. The resulting mixture was incubated at 50 °C for 48 h in a shaking incubator (200 rpm). 500 μ L sample was taken, the samples were diluted to a total volume of 600 μ L with a dDMSO containing sodium formate standard or maleic acid and analysed *via* NMR.

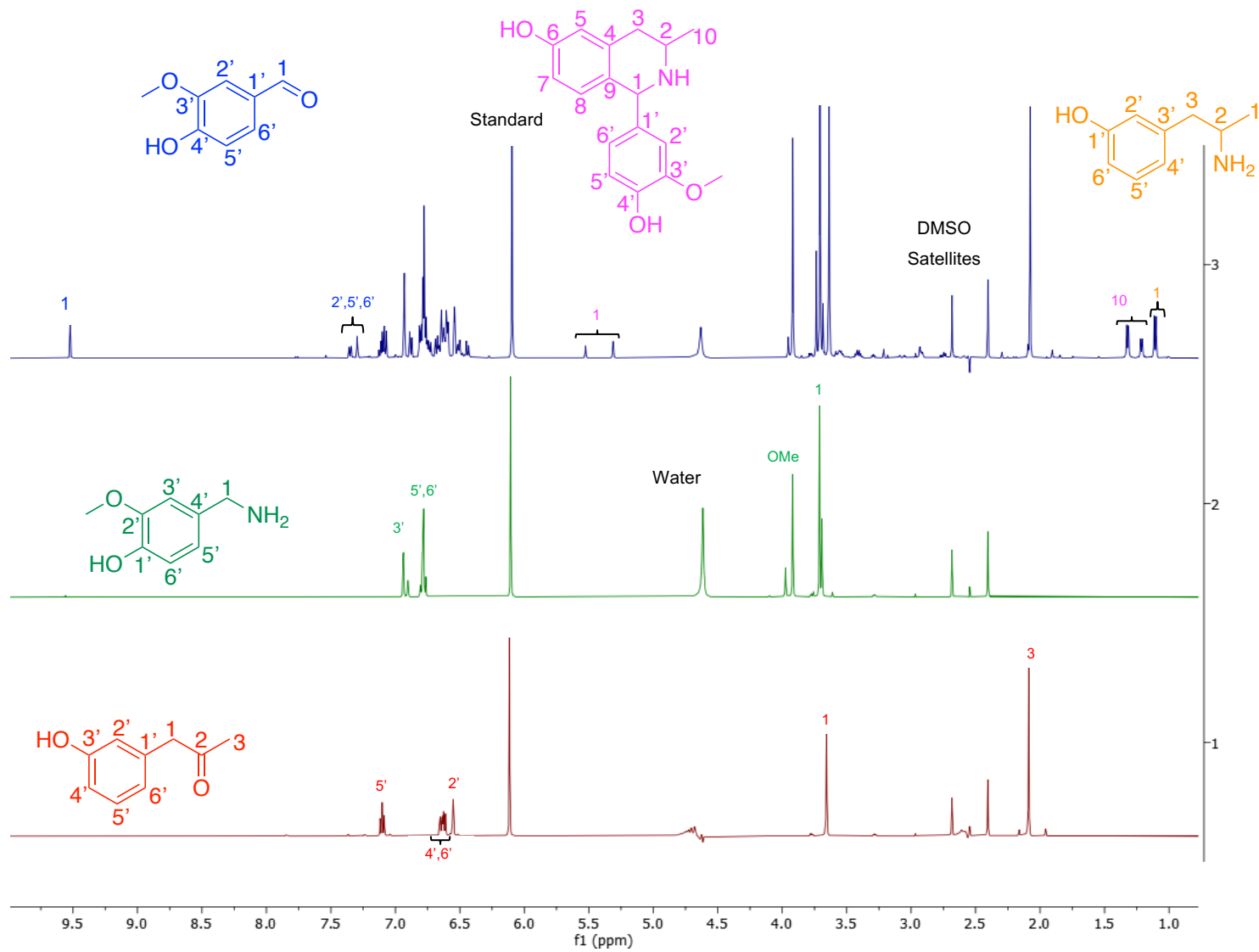
Calculation used to Work Out the Conversion of Biotransformations via Quantitative NMR Analysis

The quantitative integration of NMR spectra was undertaken by referencing peaks of interest to the known concentration of the standard peak, in this case, maleic acid. The peak for maleic acid is observed at 6.30 in the spectra, and the integration was set to concentration of the maleic acid added (50mM) * number of protons (2), thus it being set to 100.

This allowed quantitative examination of the other peaks of the NMR by referencing to this standard, as the relative integrations could then be divided by the number of protons present in the peak to give the relative concentration of the product or reactant.

To account for the dilution factor used in the experiment (where 100 μ L was added to 500 μ L of sample, to give 600 μ L total volume), the below formula was used to determine the concentration of the reagent/product of interest:

$$\text{conc. of reactant/product (mM)} = \left(\frac{\text{integration of peak}}{\text{no. of protons in peak}} \right) \times \frac{6}{5}$$



8.0 References

- 1 T. P. T. Cushnie, B. Cushnie and A. J. Lamb, *Int. J. Antimicrob. Agents*, 2014, **44**, 377–386.
- 2 A. H. Savitzky, A. Mori, D. A. Hutchinson, R. A. Saporito, G. M. Burghardt, H. B. Lillywhite and J. Meinwald, *Chemoecology*, 2012, **22**, 141–158.
- 3 H. D. Neuwinger, in *Alkaloids: Biochemistry, Ecology, and Medicinal Applications*, eds. M. F. Roberts and M. Wink, Springer US, Boston, MA, 1998, pp. 45–84.
- 4 T. Robinson, *Am. Assoc. Adv. Sci.*, 2016, **184**, 430–435.
- 5 G. R. Waller and E. K. Nowacki, in *Alkaloid Biology and Metabolism in Plants*, Springer US, Boston, MA, 1978, pp. 143–181.
- 6 J. C. Braekman, D. Dalozze and J. M. Pasteels, in *Alkaloids: Biochemistry, Ecology, and Medicinal Applications*, eds. M. F. Roberts and M. Wink, Springer US, Boston, MA, 1998, pp. 349–378.
- 7 R. Sigrist, B. Z. da Costa, A. J. Marsaioli and L. G. de Oliveira, *Biotechnol. Adv.*, 2015, **33**, 394–411.
- 8 S. Goyal, in *Natural Products: Phytochemistry, Botany and Metabolism of Alkaloids, Phenolics and Terpenes*, eds. K. G. Ramawat and J.-M. Mérillon, Springer Berlin Heidelberg, Berlin, Heidelberg, 2013, pp. 149–171.
- 9 C. Doepker, H. R. Lieberman, A. P. Smith, J. D. Peck, A. El-Sohemy and B. T. Welsh, *Annu. Rev. Food Sci. Technol.*, 2016, **7**, 117–137.
- 10 M. F. Roberts and M. Wink, in *Alkaloids: Biochemistry, Ecology, and Medicinal Applications*, eds. M. F. Roberts and M. Wink, Springer US, Boston, MA, 1998, pp. 1–7.
- 11 K. G. Zulak, D. K. Liscombe, H. Ashihara and P. J. Facchini, in *Plant Secondary Metabolites: Occurrence, Structure and Role in the Human Diet*, eds. A. Crozier, M. N. Clifford and H. Ashihara, John Wiley & Sons inc, 1st edn., 2020.
- 12 A. L. Harvey, *Drug Discov. Today*, 2008, **13**, 894–901.
- 13 P. M. Dewick, in *Medicinal Natural Products: Biosynthesis Approach*,

Wiley and Sons, 3rd edn., 2009, p. 311.

- 14 J. G. Geisler and G. G. Gross, *Phytochemistry*, 1990, **29**, 489–492.
- 15 É. Szoke, É. Lemberkovics and L. Kursinszki, in *Natural Products: Phytochemistry, Botany and Metabolism of Alkaloids, Phenolics and Terpenes*, eds. K. G. Ramawat and J.-M. Mérillon, Springer Berlin Heidelberg, Berlin, Heidelberg, 2013, pp. 303–341.
- 16 E. Leete and K. N. Juneau, *J. Am. Chem. Soc.*, 1969, **91**, 5614–5618.
- 17 B. G. de la Torre and F. Albericio, *Molecules*, 2020, **25**, 745.
- 18 C. Li, S. S. Ragab, G. Liu and W. Tang, *Nat. Prod. Rep.*, 2020, **37**, 276–292.
- 19 R. K. Zaidan and P. Evans, *European J. Org. Chem.*, 2019, 5354–5367.
- 20 M. R. Monaco, P. Renzi, D. M. Scarpino Schietroma and M. Bella, *Org. Lett.*, 2011, **13**, 4546–4549.
- 21 Y. C. Shih, P. H. Tsai, C. C. Hsu, C. W. Chang, Y. Jhong, Y. C. Chen and T. C. Chien, *J. Org. Chem.*, 2015, **80**, 6669–6678.
- 22 A. Sud, D. Sureshkumar and M. Klusmann, *Chem. Commun.*, 2009, **7345**, 3169–3171.
- 23 D. Robbins, A. F. Newton, C. Gignoux, J. C. Legeay, A. Sinclair, M. Rejzek, C. A. Laxon, S. K. Yalamanchili, W. Lewis, M. A. O'Connell and R. A. Stockman, *Chem. Sci.*, 2011, **2**, 2232–2235.
- 24 M. Rejzek, R. A. Stockman and D. L. Hughesb, *Org. Biomol. Chem.*, 2005, **3**, 73–83.
- 25 A. F. Newton, M. Rejzek, M. L. Alcaraz and R. A. Stockman, *Beilstein J. Org. Chem.*, 2008, **4**, 3–7.
- 26 J.-C. Legeay, W. Lewis and R. A. Stockman, *Chem. Commun.*, 2009, 2207–2209.
- 27 R. A. Stockman, A. Sinclair, L. G. Arini, P. Szeto and D. L. Hughes, *J. Org. Chem.*, 2004, **69**, 1598–1602.
- 28 M. S. Karatholuvhu, A. Sinclair, A. F. Newton, M. L. Alcaraz, R. A. Stockman and P. L. Fuchs, *J. Am. Chem. Soc.*, 2006, **128**, 12656–12657.
- 29 A. Pictet and T. Spengler, *Ber. Dtsch. Chem. Ges*, 1911, **44**, 2030–2036.

- 30 J. Stöckigt, A. P. Antonchick, F. Wu and H. Waldmann, *Angew. Chemie - Int. Ed.*, 2011, **50**, 8538–8564.
- 31 M. Chrzanowska and M. D. Rozwadowska, *Chem. Rev.*, 2004, **104**, 3341–3370.
- 32 W. Liu, S. Liu, R. Jin, H. Guo and J. Zhao, *Org. Chem. Front.*, 2015, **2**, 288–299.
- 33 M. Chrzanowska, A. Grajewska and M. D. Rozwadowska, *Chem. Rev.*, 2016, **116**, 12369–12465.
- 34 E. D. Cox and J. M. Cook, *Chem. Rev.*, 1995, **95**, 1797–1842.
- 35 A. Yokoyama, T. Ohwada and K. Shudo, *J. Org. Chem.*, 1999, **64**, 611–617.
- 36 R. Quevedo, E. Baquero and M. Rodriguez, *Tetrahedron Lett.*, 2010, **51**, 1774–1778.
- 37 M. J. Vanden Eynden, K. Kunchithapatham and J. P. Stambuli, *J. Org. Chem.*, 2010, **75**, 8542–8549.
- 38 M. J. Vanden Eynden and J. P. Stambuli, *Org. Lett.*, 2008, **10**, 5289–5291.
- 39 A. Hegedüs and Z. Hell, *Tetrahedron Lett.*, 2004, **45**, 8553–8555.
- 40 M. Barbero, S. Bazzi, S. Cadamuro and S. Dughera, *Tetrahedron Lett.*, 2010, **51**, 6356–6359.
- 41 T. Pesnot, M. C. Gershater, J. M. Ward and H. C. Hailes, *Chem. Commun.*, 2011, **47**, 3242–3244.
- 42 J. Zhao, D. Méndez-Sánchez, J. M. Ward and H. C. Hailes, *J. Org. Chem.*, 2019, **84**, 7702–7710.
- 43 L. Knorr, *Chem. Ber.*, 1884, **17**, 546.
- 44 F. V. F., M. C. Souza, B. V. de, A. C. Cunha, L. O. R. Pereira and M. L. G. Ferreira, *Org. Prep. Proced. Int. New J. Org. Synth.*, 2001, **33**, 411–454.
- 45 P. Nagafuji and M. Cushman, *J. Org. Chem.*, 1996, **61**, 4999–5003.
- 46 A. Alberola, A. G. Ortega, M. L. Sádaba and C. Sañudo, *Tetrahedron*, 1999, **55**, 6555–6566.
- 47 S. Michlik and R. Kempe, *Nat. Chem.*, 2013, **5**, 140–144.
- 48 I. Paterson and E. a Anderson, *Science (80-.)*, 2005, **310**, 451–453.
- 49 V. Alphand, R. Furstoss, K. Drauz and H. Waldmann, *Enzyme*

Catalysis in Organic Synthesis, Wiley-VCH, Weinheim, Germany, Third., 1995.

- 50 N. J. Turner and E. O'Reilly, *Nat. Chem. Biol.*, 2013, **9**, 285–288.
- 51 P. Anastas and N. Eghbali, *Chem. Soc. Rev.*, 2010, **39**, 301–312.
- 52 P. T. Anastas and M. M. Kirchhoff, *Acc. Chem. Res.*, 2002, **35**, 686–694.
- 53 A. Gomm and E. O'Reilly, *Curr. Opin. Chem. Biol.*, 2018, **43**, 106–112.
- 54 F. Leipold, S. Hussain, D. Ghislieri and N. J. Turner, *ChemCatChem*, 2013, **5**, 3505–3508.
- 55 G. A. Aleku, S. P. France, H. Man, J. Mangas-Sanchez, S. L. Montgomery, M. Sharma, F. Leipold, S. Hussain, G. Grogan and N. J. Turner, *Nat. Chem.*, 2017, **9**, 961–969.
- 56 G. A. Aleku, J. Mangas-Sanchez, J. Citoler, S. P. France, S. L. Montgomery, R. S. Heath, M. P. Thompson and N. J. Turner, *ChemCatChem*, 2018, **10**, 515–519.
- 57 J. I. Ramsden, R. S. Heath, S. R. Derrington, S. L. Montgomery, J. Mangas-Sanchez, K. R. Mulholland and N. J. Turner, *J. Am. Chem. Soc.*, 2019, **141**, 1201–1206.
- 58 D. Ghislieri, A. P. Green, M. Pontini, S. C. Willies, I. Rowles, A. Frank, G. Grogan and N. J. Turner, *J. Am. Chem. Soc.*, 2013, **135**, 10863–10869.
- 59 J. H. Schrittwieser, B. Groenendaal, S. C. Willies, D. Ghislieri, I. Rowles, V. Resch, J. H. Sattler, E. M. Fischereeder, B. Grischek, W. D. Lienhart, N. J. Turner and W. Kroutil, *Catal. Sci. Technol.*, 2014, **4**, 3657–3664.
- 60 I. Rowles, K. J. Malone, L. L. Etchells, S. C. Willies and N. J. Turner, *ChemCatChem*, 2012, **4**, 1259–1261.
- 61 V. Erdmann, B. R. Lichman, J. Zhao, R. C. Simon, W. Kroutil, J. M. Ward, H. C. Hailes and D. Rother, *Angew. Chemie - Int. Ed.*, 2017, **56**, 12503–12507.
- 62 B. R. Lichman, E. D. Lamming, T. Pesnot, J. M. Smith, H. C. Hailes and J. M. Ward, *Green Chem.*, 2015, **17**, 852–855.
- 63 J. H. Schrittwieser, V. Resch, S. Wallner, W. D. Lienhart, J. H. Sattler,

- J. Resch, P. MacHeroux and W. Kroutil, *J. Org. Chem.*, 2011, **76**, 6703–6714.
- 64 M. D. Truppo, J. David Rozzell and N. J. Turner, *Org. Process Res. Dev.*, 2010, **14**, 234–237.
- 65 M. Girardin, S. G. Ouellet, D. Gauvreau, J. C. Moore, G. Hughes, P. N. Devine, P. D. O'Shea and L. C. Campeau, *Org. Process Res. Dev.*, 2013, **17**, 61–68.
- 66 R. C. Simon, F. Zepeck and W. Kroutil, *Chem. - A Eur. J.*, 2013, **19**, 2859–2865.
- 67 R. C. Simon, B. Grischek, F. Zepeck, A. Steinreiber, F. Belaj and W. Kroutil, *Angew. Chemie - Int. Ed.*, 2012, **51**, 6713–6716.
- 68 S. E. Payer, J. H. Schrittwieser, B. Grischek, R. C. Simon and W. Kroutil, *Adv. Synth. Catal.*, 2016, **358**, 444–451.
- 69 E. O'Reilly, C. Iglesias, D. Ghislieri, J. Hopwood, J. L. Galman, R. C. Lloyd and N. J. Turner, *Angew. Chemie - Int. Ed.*, 2014, **53**, 2447–2450.
- 70 S. P. France, S. Hussain, A. M. Hill, L. J. Hepworth, R. M. Howard, K. R. Mulholland, S. L. Flitsch and N. J. Turner, *ACS Catal.*, 2016, **6**, 3753–3759.
- 71 N. Alvarenga, S. E. Payer, P. Petermeier, C. Kohlfuerst, A. L. Meleiro Porto, J. H. Schrittwieser and W. Kroutil, *ACS Catal.*, 2020, **10**, 1607–1620.
- 72 B. Z. Costa, J. L. Galman, I. Slabu, S. P. France, A. J. Marsaioli and N. J. Turner, *ChemCatChem*, 2018, **10**, 4733–4738.
- 73 J. Ryan, M. Šiaučiulis, A. Gomm, B. Maciá, E. O'Reilly and V. Caprio, *J. Am. Chem. Soc.*, 2016, **138**, 15798–15800.
- 74 I. Slabu, J. L. Galman, R. C. Lloyd and N. J. Turner, *ACS Catal.*, 2017, **7**, 8263–8284.
- 75 D. Koszelewski, K. Tauber, K. Faber and W. Kroutil, *Trends Biotechnol.*, 2010, **28**, 324–332.
- 76 A. C. Eliot and J. F. Kirsch, *Annu. Rev. Biochem.*, 2004, **73**, 383–415.
- 77 F. Steffen-Munsberg, C. Vickers, H. Kohls, H. Land, H. Mallin, A. Nobili, L. Skalden, T. van den Bergh, H. J. Joosten, P. Berglund, M. Höhne and U. T. Bornscheuer, *Biotechnol. Adv.*, 2015, **33**, 566–604.

- 78 R. Percudani and A. Peracchi, *BMC Bioinformatics*, 2009, **10**, 273.
- 79 P. K. Mehta, T. I. Hale and P. Christen, *Eur. J. Biochem.*, 1993, **214**, 549–561.
- 80 S. A. Kelly, S. Pohle, S. Wharry, S. Mix, C. C. R. Allen, T. S. Moody and B. F. Gilmore, *Chem. Rev.*, 2018, **118**, 349–367.
- 81 M. D. Patil, G. Grogan, A. Bommarius and H. Yun, *Catalysts*, , DOI:10.3390/catal8070254.
- 82 M. S. Humble, K. E. Cassimjee, M. Håkansson, Y. R. Kimbung, B. Walse, V. Abedi, H. J. Federsel, P. Berglund and D. T. Logan, *FEBS J.*, 2012, **279**, 779–792.
- 83 J. S. Shin and B. G. Kim, *J. Org. Chem.*, 2002, **67**, 2848–2853.
- 84 I. V. Pavlidis, M. S. Weiß, M. Genz, P. Spurr, S. P. Hanlon, B. Wirz, H. Iding and U. T. Bornscheuer, *Nat. Chem.*, 2016, **8**, 1076–1082.
- 85 K. E. Cassimjee, B. Manta and F. Himo, *Org. Biomol. Chem.*, 2015, **13**, 8453–8464.
- 86 K. E. Cassimjee, M. S. Humble, V. Miceli, C. G. Colomina and P. Berglund, *ACS Catal.*, 2011, **1**, 1051–1055.
- 87 A. P. Green, N. J. Turner and E. O'Reilly, *Angew. Chemie - Int. Ed.*, 2014, **53**, 10714–10717.
- 88 J. L. Galman, I. Slabu, N. J. Weise, C. Iglesias, F. Parmeggiani, R. C. Lloyd and N. J. Turner, *Green Chem.*, 2017, **19**, 361–366.
- 89 A. Gomm, W. Lewis, A. P. Green and E. O'Reilly, *Chem. - A Eur. J.*, 2016, **22**, 12692–12695.
- 90 C. K. Savile, J. M. Janey, E. C. Mundorff, J. C. Moore, S. Tam, W. R. Jarvis, J. C. Colbeck, A. Krebber, F. J. Fleitz, J. Brands, P. N. Devine, G. W. Huisman and G. J. Hughes, *Science (80-.)*, 2010, **329**, 305–309.
- 91 E. Busto, R. C. Simon, B. Grischek, V. Gotor-fernandez and W. Kroutil, 2014, 1937–1942.
- 92 M. A. Huffman, A. Fryszkowska, O. Alvizo, M. Borra-Garske, K. R. Campos, K. A. Canada, P. N. Devine, D. Duan, J. H. Forstater, S. T. Grosser, H. M. Halsey, G. J. Hughes, J. Jo, L. A. Joyce, J. N. Kolev, J. Liang, K. M. Maloney, B. F. Mann, N. M. Marshall, M. Mclaughlin, J. C. Moore, G. S. Murphy, C. C. Nawrat, J. Nazor, S. Novick, N. R.

- Patel, A. Rodriguez-Granillo, S. A. Robaire, E. C. Sherer, M. D. Truppo, A. M. Whittaker, D. Verma, L. Xiao, Y. Xu and H. Yang, *Science (80-.)*., 2020, **368**, eabc1954.
- 93 E. O'Reilly and J. Ryan, *Science (80-.)*., 2019, **366**, 1199–1200.
- 94 P. Yu, A. Bismuto and B. Morandi, *Angew. Chemie - Int. Ed.*, 2020, **59**, 2904–2910.
- 95 T. Delcaillau, A. Bismuto, Z. Lian and B. Morandi, *Angew. Chemie - Int. Ed.*, 2020, **59**, 2110–2114.
- 96 B. N. Bhawal, J. C. Reisenbauer, C. Ehinger and B. Morandi, *J. Am. Chem. Soc.*, 2020, **142**, 10914–10920.
- 97 P. Boehm and B. Morandi, *Chimia (Aarau)*., 2019, **74**, 724–729.
- 98 X. Dong, J. L. Röckl, S. R. Waldvogel and B. Morandi, *ChemRxiv*, 2020, **514**, 507–514.
- 99 X. Fang, P. Yu and B. Morandi, *Science (80-.)*., 2016, **351**, 832–837.
- 100 S. L. Montgomery, J. Mangas-Sanchez, M. P. Thompson, G. A. Aleku, B. Dominguez and N. J. Turner, *Angew. Chemie*, 2017, **129**, 10627–10630.
- 101 T. Knaus, F. G. Mutti, L. D. Humphreys, N. J. Turner and N. S. Scrutton, *Org. Biomol. Chem.*, 2015, **13**, 223–233.
- 102 M. P. Thompson and N. J. Turner, *ChemCatChem*, 2017, **9**, 3833–3836.
- 103 F. G. Mutti, T. Knaus, N. S. Scrutton, M. Breuer and N. J. Turner, *Science (80-.)*., 2015, **349**, 1525–1529.
- 104 J. E. Farnberger, N. Richter, K. Hiebler, S. Bierbaumer, M. Pickl, W. Skibar, F. Zepeck and W. Kroutil, *Commun. Chem.*, 2018, **1**, 1–8.
- 105 J. Xu, A. P. Green and N. J. Turner, *Angew. Chemie - Int. Ed.*, 2018, **57**, 16760–16763.
- 106 B. N. Bhawal and B. Morandi, *ACS Catal.*, 2016, **6**, 7528–7535.
- 107 B. N. Bhawal and B. Morandi, *Chem. - A Eur. J.*, 2017, **23**, 12004–12013.
- 108 F. Taday, J. Ryan, S. P. Argent, V. Caprio, B. Maciá and E. O'Reilly, *Chem. - A Eur. J.*, 2020, **26**, 3729–3732.
- 109 S. Al-Mousawi, M. M. Abdelkhalik, E. John and M. H. Elnagdi, *J. Heterocycl. Chem.*, 2003, **40**, 689–695.

- 110 A. Z. A. Elassar and A. A. El-Khair, *Tetrahedron*, 2003, **59**, 8463–8480.
- 111 J. V. Greenhill, *J. Chem. Soc.*, 1977, 277–294.
- 112 A. K. Chattopadhyay and S. Hanessian, *Chem. Commun.*, 2015, **51**, 16437–16449.
- 113 S. Fréville, P. Delbecq, V. M. Thuy, H. Petit, J. P. Célérier and G. Lhomme, *Tetrahedron Lett.*, 2001, **42**, 4609–4611.
- 114 B. T. Kametani, H. Nemoto, M. Ihara and K. Fukumoto, *J. Chem. Soc. Perkin Trans. 1*, 1980, 1607–1613.
- 115 A. S. Howard, R. B. Katz and J. P. Michael, *Tetrahedron Lett.*, 2001, **24**, 829–830.
- 116 C. Herdeis and J. Telser, *European J. Org. Chem.*, 1999, 1407–1414.
- 117 C. Herdeis, P. Küpper and S. Plé, *Org. Biomol. Chem.*, 2006, **4**, 524–529.
- 118 J. P. Michael, C. B. de Koning and D. P. Pienaar, *Synlett*, 2006, **3**, 0383–0386.
- 119 A. G. H. Wee and G. J. Fan, *Org. Lett.*, 2008, **10**, 3869–3872.
- 120 D. Bacos, J. P. Célérier, E. Marx, S. Rosset and G. Lhomme, *J. Heterocycl. Chem.*, 1990, **27**, 1387–1392.
- 121 A. I. Gerasyuto and R. P. Hsung, *Org. Lett.*, 2006, **8**, 4899–4902.
- 122 K. R. Eddington, N.D.; Cox, D.S.; Roberts, R.R.; Stables, J.P.; Powell, C.B.; Scott, *Curr. Med. Chem.*, 2000, **7**, 417–436.
- 123 J. E. Foster, J. M. Nicholson, R. Butcher, J. P. Stables, I. O. Edafiogho, A. M. Goodwin, M. C. Henson and C. A. Smith, *Bioorganic Med. Chem.*, 1999, **7**, 2415–2425.
- 124 N. N. Salama, N. D. Eddington, D. Payne, T. L. Wilson and K. R. Scott, *Curr. Med. Chem.*, 2012, **11**, 2093–2103.
- 125 G. Dannhardt, A. Bauer and U. Nowe, *J. Fur Prakt. Chemie Chem.*, 1998, **340**, 256–263.
- 126 D. L. Boger, R. J. Wysocki, S. A. Munk, T. Ishizaki, P. A. Kitos and O. Suntornwat, *J. Am. Chem. Soc.*, 1989, **111**, 6461–6463.
- 127 J. P. Michael, C. B. De Koning, G. D. Hosken and T. V. Stanbury, *Tetrahedron*, 2001, **57**, 9635–9648.
- 128 B. A. D. Neto, A. A. M. Lapis, A. B. Bernd and D. Russowsky,

- Tetrahedron*, 2009, **65**, 2484–2496.
- 129 D. Scarpi, S. Begliomini, C. Prandi, A. Oppedisano, A. Deagostino, E. Gómez-Bengoa, B. Fiser and E. G. Occhiato, *European J. Org. Chem.*, 2015, 3251–3265.
- 130 A. Arcadi, G. Bianchi, S. Di Giuseppe and F. Marinelli, *Green Chem.*, 2003, **5**, 64–67.
- 131 J. Ciesielski, D. P. Canterbury and A. J. Frontier, *Org. Lett.*, 2009, **11**, 4374–4377.
- 132 G. H. Lee, E. B. Choi, E. Lee and C. S. Pak, *J. Org. Chem.*, 1994, **59**, 1428–1443.
- 133 P. Chiu and S. K. Leung, *Chem. Commun.*, 2004, 2308–2309.
- 134 J. Schreiber, D. Felix, a. Eschenmoser, M. Winter, F. Gautschi, K. H. Schulte-Elte, E. Sundt, G. Ohloff, J. Kalvoda, H. Kaufmann, P. Wieland and G. Anner, *Helv. Chim. Acta*, 1967, **50**, 2101–2108.
- 135 R. J. Cox, D. J. Ritson, T. A. Dane, J. Berge, J. P. H. Charmant and A. Kantacha, *Chem. Commun.*, 2005, 1037.
- 136 R. E. Islas, J. Cárdenas, R. Gaviño, E. García-Ríos, L. Lomas-Romero and J. A. Morales-Serna, *RSC Adv.*, 2017, **7**, 9780–9789.
- 137 M. M. Gugelchuk, D. J. Hart and Y. M. Tsai, *J. Org. Chem.*, 1981, **46**, 3671–3675.
- 138 S. K. Ghosh, G. S. Buchanan, Q. A. Long, Y. Wei, Z. F. Al-rashid, H. M. Sklenicka and R. P. Hsung, *Tetrahedron*, 2008, **64**, 883–893.
- 139 K. Paulvannan and J. R. Stille, *J. Org. Chem.*, 1994, **59**, 1613–1620.
- 140 G. S. Buchanan, H. Dai, R. P. Hsung, A. I. Gerasyuto and C. M. Scheinebeck, *Org. Lett.*, 2011, **13**, 4402–4405.
- 141 T. Pesnot, M. C. Gershater, J. M. Ward and H. C. Hailes, *Chem. Commun.*, 2011, **47**, 3242–3244.
- 142 E. Vitaku, D. T. Smith and J. T. Njardarson, *J. Med. Chem.*, 2014, **57**, 10257–10274.
- 143 J. L. Galman, I. Slabu, F. Parmeggiani and N. J. Turner, *Chem. Commun.*, 2018, **54**, 11316–11319.
- 144 A. Rouchaud and J. C. Braekman, *European J. Org. Chem.*, 2009, **5**, 2666–2674.
- 145 O. Barbosa, C. Ortiz, Á. Berenguer-Murcia, R. Torres, R. C.

- Rodrigues and R. Fernandez-Lafuente, *RSC Adv.*, 2014, **4**, 1583–1600.
- 146 A. R. Battersby, *Nat. Prod. Rep.*, 2000, **17**, 507–526.
- 147 C. C. Hughes, A. Prieto-Davo, P. R. Jensen and W. Fenical, *Org. Lett.*, 2008, **10**, 629–631.
- 148 R. Khajuria, S. Dham and K. K. Kapoor, *RSC Adv.*, 2016, **6**, 37039–37066.
- 149 Codexis ATA Screening Kit, Frequently Asked Questions, https://aed8ea31-545e-414a-b7fa-7c34b1742e9a.filesusr.com/ugd/5a7b2a_b0a8c635f49c49048b42b931ca9da250.pdf, (accessed 5 January 2021).
- 150 M. D. Truppo, J. D. Rozzell and N. J. Turner, *Org. Process Res. Dev.*, 2010, **14**, 234–237.
- 151 Z. Wang, in *Comprehensive Organic Name Reaction and Reagents*, John Wiley & Sons, inc., 2010, pp. 1634–1637.
- 152 M. E. Welsch, S. A. Snyder and B. R. Stockwell, *Curr. Opin. Chem. Biol.*, 2010, **14**, 347–361.
- 153 B. K. Peters, S. K. Chakka, T. Naicker, G. E. M. Maguire, H. G. Kruger, P. G. Andersson and T. Govender, *Tetrahedron Asymmetry*, 2010, **21**, 679–687.
- 154 R. B. Kawthekar, S. K. Chakka, V. Francis, P. G. Andersson, H. G. Kruger, G. E. M. Maguire and T. Govender, *Tetrahedron Asymmetry*, 2010, **21**, 846–852.
- 155 T. Naicker, K. Petzold, T. Singh, P. I. Arvidsson, H. G. Kruger, G. E. M. Maguire and T. Govender, *Tetrahedron Asymmetry*, 2010, **21**, 2859–2867.
- 156 S. K. Chakka, P. G. Andersson, G. E. M. Maguire, H. G. Kruger and T. Govender, *European J. Org. Chem.*, 2010, 972–980.
- 157 N. Samanani and P. J. Facchini, *Planta*, 2001, **213**, 898–906.
- 158 H. Minami, E. Dubouzet, K. Iwasa and F. Sato, *J. Biol. Chem.*, 2007, **282**, 6274–6282.
- 159 P. Li, B. Lü, C. Fu and S. Ma, *Adv. Synth. Catal.*, 2013, **355**, 1255–1259.
- 160 W. C. Fu, C. M. So, W. K. Chow, O. Y. Yuen and F. Y. Kwong, *Org.*

- Lett.*, 2015, **17**, 4612–4615.
- 161 B. M. Trost, M. J. Bartlett, A. H. Weiss, A. J. Vonwangelin and V. S. Chan, *Chem. - A Eur. J.*, 2012, **18**, 16498–16509.
- 162 B. M. Trost and M. J. Bartlett, *Org. Lett.*, 2012, **14**, 1322–1325.
- 163 A. Kohda, K. Nagayoshi, K. Maemoto and T. Sato, *J. Org. Chem.*, 1983, **48**, 425–432.
- 164 J. Diehl and R. Brückner, *European J. Org. Chem.*, 2017, **2017**, 278–286.
- 165 P. H. Lambert, M. Vaultier and R. Carrié, *J. Org. Chem.*, 1985, **50**, 5352–5356.
- 166 B. C. Hong, F. L. Chen, S. H. Chen, J. H. Liao and G. H. Lee, *Org. Lett.*, 2005, **7**, 557–560.
- 167 Y. Li, Q. Zhang, H. Wang, B. Cheng and H. Zhai, *Org. Lett.*, 2017, **19**, 4387–4390.
- 168 M. R. Monaco, P. Renzi, D. M. Scarpino Schietroma and M. Bella, *Org. Lett.*, 2011, **13**, 4546–4549.
- 169 J. McNulty and P. Das, *Tetrahedron*, 2009, **65**, 7794–7800.
- 170 L. C. Bouchez, C. Gerbeaux, M. Rusch, M. Patoor, M. Livendahl and N. J. Press, *Synlett*, 2017, **10**, 1219–1223.